



Durham E-Theses

The role of plectin in the regulation of carcinoma cell invasion

McInroy, Lorna

How to cite:

McInroy, Lorna (2007) *The role of plectin in the regulation of carcinoma cell invasion*, Durham theses, Durham University. Available at Durham E-Theses Online: <http://etheses.dur.ac.uk/2565/>

Use policy

The full-text may be used and/or reproduced, and given to third parties in any format or medium, without prior permission or charge, for personal research or study, educational, or not-for-profit purposes provided that:

- a full bibliographic reference is made to the original source
- a [link](#) is made to the metadata record in Durham E-Theses
- the full-text is not changed in any way

The full-text must not be sold in any format or medium without the formal permission of the copyright holders.

Please consult the [full Durham E-Theses policy](#) for further details.

The role of plectin in the regulation of carcinoma cell invasion.

by
Lorna McInroy

The copyright of this thesis rests with the author or the university to which it was submitted. No quotation from it, or information derived from it may be published without the prior written consent of the author or university, and any information derived from it should be acknowledged.

A thesis submitted at Durham University for the
degree of Doctor of Philosophy

School of Biological and Biomedical Sciences
Durham University
September 2007



DECLARATIONS

I declare that the experiments described in this thesis were carried out by myself in the School of Biological and Biomedical Sciences, Durham University, under the supervision of Dr Arto Maatta. This thesis has been composed by myself and is a record of work that has not been submitted previously for a higher degree.



Lorna McInroy

I certify that the work reported in this thesis has been performed by Lorna McInroy, who, during the period of study, has fulfilled the conditions of the Ordinance and Regulations governing the Degree of Doctor of Philosophy.



Dr Arto Maatta

The copyright of this thesis rests with the author. No quotation from it should be published in any format, including electronics and the internet, without the author's prior consent. All information derived from this thesis must be acknowledged appropriately.

ABSTRACT

The research presented in this thesis endeavours to understand the role of the plakin family of cytoskeletal linker proteins in the migration and invasive potential of epithelial carcinomas. This study focuses on plectin, a plakin family member that has previously been implicated with a role in tissue integrity of the skin and muscle. I investigated the complex gene organisation of the alternative first exons in human plectin, leading to the discovery of a further novel isoform plectin-1k. A panel of colon and breast carcinoma cell lines that vary in their differentiation and metastatic potential were used to investigate the expression of the isoforms at the mRNA and protein levels, showing plectin to be expressed at higher levels in the more invasive cell types. The subcellular localisation of the alternatively spliced plectin isoforms was investigated using green fluorescent protein (GFP) and polyclonal antibodies, revealing isoform specific targeting to different actin structures. Ablation of plectin or vimentin (a major intermediate filament protein of mesenchymal cells that interacts with plectin), by small interfering RNAs suggest these proteins are able to modulate invasion, migration and attachment of the epithelial carcinoma cells. Further investigation into the novel isoform plectin-1k reveals a role in the formation of podosome like adhesion structures in a Rho kinase dependant manner that facilitate migration in the SW480 colon carcinoma cells. The above findings are novel and contribute to the understanding of migration and invasion of cancer cells. Furthermore, this understanding could provide novel targets of cancer cell metastasis.

ACKNOWLEDGEMENTS

I would like to acknowledge my husband Dale for helping me through all the times when I did not believe in myself. I am also forever in debt to my parents for supporting me in more ways I can think of, making all this possible. I would never have achieved so much without my supervisor, Dr Arto Määttä, who gave me sound advice and guidance right to the end. To all the members of the ICBL lab and beyond for making my time in Durham unforgettable, I will miss everyone dearly. Special thanks to Professor Roy Quinlan and his lab members for advice throughout my project. Acknowledgements must go to Christine Richardson for advice on confocal microscopy, to Terry Gibbons for useful tips on molecular biology, to Dr Naomi Willis for advice on the colon carcinoma cells and Pamela Ritchie for cell culture assistance. Finally, a big thank you to everyone or anything that had to listen to me blethering on about plectin isoforms and cell migration assays. This project was supported by Cancer Research UK. I dedicate this thesis to Pepper.

CONTENTS	page no.
Declaration	II
Abstract	III
Acknowledgements	IV
Contents	V
List of Tables	XII
List of Figures	XIII
1 CHAPTER 1: Introduction	1
1.1 Prologue.	2
1.2 The cytoskeleton, an overview.	2
1.2.1 Microfilaments.	2
1.2.2 Microtubules.	3
1.2.3 Intermediate filaments.	4
1.2.3.1 Keratins.	5
1.2.3.2 Vimentin.	6
1.3 Plectin, a member of the plakin family of proteins.	11
1.3.1 Role of plectin in cytoskeletal dynamics.	12
1.3.2 Role of plectin as a scaffolding protein for signal transduction.	12
1.3.3 Role of plectin in tissue and cell integrity.	13
1.4 Epithelial cell junctions.	14
1.4.1 Role of plectin in the formation of hemidesmosomes.	16
1.4.2 Type II hemidesmosomes.	17
1.4.3 Desmosomes.	18
1.5 The plakin family.	20
1.5.1 The plakin family protein domains.	20
1.5.2 Bullous pemphigoid antigen 1 (BPAG1)	24
1.5.3 Desmoplakin.	24
1.5.4 Periplakin and envoplakin.	25
1.5.5 Microtubule-actin crosslinking factor 1 (MACF 1).	27
1.5.6 Epiplakin.	28
1.6 Plakins and cancer.	28

2	CHAPTER 2: Materials and methods	30
2.1	Chemicals and reagents.	31
2.2	Bioinformatics.	31
2.3	Molecular biology.	31
2.3.1	Primer design.	31
2.3.2	RNA extraction.	33
2.3.3	cDNA synthesis.	36
2.3.4	PCR.	36
2.3.5	Cloning of alternative first exon plectin isoforms.	38
2.3.6	Competent DH5 bacterial cells.	38
2.3.7	Real time PCR.	39
2.3.8	Cloning of eGFP constructs.	40
2.4	Cell culture.	42
2.4.1	Cell maintenance.	42
2.4.2	Differentiation of THP1 cells.	44
2.4.3	Transfection of plectin-GFP vectors.	44
2.4.4	Plectin GFP stable cell lines.	44
2.5	siRNA interference.	45
2.5.1	siRNA sequences.	47
2.5.2	Transfection of siRNA.	48
2.6	Plectin isoform specific polyclonal antibodies.	48
2.7	Protein analysis.	49
2.7.1	Total cell protein extraction.	49
2.7.2	Colorimetric protein quantification using spectroscopy.	49
2.7.3	1-dimensional gel electrophoresis.	49
2.7.4	Coomassie Blue staining.	51
2.7.5	Immunoblotting.	51
2.7.6	Immunoblotting (high molecular weight proteins)	51
2.7.7	Immunofluorescence of carcinoma cells	52
2.8	Microscopy.	54
2.9	Specificity of plectin LM antibodies.	54
2.9.1	Purification.	54
2.9.2	Peptide competition assay.	55
2.9.3	Specificity of polyclonal antibodies by siRNA.	55

2.10	Cell survival assay.	55
2.11	Migration and invasion.	56
2.11.1	Collagen insert migration assay.	56
2.11.2	Gel insert invasion assay.	56
2.11.3	Scratch wound assay.	57
2.11.4	Rho kinase inhibitor assay.	57
2.12	Cell attachment assays.	57
3	CHAPTER 3: Mapping of the alternatively spliced human isoforms.	59
3.1	Introduction.	60
3.2	Results.	62
3.2.1	Human plectin gene contains a similar diversity of alternative N-terminal isoforms to mouse and rat genes.	62
3.2.2	Mapping of the alternative plectin 5' isoforms.	64
3.2.3	Identification of a novel plectin isoform; plectin-1k.	64
3.2.4	Search of EST clones reveals further possible alternative exons.	66
3.2.5	PCR sequencing and cloning of plectin alternative N-terminal first exons.	66
3.2.6	Semi-quantitative RT-PCR end point analysis shows distinct expression levels of plectin N-terminal isoforms in colon carcinoma cells.	68
3.2.7	Real time PCR: a method to quantitatively investigate mRNA expression levels.	70
3.2.8	Melt curve analysis confirms the integrity of the PCR product.	70
3.2.9	Fluorescence curves for isoform plec-1k show real-time PCR progression.	70
3.2.10	Quantitative Real time PCR shows changes in isoform expression in cancer cell lines.	77
3.2.11	Expression of plectin N-terminal isoforms in a panel of human tissues.	80
3.3	Discussion.	83

4 CHAPTER 4: Expression and subcellular expression of plectin protein isoforms in carcinoma cells.	86
4.1 Introduction.	87
4.2 Results.	88
4.2.1 Highgrade SW480 and MDA-MB-231 cells show an increase of invasive potential compared to their lowergrade counterparts.	88
4.2.2 Investigation of expression levels of cytoskeletal and related proteins in the panel of carcinoma cell lines.	90
4.2.3 Plectin is over-expressed in the more invasive cell lines	90
4.2.4 Plectin is recruited away from cell periphery in the more invasive carcinoma cells.	93
4.2.5 Invasive cell lines are not able to form a well-organised epithelial monolayer.	98
4.2.6 Plectin co-localised with the actin cytoskeleton in cancer cell lines.	101
4.2.7 Expression of eGFP-tagged alternative plectin actin binding domains in stable cell lines.	104
4.2.8 Alternative first exons target plectin actin binding domains to unique cytoskeletal structures.	106
4.2.9 Plectin-1b GFP colocalised with a transfected mitochondrial marker.	106
4.2.10 Investigation of the human plectin isoforms using polyclonal antibodies raised to plectin isoforms 1, 1b, 1f, 1k.	112
4.2.11 Polyclonal plectin isoform antibodies recognise full-length plectin.	112
4.2.12 The specificity of plectin N-terminal human antibodies was further supported by siRNA transfection experiments with total plectin.	113
4.2.13 Expression of plectin isoforms 1, 1b, 1f and 1k in cancer cell lines.	117

4.2.14	Immunofluorescence using isoform specific antibodies in carcinoma cells.	117
4.3	Discussion.	121
5	CHAPTER 5: Role of plectin and vimentin in migration and invasion of carcinoma cells.	126
5.1	Introduction.	127
5.1.1	Cell Migration.	129
5.1.1.1	Modes of cell migration.	129
5.1.1.2	Cell-matrix attachments.	130
5.1.1.3	Integrins.	130
5.1.1.4	Epithelial to mesenchymal transition.	131
5.1.1.5	Matrix degradation.	132
5.2	Results.	135
5.2.1	Transfection of short interfering RNA (siRNA) to down-regulate expression of plectin and vimentin proteins	135
5.2.2	Cell viability is not affected by either vimentin or plectin siRNA transfections.	139
5.2.3	Plectin depletion causes impairment of carcinoma cell invasion through collagen gels.	141
5.2.4	The depletion of vimentin dramatically reduces the ability of SW480 and MDA-MB-231 cells to invade through collagen gels.	141
5.2.5	Plectin ablation decreases attachment to fibrillar collagen in both MDA-MB-231 and SW480 carcinoma cells.	147
5.2.6	Vimentin ablation alters attachment to fibrillar collagen in both MDA-MB-231 and SW480 carcinoma cells.	147
5.2.7	Depletion of plectin and vimentin in SW480 cells reduce number of cells in suspension compared to scrambled control.	147
5.2.8	Scratch wound assay as a tool to measure wound closure rates in epithelial cells.	151
5.2.9	The ability of cells to close a wound in vitro was impaired by plectin siRNA in SW480 carcinoma cells but not in	

MDA-MB-231 carcinoma cells.	151
5.2.10 The ability of cells to close a wound in vitro is significantly impaired by vimentin depletion in both colon and breast carcinoma cells.	152
5.2.11 Vimentin depletion is confirmed by immunofluorescence on scratch wound monolayers.	158
5.2.12 Plectin depletion alters actin dynamics at the wound edge.	158
5.2.13 Plectin depletion alters the appearance of actin in confluent monolayers in SW480 cells.	159
5.3 Discussion.	163
6 CHAPTER 6: Characterisation of subcellular localisation and function of plectin-1k.	169
6.1 Introduction.	170
6.2 Results.	171
6.2.1 Partial co-localisation of plectin-1k and total plectin in SW480 cells.	171
6.2.2 Plectin-1k localisation in MDA-MB-231 cells.	171
6.2.3 Plectin-1k is localised in podosome-type adhesions.	171
6.2.4 Co-localisation of plec-1k with podosome components.	172
6.2.5 Plectin-1k is localised to podosomes in macrophages.	173
6.2.6 Plec-1k -Actin Binding Domain -GFP construct is targeted to Podosomes.	180
6.2.7 Inhibition of ROCK activity impairs podosome assembly and alters plectin-1k localisation.	180
6.2.8 The N-terminal Actin-binding domain of plectin-1k rescues podosome formation in plectin knockdown cells.	181
6.2.9 Plectin-1k is shown localising to actin adhesive structures in cells attaching to collagen.	181
6.3 Discussion.	190
7 CHAPTER 7: Conclusions and future outlook.	193

APPENDIX I: Plectin alternative first exon cDNA sequences.	199
APPENDIX II: Plectin alternative first exon protein sequences.	204
APPENDIX III: Additional plectin-GFP images.	208
REFERENCES	211

LIST OF TABLES	page no.
Table 1.1 The Intermediate Filament Family.	8
Table 1.2 Distribution of Keratins in Epithelia.	9
Table 2.1 Primers for rtPCR	33
Table 2.2 PCR primers used for amplifying exons 1-k for cloning into eGFP.	41
Table 2.3 Primers used for sequencing of eGFP inserts.	41
Table 2.4 Cell lines used in this study.	43
Table 2.5 siRNA sequences used in this study.	47
Table 2.6 Peptide sequences for generation of polyclonal antibodies.	48
Table 2.7 SDS-Page gel preparation.	50
Table 2.8 List of antibodies used in this study.	53
Table 3.1 Sequence alignment of human plectin alternatives N-terminal exons to mouse and rat.	63
Table 3.2 Take of points and amplification efficiency of real time PCR.	76
Table 4.1 Summary of subcellular localisations of alternative plectin N-terminal eGFP constructs.	111
Table 5.1 Summary of cell migration assays.	168

LIST OF FIGURES	page no.
Figure 1.1 Organisation of simple and stratified epithelia.	15
Figure 1.2 Composition of a Type I hemidesmosome at the basal cell surface of epithelia cells.	19
Figure 1.3 The plakin family members their domain structures.	22
Figure 2.1 RNA extraction.	35
Figure 2.2 Optimum conditions for TAQ PCR.	37
Figure 2.3 Overview of the siRNA pathway.	46
Figure 3.1 Map of plectin alternative N-terminal first exons.	65
Figure 3.2 Alternative N-terminal first coding exons in the human plectin gene.	67
Figure 3.3 Expression of plectin N-terminal isoforms in colon carcinoma cells	69
Figure 3.4 Melt curves of real time PCR of plectin N-terminal isoforms	72
Figure 3.5 Sybr green fluorescence in real time PCR of plectin-1k isoform	74
Figure 3.6 Realtime PCR of plectin N-terminal isoform mRNA expression in cancer cell lines.	78
Figure 3.7 Real-time PCR analysis of the expression of the plectin N-terminal splice variants in human tissues.	81
Figure 4.1 Collagen gel invasion of carcinoma cells.	89
Figure 4.2 Expression of cytoskeletal and related proteins in carcinoma cell lines.	92
Figure 4.3 Co-expression of keratin 8 & 18 and plectin protein in carcinoma cells.	95
Figure 4.4 Subcellular expression of vimentin in SW480 and MDA-MB-231 cells.	97
Figure 4.5 Desmoplakin and plectin immunofluorescence in colon carcinoma cells.	99
Figure 4.6 F-actin sub-cellular localisation in carcinoma cells.	102
Figure 4.7 Expression of eGFP-tagged plectin N-terminal isoforms.	105

Figure 4.8 Subcellular localisation of alternative plectin N-terminal domains.	108
Figure 4.9 Co-localisation of plec-1b-GFP and mitochondria.	110
Figure 4.10 Detection of plectin-1, 1b, 1f and 1k with polyclonal antibodies.	114
Figure 4.11 Conformation of the specificity of polyclonal antibodies using siRNA.	116
Figure 4.12 Expression of plectin isoforms in carcinoma cell lines.	118
Figure 4.13 Subcellular localisation of plectin alternative first exon isoforms using polyclonal antibodies.	119
Figure 5.1 Modes of cancer cell migration.	133
Figure 5.2 Summary of epithelial to mesenchymal transition.	134
Figure 5.3 Comparison of plectin siRNA nucleotides.	137
Figure 5.4 Comparison of vimentin siRNA nucleotides.	138
Figure 5.5 Cell survival after siRNA transfections.	140
Figure 5.6 Impaired migration of plectin siRNA transfected SW480 cells.	143
Figure 5.7 Invasion of plectin siRNA transfected MDA-MB-231 cells.	144
Figure 5.8 Impaired migration of vimentin siRNA transfected SW480 cells.	145
Figure 5.9 Impaired migration of vimentin siRNA transfected MDA-MB-231 cells.	146
Figure 5.10 Adhesion of carcinoma cells to fibrillar collagen.	149
Figure 5.11 Wound migration properties of plectin depleted SW480 cells.	153
Figure 5.12 Open wound migration distance of plectin depleted MDA-MB-231.	155
Figure 5.13 Open wound migration distance of vimentin depleted SW480 cells.	156
Figure 5.14 Open wound migration distance of vimentin depleted MDA-MB-231 cells.	157
Figure 5.15 Immunofluorescence analysis of vimentin ablation in carcinoma cell monolayers	160
Figure 5.16 Plectin knock-down inhibits actin dynamics at the wound edge of SW480 cells.	161
Figure 5.17 Plectin knock-down alters monolayer characteristics SW480 cells.	162

Figure 6.1 Plectin-1k localised to podosome-like foci.	174
Figure 6.2 Co-localisation of plectin-1k with integrin subunits.	175
Figure 6.3 Subcellular localisation of plectin-1k in SW480 cells.	177
Figure 6.4 Plectin-1k co-localised with N-Wasp in macrophages.	179
Figure 6.5 Exon 1k targets plectin actin-binding domain to podosomes and Dorsal actin ruffles.	183
Figure 6.6 Rho-ROCK signalling regulates podosome assembly and plectin-1k localisation.	185
Figure 6.7 Plectin-1k N-terminus rescues podosome assembly in plectin knockdown cells.	186
Figure 6.8 Plectin-1k localisation in cells attaching to collagen.	188
Appendix III. Sub-cellular localisation of alternative plectin N-terminal domains.	208

CHAPTER 1
INTRODUCTION

1.1. Prologue.

Plectin, a member of the plakin family of cytolinkers proteins has an integral role in skin and tissue integrity by linking the three cytoskeletal networks with each other. Furthermore, plectin tethers intermediate filaments to cell junctions and can act as a regulator of cytoskeletal dynamics. There is now emerging evidence of plectin as a scaffolding protein for a variety of signalling events. This thesis proposes that this multifunctional protein has a role to play in the migration, invasion and attachment of cells in which alterations in these processes can lead to the progression of cancer. The importance of vimentin, an intermediate filament protein that can interact with plectin will also be discussed. This chapter will address each of these elements above giving an overview of the many roles of plectin and the proteins in which it interacts with. Each of the results chapters to follow will then give a focused insight on the subject they address.

1.2. The cytoskeleton, an overview.

In order to understand the various roles plectin plays as a cytoskeletal linker protein, a brief introduction of the cytoskeleton is needed. The mammalian cytoskeleton is made up from three networks that all have specific roles in the cell, but increasing evidence has highlighted the importance of the interaction of these networks with each other in many functions including invasion, migration and metastasis. The cytoskeleton is responsible for such diverse functions as the transport and positioning of organelles in the cytoplasm, the segregation of the chromosomes during mitosis, cell shape, cell movement, and the structural integrity of the membranes (Fuchs and Karakesisoglou, 2001). The three networks, microfilaments, microtubules and intermediate filaments will be discussed below.

1.2.1. Microfilaments (actin cytoskeleton).

Actin was discovered along with myosin by Kuhne in 1861, but was not isolated until 1939-1942 by Straub, Bonga and Szent-Gyorgyi (Szent-Gyorgyi, 2004). The actin cytoskeleton is paramount to cell motility, contractility, cell remodelling, cytokinesis, cell polarity, intracellular transport and phagocytosis (reviewed in Schmidt et al., 1998). The network consists of polymers of actin (F-actin,) along with a large number of actin binding proteins and associated proteins (Stossel, 1993; Winsor et al., 1997). Actin filaments are characterised by polarised ends, where the plus (barbed) end grows

faster than the minus (pointed) end. Actin can exist as monomers (G-actin) and each monomer can bind ATP and hydrolyse to ADP when incorporated into actin filaments. The actin monomer, which is highly conserved in evolution (Kron et al., 1992), contains 375 amino acids and is a 43 kDa globular monomer with 2 domains. The actin cytoskeleton is highly dynamic and filaments can form spontaneously via non-covalent interactions, but ATP-bound actin polymerises faster than ADP-bound actin (Engel et al., 1977). The organisation of actin filaments is regulated by a large number of signalling proteins including Rho, Rac, and Cdc42, which are activated by extracellular signals (discussed in Chapter 5). Two alternate forms of actin machinery have been shown to exist at the leading edge of motile cells, lamellipodia that exerts a persistent protrusion over a surface and filopodia that performs sensory and exploratory functions (Mejilano et al., 2004). At the leading edge of the lamellipodia actin filaments are driven by activation of the actin-related protein (Arp) 2/3 complex and are organised in a branched network with the barbed ends orientated towards the membrane. The Arp2/3 complex, which stimulates new filament formation by a process termed dendritic nucleation (Mullins et al., 1998), consists of the actin-related proteins Arp2 and Arp3 along with five other proteins designated p41-, p34-, P21- and p16-arc (Machesky and Gould., 1999). In contrast at the base of the lamellipodia actin filaments are long and un-branched (Small et al., 1995, Svitkina et al., 1999). Filopodia consist of elongated parallel filaments and have been implicated in many cell processes such as epithelial sheet closure in development, wound healing and cell invasion and metastasis of cancer cells (Jacinto et al., 2001, Roth, 2003). Plectin has been implicated to play a part in regulation of actin dynamics (Andra et al., 1998) and the crystal structure of the murine actin-binding domain of plectin has been elucidated, as discussed in section 1.3 (Sevcik et al., 2004).

1.2.2. Microtubules.

Microtubules (MT), which were discovered using electron microscopy by Fawcett and Porter, 1954 and Manton and Clarke, 1952, are large polar filaments composed of heterodimers of α and β tubulin that form a cylindrical ring of 13 linear protofilaments, 25nm in diameter (reviewed by Brinkley, 1997). Microtubules assemble from the microtubule organising centre (Tucker, 1992) and undergo rapid remodelling with frequent shortening and growth transitions (Waterman-Storer and Salmon, 1997). This dynamic instability is important in cell motility and also in the

positioning of organelles and movement of vesicles in the cell via dynein and kinesin motors (Mitchison et al., 1984; Gross et al., 2007). Microtubules are also essential in spindle formation aligning chromosomes and segregation during mitosis (Sawin et al., 1993; McIntosh et al., 2002). The microtubule cytoskeleton associates with a variety of proteins; Microtubule Associated Proteins (MAPs), which have increasingly been found to interact with the other networks, especially actin supporting the idea that the networks of the cytoskeleton have interlinking roles (Mandelkow et al., 1995). Also, historically microtubules have been shown to form closely associated parallel arrays with intermediate filaments throughout the cytoplasm in fibroblasts (Goldman, 1971). Plakins, especially BPAG1 have the ability to interact with microtubules (Yang et al., 1999) and plectin has been shown by immunogold labelling to connect intermediate filaments to microtubules (Svitkina et al., 1996).

1.2.3. Intermediate Filaments.

Intermediate filaments appeared more recently in evolution compared to the other cytoskeleton networks (Rash et al., 1970). The intermediate filament family are encoded by one of the largest families of genes in the human genome (Hesse et al., 2001). The family can be classified into six major types (Hermann et al., 2000), and specific expression of intermediate filament proteins can be found in different cell types (Table 1.1). Most intermediate filaments contain a α helical rod domain that is usually 310 residues long and is flanked with a non-helical carboxy and amino terminal that vary depending on the intermediate filament type (Coulombe et al., 2001). The rod domain contains heptad repeats (subdomains 1A, 1B, 2A, 2B) that facilitates dimerisation between the rod domains (Coulombe et al., 2001). Intermediate filaments can spontaneously assemble into non-polar tetramer filaments in the absence of ATP and GTP (Strelkov et al., 2003), with a diameter of 8-9nm, which assemble in a rope like array to form the final filament. Free tetramers are rare in the cell, but a cell can regulate the assembly by phosphorylation of serine specific residues in the amino head domain (Izawa et al., 2006). Intermediate filaments are thought to play a role in flexible structural support and are essential to the integrity and organisation of skin and muscle (Fuchs et al., 1998). Recent research has shown intermediate filaments to be more motile than once thought. The motile and dynamic properties of each type vary due to their various N and C- terminal sequences and binding capacity to other parts of the cytoskeleton (see review Helfand et al., 2004). For the considerations of this work

the keratins and vimentin intermediate filaments will be discussed due to their important interactions with plectin in epithelial cells (Pytela and Wiche, 1980; Foisner et al., 1988; Nikolic et al., 1996). However, plectin can also interact with desmin, glial fibrillary acidic protein (GFAP) neurofilaments and lamin-B (Schroder et al., 1999, Tian et al., 2006; Errante et al., 1994 and Foisner et al., 1991).

1.2.3.1. Keratins.

Keratins are encoded by a large multi-gene family whose 54 members are divided into two major groups, type I and type II on the basis of gene structure and sequence homology (Gu et al., 2007). They form the main constituents of epithelial cells, which contain a variety of keratins that are expressed in a tissue, and differentiation specific pattern as illustrated in Table 1.2 (Coulombe et al., 2002; Schweizer et al., 2006). The diversity of keratin expression is most pronounced in skin, where each layer has a distinct keratin expression (Gu et al., 2007). Keratins display a network that extends from the nucleus to the plasma membrane, where they form attachment at desmosomal and hemidesmosomal complexes. They also act as protein scaffolds with structural and regulatory functions in a cell-type specific manner (Magin et al., 2007). The importance of keratins in skin integrity has been underlined by the large number of epidermal diseases found to have keratin mutations (reviewed in Uitto et al., 2007). The role of keratins in wound healing and migration has been widely studied recently with contrasting results, possibly due to cell specific settings. Specifically, no defects were found in embryonic wound healing at mid-gestation of keratin 8 deficient mice. However, siRNA ablation of keratin 8 and keratin depletion in hepatocytes from keratin null mice was recently shown to inhibit collective sheet migration and spreading (Long et al., 2006; Galarneau et al., 2007). Contrasting this, wound healing was accelerated in absence of keratin 8 in vimentin positive cells (Long et al., 2006). Keratins 8 and 18 are mainly expressed in simple epithelia as found in gastrointestinal tract, liver and exocrine pancreas, from which many carcinomas arise (Nishizawa et al., 2004). Overexpression of keratins 8 and 18 along with vimentin in melanoma is associated with metastasis (Hendrix et al., 1992), and transfection of keratins 8 and 18 in mouse fibroblasts and melanoma cells increases the invasiveness of the cells (Chu et al., 1993; Chu et al., 1996). Keratins have been used in the finger printing of carcinomas due to their specific expression in different epithelia, as when epithelium undergoes malignant transformation its keratin profile usually remains constant. For

example, over 90% of colorectal adenocarcinomas express keratin 20 regardless of the degree of differentiation or origin of biopsy from either the primary tumour or metastatic spread. Also, 90% of colorectal adenocarcinomas don't express keratin 7; this expression of K7-/K20+ is very specific to colon adenocarcinoma and is rarely seen in other carcinomas (Chu et al., 2002).

1.2.3.2. Vimentin.

Klaus Weber coined the name vimentin for the intermediate filaments that were found to decorate mouse 3T3 cells and mesenchymal derived cells but not epithelial derived cells (Franke et al., 1978). Later, it was confirmed that vimentin is the major intermediate filament expressed in cells of mesenchymal origin such as fibroblasts and endothelial cells (Frank et al., 1987). In the same year, it was demonstrated that in quail embryo fibroblasts, vimentin intermediate filaments were connected to focal contacts (Bershadsky et al., 1987). Vimentin is classed as a type III intermediate filament protein (Table 1.1) and can homo-polymerise to form 10 nm filaments in vitro and vivo. Few of the other group B proteins can do this and require involvement of other group B proteins, often vimentin (Coulombe et al., 2001). Vimentin shows a high degree of sequence homology between species suggesting important evolutionary conserved physiological roles (Herrmann et al., 1989; Schaffield et al., 2001). Vimentin is often used as a developmental marker of cells and tissues. The protein is first expressed in the mouse around E8.5 in the cells of the parietal endoderm and also in the cells that delaminate through the primitive streak to become the primary mesoderm (Franke et al., 1982; Lane et al., 1983). Later, expression is seen in early pre-differentiated cell types during development of the neural and myogenic tissue before being replaced by glial fibrillary acidic protein GFAP and desmin (Cochard et al., 1984; Furst et al., 1989). In adults, endothelial cells, fibroblasts and cells of the haemopoetic lineages, only express vimentin. Vimentin has been used widely in the study of intermediate filament dynamics. Using microinjection it was shown that filament polymerisation was regulated by subunit exchange (Vikstrom et al., 1989). Yoon et al., 1998 demonstrated that filaments were constantly changing their configurations in vivo, extending and shortening. Furthermore, Time-lapse imaging of GFP-vimentin in epithelial cells showed short vimentin “squiggles” at the cell periphery, which then move towards the cell centre. Keratin filaments also display these squiggles; however the dynamic properties of keratin short fibrils are

dramatically different to those of vimentin in the same region. This suggests that there are different factors regulating the dynamic properties of different types of intermediate filaments within the same cytoplasmic regions (Yoon et al., 2001). GFP tagged vimentin has also been shown to move along microtubules, further supporting the interaction of the different cytoskeletal networks (Martys et al., 1999). Phosphorylation of the protein has been shown to have a central role in regulating the dynamics of vimentin assembly into polymers (Inagaki et al., 1997) and also regulating the connections between intermediate filaments and associated proteins (Ku et al., 1998). At first inspection, vimentin knockout mice do not show serious differences from wild type mice in vivo (Eckes et al., 1998). However, impaired wound healing in embryonic and adult mice was visible (Eckes et al., 2000). Furthermore, fibroblasts were shown to have impaired mechanical stability and migration and the reorganisation of collagen fibrils and contraction of collagen lattices was severely impaired (Eckes et al., 1998).

Table 1.1. The Intermediate Filament Family.

Name	Assembly group	Class	Distribution	Predicted protein size kDa
Keratin (acidic)	A	I	Epithelia	40-60
Keratin (basic)	A	II	Epithelia	56-68
Vimentin	B	III	Heterogenous	55
Desmin	B	III	Muscle	53
GFAP	B	III	Glial cells	50-52
Peripherin	B	III	PNS neurons	54
Syncoillin	B	III/IV	Muscle	54
NF-L	B	IV	CNS neurons	62
NF-M	B	IV	CNS neurons	102
NF-H	B	IV	CNS neurons	110
α -Internexin	V	IV	CNS neurons (embryonic)	66
Nestin	B	VI	Heterogenous progenitor cells & mesenchymal cells	240
Synemin	B	VI	Muscle	182
Desmuslin	B	VI	Muscle	140
Lamin A/C	C	V	Nuclear	76/62
Lamin β 1	C	V	Nuclear	6
Lamin β 2	C	V	Nuclear	78
Phakinin/CP49	D	?	Lens	46
Filensin	D	?	Lens	83

(Adapted from Coulombe et al., 2001)

Table 1.2 Distribution of Keratins in Epithelia.

Epithelial type	Type I	Type II	Distribution
Simple epithelia	8	18	Most secretory and parenchymatous cells
	7	19	Ductile epithelia (bile and pancreatic duct, renal collecting ducts) and gastrointestinal epithelia*
		20	Gastrointestinal epithelia, merkel cells of the skin and taste buds of the oral mucosa.
Stratified Squamous epithelia	5	14	Basal cells of squamous and glandular epithelia, myoepithelia, mesothelium
		15	Squamous epithelia
	8	18,19	Non-cornifying stratified squamous epithelia
Suprabasal cells	1	10,11	Epidermis
		9	Epidermis of palms and feet
	2e		High layers of epidermis
	2p		Gingival, hard palate
	3	12	Corneal epithelium
	4	13	Non-keratinising stratified squamous epithelia of internal organs.
	6	16,17	Hyperproliferative squamous epithelia.**

*K7 is absent ** In addition K17 is most typically expressed in basal cells of complex epithelia. (Table from Chu and Weiss, 2002)

Table 1.1. The intermediate filament family.

Intermediate filaments are classified into six major types (I-VI) dependant on genomic structure and nucleotide sequence homology. There are four assembly groups (A-D) at the protein level dependent on the polymerisation properties. Type I (acidic) and Type II (basic) encode the epithelial expressed keratins that co-polymerise to form assembly group A. Type III, type IV and type VI assemble into protein group B. Type II and Type VI are mostly expressed in muscle except for GFAP, peripherin and nestin. Type IV genes encode the neurofilament triplicate proteins which are obligate heteropolymers. Type V genes encodes for the nuclear lamins, which form a meshwork at the nuclear membrane, lamin proteins cannot co-polymerise with other intermediate filament proteins and assemble into group C. Finally, phakinin/CP49 and filensin are found in the eye lens and do not conform to any of the above groups and form the group D proteins (Reviewed in Coulombe et al., 2001 and Oshima, 2007).

Table 1.2. Distributions of keratins in epithelia.

Type I (acidic) and Type II (basic) keratins, co-polymerise in an exclusive obligatory fashion that have epithelial tissue specific distributions as shown in the table. Simple epithelia generally express the simple epithelial keratins 7, 18, 19, and 20, while complex epithelia express complex epithelial keratins 5/6, 10, 14, and 15.

1.3. Plectin, a member of the plakin family of proteins.

In studies of tissues that experience mechanical stress, such as epithelia (Leung et al., 2002), the cytoskeleton field is becoming increasingly aware, that the three networks do not just act alone but are interlinked and together play dynamic roles in cellular architecture and integrity. Plectin, along with related proteins termed the plakins, is a definite candidate for mediating these interactions (Figure 1.3). The plakins were first discovered as linkers tethering the intermediate filament network to cell-cell and cell matrix junctions. Uitto et al., 1996 defined the name plakins to encompass a family of protein cytolinkers that were all discovered in very different ways. Further studies have opened up this family's role, where plakins can link to actin to microtubules in the nervous system (Sun et al., 2001) and also act as a scaffold for various signalling events (Sonnenberg et al., 2007).

Plectin was originally isolated as a major intermediate filament-associated protein in cultured cells (Pytela and Wiche, 1980). Additionally, a novel hemidesmosome protein named HD1 was isolated in bovine corneal epithelial cells, that was later identified as plectin (Owaribe et al., 1991; Hieda et al., 1992; Okumura et al., 1999). The protein has an estimated molecular weight of >500kDa and is found expressed widely in a variety of cell types, including skin and striated muscle. Plectin plays a role in cell and tissue integrity by cross-linking between the three cytoskeletal networks and stabilising cell-matrix and cell-cell contacts (Wiche et al., 1998; Leung et al 2002). It has been shown that plectin stabilises intermediate filaments to desmoplakin in desmosomes, links intermediate filaments directly with β 4-Integrin (Niessen et al., 1997) and is present in focal adhesion contacts and distributes with actin stress fibres (Seifert et al., 1992 and Sanchez-Aparicio et al., 1997). The intermediate filament-binding site has been mapped to 50 amino acids at the end of the fifth repeat (Nikolic et al., 1996). Interaction of plectin with microtubules has been suggested at the C-termini domain of plectin (Herrmann et al., 1987; Svitkina et al., 1996). Furthermore, plectin has been established as a novel component of focal contact complexes and it has been suggested that plectin plays a role as mediator between intermediate filaments and actin filaments (Seifert et al., 1992). Extensive analysis of the murine plectin gene shows plectin contains over 40 exons on Chromosome 15 and exhibits an unusual 5' transcript complexity of plectin isoforms (Fuchs et al., 1999 and Rezniczek et al., 2003). In the human gene, plectin spans over 32 exons on 32kb located in the telomeric region (q24)

on chromosome 8. When this project commenced; only 4 isoforms in human and rat had been identified (Andra et al., 2003; Elliott et al., 1997). However, a subsequent bioinformatics search identified eight putative first exons also in the human plectin gene (this study and Zhang et al., 2004).

1.3.1. Role of plectin in cytoskeletal dynamics.

Plectin has been shown as a regulator of actin filament dynamics beyond its role in scaffolding and mechanical stability (Andra et al., 1997). The plectin actin binding domain (ABD) is highly conserved consisting of a pair of calponin homology (CH) subdomains that had been shown to interact with polymeric actin and also bundle actin filaments via dimerisation of the ABD (Fontao, 2001). The crystal structure of the plectin actin-binding domain shows the domain to adopt a closed conformation with intramolecular contacts between the two CH domains (Garcia-Alvarez et al., 2003). Plectin has been shown to regulate actin filament dynamics via phosphatidylinositol, 4,5-bisphosphate (PIP2) (Andra et al., 1998). Stress fibres and focal contacts were more prominent in plectin depleted fibroblasts, which display reduced migration and increased adhesion (Andra et al., 1998). Contrasting this, plectin deficient keratinocytes display a reduced rigidity of the keratin network and fewer hemidesmosomal attachments (Osmanagic-Myers et al., 2006). A recent study has also identified plectin as an early substrate for caspase 8 suggesting that plectin may also play a role in the reorganisation of the actin cytoskeleton during death receptor mediated apoptosis (Stegh et al., 2000).

1.3.2. Role of plectin as a scaffolding protein for signal transduction.

An emerging role of plectin in controlling signalling pathways is being explored (Sonnenberg et al., 2007). Mapping of the protein-protein interactions of plectin has identified binding sites for several signalling molecules, such as AMP-activated protein kinase (Gregor et al., 2006), RACK-1 receptor for activated protein C kinase 1, (Osmanagic-Myers and Wiche, 2004) and Fer kinase (Lunter and Wiche, 2002). Furthermore, the kinase activity of Erk1/2, c-Src and PKC δ has been shown to be upregulated in plectin deficient keratinocytes (Osamanagic-Myers et al., 2006). These data suggest that plectin, along with the role as a cytoskeletal linker protein, may be able to effect carcinoma cell migration and invasion via regulation of signalling processes.

1.3.3. Role of plectin in tissue and cell integrity.

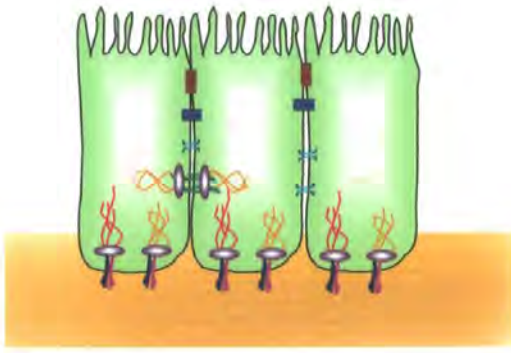
In stratified epithelia, plectin has been localised at the basal cell surface membranes, in peripheral areas of epithelial cells and all cell layers (Wiche et al., 1983). Plectin, present in hemidesmosomes, serves as anchorage sites for intermediate filaments to mediate firm adhesion of the basal cells to the basement membrane (Borradori et al., 1999, Jones et al., 1998). In other studies, plectin has been also been localised to Z-discs and dense plaques of striated muscle (Wiche et al., 1983; Wiche et al., 1984; Zernig et al., 1985). At these sites plectin is found associated to desmin peripheral myofibrils, to costameres at the sarcolemma and can link adjacent myofibrils to one another (Sonnenberg et al., 2007). Furthermore, the predominant expression of plectin at pia/glia and endothelia/glia interfaces in the human brain indicates that plectin may also have an integral role in the structural organization of the blood-brain barrier and the leptomeninges (Lie et al., 1998).

More evidence for an essential role of plectin in the integrity of muscle and skin architecture is demonstrated in plectin null mice. Plectin deficient mice exhibit severe skin blistering with a reduction of hemidesmosomes and abnormalities in skeletal heart and muscle (Andra et al., 1997). The role is further supported by human patients with plectin abnormalities, who exhibit epidermolysis bullosa simplex (a skin blistering disease) with muscular dystrophy (EBS-MD) (McLean et al., 1996). The majority of patients have nonsense mutations in the plectin rod-domain, which lead to premature termination of translation (Pfender et al., 2003). Hemidesmosomes can still be found in EBS-MD patients but the anchorage to intermediate filaments is impaired and blisters form at the basal layer (McLean et al., 1996 Smith et al., 1996). Plectin mutations at the end of the coiled-coiled rod domain have also been found in patients with EB simplex of the Ogna type, a rare autosomal disorder. Finally, recent studies have shown plectin mutations in patients with EB pyloric atresia (EB-PA) an autosomal recessive syndrome that is often lethal and causes neonatal blistering with gastric abnormalities (reviewed in Pfender et al., 2003).

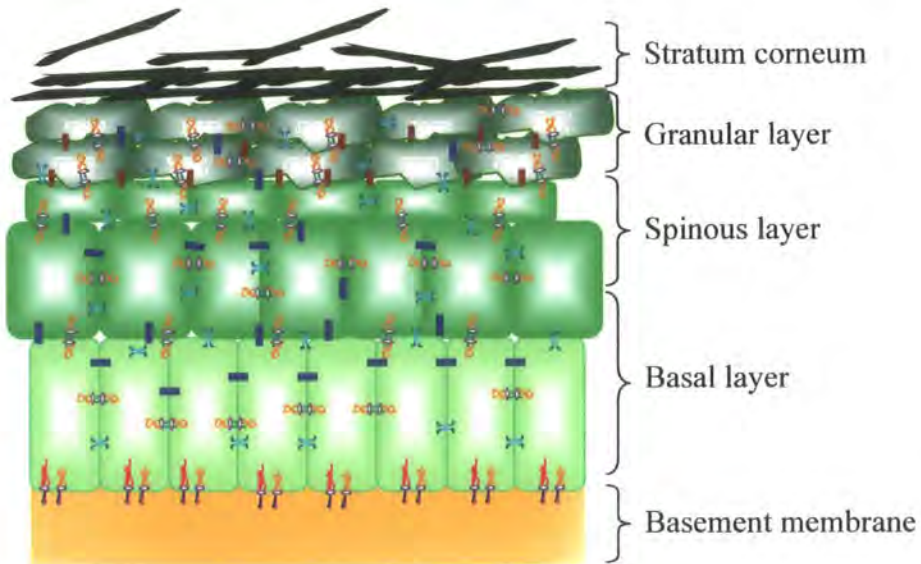
1.4. Epithelial cell junctions.

Epithelia, found in multi-cellular organisms, are cohesive sheets of ordered epithelial cells (Perez-Moreno et al., 2003). The main types of epithelia are the stratified epithelia of the skin layers and simple epithelia, such as those that line the gut (Figure 1.1). The epithelial sheets are anchored to the basement membrane via cell-matrix attachments mediated via the integrin family of transmembrane receptors discussed in Chapter 5. The basement membrane separates the epidermis from the underlying dermis (Marinkovich et al., 1992). Hemidesmosomes (Figure 1.2) are the main mediators of adhesion to the basement membrane along with focal contacts. Also important for epithelial integrity are the cell-cell adhesions mediated via the calcium dependent cadherin family of proteins. There are several types of cell-cell junctions found in epithelial layers; tight junctions, adherens junctions, gap junctions and desmosomes. Adhesions can be connected through intermediate filaments at desmosomes or to microfilaments at adherens junctions and tight junctions (Reviewed by Braga, 2002). Tight junctions prevent mixing between apical and baso-lateral membranes and render the epithelial sheet impermeable to ions and solutes. Adherens junctions in epithelial cells depend on the homophilic, calcium dependent binding of the extracellular domain of transmembrane cadherins (Takeichi et al., 1991). Gap junctions allow the exchange of ions, second messengers and small metabolites between adjacent cells formed from connexin and pannexin protein families (reviewed in Mese et al., 2007). Cell junctions are also considered highly dynamic complexes that integrate signalling processes with the cytoskeletal network. Cell-cell adhesion also involves the activation of a number of signalling pathways; Small Rho GTPases, Rho, Rac and Cdc42 are members of the rho GTPase subfamily and have been implicated in adherens junctions. Other related family members of the super family Ras have also been identified as regulators of cell-cell adhesion (Reviewed by Braga, 2002).

A



B









-  Tight junctions
-  Hemidesmosomes
-  Focal contacts
-  Desmosomes
-  Adherence junction (e.g. E- Cadherin)
-  Gap junctions

Figure 1.1. Organisation of simple and stratified epithelia.

(A) Simple epithelia of one layer thick attaches to the basement membrane (yellow) by focal contacts and type II hemidesmosomes. Cell-cell attachments are mediated by adherence junctions (blue) and desmosomes. Tight junctions (red) ensure a water tight impermeable barrier and cell polarity and gap junctions allow the exchange of ions and metabolites between adjacent cells. (B) The stratified squamous epithelia is made up from four layers; stratum corneum, granular layer, spinous layer and the basal layer. Hemidesmosomes and focal contacts link the basal layer to the basement membrane. Adherens junctions and desmosomes form cell-cell junctions. Tight junctions are present in the late spinous layers and throughout the granular layers. Connexins present in gap junctions display distinct and overlapping expression patterns in the skin. Adapted from Perez-Moreno et al., 2003.

1.4.1. Role of plectin in the formation of hemidesmosomes.

Hemidesmosomes were first identified as electron dense plaques at the plasma membrane connecting basement membrane to intermediate filaments (originally termed "bobbins" by Weiss and Ferris, 1954). These junctional complexes were found to bind epithelial cells to the basement membrane in stratified and complex epithelia forming a tight link between the intracellular intermediate filament system and the extracellular matrix (Geerts et al., 1999). The hemidesmosomes' main role is providing mechanical stability to the layers of the skin as demonstrated with plectin deficient mice that exhibit severe skin blistering with a reduction of hemidesmosomes and abnormalities in skeletal heart and muscle (Andra et al., 1997). Hemidesmosomes are dynamic structures that constantly renew during migration and invasion and division. The plakin proteins BPAG-1 (also named BP230) and plectin form the hemidesmosomal plaque proteins that bind intermediate filaments to the hemidesmosomes (Stanley et al., 1981; Gache et al., 1996; Borradori, 1996; Green et al., 1999 and Burgeson, 1997). Along with the hemidesmosomal plaque proteins, the transmembrane proteins, integrin $\alpha6\beta4$ and BPAG2 (also named BP180) mediate anchorage of the basal epithelial cells to the basement membrane (Jones et al., 1991; Sonnenberg et al., 1991; Li et al., 1992). The integrin $\alpha6\beta4$ binds particularly to laminin-5 (a non-collagenous glycoprotein) that is prominently expressed in the basement membrane of epithelial layers (Niessen et al., 1994). The binding of integrin $\alpha6\beta4$ to plectin is suggested as the first step in hemidesmosomal assembly, as BPAG1 or BPAG2 are not recruited efficiently when $\beta4$ cannot bind plectin (Koster et al., 2004). The tetraspannin protein CD151 is also an early constitute of the hemidesmosomal adhesion structures as it was found strongly associated with laminin-binding integrin $\alpha3\beta1$ in keratinocytes forming pre-hemidesmosomal clusters (Sterk et al., 2000). These integrin clusters are speculated to be the nucleation site for assembly of $\alpha6\beta4$ hemidesmosomes. Furthermore CD151 binds to $\alpha6$ and on maturation of the complex and then $\alpha3\beta1$ is recruited to focal contacts after hemidesmosomes are assembled. However, this interaction is not thought to be essential, as CD151 null mice still form hemidesmosomes (Wright et al., 2004).

The $\beta4$ subunit of $\alpha6\beta4$ integrin is unique to the other integrins in that it possesses a 1000 amino acid cytoplasmic domain compared to 59 amino acids in the other β subunits (Suzuki et al., 1990). The cytoplasmic domain contains two pairs of

fibronectin type III repeats separated by a connecting segment (Borradori et al., 1999). The first and second fibronectin repeats form a complex with plectin (Spinardi et al., 1993). The Ser-1325 in the connecting segment of β 4 was found to be essential for the recruitment of plectin into hemidesmosomes in vivo. Furthermore, CH1 domain of plectin associates with the groove between the two FNIII domains of β 4, inducing a conformational change in the cytoplasmic domain in which the additional plectin-binding site at the C-terminus becomes exposed (Geerts et al., 1999). Two proline residues in the C terminal of β 4 have been found to be critical for the recruitment of plectin to hemidesmosomes (Koster et al., 2004). An additional interaction of the plakin domain with the C-terminal tail of β 4 has been suggested to stabilise the association and to enable the recruitment of plectin to hemidesmosomes (Koster et al., 2004; Reznicek et al., 1998). Furthermore, β 4 can adopt a folded conformation regulating the binding of plectin (Schaapveld et al., 1998). A recent study has shown that plectin β 4 tail interactions may play an important role in connecting α 6 β 4 with vimentin (Homan et al., 2002). Interestingly, it has been found that F-actin was not present in hemidesmosomes and that plectin associates in a mutually exclusive manner with either actin or β 4 as a result of competitive binding (Geerts et al., 1999). The third fibronectin repeat is essential for binding BPAG2 (Borradori et al., 1997; Aho et al., 1998; Schaapveld et al., 1998) BPAG2 is a type II transmembrane collagen expressed exclusively in epithelial tissues and is suggested as a possible laminin-5 (laminin-332) receptor (Nishizawa et al., 1993; Aho et al., 1999). Finally the third and fourth fibronectin repeats are important in the binding of BPAG1 (Hopkinson and Jones, 2000; Koster et al., 2003).

1.4.2. Type II hemidesmosomes.

Hemidesmosomes, found in intestinal epithelial cells do not contain all the proteins found in the classical hemidesmosome (Uematsu et al., 1994 and Orion-Rousseau, 1996). Type II hemidesmosomes, that form an adhesion complex lacking BPAG1 (BP230) and BPAG2 (BP180) but containing plectin and α 6 β 4 integrin, have been described in some cell types and tissues (Jones et al., 1991; Uematsu et al., 1994; Orion-Rousseau et al., 1996; Fontao, 1997). Fontao and colleagues characterised a type II hemidesmosomes in HT29 cells with electron microscopy showing electron dense regions connected to cytokeratin filaments that could be modulated by the extracellular matrix. They found that assembly requires actin filaments but not microtubules

(Fontao et al., 1999). Further evidence was found in intestinal epithelial cells, where plectin and $\alpha6\beta4$ associated in type II hemidesmosomes which co-distributes with laminin-5 in intestinal mucosa (Simon-Assmann et al., 1994). These studies demonstrate that plectin is essential for the integrity of the hemidesmosomal complex in both hemidesmosome types.

1.4.3. Desmosomes.

Plectin was found to co-immunoprecipitate with plakin family member desmoplakin (described below) and was suggested to be involved in the anchorage of intermediate filaments to desmosomes and to the sub-membranous skeleton in MDCK cells (Eger et al., 1997). Desmosomes are important in tissue architecture as they connect intermediate filaments to neighbouring cells providing a continuous network throughout tissues (Green et al., 1990). They function as cell-cell attachment sites in epithelia, cardiac muscle, and dendritic cells of the lymphoid system. Transmembrane members of the cadherins family, desmogleins and desmocollins, form an adhesive interface (Garrod et al., 2002) and the cytoplasmic tails interact with armadillo proteins, plakoglobin and plakophilins (Schmidt et al., 2005). The plaque proteins then interact with desmoplakin which links to the intermediate filaments at the desmosomal plaque (reviewed in Godsel et al., 2005). Cell-cell contacts are thought to trigger the initiation of desmosomes with recruitment of desmoplakin that is regulated by intermediate filament and actin interactions (Godsel et al., 2005). This is supported with the recent finding that keratin 8 is involved in the modulation of desmoplakin deposition at desmosomes through a phosphoserine dependent process (Loranger et al., 2006). Although desmoplakin is the main candidate for mediating the intermediate filament linkage in stratified cells it is suggested that plectin could possible participate in the linkage in simple epithelial cells (Eger et al., 1997).

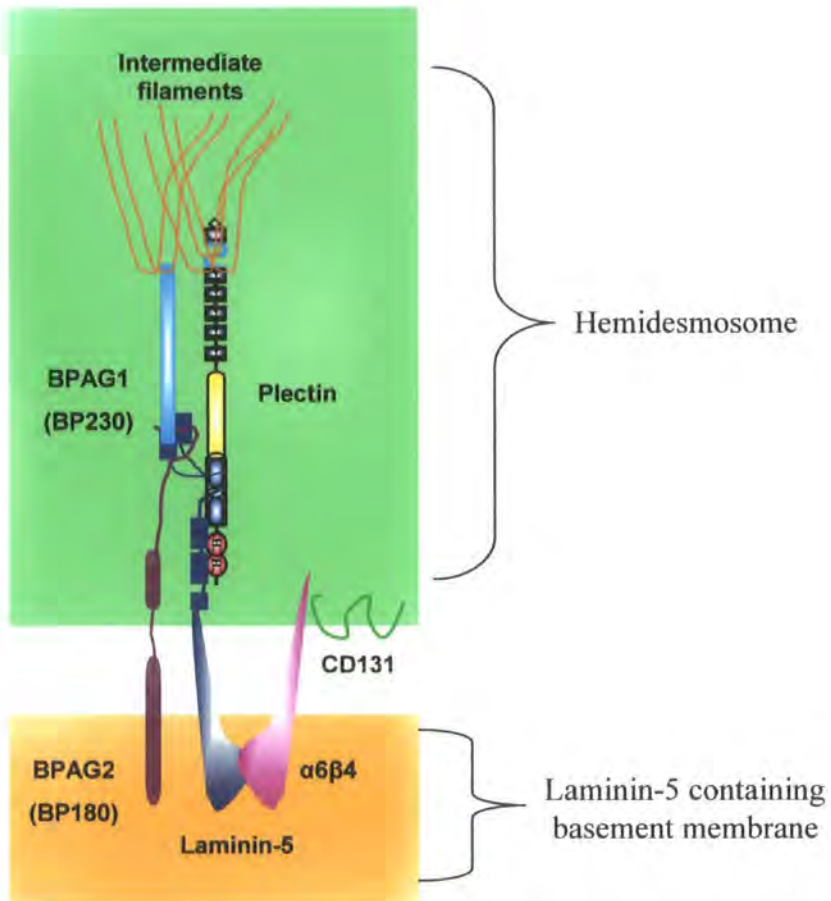


Figure 1.2. Composition of a Type 1 hemidesmosome at the basal cell surface of epithelia cells.

Schematic drawing of a hemidesmosome showing plectin as a key component linking intermediate filaments to the $\beta 4$ integrin. The plakin domain and the actin binding domain of plectin are important in the $\beta 4$ interaction (see Figure 1.3 for plectin domains) and the C-terminal plakin repeat domains mediate linkage to the intermediate filament cytoskeleton. BPAG1 (BP230), BPAG2 (BP180) and tetraspanning CD131 all have key roles in the recruitment, assembly or stability of the hemidesmosome along with plectin. Adapted from Litjens et al., 2006.

1.5. The plakins family.

Plectin, BPAG1 and desmoplakin, that were discussed previously in their role of stabilising epithelial junctions, are all members of the mammalian plakins family along with microtubule crosslinking factor (MACF7), envoplakin, periplakin and epiplakin (Figure 1.3). The mammalian plakins are evolutionary related to the spectraplakins, cytoskeletal giants with characteristics of both plakins and spectrins (Roper et al., 2003, reviewed by Määttä et al., 2004). The spectraplakins were named by Roper and colleagues to encompass proteins that have similarities to plakins and spectrin family proteins such as *shortstop* gene in *Drosophila* and the *dystonin*/BPAG1 and MACF1 genes in mammals and consist of spectrin repeats that are 38 residues long, connected by loops and organised in tandem arrays (Jefferson et al., 2004). Sonnenberg and Liem now propose that the plakins are all members of a spectrin superfamily that have evolved to encode additional domains and functions (Sonnenberg et al., 2007). The plakins are highly conserved through evolution, with plectin-like proteins also being found in the green alga, *Chlamydomonas eugametos*, expressed at perinuclear region and localized near the cell wall, probably attaching to the cytoplasmic membrane (Hendrychova et al., 2002). The invertebrate plakins in *Drosophila melanogaster* and *Caenorhabditis elegans* were discovered from genetic screens for mutations that produced defects in cell adhesion and morphogenesis (reviewed in Jefferson et al., 2004). The *Drosophila* gene, *Shortstop* and its protein product shot (sometimes referred to as Kakapo) was identified in a screen for phenotypes that were similar to that produced in the position specific integrins (Walsh et al., 1998; Prout et al., 1997). The *Caenorhabditis* plakins, VAB-10A/B were identified in genetic screens for embryonic morphological defects, where mutants failed to elongate, the epithelium is detached from the cuticle, and the muscles produced irregular body morphologies (Bosher et al., 2003).

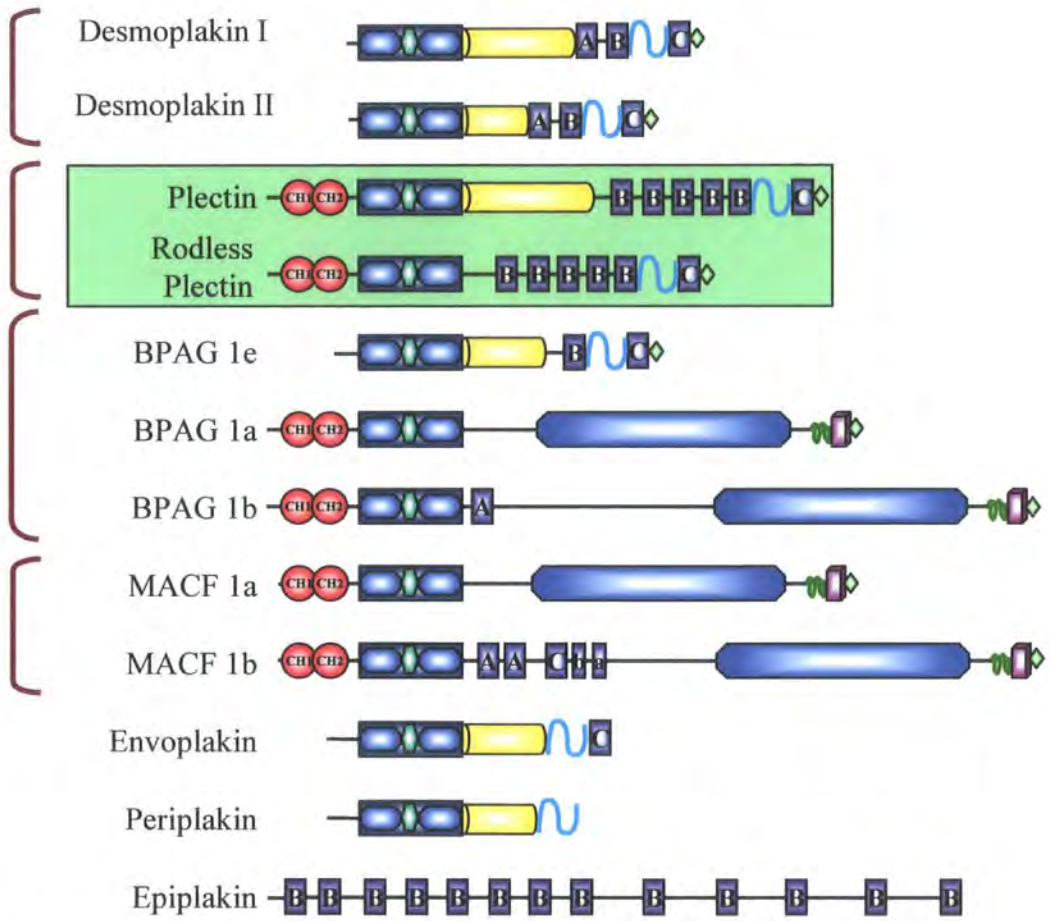
1.5.1. The plakins family protein domains.

The plakins proteins are composed of distinct subdomains as shown in Figure 1.1.

The calponin-homology (CH) domain consists of four α -helices connected by loops and a few short helices. Each domain contains ~10 residues and is present in both signalling and cytoskeletal proteins (Stradal et al., 1998; Gimona et al., 2002). Calponin-homology domains are sub grouped into CH1 and CH2 due to functional diversity. CH1 and CH2 together form an actin-binding domain in some plakins. The

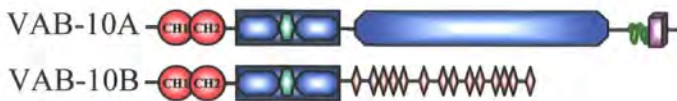
CH1 domain binds actin alone but with a lower affinity than CH1-CH2 and CH2 has an even lower affinity to actin than CH1 (Winder et al., 1995). The actin-binding domains of plakins are also able to homodimerise and heterodimerise with each other, contributing to the crosslinking of the actin network (Fontao et al., 2001; Young et al., 2003). Most of the plakin family harbour a characteristic 'plakin box' domain consisting of alpha-helical spectrin repeats and a putative SH3 domain that plays a role in protein-protein interactions (Leung et al., 2002; Rezniczek et al., 2004; Jefferson et al., 2007). The presence of spectrin repeats in the plakin domain of plectin and BPAG1 were recently confirmed by crystallography (Jefferson et al., 2007; Sonnenberg et al., 2007). The epithelial plakins contain a coiled-coiled rod domain, which is made up from heptad repeats that mediate homodimerisation, or in some plakins heterodimerisation. The plakin repeat domains (PRD) are found at the carboxyl termini of the epithelial plakins and some spectraplakins. A plakin repeat domain is composed of 4.5 copies of a 38 amino acid sequence repeat that adopts a globular structure with a unique fold (Choi et al., 2002) and is important in binding plakins to intermediate filaments where two or more repeats gives a higher binding affinity. It is also suggested that the linker sequence found in some of the plakins may be required to allow two domains to simultaneously bind to intermediate filaments (Sonnenberg et al., 2007). Finally, there is the gas2 related (GAR) domain that is thought to be important in binding to microtubules. The GAR domain is located at the carboxyl terminus of some BPAG1 and MACF isoforms. Plakins without this domain that bind to microtubules have been suggested to bind through glycine serine arginine GSR repeats (Sun et al., 2001, Yang et al., 1999), which are also present in the GAR domains. Preceding the GAR domain are two putative calmodulin-like EF hands. Dystrophin and utrophin, members of the spectrin superfamily, connect the actin-based cortical cytoskeleton to the laminin in the extracellular matrix through the glycoprotein complex (Culligan et al., 1998; Winder et al., 1995). The EF-hand domains in proteins of the dystrophin family mediate binding to the transmembrane proteins in the complex, linking the cortical actin cytoskeleton to the extracellular matrix through the dystrophin (Chung et al., 1999).

A Mammalian Plakins.

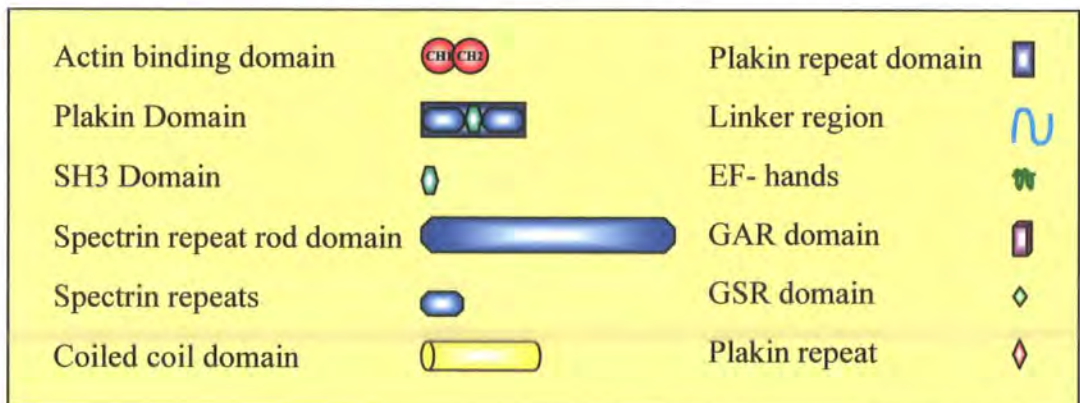
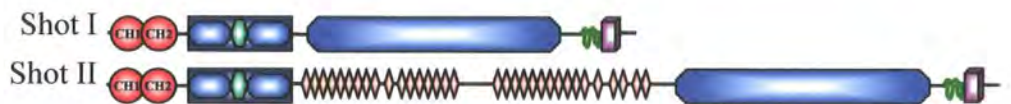


B

Caenorhabditis plakins



Drosophila melanogaster plakins



Adapted from Sonnenberg and Liem, 2007

Figure 1.3. The plakins family members their domain structures.

Schematic diagram of the mammalian (A) and invertebrate (B) plakins family members. All the plakins, except epiplakin, contain a plakins domain that consists of 4-8 spectrin repeats with a central SH3 domain. The actin-binding domain is present in plectin, BPAG1a/b and MACF1a/b consisting of two calponin homology domains (CH); upstream of this these proteins also contain alternative N-termini. The coiled-coiled domain is only present in the epithelial plakins. The spectrin repeat rods are present in BPAG, MACF and the invertebrate plakins VAB-10A and ShottII. The C-termini of these proteins contain a microtubule-binding domain, consisting of EF hands and a gas2 related (GAR) domain with a glycine-serine-arginine (GSR) domain. There are three plakins repeat domain (PRD) subunits; A, B and C, with incomplete A and B PRD labelled a and b. The invertebrate plakins contain plakins repeats that are not organised into PRD domains. There is a linker region found in the epithelial plakins at the C-termini. The C-termini of desmoplakin, plectin, BPAG1e and envoplakin/periplakin can interact with intermediate filaments. The key for domains is in the yellow box and plectin is highlighted in green.

1.5.2. Bullous pemphigoid antigen 1 (BPAG1).

BPAG1e, a 230 kDa epithelial form of BPAG1 was discovered along with BPAG2 as a target for autoantibodies against hemidesmosomes in patients with the skin blistering disease Bullous Pemphigoid (Stanley, et al., 1988). The C-terminus of BPAG1 was found to bind to intermediate filaments *in vivo* (Leung et al., 1999). BPAG1 has a large number of different isoforms; a b, e (epithelial) and n (neuronal) that result from different transcriptional start sites as well as alternative splicing. The isoforms exhibit tissue specific expression, primarily BPAG1a is expressed throughout the nervous system primarily at the pituitary primordia and the dorsal root ganglia (Leung et al., 2001) and BPAG1-b is expressed more in heart, skeletal muscles and bone cartilage of developing mouse embryos (Leung et al 2001). BPAG1-e (structurally similar to desmoplakin Figure 1.3), is expressed in basal epithelial cells localising near hemidesmosomes as discussed in Section 1.5.3 (Leung et al., 2002). BPAG1-n expressed in neurons was found to bind actin and neurofilaments (Yang et al., 1999). Surprisingly, knock out mice show primary defects in the nervous system rather than epithelia (Guo et al., 1995), which can be explained by longer splice variants of BPAG1 found in neurones bind to neuronal filaments, actin and microtubules (Guo et al., 1995; Yang et al., 1999). There have been very few reports of BPAG1 defects in disease, however recently BPAG1 had been identified as a component of the disc 1 interactome, which is disrupted in schizophrenia (Camargo et al., 2007). BPAG1 that has several N-terminal splice variants was also found localised to actin filaments and to the nucleus via regulation by the N-terminus similar to the plectin N-terminal isoforms (Young et al., 2003) that will be discussed in Chapter 3.

1.5.3. Desmoplakin.

Desmoplakin was originally identified in bovine tongue desmosomes (Franke et al., 1981) and found linked to desmosomes isolated from epithelia (Skerrow et al., 1974). Desmoplakin protein was shown to migrate in SDS-page as two bands at 322 kDa (DPI) and 295kDa (DPII) (Kowalczyk, 1994), due to alternative splicing within the rod domain. The heptad-repeat-containing rod domain mediates parallel dimers so desmoplakin II may be present as a monomer (O'Keefe et al., 1989). Desmoplakin I is present in all tissues (Angst et al., 1990) and desmoplakin II is found in lower levels in non-stratified tissues and absent in the heart (Green et al., 1996). As discussed in Section 1.4.3, desmoplakin is targeted to desmosomes through interaction of its N-

terminal plakin domain with plakoglobin and plakophilins which then interact with the desmosomal cadherins. Desmoplakin null mice were found not to survive past E 6.5 due to impairment of egg cylinder formation, and it was suggested that desmoplakin plays a central role not only in establishing intermediate filament cytoskeletal architecture, but also in assembly and or stabilisation of the desmosome (Gallicano et al., 1998). Intriguingly, a subsequent study revealed that ablation of desmoplakin in the developing mouse epidermis had little effect on the structure of desmosomes, however the association to intermediate filaments is disrupted and this leads to skin fragility (Vasioukhin et al., 2001). Thus, cell type and developmental factors may influence the formation and stability of desmosomes (Sonnenberg et al., 2007). Mutations in the human desmoplakin gene cause the skin disorder, striate palmoplantar keratoderma. The C-terminally truncated desmoplakin causes dilated cardiomyopathy, woolly hair and keratoderma in humans (Norgett et al., 2000). The C-terminus of desmoplakin may play a role in regulation of interactions between intermediate filaments and desmosomes as binding is much weaker when S2849 residue of desmoplakin is phosphorylated (Stappenbeck et al., 1994). Desmoplakin has a proposed role in the formation of complex adherens junctions that are found only in endothelial cells that constitute capillaries and lymph vessels (Schmelz et al., 1994; Kowalezyk et al., 1998). This role is demonstrated in desmoplakin siRNA treated endothelial cells that failed to form microvascular tubes in Matrigel (Zhou et al., 2004). Furthermore, mouse embryos depleted of desmoplakin have leaky and poorly formed capillaries (Gallicano et al., 2001). Desmoplakin also been recently implicated in the rearrangement of microtubules during epidermal differentiation, where loss of desmoplakin prevents accumulation of cortical microtubules (Lechler et al., 2007).

1.5.4. Periplakin and envoplakin.

Periplakin (195 kDa) was identified along with envoplakin (210kDa) as constituents of the cornified envelope and desmosomes (Simon and Green, 1984; Ruhrberg et al., 1996; Ruhrberg et al., 1997). The cornified envelope is a layer of transglutaminase-crosslinked protein that is below the plasma membrane in terminally differentiating keratinocytes (Kalinin et al., 2001). Ceramide lipids are found covalently attached to these proteins (Marekov et al., 1998) and they have been proposed to act as an interdesmosomal scaffold on which the cornified envelope is assembled (Ruhrberg et al., 1997). Envoplakin and periplakin have smaller C-terminal domains than the other

plakins with periplakin lacking the plakin repeat domain, (Figure 1.3). They also have the potential to heterodimerise with each other (Ruhrberg et al., 1997). Periplakin has a wide tissue expression, but expression is more limited in tissues with envoplakin. Envoplakin is expressed in the suprabasal layers of stratified squamous epithelia, but not in simple epithelia or non-epithelial tissues. Contrasting this, periplakin is expressed in a variety of epithelial and non-epithelial tissues such as brain. Periplakin contains an L subdomain that contains a sequence homology to the linker region between the plakin repeat domains B and C in desmoplakin; this domain is thought to be important in binding to intermediate filaments (Kazerounian et al., 2002; Fontao et al., 2003). Supporting original findings by Di Colandrea and colleagues, who found periplakin co-localised with intermediate filaments (Di Colandrea et al., 2000). The tail of periplakin has been found to specifically bind to keratin 8 and vimentin (Kazerounian et al., 2002). Furthermore periplakin was found to participate in the re-organisation of keratins in migrating cells (Long et al., 2006). Recently, in an attempt to further characterise the function of periplakin, a number of novel interactions have been identified. Periphilin interacts with periplakin at the cell-cell junctions and cell periphery and is thought to contribute to epidermal integrity and barrier formation (Kazerounian et al., 2003). A novel protein kazrin was found to interact with the N-terminus of periplakin at desmosomes and the interdesmosomal plasma membrane (Groot et al., 2004). Additionally periplakin interacts with protein kinase B and can relocate the kinase between cellular compartments (Van der Heuvel et al., 2002) and also with mannose 6-phosphate receptor, which target newly synthesised lysosomal enzymes through their ability to cycle between the trans-golgi network (Le Borgne et al., 1998). The diversity of periplakin protein interactions was further demonstrated where periplakin was shown to have a direct interaction with FcγRI (CD64) an IgG receptor that is upregulated during inflammation with a role in controlling receptor endocytosis and ligand binding capacity (Beekman et al., 2004). Interestingly, periplakin null mice do not display any abnormal skin defects. Similarly, envoplakin knockout mice show only a subtle barrier defect; in both cases the cornified envelope was normal (Aho et al., 2004; Määttä et al., 2001). Of most significance to this study was the discovery of plectin as a periplakin interacting protein, where ablation of plectin compromised the subcellular distribution of periplakin in HaCaT keratinocytes. In addition, ablation of periplakin, plectin or both proteins simultaneously impaired migration of MCF7 epithelial sheets (Boczonadi et al., 2007). These findings suggest

that different plakin family members can form complexes, thus influence cytoskeletal organisation and cell migration.

1.5.5. Microtubule-actin Crosslinking factor 1 (MACF 1).

MACF1 belongs to the plakin family due to similarities of the N-terminal actin binding to that found in plectin and BPAG1 (Bernier et al 1996; Byers et al., 1995). It was first identified as a partial human cDNA and named by Kunkel and colleagues as ACF7 (it also has been named α -trabeculin and macrophin by Sun et al., 1999 and Okuda et al., 1999 respectively). It is suggested that MACF1 is a hybrid derived from ancestral gene for plectin and dystrophin due to the intron positions within the spectrin repeats (Gong et al., 2001). There are two major isoforms, MACF1a similar to BPAG1a and MACF1b similar to BPAG1b (Lin et al., 2005). There has been no disease yet linked to mutations in MACF1, this may be due to the severity of the phenotype found in knockout mice (Chen et al., 2006). The MACF1 knock out mice die at the gastrulation stage and show a head without a trunk phenotype similar to the *Wnt3*^{-/-} mice (Chen et al., 2006) and in fibroblasts, the microtubules no longer grow along polarised actin-rich cortical structures but exhibited skewed cytoplasmic trajectories and altered dynamic stability (Kodoma et al., 2003). Thus, MACF1 has been proposed to connect and coordinate actin and MT cytoskeleton. However, studies on the drosophila homologue showing that it plays a significant role in neuronal and muscular development indicate that MACF1 may be involved in this also (Lin et al., 2005; Kodoma et al., 2003). MACF1 protein has a proposed role in signalling; in MACF1 deficient fibroblasts a constitutively active Rho effector mDia (which is normally necessary for the orientation microtubules) could not promote microtubule stability (Kodoma et al., 2003). Furthermore, MACF1 was found to effect the cortical localisation of CLASP2, a microtubule tip binding protein (Drabek et al., 2006). The role of MACF1 in signalling suggests that it could be involved in cancer (Sonnenberg et al., 2007). Supporting this MACF1 was found mutated in 12% of breast and colon cancers in a recent screen (Sjoblom et al., 2006).

1.5.6. Epiplakin.

Epiplakin, first identified as an autoantigen in a patient suffering from skin blistering disease, is unusual in that it contains exclusively plakin repeat domains encoded by a single exon (Fujiwara et al., 1992). The human form contains 13 repeats and the mouse 16 repeats with the final C-terminal six repeats being almost identical (Fujiwara et al., 2001; Spazierer et al., 2003). Epiplakin is thought to have a role in bundling keratin intermediate filaments (Fujiwara et al., 1996; Spazierer et al., 2003) where it is widely expressed in a variety of tissues with higher amounts in the liver, salivary gland, and the digestive tract and in the entire epidermis of the skin (Fujiwara et al., 2001). No mutations in epiplakin have been reported to cause disease as yet and epiplakin knockout mice have no obvious defects. However, epiplakin deficient keratinocytes display increased migration further supporting the role that plakins may play in cancer progression (Goto et al., 2006; Spazierer et al., 2006).

1.6. Plakins and cancer.

The variety of impairments in plakin deficient mice and in patients with plakin mutations underline the versatility and many roles that plakin proteins play in tissue and cell integrity, linking at cell-cell and cell-matrix junctions. The plakin proteins were found able to link to all three cytoskeletal networks with roles in the regulation and dynamics of each network. Furthermore, plakins have been shown to interact with a variety of signalling molecules and may impact various signalling processes by affecting localisation or the stability of the cytoskeleton (Sonnenberg et al., 2007). Commencing this study, there was a lack of knowledge of the role that plakin proteins may play in the progression of cancer, prompting our laboratory to investigate this field.

The ability of cancerous cells to metastasise makes it difficult to treat cancer surgically or with localised radiation and this contributes to the main cause of death from cancer. For a cancer cell to spread to another site in the body it must undergo changes in these properties. From a benign tumour in the epithelium a cell undergoes loss of adhesion to its neighbours. Eat its way through other tissues, break though the basal lamina, invade the blood capillaries, adhere to the capillary wall at its destination invade into the tissue and proliferate into the new tissue such as the lung or liver (refer to Chapter 5). An understanding of the cellular and molecular mechanisms of migration and

invasion should lead to the effective design of treatments able to block the process of metastasis. Plectin along with the other epithelial plakins have been traditionally studied in their role in skin and tissue integrity due to the role these proteins play at cell junctions and the severity of blistering diseases found caused by plectin mutations (Wiche, 1998). However, recent studies have implicated other plakin family members in the progression of cancer, where there was down regulation of desmoplakin in poorly differentiated breast tumours (Davies et al., 1999) and mutations of MACF1 in breast cancer tumours (Sjoblom et al., 2006). Interacting partners of plectin have been previously shown to have roles in cancer progression with integrin $\alpha 6\beta 4$ upregulated in many cancers (see review by Mercurio et al., 2001 and Chapter 5). Furthermore, laminin-5 has been found to inhibit human keratinocyte migration (O'Toole et al., 1997) and laminin signalling has been implemented as a key event in tumour invasion and metastasis (reviewed by Givant-Horwitz et al., 2004).

This thesis aims to address if plectin plays a role in cancer cell invasion and if so are the plectin isoforms (described in Chapter 3) variably expressed in cancer. Thus, can plectin isoform expression lead to a change in the aggressiveness of cancer?

CHAPTER 2
MATERIALS AND METHODS

2.1. Chemicals and reagents.

All chemicals and reagents used in this study are of analytical grade and unless otherwise stated are supplied from Sigma Aldrich UK or BDH laboratory supplies.

2.2. Bioinformatic methods used for unravelling the human N-terminal alternative first exons of plectin.

Based on available information on mouse and rat plectin sequences, (Fuchs et al., 1999; Elliott et al., 1997, respectively) the National Center for Biotechnology Information (NCBI) blast tool was used to search the mouse and rat sequences against the human genome. Blast, is the abbreviation for **B**asic **L**ocal **A**lignment **S**earch **T**ool that finds regions of local similarity between sequences and returns significant matches of DNA sequences. All assemblies of the genome were selected in the NCBI database to date (19th November 2003, Build 34 version 2). Ensemble, a joint project between EMBL - EBI and the Sanger Institute, which produces and maintains automatic annotation on selected eukaryotic genome, was also used to search the human genome against the mouse plectin isoforms to check that the returned results were similar to the NCBI sites. The whole genomic plectin DNA sequence was then compared against the expressed sequence tag (EST) database (NCBI) using Blast algorithm (NCBI) to further identify potential alternative first exons in the human plectin gene. The EST database contains partial single pass cDNA sequences (refer to Boguski et al., 1993 and Boguski, 1995 for in depth explanation) and has been used to identify previously unknown gene products for mapping. ExPASy translate tool (**Expert Protein Analysis System** proteomics server for the Swiss institute of bioinformatics) was used to conveniently convert the DNA sequence to protein sequences for each plectin isoform for further use in comparing species.

2.3. Molecular Biology.

The following section will contain the methods used for RNA extraction, rt- PCR, real time PCR and cloning of the plectin isoforms into GFP constructs.

2.3.1. Primer design of plectin alternative first exon N-terminal isoforms.

Oligonucleotide primers were designed for human plectin splice variants corresponding to mouse exons 1 – 1g and subsequently for the novel exon 1k. The

primers were identified for each of the exons using, where possible, the following considerations; between 18-20bp long, a melting temperature of 54-58°C, GC nucleotide content between 40-60%, primers ending on a G, C (to act as a clamp), no primer dimers, no repeats, no stretches of polynucleotide G or C. The size of the template determines the temperature and annealing time, if the primer is too long then inefficient priming annealing can take place and if the sequence is too short then the primer may not be specific enough for to prime for the correct sequence of interest. The annealing temperature for the forward and reverse primer should be kept similar, as miss-priming can occur of the higher temperature primer at the lower temperature. The GC nucleotide content of the primer is important as the GC pairs form 3 hydrogen bonds, raising the annealing temperature of the PCR, leading to inefficient amplification, However, including G or C nucleotides at the 3' end of the primer provides a GC clamp that ensures the correct binding due to the strong hydrogen bonds. It must be noted that poly G and C stretches can promote non-specific binding and stretches of poly A and poly T can open up the template resulting in lower amplification efficiency, so should be avoided. The primers should also be designed so that they are not self-complimentary and therefore, cannot form hairpin loops (primer dimers), which would reduce the amplification efficiency significantly. (Sourced from Qiagen critical factors for successful PCR and real time PCR). The reverse primer was chosen located in exon 4 of the plectin gene due to the presence of possible alternative 2nd and 3rd exons that were also short and GC rich. The program Fast PCR (Kalendar et al., 2007) was used as a quick reference to temperatures and presence of primer dimers, the actual position was manual selected. Sequences of oligomers, which were sent to MWG biotech for synthesis, are shown in Table 2.1.

Primer Name	Sequence
Reverse exon 4	attctgcagcttgtggaacg
Plec 1	tgcttgctaccaccag
Plec 1a	tacctggctgtgctcag
Plec 1b	agcctgttccctccctg
Plec 1c	cggtcattcgcatcgag
Plec 1d	ccgatgaagatcgtgcc
Plec 1e	atccagaacgagatcagc
Plec 1f	ttcatccaggcctacgagg
Plec 1g	tacctctaccagcagctg
Plec 1k	catggacaggtacagcatgg

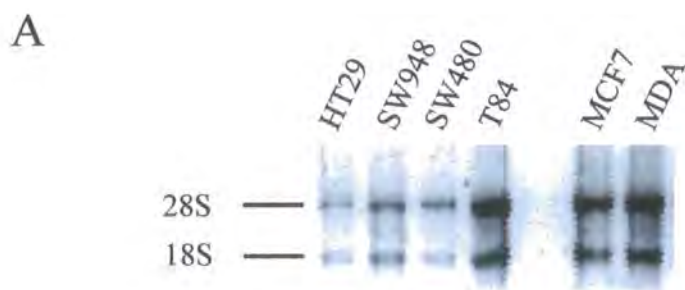
Table 2.1. Primers used in rtPCR.

The above table lists the exons and the corresponding primers used for reverse transcriptase-PCR and real-time PCR of the alternative first exons of plectin.

2.3.2. RNA extraction and purification of carcinoma cells.

In order to create an RNase free environment and, therefore, avoid RNA degradation the following procedures were used. Sterile techniques were used with disposable RNase free plastics and tips, Diethyl pyrocarbonate treated (DEPC) water was used (Ambion) and isopropanol, ethanol and chloroform were of molecular grade and reserved for RNA work (Sigma). Finally, surfaces were wiped clean with RNase away spray (Fisher Scientific) to reduce the chance of contaminating RNA from the environment. RNA was isolated from 70% confluent T75 flask (Greiner Bio-one UK) cultures of HT29, SW948 SW480, T84, MCF7 and MDA-MB-231 using Tri Reagent (Sigma-Aldrich, UK) following the protocol provided by the manufacturer. Briefly, a T75 flask of cells was lysed using 2 ml of Tri reagent and the lysate homogenised through a 1ml tip, and allowed to stand for 5 minutes to allow for dissociation of

nucleotide complexes. Next, 0.4 ml chloroform (molecular grade, Sigma Aldrich UK) was added to the lysate that was transferred to 2 x 1.5 ml eppendorfs, shaken vigorously, before standing for 15 min at room temperature. This was then centrifuged at 12000 x g for 15 min 4°C to separate the phases containing, a red organic protein phase, DNA containing inter phase and a colourless RNA containing upper phase. The RNA phase was removed, with care to prevent DNA contamination, and 1 ml isopropanol (molecular grade, Sigma Aldrich UK) was added and left to stand for 10 minutes at room temperature before centrifuging again at 12000 G 10 min 4°C, to precipitate the RNA, visualised as a white pellet. The isopropanol was removed and the pellet washed with 75% ethanol (molecular grade, Sigma Aldrich UK) to remove residual salts, then the sample was re-centrifuged 7500 x g 5 min to remove the ethanol. The pellet was air dried briefly and then resuspended in DEPC water at 50°C, pipetting gently to dissolve the pellet. Residual DNA was removed by treatment with DNase 1 enzyme (Qiagen UK) 6.25 Units with up to 87.5 µl RNA made up to 100 µl in suppliers buffer, incubated 10 minutes at room temperature. RNA clean up kit spin columns (Qiagen UK) removed any contaminating DNA by only binding strands of nucleotides in the silicon membrane that are longer than 100 bp, hence removing the enzyme fragmented DNA and retaining the longer RNA strands in high salt buffers. DEPC water (Ambion UK), 2 x 30 µl, was used to elute the RNA. The RNA was quantified using Beckman DU-600 spectrophotometer absorbance A_{260} read at 260 nm, 280 nm and 320nm. The RNA was deemed good quality if the ratio $A_{260}/280$ ratio was between 1.7 and 2.0. The quantity of RNA was measured, as one A_{260} unit equals 50 µg of double-stranded RNA/ml. The quality of RNA was further verified by running on a denaturing agarose gel. Samples were combined with formaldehyde loading dye (1 x MOPS/ 13.5% formaldehyde/ 50% formamide) and heated to 65°C for five minutes to denature the RNA structures. The samples were loaded onto a 2% agarose gel, containing MOPS buffer (0.2 M MOPS; pH 7.0 0.08 M NaAc 0.01 M EDTA 0.01% bromophenol blue) with 12.3 M formaldehyde and samples were run at 100 V, 1/3 down the gel (3-4cm). The gel was stained with ethidium bromide solution (2 mg/ml in MOPS running buffer). Expected bands of the small 18S (~2 kb) and large 28S (~5 kb) ribosomal RNA were visualised and photographed with UV light using the FujiFilm Intelligent Dark Box II. RNA was stored in DEPC treated water at -20°C or -80°C for long-term storage. The RNA is of good quality if the 28S subunit is twice as intense as the 18S subunit band. Figure 2.1 shows a representative RNA extraction used in this study and the spectrophotometer reading output showing the quality of the RNA used for realtime PCR.



B

Sample	260 nm	280 nm	Background 320 nm	260/28 0	Concentration $\mu\text{g/ml}$
HT29	0.3819	0.2091	0.0190	1.9092	0.5530
SW948	0.5386	0.2831	0.0053	1.9200	0.8112
SW480	0.4864	0.2512	0.0030	1.9476	0.7316
T84	1.2989	0.7088	0.0159	1.8516	1.9759
MCF7	1.1313	0.6131	0.0148	1.8660	1.7149
MDA	1.6472	0.8940	0.0168	1.8587	2.5076

Figure 2.1. RNA extraction.

(A) Extracted total RNA from carcinoma cell lines were run on a 2% agarose electrophoresis gel. Two bands of the more intense 28S subunit and the lower 18S RNA subunit was visible on the gel. (B) For quantification and indication of quality, samples were analysed using a spectrophotometer at 260, 280 and 320 nm. Note the ratio of 260/280 is above 1.8 for each of the extractions.

2.3.3. cDNA synthesis from RNA extractions.

SuperScript III RNase H reverse transcriptase (Invitrogen UK) was used to engineer cDNA from RNA extracts. For routine PCR and cloning Oligo-dT primers (Invitrogen, UK) were used. For real time PCR applications Random hexamers (Invitrogen) were used to prime the cDNA synthesis. Oligo-dT primers reverse transcribe from the poly-A tail at the 3' end whereas random hexamers enable reverse transcription from the entire RNA population producing short cDNA this ensures that a representative population of the alternative plectin n-terminal isoforms is made. 100 ng of total RNA of was used in a 20 µl cDNA reaction with 1µl of 10 mM dNTP mix, 1µl random primers 100 ng, 1 µl 0.1 M DTT, 1 µl RNase OUT, 4 µl 5 x strand buffer (250 mM Tris-HCl pH 8.3, 375 mM KCl, 15 mM MgCL₂) and 1 µl superscript III reverse transcriptase (Invitrogen UK). The reaction was heated to 50°C for one hour and then the enzyme was inactivated by heating at 70°C for 15 min. The samples were incubated for 20 min at 37°C with 1µl per reaction of E. coli RNase H (Invitrogen UK) to remove RNA complementary to the cDNA.

2.3.4. PCR of alternative exons in human cell lines.

PCR was carried out using Taq polymerase (Promega UK) on Hybaid MBS 2.0 cycler using cDNA synthesised from the cell lines. The efficiency of the PCR was optimised by altering the concentration of MgCl₂ and the annealing temperature for each isoform (Figure 2.2). MgCl₂ is an essential co-factor for Taq polymerase, but the efficiency of the PCR is dependent on the concentration, as excess free magnesium can reduce the enzymes fidelity and increase non-specific amplification (Eckert and Kunkel, 1990; Williams, 1989; Ellsworth *et al.* 1993). PCR samples were separated on a 2% agarose DNA gel in TAE buffer (40 mM Tris-acetate, 1mM EDTA pH 8.0).

A

Cycled
for 25 x {
94°C 2min
94°C 30 sec
Annealing temperature 30 sec
72°C 1 minute
72°C 5 minute
4°C Hold

B

Target	MgCl ₂ mM*	Annealing temperature °C
Plec-1	12.083	58.8
Plec-1a	2.083	58.8
Plec-1b	2.083	58.8
Plec-1c	1.25	58.8
Plec-1d	2.5	58.8
Plec-1e	2.083	54.0
Plec-1f	2.083	54.0
Plec-1g	1.25	58.8
Plec1k	N/A**	N/A**
Periplakin	2.5	55.4
Actin	2.5	65

Figure 2.2 Optimum conditions for TAQ PCR

(A) The cycle program that gave the optimum result for PCR product. (B) Table of optimum conditions for each forward primer listed in table 2.1 when paired with reverse primer exon 4. * Stock 25mM end concentration in 30µl reaction listed. ** was optimised using SYBR green kit.

2.3.5. Cloning of alternative first exon plectin isoforms into pGEM-T easy and sequencing of constructs.

PCR samples were run on a 1-2% agarose DNA gel. Correct DNA bands were cut from the gel and purified using Qiagen gel Extraction Kit. Purified PCR samples were then ligated into pGEM-T Easy Vector System 1 (Promega UK). This vector system is useful for easy cloning of PCR products for sequence identification or future sub-cloning. This vector has 3'-T overhangs, which allow direct insertion of the PCR products generated by Taq DNA Polymerase (generates single base 3' adenine overhangs). Purified bands were ligated into the plasmid using T4 DNA ligase (Invitrogen UK) 5 Units (1 μ l) with up to 10 μ l of DNA, at 1:3 ratio of plasmid: insert, in 2 μ l of 10 X ligation buffer (400 mM Tris-HCl, 100 mM MgCl₂, 100 mM DTT 5 mM ATP. pH 7.8), made to 20 μ l in DEPC water (Ambion UK). The reaction was incubated at room temperature for one hour and enzyme deactivated by heating to 65°C for 10 minutes. Ligated plasmids were then transformed into competent DH5 α bacteria cells (refer to Section 2.3.1) by incubating together on ice for fifteen minutes then heatshocking ninety seconds at 42°C. Samples were incubated in Luria-Bertani Media (LB) for 1 hour 37°C with shaking 250 rpm to induce antibiotic resistance. Bacteria was spread onto LB agar and grown overnight at 37°C with ampicillin (1/1000 50 mg/ml) and X-gal selection. When insert is introduced into the vector it interrupts the Lac Z gene cassette responsible for synthesising beta-galactosidase, which digests the X-gal and produces a blue by-product. White colonies containing the vector were picked out and grown in an overnight culture of 5 ml LB. Plasmids were then prepared from the bacteria using Gene Elute Plasmid Mini Prep Kit (Sigma Aldrich UK), digested with EcoRI restriction enzyme (Invitrogen UK) and run on 2% agarose gel to verify presence of an insert and the expected size. Samples were sent to be sequenced using M-13 reverse primer (Durham University Sequencing unit UK). The sequences were then compared to plectin genome using a BLAST search (NCBI) to confirm the correct sequence.

2.3.6. Generation of competent DH5 Bacterial cells for use in transformation.

DH5 α bacteria from glycerol stocks (gift of Professor Quinlan) were spread onto LB agar plates and grown overnight 37°C. A single colony was used to inoculate a 5ml starter culture incubated overnight 37°C. The starter culture (1 ml) was used to inoculate 100 ml of LB media that was then incubated at 37°C shaking 250 rpm until

A_{600} reached 0.25-0.5 units. The cells were chilled on ice for 10 min and then centrifuged at 2500 rpm for 10 min at 4°C. The supernatant was discarded and the pellet resuspended in 20 ml buffer 1 (20ml 1M KCL, 12 ml 1M CaCl₂, 30ml glycerol, 1.2 ml 3 M KAcetate, pH 5.8 with 0.2 M acetic acid, filter sterilised) and incubated for 60 min on ice. Cells were further centrifuged at 3000 rpm for 5min 4°C and the pellet resuspended in 4 ml buffer 2 (2 ml 1M KCl 15 ml 1m CaCl₂, 30 ml glycerol 2ml MOPs pH 6.8 10M NaOH/HCL, filter sterilised) and incubated on ice before being aliquoted 0.2 ml and stored at -80°C.

2.3.7. Real time PCR of plectin alternative first exons isoforms.

Real time PCR is a technique where the amplification and quantification of a specific nucleic acid sequence can be detected in real time. This is achieved at each cycle by detecting fluorescence of the sample, where the amount of fluorescence is directly proportional to the amount of product. In this study I used SYBR Green which is a fluorescent dye that binds all double stranded DNA molecules, emitting a wavelength of 521 nm on binding. The Fluorescence was detected during the extension step of the PCR. Real time PCR was carried out on Rotor-gene 3000 (Corbet Research, UK) using Rotor Gene 6 software. Initially, SYBR green (Clontech Invitrogen UK) 1:60,000 stock (1:600 stock 1:100 per reaction) was added to the optimised TAQ (Promega UK) PCR as above (2.3.1). Subsequently, QuantiTech, SYBR Green PCR kit (Qiagen UK) was used according to the manufacturer's protocol. This provided an improved reliability of product (based on melt curves and agarose gel analysis) and was used for the results presented in Chapter 3. The primers were designed manually to generate a PCR product of 150-250 bp; this is to enable comparison of different targets and to increase amplification efficiency (Table 2.1). The reaction total volume was 50 µl, primers were used at a concentration of 0.5 µM and template at 1 µl of cDNA reaction (20 µl reaction volume using starting total RNA 100 ng). Omitting enzyme or template as a control assessed the possibility of DNA contamination. Data acquisition was performed during the extension step and melt curve analysis. Using Rotor-gene analysis tools, comparative quantification between the lowest grade and higher grade carcinomas was acquired. Based on the Takeoff point and the reaction efficiency, the relative concentration of each cell line compared to HT29 for each isoform is calculated. The second derivative of the amplification plot produces peaks corresponding to the maximum rate of fluorescence increase in the reaction, the take

off is the point at which is the point where the second derivative is at 20%, and the reaction efficiency is where a value of two is 100% (doubling of product with every cycle). Agarose gels (2%) were run to evaluate the product along with GeneRuler 100bp Marker (MBI Fermentas UK Life Sciences) to provide further confirmation of correct size of products.

2.3.8. PCR of plectin isoforms for cloning into eGFP constructs.

Constructs primers (Table 2.2) for the alternative exons were designed to include the predicted start codon and to encompass exons 1-8 (i.e. the whole actin-binding domain) and restriction sites; BamHI and HindIII for direct cloning into eGFP-N vector (Clontech Invitrogen UK). Platinum Taq DNA Polymerase High Fidelity (Invitrogen, UK) was used to amplify the inserts. The vector and inserts were double digested with BamHI and Hind III restriction enzymes at 37°C for 2 hrs and digests were run on a 1% agarose gel and purified using Qiagen gel Extraction Kit (Qiagen UK). The vector was then treated with shrimp alkaline phosphatase (Fermentas UK), 1 unit per 50 ng of cut vector, which catalyses the release of 5' and 3' phosphate groups. This ensures empty vectors do not ligate after digestion and no false positive colonies are selected, the enzyme is inactivated by heating to 65°C for 10 minutes then chilled on ice. The vector and inserts were ligated with T4 DNA ligase (Invitrogen UK) 1:3 ratio of vector to insert. The ligated vectors were transformed into One Shot TOP10 competent cells (Invitrogen UK) and selected on kanamycin (50µg/ml) LB agar plates. Individual colonies were used to inoculate 5 mls LB overnight 37°C. The plasmids were purified and eluted in 2 x 30 µl of sterile distilled water using Qiagen mini prep kit, which used silicon membrane spin technology to purify plasmids from bacterial cultures. The correct clones were verified by sequencing using primers that would cover the whole sequence and ligation points (Table 2.3). Correct clones were then grown in 200 mls LB and plasmids were purified and resuspended in 150 µl using Midi prep kit (Qiagen UK). DNA concentration was measured on Beckman DU-600 spectrophotometer with absorbance A read at 260 nm, 280 nm and 320 nm (background correction). Quality was checked ensuring a ratio of 1.8-2.0 at 260/280; good preparations yielded ~200 µg. The final concentration was adjusted to 1 µg/µl in water and the plasmids were stored at -20 or -80°C.

Table 2.2. PCR primers used for amplifying exons 1-k for cloning into eGFP vector.

Primer Name	Sequence
Reverse exon 8 GFP	GCGGATCCGATCCTGCACGTCCGGCA
Plec 1 GFP	GCCAAGCTTCGGCTCCAGCAGCCATG
Plec 1a GFP	GCCAAGCTTCAGCATGTCTCAGCACCA
Plec 1b GFP	GCCAAGCTTCGGCTATGGAGCCCTCGG
Plec 1c GFP	GCCAAGCTTCCATGTCGGGTGAGGACGC
Plec 1d GFP	GCCAAGCTTCCCGATGAAGATCGTGCCCG
Plec 1e GFP	GCCAAGCTTCAGACATGGACCCCTCG
Plec 1f GFP	GCCAAGCTTCCGGCATGGCCGGCCCGCTG
Plec 1g GFP	GCCAAGCTTGCCGAACCAGGGCTCCGG
Plec 1k GFP	GCCAAGCTTCATGGACAGGTACAGCATG

Table 2.3. Primers used for sequencing of eGFP inserts.

Name	Sequence
EGFP826_Rev	CGAACGGCCACCACGTCTAC
EGFP_N_RevSeQ	GTCGCCGTCCAGCTCGACCA
Exon7_FWDSEQ	CAGACCAACCTGGAGAACCTG
EGFO826_REV	TGGTGCAGATGAACTTCAGG

2.4. Cell culture.

The following sections contain the cell culture methods with Table 2.4 listing the cell types used in this study.

2.4.1. Cell maintenance.

All cells were cultured in a humidified atmosphere, with 5% CO₂, all media was supplemented with 10% fetal calf serum (Sigma Aldrich UK) and 50 units/ml penicillin, 50 µg/ml streptomycin. The McCoy's 5A media (Sigma Aldrich UK) and Dulbecco's modified Eagle's medium (DMEM) (Gibco, Invitrogen UK) were supplemented with 5% glutamine; however DMEM/NUT.Mic F-12 (Gibco, Invitrogen UK) was pre supplemented with 5% Glutamax. Standard sterile tissue culture techniques were used and cells were propagated in T25 or T75 flasks (Griener Bio-one UK), where appropriate, and never grown above 70-80 % confluence. When cells reached above 80% they tend to differentiate and were discarded. Cells were passaged using Trypsin EDTA (Sigma Aldrich UK) and all washes performed with 1x PBS (Sigma Aldrich UK tissue culture grade). Experiments were always conducted up to 7 passages above starting passage (Table 2.4) to ensure consistency of results as cells can change in nature due to selection or differentiation at later passages. For long term storage cells were centrifuged at 800 rpm for 5 minute to remove old media and resuspended on ice in antibiotic free media containing 10% dimethyl sulphoxide (DMSO) and finally transferred to -140°C freezer or liquid nitrogen cell bank.

Table 2.4. Cell lines used in this study.

Cell line	Type	Media conditions	Passage *	Origin	Reference
HT29**	Human (Caucasian) colon adenocarcinoma (grade II)	McCoy's 5A modified medium (Sigma)	P149	ATCC HTB-38 J Fogh	Fogh, 1975
SW948	Human colon epithelial carcinoma (grade II-III)	DMEM/N UT.MixF-12 (Gibco)	P65	ATCC CCL-237 A Leibovitz	Leibovitz et al., 1976
SW480	Human colon epithelial carcinoma (grade III-IV)	DMEM/N UT.MixF-12 (Gibco)	P116	ATCC CCL-228 A Leibovitz	Fogh et al., 1977.
T84**	Human lung metastasis from colon epithelial	DMEM/N UT.MixF-12 (Gibco)	P66	ATCC CCL-248 H Masui	Murakami et al., 1980
MCF7**	Human Caucasian breast adenocarcinoma (grade II)	DMEM (Gibco)	P24	HTB-22 ATCC CM McGrath	Soule et al., 1973
MDA-MB-231**	Human Caucasian breast adenocarcinoma (grade III-IV)	DMEM/N UT.MixF-12 (Gibco)	P17	ATCC HTB-26 R Cailleau	Cailleau et al., 1974
THP1	Human acute monocyte leukaemia	RPMI-1640 (Sigma)	P25	ATCC TIB-202 S Tsuchiya	Tsuchiya et al., 1980

* Passage refers to the number of times the cells have been split and is a rough indicator of the age of the culture.

** Cells were obtained through the European collection of cell cultures (ECACC), although HT29, T84, MCF7 and MDA cells originate from the ATCC.

2.4.2. Differentiation of THP1 cells into macrophage like cells.

THP1 cells grow in suspension culture and are monocytic in origin. The cells, upon phorbol 12-myristate 13-acetate (PMA) treatment can be stimulated to differentiate into macrophage like cells (Auwerx et al., 1988 and Schwende et al., 1996). PMA is a potent tumour promoter, which activates protein kinase. Cells were plated at a density of 1×10^5 cells per well with media containing 12.5 ng/ml PMA (Sigma Aldrich UK) for 48 hours (adapted from Tsuboi, 2007). After 48 hours adherent macrophages were fixed with 4% paraformaldehyde and processed for immunofluorescence (Section 2.8.1).

2.4.3. Transfection of plectin-GFP vectors into carcinoma cells.

The constructs were transfected using GeneJuice (Merck Biosciences, UK). Cells were counted to 1×10^5 cells per 6 x well plate (Griener Bio-one UK) using a haemocytometer. Cells were put into suspension in media using Trypsin EDTA (Sigma Aldrich UK) and diluted 1:1 with Trypan Blue (Sigma Aldrich UK), which checks for cell viability as dead cells take up the blue dye. 10 μ l of the Trypan blue cell suspension was loaded into the haemocytometer, ten fields consisting of 16 small squares were counted, then the average of these was multiplied by 20,000 to find cells per ml, this was repeated twice. Cells were then transfected with 1 μ g of plasmid and 3 μ l of GeneJuice for 48 hours and then the media was changed. The transfection reagent uses a non-toxic cellular protein and a polyamine to introduce plasmids inside the cells, which form a complex with the reagent. Once inside the cell, the plasmid can then express the gene of interest from the internal plasmid promoter using the cells machinery. Cells were then used for protein extraction (2.7.1), staining with fluorescent antibodies (2.8.1), or used to generate stable cell lines (2.4.4).

2.4.4. Establishing stable plectin GFP stable cell lines in SW480 cells.

After a 48 hour transfection (refer to Section 2.4.3) with eGFP vectors, cells were selected using antibiotic G418, Geneticin (Invitrogen) at 600 μ g/ml. The media was changed every two days for 3 weeks until isolated colonies appeared. Stable clones were frozen down for use as a mixed stable cell line or single cell clones were selected by serial dilution to a concentration of 0.25 cells per well in a 96 well plate, to increase the chance of single cell clones. Clones were grown up to larger flasks and analysed by immunofluorescence and immunoblotting, those expressing the correct GFP vector at

an intermediate level were passaged and frozen for future use. High expressing clones could potentially effect the results due to the GFP and not the insert and low expressing clones may not provide a strong dominant negative effect or be hard to image.

2.5. siRNA interference as method of protein depletion in cells.

Short interfering RNA can be used to knockdown a protein of interest and therefore determine a proteins function in a negative manner. The siRNAs act via formation of a RNA-induced silencing complex (RISC), which is a multi-protein complex that cleaves double, stranded RNA (Figure 2.3). After unwinding into single strands, the siRNA recruits RISC complex to the complementary RNA molecules, where it cleaves the native complementary RNA or stops ribosome translation of the RNA and therefore stops translation of the protein (first described in mammalian cells by Elbashire et al., 2001).

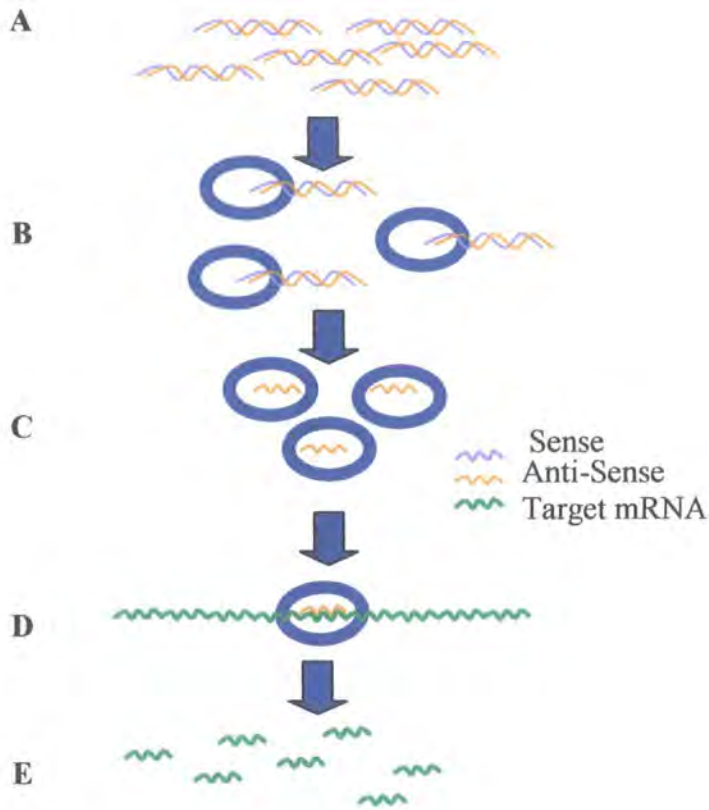


Figure 2.3. Overview of the siRNA pathway.

Short interfering RNA is introduced into the cell via transfection (A), which then binds to a multidomain complex to form the RNA-induced silencing complex (RISC) (B). One of the main proteins of the RISC is the argonaute protein, which cleaves and discards the passenger (sense) strand of the siRNA duplex leading to activation of the RISC complex (C). The antisense strand of the siRNA then guides the RISC complex to its homologous mRNA (D), resulting in the endonucleolytic cleavage of the target mRNA (E). Reviewed in Bantounas et al., 2004.

2.5.1. siRNA sequences in this study.

Using the online siRNA database from Ambion non-validated pre-designed siRNA oligos standard purity were purchased for human plectin and vimentin (Table 2.5). The plectin siRNAs target to exons 5, 23 and 32 which are common to all plectin isoforms including the rodless isoform lacking exon 31 ensuring total knockdown of all isoforms. Vimentin siRNAs are targeted to exons 4, 8 and 9.

Table 2.5. siRNA sequences used in this study.

Name	Sequence 5'-3'	Target exon	Level of knock down
Silence negative control no 1	19bp scrambled sequence 3 dt overhangs Sequence withheld	None	No interference observed
Plectin 1 Id144451	Sense: GGAAUGAUGACAUCGCUGAtt Antisense: UCAGCGAUGUCAUCAUUCCTg	Exon 5	High
Plectin1 ID 144452	Sense: GGCACUGCGUAGGAAAUAActt Antisense: GUAUUUCCUACGCAGUGCCTc	Exon 23	Medium
Plectin1 ID 144453	Sense: GGCAGAACACUAACCUGAtt Antisense: UCAGGUUAGUGUUCUGCCctt	Exon 32	Low
Vimentin ID 138993	Sense: GCAUGUCCAAAUCGAUGUGtt Antisense: CACAUCGAUUUGGACAUGCtg	Exon 4	High
Vimentin ID 138994	not available	Exon 8	Low
Vimentin Id 138995	Sense: GCAAGUAUCCAACCAACUUt Antisense: AAGUUGGUUGGAUACUUGCtg	Exon 9	High

2.5.2. Transfection of siRNA into carcinoma cells.

Oligofectamine (Invitrogen, UK) was used to transfect the SW480 and MDA-MB-231 cell lines with 60 pmol siRNA per 24 well, 240 pmol per 6 well and 1.920 nmol per 10 cm dish. Since starting this project several new recommended siRNA transfection reagents, such as lipofectamine 2000 (Invitrogen UK) have become available that use only 20 pmol per 24 well, I decided not to change method since the previous was producing excellent knockdowns. Transfections were carried out in antibiotic free media that was changed 48 hours after transfection. Cells were processed for immunofluorescence, immunoblotting or assaying at 72-96 hours after transfection,

2.6. Generation of plectin isoform specific polyclonal antibodies.

Polyclonal antibodies were raised against the first exons of plec 1, 1b, 1f and 1k peptide (Table 2.6). The peptides were chosen as the most hydrophilic (antigenic) sites and a cysteine residue was added to the start of the peptide sequence for conjugation to the carrier protein keyhole limpet hemocyanin (KLH). Carrier proteins, once coupled to the peptides, provide additional motifs required for association with Class II molecules and T-cell receptors and in turn generate a stronger antibody response. Two rabbits were inoculated with each peptide to increase positive results. The peptide synthesis, raising of antibodies and collection of the serum was conducted by Cambridge Research Biochemicals, Billingham, UK.

Table 2.6. Peptide sequences for generation of polyclonal antibodies.

Name	Isoform target	Peptide sequence	Properties
LM1/2	Plec 1	SPPKRGPLPTEEQRVYRRK	Amide
LM3/4	Plec 1b	RRGRRWAQDEQ	Acid
LM5/6	Plec 1f	QDFIQAYEEVREKYK	Acid
LM7/8	Plec 1k	DRYSMEELIQ	Amide

2.7.1. Total cell protein extraction from carcinoma cell lines.

For extraction of total cell protein, media was removed from the adherent cells and the cells then washed in 1x phosphate buffered saline (PBS) (135 mM NaCl, 2.7 mM KCl, 10 mM Na₂HPO₄, 2 mM KH₂PO₄ pH 7.4). Cells were lysed on ice in 2x Laemmli

sample buffer (50 mM trishydroxymethylaminomethane-hydrochloric acid (Tris-HCl) pH 6.8, 20% v/v glycerol, 1 mM ethylenedinitrilotetraacetic acid (EDTA) 1% Sodium dodecyl sulphate (SDS)) supplemented with protease inhibitor cocktail, 1 tablet per 10 ml sample buffer (Roche, UK). Using a low temperature and the protease inhibitors during protein extraction is an important step to stop degradation of the proteins. Samples were boiled for 5 min and then homogenised through a 25G needle to shear DNA. Finally, samples were used fresh or aliquoted and stored for 1 month at -20°C or for longer at -80°C (Laemmli et al., 1970).

2.7.2. Colorimetric protein quantification using spectroscopy.

Extracted proteins were quantified using bicinchoninic acid, BCA protein assay reagent kit (Pierce UK), which is a colorimetric assay where the samples are read at 562 nm. Standards were made using bovine album serum BSA (Sigma Aldrich UK) diluted in the exact sample buffer that the protein samples were stored in. Standard concentrations were; 0, 0.1, 0.25, 0.5, 1.0, 1.5, and 2.5 mg/ml, and the protein samples were used at dilutions of 1:5 in the assay. Samples were read on Beckman DU-600 spectrophotometer, which produces a standard curve at which the absorbance of unknown samples can be correlated to the concentration.

2.7.3. 1-dimensional gel electrophoresis (20-200 MW proteins) and immunoblotting.

Protein samples were separated under reducing conditions using the Thermo Electron mini gel system. Sodium dodecyl sulphate (SDS) is an anionic detergent which denatures proteins by "wrapping around" the polypeptide backbone. Samples were mixed with equal volumes of loading buffer dye (sample buffer supplemented with 0.2% bromophenol blue and 1% β -mercaptoethanol) and resolved on SDS-Page gels, at 100V through the stacking and 200 V in the resolving gel in 1 X SDS-Page buffer (25 mM Tris, 250 mM Glycine, 0.1% SDS). Depending on the size of the proteins of interest, resolving gels of 4% to 12% were used for higher resolution in the upper and lower part of the gel, respectively (Table 2.7).

Table 2.7. SDS-Page gel preparation.**A**

Component	Stacking gel 4%
dH ₂ O ml	6.1
1.5M Tris	2.1
pH 6.8 ml	
10% SDS μ l	100
Acrylamide	1.35
30% ml	
10% APS μ l	5
TEMED μ l	10
Total ml	10

B

Component	Resolving Gel			
	4%	7.5%	10 %	12 %
dH ₂ O ml	6.0	4.85	4.01	3.34
1.5M Tris pH	2.5	2.5	2.5	2.5
6.8 ml				
10% SDS μ l	100	100	100	100
Acrylamide	1.35	2.5	3.33	4
30% ml				
10% APS μ l	50	50	50	50
TMed μ l	5	5	5	5
Total ~ml	10	10	10	10

2.7.4. Coomassie Blue staining of SDS Page gels.

To visualise proteins separated in the gel, coomassie blue solution (40% methanol 10% acetic acid 0.1% Coomassie Blue G-250 (Sigma Aldrich UK)) was used to stain the gels for 1 hour after which they were destained at room temperature with a solution of 40% methanol, 10% acetic acid in dH₂O, for up to a day changing the solutions frequently.

2.7.5. Immunoblotting of whole cell protein extractions.

Proteins from the gel were transferred to Hybond nitrocellulose membranes (Amersham Pharmacia Biotech UK) in 1X Towbin buffer (25mM Tris pH 8.3 20 % methanol 0.1% SDS) (Towbin et al., 1979), using the Thermo Mini Blot module at 15 V for 1.5 hours. This method uses semi-wet blotting, where the membrane and gel are sandwiched between filter paper and then sponges which are contained in a closed cassette filled with buffer. This method is unlike wet blotting, where the whole tank is filled with buffer or semi-dry blotting, where only the filter papers are soaked in buffer. The membranes were then rinsed in 1x TTBS (10 mM Tris pH 7.4, 137 mM NaCl, 2.68 mM KCl, 0.2% Tween 20) and stained with Ponceau-S red (Sigma Aldrich UK) to check transfer efficiency. Ponceau-S solution stains total protein and this method can be used as a visual to check equal protein loading levels and transfer. Membranes were blocked for 2 hrs or overnight in 5% milk 1x TTBS, probed with primary antibody (listed in table 2.8) for 2 hours followed with, 1 hour incubation with horseradish-peroxidase conjugated secondary antibody (Dako UK). Washes and antibody incubation was performed with 2.5% Milk 1x TTBS with 5 x 5 min washes between incubations. Bound antibodies were visualised using Enhanced Chemiluminescence (Amersham Pharmacia Biotech UK) and FujiFilm Intelligent Dark Box II. When analysis of the intensity of bands obtained during immunoblotting was carried out, Image J software was used to calculate area and pixel value statistics of each band, which was then compared to a control band (on the same blot) to give a percentage change of band intensity.

2.7.6. 1-dimensional gel electrophoresis and immunoblotting (for high molecular weight proteins).

Plectin has an estimated MW of 500 KDa, although 4% SDS PAGE gels can be used, more consistent results were obtained using the NuPAGE Mini-Cell system

(Invitrogen UK). Furthermore, using gradient gels allowed a check of proteins at lower molecular weights simultaneously. Proteins were resolved on NuPAGE 3-8% Tris-acetate Gradient gels (Invitrogen) using 1X NuPAGE Tris-acetate running buffer. Tris acetate gels have a lower pH than traditional SDS PAGE gels and have improved separation of high molecular weight proteins due to clearer bands and increased gel stability. Proteins from the gel were transferred to Hybond nitrocellulose membranes (Amersham Pharmacia Biotech), using NuPAGE transfer buffer (Invitrogen UK) and 20% methanol, at 30 V constant for 1.5 hours using the XCell II Blot Module (Invitrogen UK). Membranes were then treated as above in section 2.7.5.

2.7.7. Immunofluorescence of carcinoma cells.

For fluorescent microscopy, cells were grown on 13 mm glass coverslips that were non-coated unless specified. Cells were then fixed with 4% paraformaldehyde in PBS using a 16% paraformaldehyde solution stock (Agar Scientific UK) for 10 minutes and permeabilised in 0.02% Triton X-100 (Sigma Aldrich UK). Alternatively, cells were fixed with chilled 1:1 methanol: acetone for 15 minutes. Methanol: acetone fixation can be useful when looking at the cytoskeleton because the cell membranes are broken and unbound lipids and proteins are released allowing clearer visualisation of the filaments. Cells were blocked for 40 minutes using 0.2% fish skin gelatin (Sigma Aldrich UK). The primary antibodies used are listed in the Table 2.8. Filamentous (F) actin was stained with TRITC labelled phalloidin (Sigma Aldrich UK). Primary antibodies were incubated for 1 hour and detected using Alexa 488 or 594-labelled secondary antibodies (Invitrogen UK). At each step the cells were washed three times with cell wash buffer (1x PBS 0.02% NaAz 0.02% BSA). The cells nucleus was visualised using 4', 6-Diamidino-2-phenylindole (DAPI) 100ng/ml (Invitrogen UK), which binds to double stranded DNA. The coverslips were positioned cell-side down onto glass slides using Immunomount (Thermo UK), dried overnight and then stored in the dark at 4°C.

Table 2.8. List of antibodies used in this study.

Antibody	Antibody type	Dilution		Source
		IF	IB	
Actin AC-40	Mouse monoclonal	NA	1/1000	Sigma
Cytokeratin 8/18	Mouse monoclonal	1:1000	1:1000	
Cortactin	Mouse monoclonal	1:100		Abcam
Desmoplakin DP1/2	Mouse Monoclonal	1:100	1:1000	ICN
Desmoplakin AMP320	Rabbit polyclonal	1:100	1:1000	Serotech
Dynamin	Mouse monoclonal	1/100	N/A	BD Biosciences
GFP	Mouse Monoclonal	N/A	1:500	Clonetech
Periplakin TD2	Rabbit polyclonal	1:100	1:200	Di Coleandra et al., 2000
α 3 Integrin F35 177-1	Mouse Monoclonal	1/100	N/A	Abcam
α 6 Integrin MP 4F10	Mouse monoclonal	1/100		CRUK
β 1 Integrin 4B7	Mouse monoclonal	1/100	N/A	CRUK
β 4 Integrin 439-9B	Rat Monoclonal	1/200	N/A	Abcam
LM1	Rabbit polyclonal	1:200	1:500	This study
LM2	Rabbit polyclonal	1:200	1:500	This study
LM3	Rabbit polyclonal	1:200	1:500	This study
LM4	Rabbit polyclonal	1:200	1:500	This study
LM5	Rabbit polyclonal	1:200	1:500	This study
LM6	Rabbit polyclonal	1:200	1:500	This study
LM7	Rabbit polyclonal	1:200	1:500	This study
LM8	Rabbit polyclonal	1:200	1:500	This study
N-Wasp	Rat Monoclonal	1/100	N/A	Michael Way
Plectin c-20	Goat polyclonal	1:200	1:500	Santa Cruz
Talin-NCL	Mouse monoclonal	1:200	1:500	Nova Castra
T-Plastin (c-15)	Goat polyclonal	1:50	1:200	Santa Cruz
Vinculin clone V-11-5	Mouse monoclonal	1:500	1:100	Sigma
3052 Vimentin	Rabbit polyclonal	N/A	1:2000	Dundee
Vimentin clone V9	Cy3 conjugated mouse monoclonal	1:1000	N/A	Sigma

2.8. Microscopy.

Specimens were viewed using a Zeiss fluorescence Axioplan microscope fitted with a 40-x/1.30-oil immersion plan-NEOFLUAR lens. Confocal images were obtained with Zeiss LSM 510 Confocal microscope using 40x N/A1.3 or 60 X/1.10 oil immersion objectives. The pinhole on the confocal was adjusted so that it matches the diameter of the airy disc; the inner light circle of the diffraction pattern of a point light source, this gives the best signal to noise ratio. The images were collected at a scan speed of 12.8 μ s per pixel and a resolution of 1024 x 1044. Composite panels were generated using Adobe Photoshop CS (Adobe Systems) and LSM510 image browser software (Carl Zeiss) and only linear adjustments to brightness and contrast were made.

2.9. Verification of specificity and optimisation of plectin isoform antibodies.

The polyclonal antibodies received from Cambridge Biosciences (section 2.6) were checked for specificity to the protein product by immunoblotting as below. Prior to use, the antibodies were purified from the serum to reduce background noise. Further purification of the specific antibody could be carried out using affinity-binding chromatography, but this was not necessary as antibodies gave a good result without this procedure.

2.9.1. Purification of antibodies from serum.

Plectin LM antibodies were purified using saturated ammonium sulphate. Polyclonal serum was diluted with 1:1 1xPBS and centrifuged to remove any precipitate. Saturated ammonium was prepared (70 g in 1 ml of 1 M NaOH and 75 ml dH₂O) and 0.67 ml was added slowly in aliquots per ml of diluted antibody vortexing each time. Samples were incubated at 4°C for 30 minutes and then centrifuged at 4°C, 30 minutes, 3000 rpm decanting the supernatant. The pellet was then resuspended in water and ammonium sulphate removed using a PD-10 desalting column (GE healthcare UK). Reading at 280 nm and using the extinction coefficient of 1.4 mg/ml/cm measured the yield obtained from extraction. The antibody was diluted to 1 mg/ml in PBS and stored at -20°C.

2.9.2. Peptide competition assay.

To ensure that the antibody is specific for the peptide raised the following assay was used. Protein extract from SW480 cells, which express the plectin isoforms, was used. Immunoblotting of the sample was carried out as Section 2.7.3, except at the primary incubation stage the membranes were incubated with; antibody alone, antibody pre blocked with peptide overnight (1 µg of antibody incubated with 50 µg of peptide in PBS), antibody pre blocked with control peptide overnight and pre immunised serum, with the lowest dilution to produce a positive band used. The antibody is shown to be specific if there is no band produced in the peptide blocked incubated membrane.

2.9.3. Conformation of polyclonal antibody specificity by siRNA.

Another method to further confirm the specificity of the antibodies is to immunoblot the antibodies against plectin siRNA protein samples. A knockdown of the band should be seen if the antibody is specific to the protein. This method was considered as the most convincing and was used to confirm all the antibodies. Furthermore, the bands produced were visualised at the expected sizes using HiMark (Invitrogen UK) protein ladder, which contains a 500-kDa band. In this study, this was the most convincing method and is presented in Chapter four.

2.10. Cell survival assay after siRNA transfection.

Equal numbers of cells were transfected in triplicates with siRNA as described in section 2.5.3 onto 12 well plates, (Cells were counted using a haemocytometer and were plated at 50% confluency prior to transfection). CellTiter 96[®] AQueous One Solution Cell Proliferation Assay (Promega UK) was modified to assess the cell survival after 3 days transfection in 12 well plates. After 72 hour of transfection, cells were incubated with 100µl of solution added to 800 µl of cell media and incubated for 2 hours, 3 x 100µl from each well was read at 490nm with a spectrophotometric plate reader (Anthoslucyl).

2.11. Migration and Invasion.

To study the ability of the cancer cell lines to migrate and invade the methods described below were used.

2.11.1. Collagen insert Migration assay.

Cells were serum starved for 24 hrs and subsequently seeded at 1×10^5 cells onto 24 well cell culture inserts with 8 μm pore size, Thincerts, (Greiner Bio-one UK) coated with 100 μl of 100 mg/ml type I collagen (First Link Birmingham Ltd UK) overnight. Lower chambers contained 10% Fetal Calf Serum in media as a chemoattractant. Invasion was stopped at indicated time-points by removing non-invaded cells in the upper chamber using swabs and washing with PBS. Invaded cells were fixed with ice-cold methanol and stained with Dapi (Molecular Probes Invitrogen UK). It was observed that invaded cells always attached to the bottom of the membrane and did not attach to the bottom of the plate. Membranes were removed from the cell culture inserts with a scalpel and mounted onto slides where 3 fields of triplicate membranes were counted. In order to produce an unbiased result blind counting was used where sample identity was unknown. Mean of invaded cells and standard deviation are shown in the graphs.

2.11.2. Gel insert invasion assay.

Cells and inserts were prepared as above with the exception that the wells were coated instead with a collagen gel or with a basement membrane mix gel; Matrigel (BD Biosciences). The collagen gels were made by adding 50 μl of collagen (2.1 mg/ml type I) (First Link Birmingham Ltd UK) 1:3 in PBS to the top of the insert and allowing gelling 4 hours at 37°C. The Matrigel was prepared on ice diluting 8 mg/ml 1:3 and adding 30 μl to the top of each well. Ice and use of ice-cold pipette tips are necessary to ensure even coating, as Matrigel gels at temperatures above 4°C. The Matrigel layers were then gelled for 4 hours at 37°C following rinsing with PBS, with care taken not to disturb the gel layer. In this assay MDA-MB-231 were seeded at a lower density (0.5×10^5 cells), due to increased cell size. The cells were allowed to invade for 6-8 hours into the collagen gels and 24 hours for Matrigel. These were determined as the optimum time points when most cells had invaded.

2.11.3. Scratch wound assay.

Cells were grown to monolayers on 13 mm (VWR) coverslips in 24 well dishes (Greiner Bio-one UK). A 10 µl pipette tip (Star Lab UK) was used to scratch a line through the cell layers. Cells were then fixed with 4% paraformaldehyde (section 2.8.1) after wounding at the following time points 0, 30 min, 1 hr, 2hr, 4 hr, 6 hr, 12 hr, and 24 hr after to allow for immunofluorescence staining for observing the changes at the wound edge. Alternatively for real time wound closure measurements, the glass just above the centre of the wound was marked to ensure consistency and photographed at the time points using x10 objective lense. It was observed that the main steps of initiating wound closure initiation occurred between 0 and 2 hours. Therefore, future immunofluorescence experiments used these parameters.

2.11.4. Rho kinase inhibitor assay.

For the Rho kinase inhibitor assay confluent layers of SW480 cells were pre-incubated with inhibitors (Calbiochem UK): H-1152, 300nm and/or Y-27632, 3 µm (concentrations from Xie et al., 2005) for 2 hours. Monolayers were then scratched at intervals then fixed and processed for immunofluorescence, as in section 2.8.1.

2.12. Cell attachment assays.

Twelve well plates (Greiner) were coated with collagen, 2.1 mg/ml (First link Birmingham Ltd UK) for two hours at 37°C. The excess collagen was removed and the plates washed in PBS, it was observed that if the collagen was allowed to dry uneven coating could occur. The cells, suspended by trypsin treatment, were washed 3x to remove trypsin and resuspend to give 500,000 cells per well. Cells in suspension were allowed to recover with frequent agitation for 1 hour. Cells were seeded onto of the collagen coating, and after 5 min, 10 min, 20 min and 40 min, the wells were then washed gently three times with PBS to remove non adhering cells. The wells were replaced with 800 µl of media and the CellTiter 96[®] AQueous One Solution Cell Proliferation Assay (Promega UK) was modified to asses the attachment in 12 well plates. Then, 60 µl of dye solution was added to each well and incubated for up to 2-3 hours (when colour starts to change). A volume of 3 x 100 µl from each well was read at 490 nm with a spectrophotometric plate reader (Anthoslucy1). For immunofluorescence, 13 mm coverslips (VWR UK) were coated as above with collagen in 24 well plates. Cells were seeded at 50 000 cells per well and were washed

and gently three times with PBS and fixed immediately with 4% paraformaldehyde at each time point. Finally, immunofluorescence staining was performed as in section 2.8.1.

CHAPTER 3
MAPPING OF THE ALTERNATIVELY
SPLICED HUMAN PLECTIN ISOFORMS.

3.1. Introduction.

The aim of this study was to investigate the role of the cytolinker protein, plectin in the migration and invasion of cancer cells. I decided to start this study by looking at the human plectin gene and its expression at transcriptional level in human cells and tissue to see if there were changes in expression levels between higher grade and lower grade cancer cells and different tissue types that could lead to an invasive or migratory phenotype.

The complex organisation of the plectin gene has the potential to generate large number of alternatively spliced transcripts. Alternative splicing is viewed as a major mechanism in the multiplicity of protein forms in higher eukaryotes (Black, 2003). In a genome wide search a large number of mammalian genes that contained multiple variable first exons were identified along with plectin, which in all cases are spliced into a common downstream exon (Zang et al., 2003). Plectin is not the only member of the plakin family to demonstrate a complex alternative splicing arrangement as both BPAG1 (Jefferson et al., 2006) and MACF (Bernier et al 1996, Gong et al., 2001, Lin et al., 2005) also display several alternative spliced N-termini. BPAG1 has three alternative spliced isoforms: BPAG1e, which is found in skin and has a characteristic structure of the plakins; BPAG1a, a predominantly neuronal isoform that differs from BPAG1e by containing a spectrin repeat rod domain and MT binding domain at the C-terminus; and BPAG1b, predominantly expressed in muscle and structurally similar to BPAG1a except for the presence of additional plakin repeats. Within the above isoforms further splicing takes place at the N-terminus resulting in three alternative first exons for BPAG1a and BPAG1b while BPAG1e has only one possible N-terminus (Jefferson et al., 2006). In 2001, Gong et al., identified a fourth isoform of the MACF1 gene. MACF1 isoforms 1 and 2 have identical ABD but differ in the upstream N-terminal sequences (Bernier et al., 1996 and Leung et al., 1999); isoform 3 contains a unique 5'UTR, a longer N-terminal sequence and just the second half of the actin binding domain (Bernier et al., 1996); and isoform 4 is distinct from the others by containing plectin repeats at the N-terminus (Gong et al., 2001).

Analysis of the mouse plectin gene shows that it contains over 40 exons on chromosome 15 and exhibits an unusual 5' transcript complexity (Fuchs et al., 1999; Rezniczek et al., 2003). At the time this study commenced, 16 mouse plectin isoforms had been identified, of which 11 (1-1j) are spliced into a common exon two. In addition, two short alternative exons were found for both 2nd and 3rd exons (named 2 α and 3 α), increasing diversity in the region of the gene that encodes the calponin homology actin-binding domain (exons 2-8). Finally, three non coding exons (named exons -1,0a and 0) that are located 5' to the first coding exon, 1c, were identified (Fuchs et al., 1999). The 8 alternative protein-coding first exons of the mouse plectin gene all differ in length and have no sequence similarity to each other (Fuchs et al., 1999; Zang et al., 2004). The alternative plectin transcripts were found to exhibit distinct tissue specific expression patterns (Fuchs et al., 1999). Furthermore, the likelihood that there is multiple promoters in the 5' end of the mouse plectin gene was suggested by the presence of CpG islands upstream of alternative 1st exons, leading to a hypothesis that tissue specific expression patterns are determined by differential promoter activation and alternative *cis* splicing (Zang et al., 2004). The human plectin gene spans over 32 exons on 32kb located in the telomeric region (q24) on chromosome 8 (Lui et al., 1996; McLean et al., 1996). At the start of this project only four alternative N-terminal first exon splice variants had been identified in the human and rat plectin genes (Andra et al., 2003; Elliott et al., 1997), while in rat additional transcripts were identified that lacked the C-terminal exon 31 encoding for the rod domain (Elliott et al., 1997). A subsequent bioinformatics search that was published after this project had started, identified eight putative first exons also in the human plectin gene corresponding to the previously identified mouse exons (Zhang et al., 2004). Notably, all of the plectin isoforms discovered so far have been found to contain alternative exons at the 5' end of the gene with only the rodless form being an exception. The previously published work on mouse and rat plectin isoforms had lead to unanswered questions on the characterisation of the human plectin gene. This chapter reports on the gene organisation of the human alternative first exons, with the subsequent identification of a novel isoform plectin-1k. The mRNA expression levels of the N-terminal isoforms are also investigated using quantitative real-time PCR in a panel of breast and colon carcinoma cells and human tissues showing changes in expression levels between the cell lines and also revealing that several of the human plectin isoforms have unique tissue specific expression patterns.

3.2. Results.

3.2.1. Human plectin gene contains a similar diversity of alternative N-terminal isoforms to mouse and rat genes.

The published mouse first exon sequences (Fuchs et al., 1999) were compared to the human genome to find related sequences. Using BLAST algorithm set to search for highly similar sequences across genomes, sequences of over 81% similarity were found in the human for eight of the alternative mouse coding first exons (exons 1, 1b, 1a, 1c, 1d, 1e, 1f, 1g). Furthermore, when the human exons were compared to the rat genome highly similar (>81%) sequences were also found for the exons 1d, 1e, 1f, 1g in addition to the previously identified rat exons 1, 1a, 1b, 1c (Elliot et al., 1997). Table 3.1 summarises the alignments of human alternative N-terminal exons with corresponding rat or mouse sequences using BLAST2 algorithm tool (NCBI). Exons 1a, 1b, 1d, 1e and 1k were identical in length in all three species. However, even though the exons 1, 1c, 1f and 1g are highly conserved in mouse and rat these exons were found to be shorter in the human. In the exon 1, mouse and rat genes have extra 18 nucleotides inserted into the second half of the exon compared to human exon 1, whereas the exon 1c is 12 nucleotides longer in the mouse and at compared to the human. Likewise the, the exon 1f of the mouse and rat plectin genes has a 15 bp insertion after the ATG start codon before the similarity to the human exon 1f commences. Finally, the human exon 1g does not show similarity to the corresponding mouse or rat exons until 28 base pairs after the ATG start site. (Appendix I lists the sequences of the alternative N-terminal exons in mouse, rat and human). Fuchs et al., 1999, identified two possible ATG start sites in plectin 1g that were 168 bp apart. The human plectin gene did not contain the first ATG site and similarity between human and mouse exons 1g can only be seen in the region following the second ATG codon. Furthermore, expression of a truncated plectin-1g protein (exon 1g-8) in a GFP vector found that this second ATG is functional to translate the protein (as seen in chapter 4). Taken together, these results show that the human plectin gene as well as the rat plectin gene could potentially express all eight alternative isoform proteins that are present in the murine gene. However, the alternative first exons are not completely conserved in the human gene as several of them contain deletions compared to alternative first exons in the mouse and rat plectin genes.

Table 3.1. Sequence alignment of human plectin alternatives N-terminal exons to mouse and rat.

Exon	Human exon length (bp)	Matches compared to mouse genome (bp)	Gaps compared to mouse genome (bp)	Matches compared to rat genome (bp)	Gaps compared to rat (bp)
Plec-1*	522	456/451 84%	20/451 3%	455/452 83%	22/452 4%
Plec-1a	112	99/112 88%	0/112 0%	99/112 88%	0/112 0%
Plec-1b	112	95/112 84%	0/112 0%	95/112 84%	0/112 0%
Plec-1c*	193	167/202 82%	12/202 5%	165/202 81%	12/202 5%
Plec-1d	16	16/16 100%	0/16 0%	16/16 100%	0/16 0%
Plec-1e	46	43/46 93%	0/46 0%	42/46 93%	0/46 0%
Plec-1f**	70	52/55 94%	0/55 0%	61/66 92%	0/66 0%
Plec-1g**	124	80/98% 81% §	5/98 5%	81/97 83%	0/97 0%
Plec-1k	43	41/43 95%	0/43 0%	40/43 93%	0/43 0%

The base pair (bp) matches and gaps observed when the human alternative first exon sequences were compared to the mouse and rat genome using the NCBI BLAST2 tool. Sequences for plec-1, 1c, 1f and 1g are longer in the rat and mouse compared to the human sequence. * plec-1 and plec-1c have additional nucleotides insertions contained within the sequences. ** plec-1f alignment starts at human bp 16 in the mouse and human bp 5 in the rat and plec1-g at bp 28 of the human, where there is no significant similarity found before this. § Fuchs et al., 1999 predicted two ATG start sites for mouse plec-1g, the second start site was used for the alignment above as the human does not contain the first ATG. (See Appendix I and Appendix II for sequences).

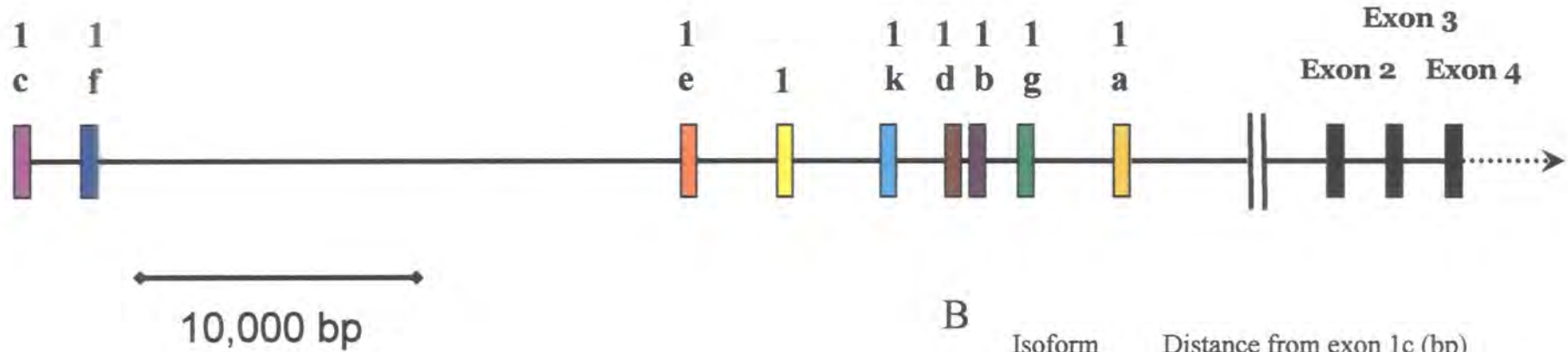
3.2.2. Mapping of the alternative plectin 5' exons.

In order to characterise the human plectin genome further, the isoforms were mapped onto the genome to show the relative positions of the exons (Figure 3.1A). The whole plectin gene from the furthest 5' end coding exon, 1c, was downloaded from the NCBI database (NT 02364 954724-1015724) and the positions of the alternative isoforms on this sequence were found by a blast search using the previously identified sequences above. The same procedure was carried out on the rat (NW047780 8864975-8805175) and mouse (NT039621 37491514-37429514) genome. The alternative first exons are located in identical order on the genomes of human mouse and rat and the relative spacing is similar (Figure 3.1B). Human exons 1c and 1f are located 19553 bp upstream of 1e, where the remaining exons cluster over 14329 kb (1, 1k, 1d, 1b, 1g and 1a). The results show that human genome contains similar distribution of alternative exons as compared to the mouse and rat.

3.2.3. Identification of a novel plectin isoform; plectin-1k.

A novel plectin N-terminal isoform that was named 1k (the mouse exons 1h, 1i and 1j are alternative noncoding 5'-UTR exons) was identified during the bioinformatics search for alternative plectin first exons. Exon 1k encodes for a 14 amino acid residue (Appendix II). The translation start site in the exon 1k (accATGgac) resides in a consensus Kozac sequence (gccgcc(A/G)ccAUGG) and is preceded by an in-frame stop codon 96 nucleotides upstream. Furthermore, a subsequent bioinformatics search revealed a human 5' EST clone that contained the exon 1k (accession number BP315239; Sugano cDNA library, mammary gland OCUB-F Homo sapiens cDNA clone OFR08117 5', mRNA sequence). The exon 1k is located between exon 1 and 1d in the human plectin locus; about 1.6 kb upstream of the exon 1d and 3.8 kb downstream of the exon 1 (Figure 3.1). Similar sequences of 95% in mouse 93% in the rat genome were identified that further validate the exon 1k (Table 3.1), and when translated at the protein level the amino acid sequence is identical in all three species (Appendix II). Therefore, the exon 1k adds to the diversity of the alternative first exon isoforms in plectin.

A



B

Isoform name	Distance from exon 1c (bp)		
	Rat	Mouse	Human
1f	1992	1928	1899
1e	21809	19330	21452
1	24654	25202	24563
1k	28560	29122	28979
1d	30408	30888	30634
1b	31101	31680	31474
1g	32633	33264	32847
1a	35351	35805	35781

Figure 3.1. Map of plectin alternative N-terminal first exons.

(A) Schematic map of the localisation of the 9 coding first exons 1 – 1k in the human plectin gene. Scale bar gives an indication of distance between exons 1c and 1a only. All human N-terminal first exons splice directly to exon 2.

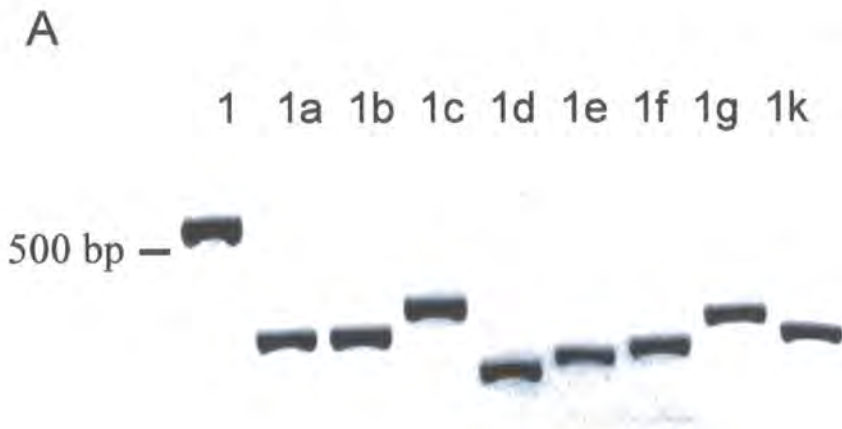
(B) Table of the distance in base pairs (bp) from exon 1c in rat, mouse and human genome.

3.2.4. Search of EST clones reveals further possible alternative exons.

The unusual complexity of the plectin alternative first exons prompted a blast search to compare the EST database against the human plectin locus. In addition to the plectin-1k isoform, a 5' EST clone was identified that is contained in the human plectin gene (accession number AL55160 Homosapiens PLACENTA COT 25-NORMALIZED Homo sapiens cDNA clone CS0DI063YN08 5-PRIME, mRNA sequence). This exon named in this study plect-1l is located 14715 bp downstream of plec-1f and 4838 bp upstream of plec-1e. The translation start site in the exon 1l (gccaccATGgat) resides also in a consensus Kozac sequence and is preceded by a stop codon 186 bp up stream. Several attempts were made to amplify this sequence (Appendix I) without success, probably due to tissue specific mRNA expression, as the EST clone was found in embryonic sample. This evidence leads to speculate that the previously identified first exons do not represent the full diversity of the alternative first exons in plectin.

3.2.5. PCR sequencing and cloning of plectin alternative N-terminal first exons.

In order to confirm the expression of the alternative human first exons, PCR was carried out using primers targeted for each of the alternative exons (Table 2.1). The reverse primer was chosen to be located in exon 4 due to the presence of the possible alternative second and third exons. Furthermore, exons 2 and 3 were not suitable due to the short length and GC richness. cDNA samples from human cell lines were used (HT29, SW480, MCF7, and U373 cells) as a template for each isoform and products were cloned into pGEM T-easy for sequencing. The PCR products were run on a 2% agarose electrophoresis gel that enhances comparison of the sizes of the alternative first exons (Figure 2.3A, Figure 3.2B). The remarkable short sizes of the alternative first exons, from plec-1 at 522 nucleotides to only 16 nucleotides in plec-1d, should be highlighted for the results that follow in this study. Sequencing of the PCR clones extending to the end of the ABD demonstrated that the all of the human alternative first exons splice to the exon 2 then 3 and 4. None of the sequences contained the alternative second exon 2 α or third exon 3 α as proposed for the mouse (Fuchs et al., 1999). These results confirm that all nine alternative plectin N-terminal first exons, including the novel exon 1k, are expressed in human cell lines.



B

Isoform	(a) Exon length (bp)	(b) Expected size (bp)
1	522	652
1a	112	242
1b	112	242
1c	193	323
1d	16	146
1e	46	176
1f	70	200
1g	124	254
1k	43	173

Figure 3.2. Alternative N-terminal first coding exons in the human plectin gene.

(A) Agarose gel electrophoresis of rt-PCR products of alternative N-termini of the human plectin gene. Exons 1-4 were amplified starting from each indicated alternative exon 1. The PCR products correspond to the predicted sizes (B) and were cloned and sequenced for confirmation. In the above table column (a) is the length of each alternative N-terminal first exon and column (b) is the expected length of the PCR products on agarose gel above using the exon 4 reverse primer.

3.2.6. Semi-quantitative RT-PCR end point analysis shows distinct expression levels of plectin N-terminal isoforms in colon carcinoma cells.

Plectin N-terminal isoform expression was investigated at the mRNA level in a panel of colon carcinoma cell lines, HT29, SW940 and SW480. These cell lines originated from grade II (HT29) to grade III/IV (SW480) cancer. The Cancer grading system set by, The American Joint commission on pathology is based on pathology of the cancer cells. The grading describes the extent or severity of an individual's cancer based on the extent of the original (primary) tumour and the extent of spread in the body. Grade I cells are early stage carcinomas and are well differentiated and slow growing, whereas grade IV cells are considered to be aggressive and undifferentiated. The expression was first investigated using semi-quantitative rtPCR, where the expression levels are evaluated at the PCR end point. The PCR was run for 25 cycles, as this was the lowest number that gave comparable product, therefore was below the plateau phase of PCR. Interestingly, in the higher grade SW480 cells compared the lower grade HT29 cells, expression of plec-1 was elevated and plec-1e was decreased (Figure 3.3). Periplakin and actin expression are shown as positive controls to mRNA levels and quality. The findings above show that plectin isoforms 1 and 1e are altered between the grades in colon carcinoma cells. Intriguingly in the murine studies, at the protein level plectin-1 was found in the nucleus with faint actin staining and 1e decorated stress fibres, indicating that these isoforms have specific localisations (Rezniczek et al., 2003). Plectin-1 was also found as the major transcript expressed in cells of mesenchymal origin (Fuchs et al., 1999) and its long sequence gives increasing potential to accommodate isoform-specific binding partners (Abrahamsberg et al., 2005). These findings prompted the investigation into the expression levels of the other alternative first exons using the quantitative method of real-time PCR, in an attempt to isolate the isoforms that are expressed more prominently in the more aggressive cancer cells compared to the low-grade cells. Also, the tissue specific expression of plectin transcripts will be investigated in the human as previous studies have looked only at expression levels in mouse tissues (Fuchs et al., 1999).

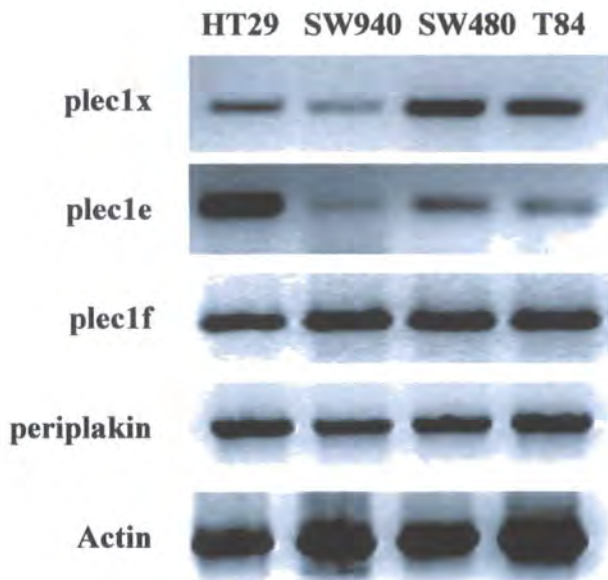


Figure 3.3. Expression of plectin N-terminal isoforms in colon carcinoma cells.

Equal volumes of PCR end products were loaded onto 2% agarose electrophoresis gel. Note the change in expression of isoform 1x and 1e, whereas 1f is uniform. Periplakin and actin is used positive control for RNA.

3.2.7. Realtime PCR: a method to quantitatively investigate mRNA expression levels.

Real Time PCR was used on the panel of colon carcinoma cell lines including the breast carcinoma cell lines MCF7 (grade II) and MDA-MB-231 (grade III-IV) to investigate expression levels of plectin N-terminal isoform transcripts. The breast carcinoma cell lines were used to investigate if any altered expression levels identified are a product of cancer cell aggressiveness or are specific for cancer cell types. The method of real-time PCR is reviewed in section 2.3.8. Due to the large amounts of data generated in real-time PCR the following sections 3.2.8 will show examples of the products for each N-terminal isoform and 3.2.9 will report on the novel isoform plectin 1k as an example to demonstrate the method. Finally, sections 3.2.8 and 3.2.9 will report on the end results of the carcinoma cell and human tissue expression study in condensed graphical form.

3.2.8. Melt curve analysis confirms the integrity of the PCR product.

The integrity of the real time PCR products were observed using melt curve analysis (Figure 3.4). After the completion of PCR cycling, the temperature is raised in 1°C steps and the product should produce one peak, representing the decreased fluorescence at the melting point of the product. Single peaks were observed in the analysis of all the nine of the plectin isoforms and in the actin control. Additional peaks, which indicate non-specific products or primer or template dimers, were not present in any of the samples (Figure 3.4). The results demonstrate that each primer pair was specific for the expected size that had previously been cloned and sequenced in Figure 3.2 for each alternative N-terminal isoform. Analysis of the final PCR products on a 2% agarose gels provided further evidence on the reliability of the method, although differences in the expression levels can no longer be observed due to the PCR reactions reaching the plateau before the 50 cycles terminates (data not shown). No non-specific bands or primer dimers were detected in the agarose gel, which confirms the results of the melt-curve analysis.

3.2.9. Fluorescence curves for isoform plec-1k show real-time PCR progression.

The representative fluorescence curve of amplification of the isoform plec-1k in the colon and breast cancer cell lines shows the progress of the real time PCR (Figure 3.5 A & C). The take off point (the point at which the PCR enters the exponential phase,

where the second derivative is at 20% of maximum level and noise level ends) of the PCR is around 29.7-33 cycles, which is relatively late compared to cycle 11.3-12 of actin PCR reactions (Table 3.2). The take off point is related to the starting copy number, but also takes into account the PCR efficiency. The efficiency of PCR is largely dependent on primer annealing, GC content and length of PCR product. Next, the curve enters the exponential phase where, as each cycle progresses, a doubling of product should be taken place if the efficiency of the PCR reaction is 100%, which most reactions do not reach due to limitations such as primer annealing efficiency, enzyme affinity to RNA or again product length. For plec-1k the average efficiency is 1.75 across the different samples, the other exons range from 1.7-1.8 with the control actin having a lower efficiency at 1.65 (Table 3.2). For the mRNA concentration of each sample to be comparable, the amplification efficiency should be around the same value. Because the results show that the deviation was less than 2.5 % for any of the reactions, this was deemed acceptable (Table 3.2). After the exponential phase, the PCR reaches the plateau, where the reaction is no longer in log-linear growth due to depletion of PCR components and renaturation of product that prevents further annealing. The height of the curve indicates the final product concentration. However, identical amounts of starting templates do not always result in identical yields that further support the need for real time analysis over semi-quantitative PCR. Figures 3.5B and 3.5C show the second derivative amplification plots, where the peak corresponds to the maximum rate of increase in fluorescence at each cycle. These plots give the comparative analysis between the samples. The relative concentration of each sample compared to the low-grade carcinomas was calculated based on the efficiency and take off point. The results show that in the colon carcinoma cells plec-1k expressions is increased in the aggressive SW480 colon cancer cell line but decreased in the aggressive MDA-MB-231 breast cancer cell line compared to the corresponding low grade HT29 and MCF7 cells. Similar calculations were carried out for all nine of the alternative N-terminal isoforms. Due to the variable efficiencies of different primer pairs for each N-terminal isoform, no attempt was made to quantify expression levels between the isoforms, but instead differences between cell lines for each isoform were investigated, as this was more relevant to the project.

Figure 3.4. Melt curves of real time PCR of plectin N-terminal isoforms.

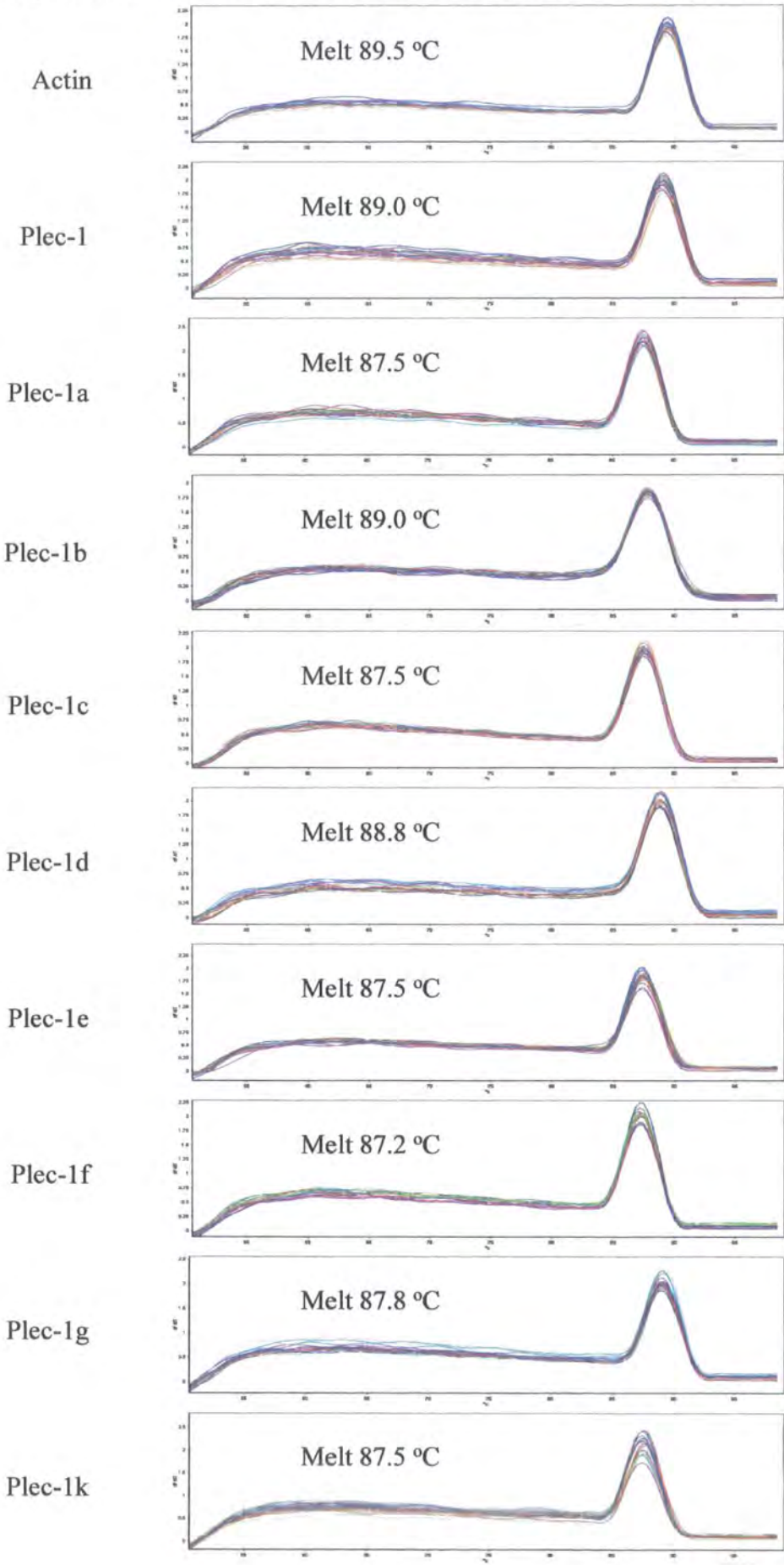


Figure 3.4. Melt curve analysis of real time PCR product.

Figure shows representative melt curves for each plectin alternative isoform from a real time PCR experiment with carcinoma cell lines. Y-axis is the relative fluorescence intensity (dF/dT) and X-axis measures the increase in melting temperature (°C). A single peak is shown where the PCR product melts and the decrease in fluorescence is detected. The temperature at which each product melts corresponding to the peaks is displayed.

Figure 3.5. Sybr green fluorescence in real time PCR of plectin-1k isoform.

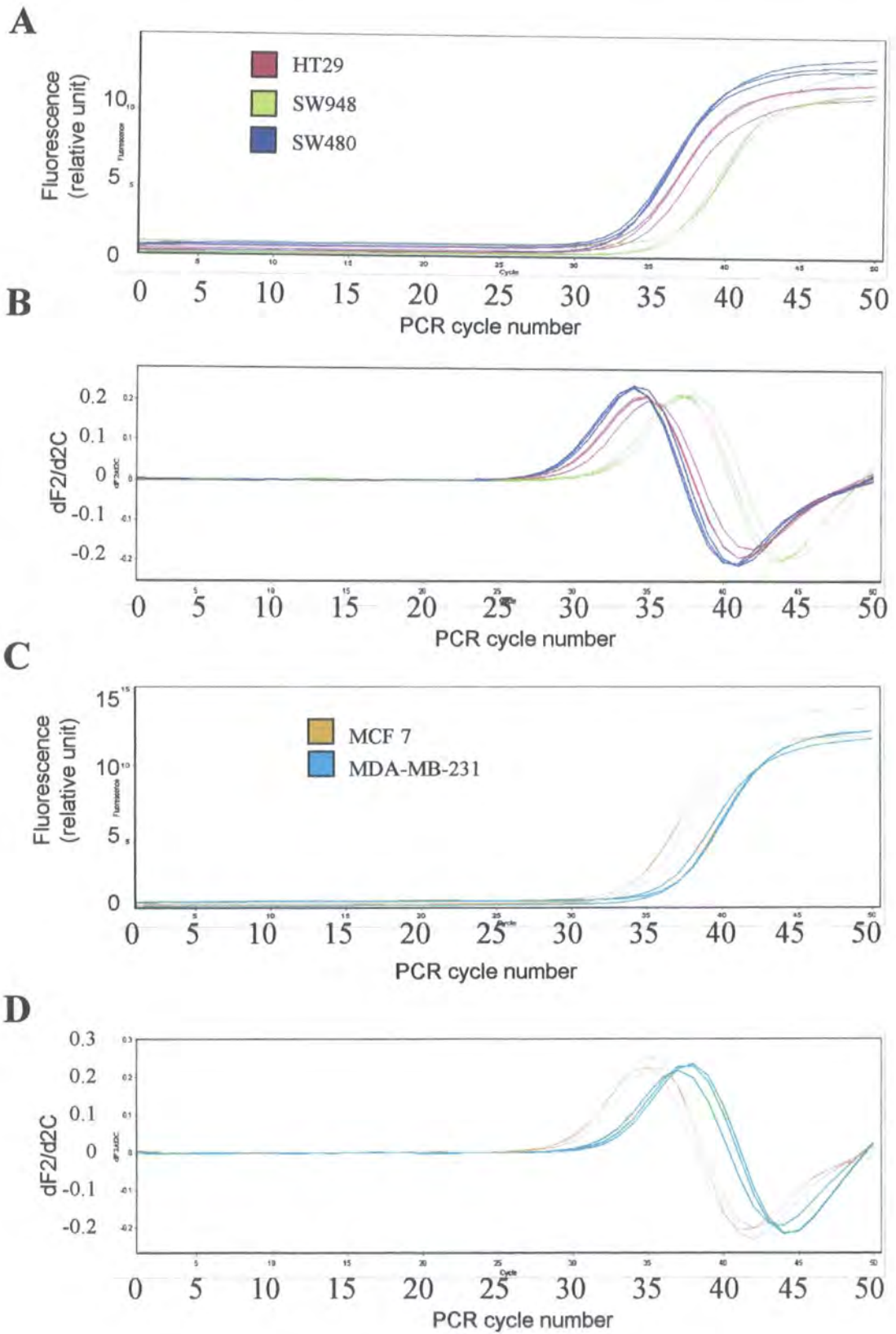


Figure 3.5. Sybr green fluorescence in realtime PCR of plectin-1K isoform.

Representative real-time PCR amplification plots showing an increase in Sybr green fluorescence from colon carcinoma cells HT29, SW948 and SW480 (A) and breast carcinoma cells MCF7 and MDA-MB-231 (C). The second derivative $dF2/d2C$ is plotted against cycle number for comparative quantification of colon (B) and breast (D) carcinoma cells.

Table 3.2. Take off points and amplification efficiency of real time PCR.

(a) The take off range lists the threshold cycle range obtained during realtime PCR of colon and breast cell lines for each exon (this is related to starting template). (b) The amplification efficiency lists the amplification of product for each cycle in the linear range and the deviation (+/-) between each sample for each exon PCR.

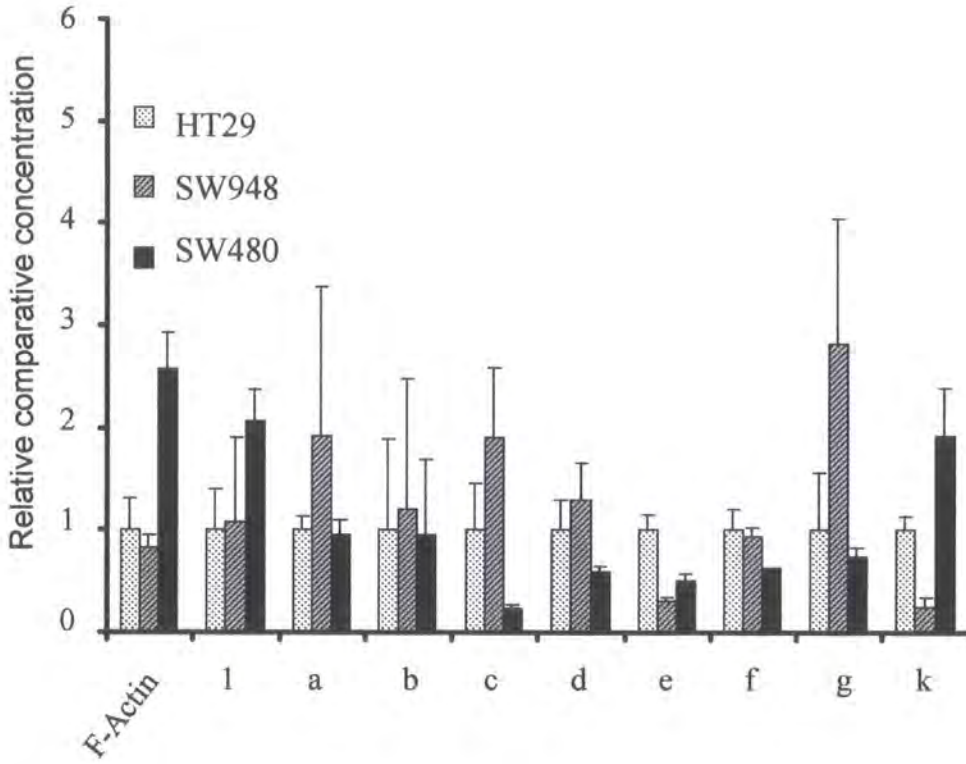
Exon	Take of range (cycle) (a)	Amplification efficiency (b)
Actin	11.3-12	1.64 +/- 0.03
1	24.5-26.8	1.73 +/- 0.03
A	26.7-29.3	1.72 +/- 0.02
B	26.6-29.6	1.73 +/- 0.02
C	23.2-27.4	1.74 +/- 0.02
D	23.3-25.5	1.73 +/- 0.04
E	17.9-20.0	1.74 +/- 0.04
F	24.7-28.1	1.70 +/- 0.02
G	21.7-24.9	1.77 +/- 0.03
K	29.7-33.5	1.74 +/- 0.02
Periplakin	17.5-20.6	1.70 +/- 0.02

3.2.10. Quantitative Real time PCR shows changes in isoform expression in cancer cell lines.

Comparative analysis was used in order to investigate the relative expression of N-terminal isoforms between low grade and high-grade colon and breast carcinoma cells. These data (Figure 3.6) were obtained from three independent RNA extractions and triplicate runs from each cell type shown. The grade II cell lines are used as the reference sample, to which all other cell lines are compared to in order to show changes between the grades. Actin, which is usually used as an endogenous reference gene (a gene that has stable expression between samples and used as a control), is not equal in all cell lines so can only be used as a positive control in the experiments. The starting RNA was quantified to ensure that comparable total cDNA levels from each cell line were used and, as further validation, comparison of independent RNA preparations confirmed constant levels of actin expression in the cell lines (note error bars for actin in Figure 3.6.). The high grade SW480 colon carcinoma cells show an increase in mRNA expression of isoforms 1 and 1k, and a decrease in the expression of isoforms 1c, 1d, 1e, 1f and 1g compared to HT29 cells, whereas the expression of isoforms 1a and 1b remain unchanged. The results for the intermediate SW948 cell line were less clear, owing to large variation between the samples (see error bars in Figure 3.6 A). Intriguingly, the breast carcinoma high-grade MDA-MB-231 cells have a relative increase in expression of isoform 1d and less so 1a when compared to the MCF7 cells. There is also a decrease in the expression levels of 1c and 1k, whereas the change in expression of the remaining isoforms 1, 1b, 1e, 1f and 1g is negligible. In summary, the correlation between invasiveness and expression of the isoforms is not uniform between colon and breast cancer cells. However, changes in mRNA expression of isoforms are observed in a cell type specific manner and this may contribute to the invasive potential of each cell line.

Figure 3.6. Real-time PCR of plectin N-terminal isoform mRNA expression in cancer cell lines.

A



B

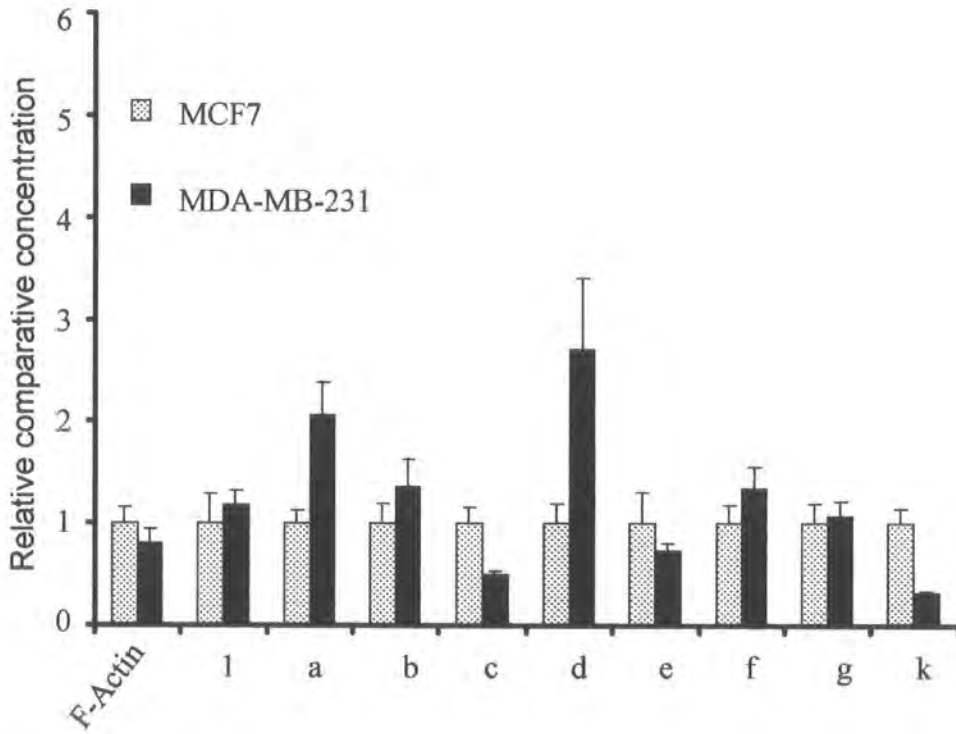


Figure 3.6. Realtime PCR of plectin N-terminal isoform mRNA expression in colon and breast cancer cells.

Realtime PCR analysis of the expression of plectin alternative N-terminal isoforms mRNA in a panel of colon (A) and breast carcinoma cells (B). Expression levels (from three independent RNA extractions with each sample run three times) are shown relative HT29 (A) or MCF7 (B). Error bars show mean standard deviation. Actin expression (right hand panel) was analysed as a positive control for each mRNA sample.

3.2.11. Expression of plectin N-terminal isoforms in a panel of human tissues.

Plectin is a ubiquitous protein that is expressed in all tissues. Detailed analysis of the expression of the mouse plectin isoforms reveals that there are tissue-specific differences in the expression of the alternative first exons (Rezniczek et al., 2003). To analyse the tissue distribution of the alternatively spliced isoforms of human plectin gene, I investigated a panel of human tissue RNAs by quantitative PCR (Figure 3.7). The human tissue RNAs were obtained from Ambion. First Choice Human Total RNA survey panel consists of pools of total RNA from 20 different normal human tissues and each pool consists of at least three tissue donors. Due to the high cost of the RNA panel the results have been repeated only twice to investigate any major differences between tissues. Plectin isoforms 1b, 1c, 1e and 1g show a constitutive expression pattern in the studied tissues. In contrast, the novel isoform 1k, as well as plectin-1, 1a, 1d and 1f displayed tissue specific differences in their expression patterns. Interestingly, plectin-1k expression was elevated in the colon and oesophagus. Plectin-1 expression was elevated significantly in the brain, oesophagus and thyroid. Plectin 1a was elevated in the placenta and ovary. Plectin-1d was upregulated remarkably in the heart and brain and also elevated in the spleen. Finally, plectin-1f expression was elevated in the brain and was hardly detectable in the kidney. These results show that there are tissue specific differences in the expression of a subset of human plectin isoforms.

Figure 3.7. Real-time PCR analysis of the expression of the plectin N-terminal splice variants in human tissues.

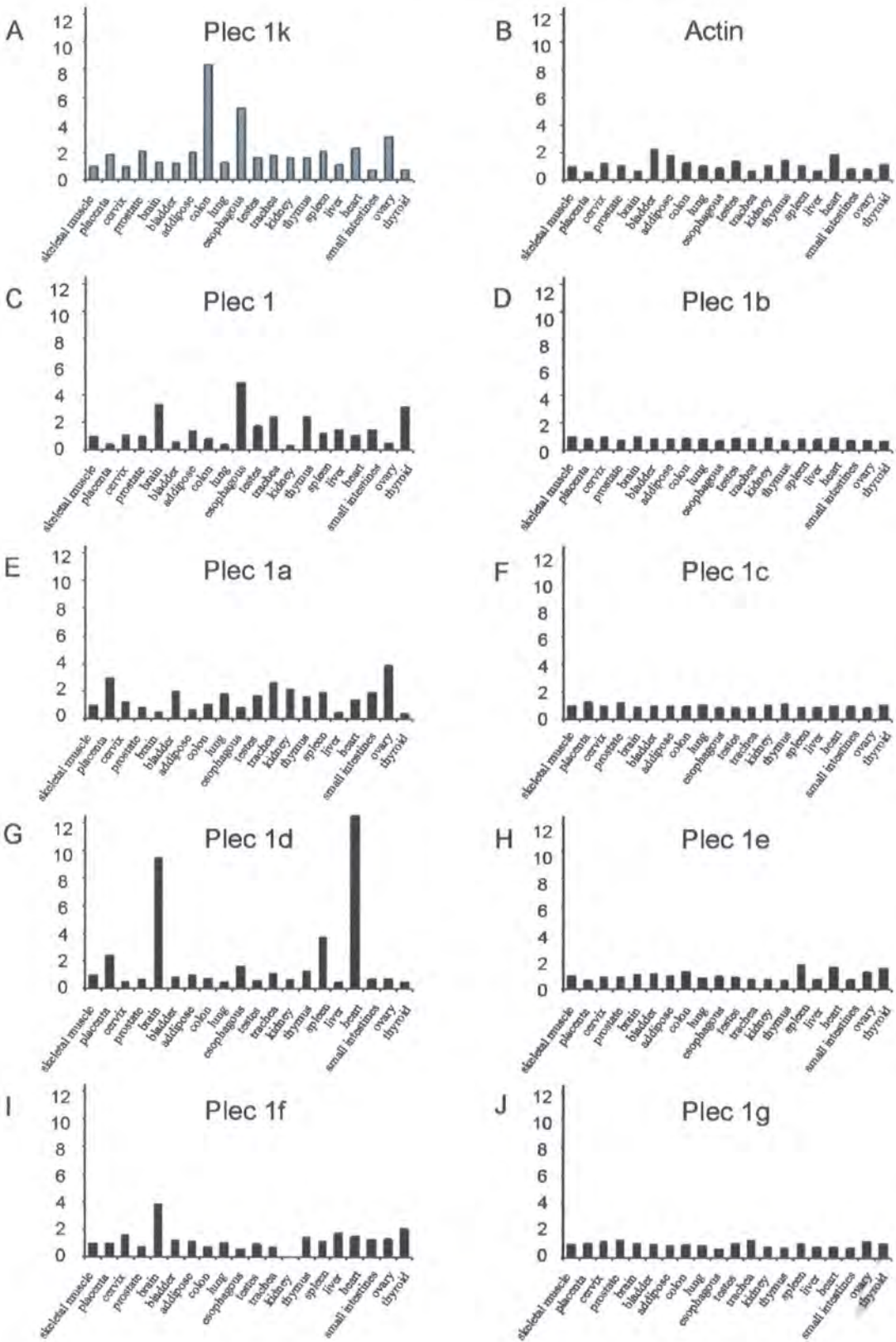


Figure 3.7. Realtime PCR analysis of the expression of the N-terminal splice variants in human tissues.

Real-time PCR was used to investigate the expression of plectin isoforms in a panel of total RNA samples from human tissues. Each isoform was analysed separately and the expression in different tissues is shown relative to mRNA levels in the skeletal muscle. The bars display two independent analyses.

3.3. Discussion.

The human plectin gene was shown to have similar diversity of plectin N-terminal isoforms as the mouse gene. In this study, the precise genomic localisation was determined for all plectin alternative N-terminal exons identified in the human gene and was found to be identical to both rat (Elliot et al., 1997) and mouse genes (Fuchs et al., 1999). Alternative splicing of the exons 2 and 3 (2α and 3α) that are found in the actin-binding domain of the mouse plectin were not identified in the human gene in this study since sequencing of all the PCR products showed direct splicing to a common exon 2.

Using semi-quantitative PCR to measure mRNA expression in the colon carcinoma cell panel, it was shown that isoform 1 was up-regulated and 1e down-regulated in the higher grade carcinoma cell SW480 compared to the lower grade HT29 and isoform 1f was constitutively expressed. These results indicated that a subset of plectin isoforms could be altered during progression of cancer. To further investigate these results, Real-Time PCR was used to provide a quantitative analysis of the plectin isoform expression in the colon carcinoma cell line panel and in two breast carcinoma cell lines. The results of upregulation of the isoform 1 and down regulation of the isoform 1e correlated with the semi-quantitative PCR results. Furthermore, the down regulation of isoforms 1c 1d 1e 1f was observed in high grade SW480 cells compared to low grade carcinoma cells. The intermediate SW948 (grade II/III) cell line showed large variation between the samples. One possible explanation is presented in chapter four (Figure 4.5B) where the SW948 cells are shown to grow in unusual stratifying colonies of variable size which may affect the plectin isoform mRNA levels between samples. The results from the breast carcinoma cells were partially different than in the colon carcinoma panel. This result is of interest as it shows that even though the expression levels of plectin isoforms do change when low grade carcinoma cells are compared to high grade cells, the changes are cell type specific. The study of the role of these isoforms in human carcinoma cell invasion and migration will be investigated at the protein level in the subsequent chapters.

Interestingly, the upregulation of isoform 1 in the higher-grade carcinoma cells may support a recently found role for isoform 1 in cell migration. Dermal fibroblasts

isolated from plectin-1-deficient mice exhibited abnormalities in their actin cytoskeleton and impaired migration (Abrahamsberg et al., 2005). Evidence that the expression of the N-terminal exons has an important role in the subcellular localisation of plectin was found when a GFP-plectin-ABD fusion protein was expressed without any of the first exon sequences. Transfections of this construct resulted in mostly diffuse, only weakly stress fibre -associated expression pattern, which is in stark contrast to localisation of protein domains containing the alternative first exons to either stress fibers or focal adhesion sites (Rezniczek et al 2003). My results suggest that changes in regulation of mRNA levels of the plectin N-terminal isoforms take place during cancer progression and it may, thus, be worthwhile to investigate plectin isoform mRNA expression levels in carcinomas compared to normal tissues or less aggressive cancers.

This study also provides the first quantitative realtime analysis of plectin alternative N-terminal first exon expression in human tissue samples. The results indicate that several isoforms have unique tissue-specific expression patterns, whereas some isoforms, such as plectin-1b that co-localises with mitochondria (Rezniczek et al., 2003), are constitutively expressed in all tissues contained in the RNA panel (Figure 3.7). Thus, it is likely that the regulation of the alternative plectin promoters is complex and may involve both shared and unique, tissue-specific regulatory elements. Previously the expression levels of some plectin N-terminal isoforms has been investigated using RNA protection assays of total RNA isolated from various mouse (Fuchs et al., 1999) and in rat (Elliot et al., 1997) tissues. The mouse study used a small panel of tissues including lung, brain, kidney, small intestine, heart, muscle, skin, liver, uterus, spleen and salivary gland. The mouse plectin isoforms 1d and 1b were exclusively found in skeletal muscle, heart and skin. Plectin-1a was found in epithelial tissue types such as lung, small intestine and skin. Plectin=1 transcripts were found in tissues with high connective tissue content such as muscle skin and uterus. Finally, isoforms 1e, 1f and 1g had a broad expression pattern. The rat study included muscle, heart, brain, testis, lymph nodes, thymus, and kidney tissues. Transcripts containing exons 1, 1a and 1b were found in all the investigated tissues. Plectin-1 and 1b were expressed in heart muscle in heart, whereas plectin-1a was predominantly expressed in lymph nodes, thymus and kidney. When comparing the human, mouse and rat data, it is apparent that there are tissue specific expression differences in

expression of plectin isoforms across the species. The subset of isoforms that show specific differences in human tissues, plectin isoforms 1, 1a and 1d are also variably expressed in the mouse tissues and the constitutively expressed isoforms 1e, 1f and 1g are also broadly expressed in the mouse tissue panel. However, the expression of isoforms 1b and 1c is variable in the mouse tissues but constitutive in the human RNA panel. Although variable expression pattern of the isoforms is in most cases conserved between different species, the tissue-specific differences between are not always conserved. This is most evident in the case of plectin-1d that shows elevated expression in murine skeletal muscle and heart tissues and low expression in the brain whereas in the human study plectin-1d mRNA is markedly elevated in brain and heart tissues compared to the skeletal muscle. The tissue specific expression of the N-terminal plectin isoforms suggests that multiple promoters may control expression of the gene. The complexity of the plectin gene was further underlined by findings that the 5' end on the plectin-1 gene overlaps in a head to tail manner with the 3' end of the Parp-10 gene, a recently identified poly (ADP-ribose) polymerase (Lesniewicz et al., 2005). This result indicates that the promoter of plectin-1 isoform is actually located in the Parp-10 gene and could provide an interesting example of regulated gene expression.

In summary the complexity of the human plectin gene with the ability to generate several N-terminal isoforms that show tissue specific expression could provide an important regulatory mechanism of protein function. Furthermore, understanding the expression of plectin isoforms in cancer may lead to a better understanding of metastatic potential.

CHAPTER 4
EXPRESSION AND SUBCELLULAR
LOCALISATION OF PLECTIN PROTEIN
ISOFORMS IN CARCINOMA CELLS.

4.1. Introduction.

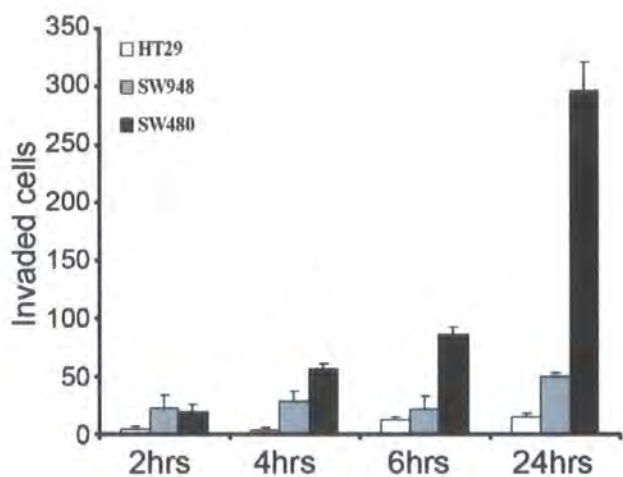
There has been no published study investigating the localisation of plectin in cancer cells of increasing invasiveness, as focus has been mainly on the expression in the epidermis and muscle and their related diseases. Plectin was originally identified as a component of hemidesmosomes, where it was shown to localise to the cellular periphery at cytoskeleton-membrane interaction sites in frozen sections of stratified skin epithelia and muscle tissues (Wiche et al., 1983, 1984; Hieda et al., 1992; Foisner et al., 1994). Additionally, Eger et al., 1997 showed that upon a loss of cell polarity plectin is relocated from the cell periphery at the desmosomal plaque to a cytoplasmic vimentin- and cytokeratin-related network. Further work investigating cytoskeletal dynamics in plectin null fibroblasts has established that, in addition to its structural role, plectin regulates actin dynamics as plectin-deficient fibroblasts show delayed actin re-organisation and impaired motility (Andra et al., 1998). Plectin has the ability to interact with actin through its N-terminal calponin homology actin-binding domain. Moreover, Rezniczek et al., 2003 showed that small alternative N-terminal sequences (5-180 residues) coding for eight of the mouse plectin isoforms could profoundly affect the sub-cellular localization of plectin. Thus, it was interesting to find out, if the human N-terminal plectin isoforms characterised in Chapter 3 could also effect the sub-cellular localisation of plectin in the carcinoma cells and whether the localisation could have a specific role in migration and invasion. In this chapter, I first characterise the breast and colon carcinoma cell lines using a collagen invasion assay to determine the invasive potential. Next, the expression of plectin and other cytoskeletal proteins was investigated in the panel of carcinoma cell line using immunofluorescence and immunoblotting.

4.2. Results.

4.2.1. High-grade SW480 and MDA-MB-231 cells show an increase of invasive potential compared to their lower grade counterparts.

To investigate whether the observed changes in plectin isoform expression levels were related to invasive phenotype of the cells, it was important to determine the invasiveness of the studied cancer cell lines. The invasive potential of the carcinoma cell lines was investigated using collagen coated Boyden chambers (Figure 4.1). Collagen gels, rather than basement membrane preparations, were chosen, as we were interested in invasion through the stroma in the later stages of cancer cell invasion. Fibrillar collagen is the main constituent of the connective tissue matrix that is degraded by several proteases during cell invasion (Wolf et al., 2003). Within the colon carcinoma cell panel, SW480 (grade III/IV) cell line displayed approximately 20 fold increase in the invasion through collagen compared to lower grade HT29 (grade II) cells. The intermediate grade SW948 cell line was only slightly more invasive than the HT29 cell line. The breast carcinoma cells panel were more invasive than the colon carcinoma cells (note scale difference), with the MDA-MB-231 cell line demonstrating an invasive potential that significantly exceeded the lower grade MCF7 cells by 9 times. The results show that in a collagen invasion assay the higher grade SW480 and MDA-MB-231 cells invade more aggressively than their lower grade counterparts. The mechanisms of invasion will be further discussed and investigated in Chapter 5. In conclusion the breast and colon panel of cell lines, with the demonstrated differing invasive potential is a powerful tool for the further investigation of the role of plectin in cancer cells.

A



B

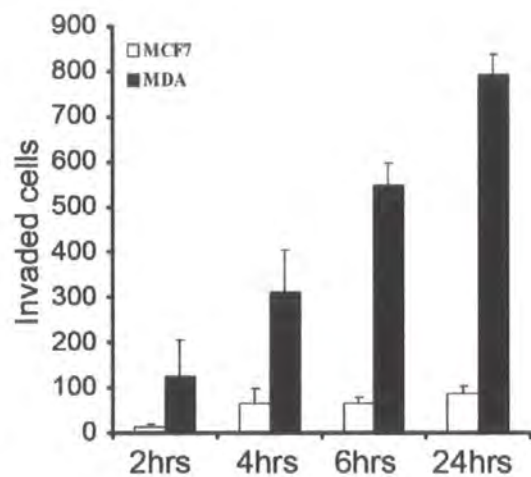


Figure 4.1. Collagen gel invasion of carcinoma cells.

(A) Invasion assay of colon carcinoma cells through collagen-coated cell culture inserts. Mean invaded cells/microscopic field from three independent experiments are shown. Error bars denote standard deviation. (B) Migration assay of breast carcinoma cells.

4.2.2. Investigation of expression levels of cytoskeletal and related proteins in the panel of carcinoma cell lines.

In order to study migration and invasion in the panel of cell lines and to expand on the results of mRNA expression analysis, the expression levels of plectin and other related cytoskeletal proteins were investigated at protein level. Immunoblotting of total cell extracts from the panel of breast and colon cells allowed identification of proteins that could play a key role in the invasive potential of carcinoma cells. The total cell extract from five independent experiments was quantified and identical quantities of protein were loaded to each lane so they could be compared. Actin was originally used as a loading control, but it's to be noted that the cell lines have slight differences in actin expression; therefore the BCA protein assay (Section 2.7.2) was used to quantify protein levels prior to loading of the gel. Equal loading was further confirmed visually by staining of the filters with Ponceau S (which stains total proteins red). Molecular weight markers were used to identify correct band sizes of the proteins.

4.2.3. Plectin is over-expressed in the more invasive cell lines.

Strikingly, plectin was found to be over-expressed in the invasive SW480 and MDA-MB-231 cell line compared to the less invasive cells. Furthermore, desmoplakin is down regulated in the invasive colon and breast carcinoma cells which correlates to the previous study on breast tumours (Davies et al., 1999). Surprisingly, there is a high expression of desmoplakin in SW948 cell line; this will be investigated using immunofluorescence. The invasive phenotype is also associated with vimentin expression with a decreased keratin expression in MDA-MB-231 cells, which is typical of epithelial to mesenchymal transition (Franke et al., 1982) that will be discussed in Chapter 5. Interestingly, periplakin, another member of plakin family of cytoskeletal linker proteins, also shows an increase of expression levels in the more invasive cell lines. Periplakin has been implicated in formation of the cornified envelope (Di Colandrea et al., 2000), but recent work has shown that periplakin can co-distribute with plectin to regulate keratin organisation and epithelial migration (Long et al., 2006 and Boczonadi et al., 2007), so its not surprising that an upregulation of periplakin is seen along with plectin in more invasive cells. Vinculin and talin, which are components of the focal adhesion complex, were up regulated in the invasive MDA-MB-231 cell line compared to MCF7 cells, but in the colon carcinoma cells only the metastasis-derived T84 cell line demonstrated an upregulation

compared to HT29. Vinculin is traditionally viewed as a stabiliser of focal adhesions (Gallant et al., 2005) that suppresses cell migration, however vinculin has been found to modulate signalling pathways regulating focal adhesion dynamics (reviewed in Ziegler et al., 2006). Furthermore, focal adhesions located at the edge of several endothelial cell types show association with both the microfilament and vimentin intermediate filament cytoskeletons (Gonzales et al., 2001). It is, therefore, not necessarily surprising that the MDA-MB-231 cells, which express a vimentin cytoskeleton instead of the keratins 8 and 18 have a high expression of vinculin. HSP27 a small heat shock protein is upregulated in SW480 cells, which is in agreement with several studies showing an increase in HSP27 expression in many cancers (reviewed by Ciocca et al., 2005). However, contrasting this, down regulation of HSP27 was seen in the more invasive MDA-MB-231 breast carcinoma cells, HSP27 expression in breast carcinoma cells has been widely studied and over expression in the MDA-MB-231 cell line leads to an increase in invasiveness but decreased motility (Morino et al., 1997, Lemieux et al., 1997). E-cadherin expression is down regulated in the invasive SW80 cell line compared to HT29 with recovery in the T84 cell line. Even more pronounced is the absence of E-cadherin expression in MDA-MD-231 cells compared to MCF7 cells. E-cadherin has also been widely studied in cancer with down-regulation of the protein seen in the progression of many cancers leading to a decreased survival in patients (see reviews by Mareel et al., 1992, Mareel et al., 1994, Jiang et al., 1996 and Bremnes et al., 2002).

These results show that that a subset of cytoskeletal proteins is altered as the invasive potential increases. The localisation of these proteins in cancer cells and their possible roles in migration and invasion will be investigated in the Chapters to follow. The elevated expression of plectin in the invasive SW480 and MDA-MB-231 cells was intriguing as previous studies on plectin in epithelial cells have concentrated on its role as a hemidesmosomal protein but not addressed the role of plectin in invasive carcinoma cells. Furthermore, the difference in vimentin, keratin and vinculin expression between the invasive MDA-MB-231 and SW480 cells may indicate that these cells use different mechanisms of migration invasion and attachment.

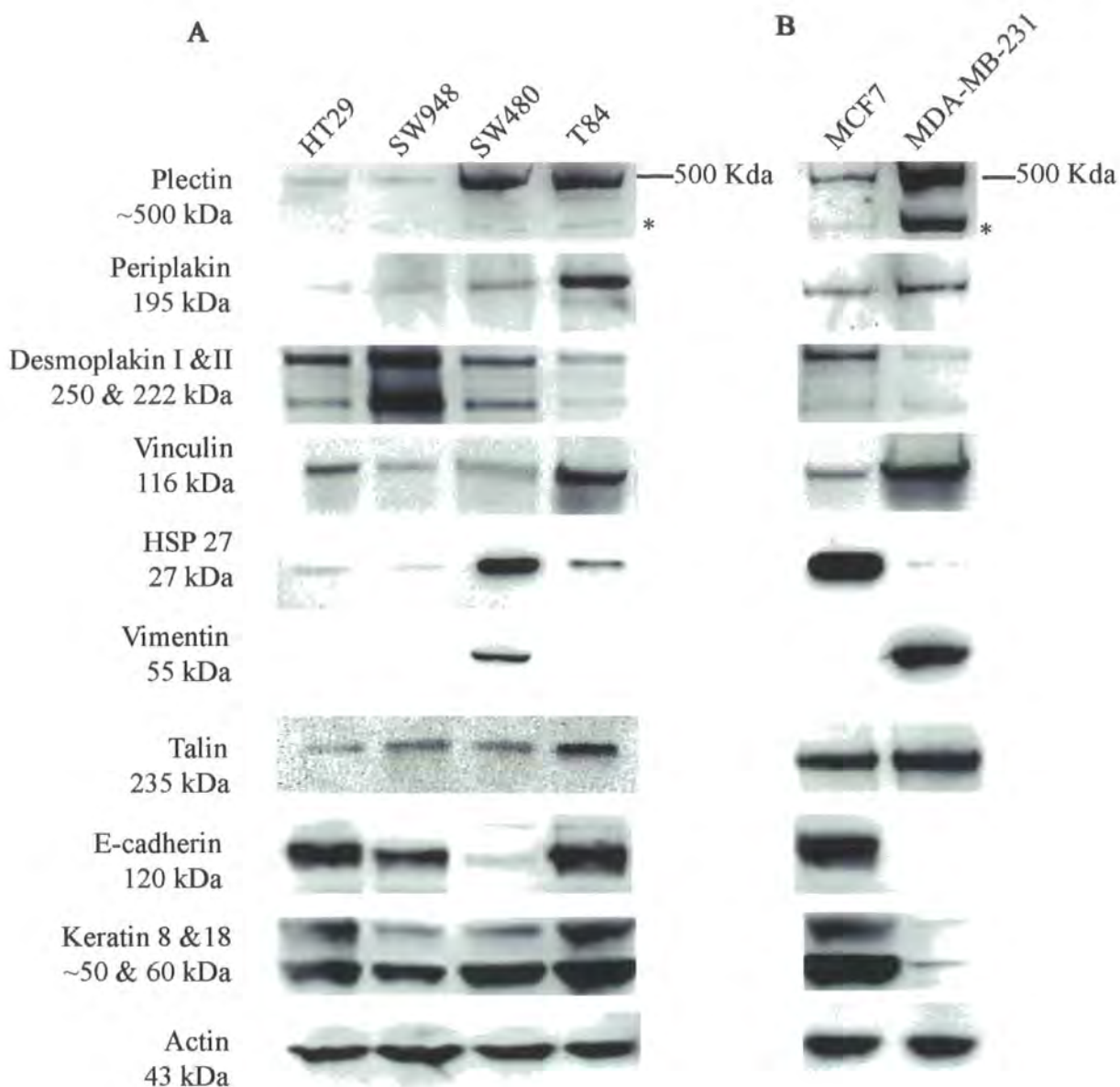


Figure 4.2. Expression of cytoskeletal and related proteins in carcinoma cell lines.

The changes in expression of cytoskeletal proteins, in a panel of carcinoma cell lines, is investigated by immunoblot analysis. Actin is used as positive control between cell extracts. Shown is a representative immunoblot of at least three independent cell extracts for each protein. (A) Immunoblot analysis of expression of cytoskeletal proteins in colon carcinoma cell lines. (B) Immunoblot analysis of cytoskeletal proteins in breast carcinoma cell lines. Note, the plectin antibody detects two distinct bands and several faint bands lower than the 500 kDa marker, possibly due to alternative isoform expression.

* denotes a lower molecular weight band of the rodless plectin.

4.2.4. Plectin is recruited away from the cell periphery in the more invasive carcinoma cells.

To study the role of the cytoskeletal proteins further, immunofluorescence was used to investigate their subcellular localisation and organisation within the colon and breast carcinoma cell lines. The results obtained in this study show that in the non-invasive HT29 cells, plectin is localised to the cell periphery and lamellipodia, co-localising with the keratin 8/18 filaments (Figure 4.3A, arrow). The plectin expression in SW948 cells, which have similar invasive potential to HT29 cells, (Figure 4.1) is also found at the cell periphery localising with keratin bundles. Contrasting this, plectin localisation in the invasive SW480 cells plectin is found throughout the cytoplasm localising with the cytoplasmic keratin 8/18 network and not especially to the cell periphery in the manner observed in the HT29 cells (Figure 4.3A). The T84 cell line, derived from lung metastasis has a less well-defined intermediate filament network where plectin expression is cytoplasmic. Plectin is also found at the cell edges along with keratin bundles in T84 cells. In all studied colon carcinoma cell lines, plectin is observed to colocalise with the keratin cytoskeleton (Figure 4.3A), which supports both previous work showing that the C-terminal domain of plectin links to the intermediate filament cytoskeleton (Sevcik et al., 2004) and initial studies showing the co-purification of plectin with the intermediate filament protein vimentin (Wiche et al., 1982). Similar observations were made in the breast carcinoma cells. In MCF7 cells, plectin is preferentially localised at the cell periphery (Figure 4.3B), where it is co-localised with keratin. MDA-MD-231 cells, that almost exclusively express vimentin with extremely low levels of keratin 8/18 (as shown immunoblotting Figure 4.2), show a dense vimentin network around the nucleus with plectin co localisation. Plectin and vimentin expression is also found throughout the cytoplasm and at cell periphery in these cells (Figure 4.4B). Plectin was also shown to localise with the vimentin cytoskeleton in SW480 cells (which expresses vimentin along with the keratin 8/18 network). In these cells, vimentin is localised both to the perinuclear area in a dense cage together with plectin (Figure 4.4A) and throughout the cytoplasm. When the sub-cellular localisation of vimentin and keratin 8/18 networks was investigated by double staining (Figure 4.4C), it was found that they both co-localised in a cytoplasmic network, but vimentin expression was more intense at the perinuclear region than the keratin expression. To summarise the above findings, plectin was found at the cell periphery of non invading cells co-localising with the keratin 8/18 network, whereas in the invasive cells that

express vimentin, the strongest plectin expression was observed in the vimentin rich cage surrounding the nucleus.

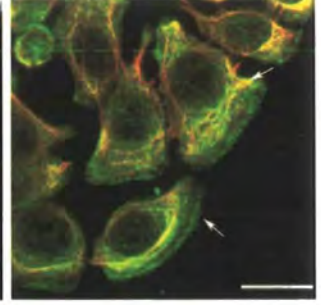
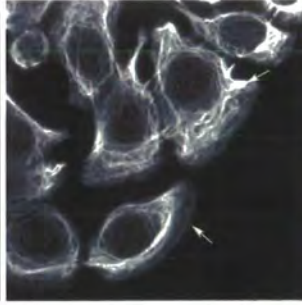
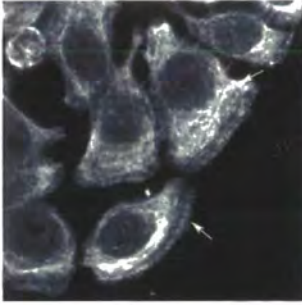
A

Plectin c-20

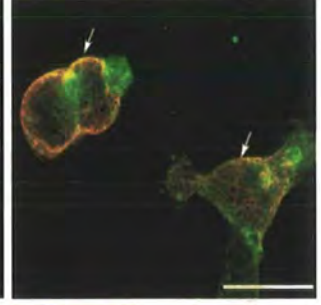
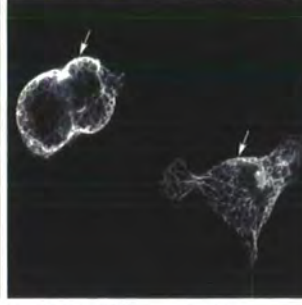
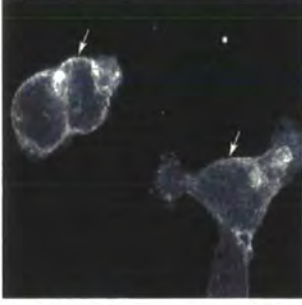
Keratin 8 & 18

Merge

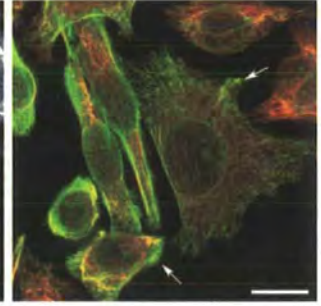
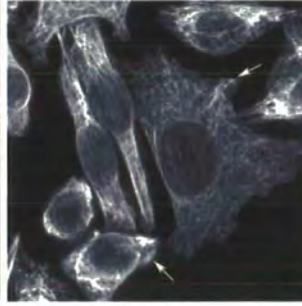
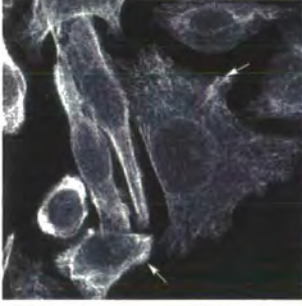
HT29



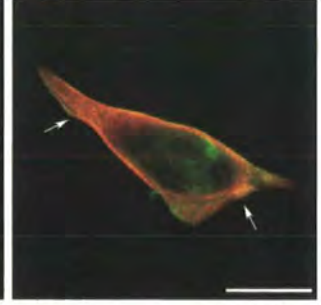
SW948



SW480



T84



B

MCF7

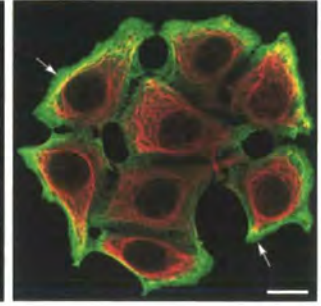
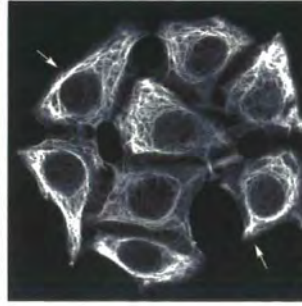
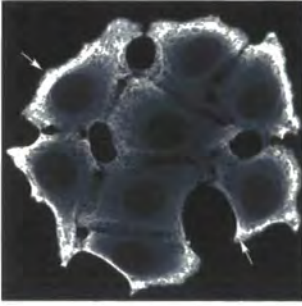


Figure 4.3. Co-expression of keratin 8 & 18 and plectin protein in carcinoma cells. (A) Confocal microscopy of single plane immunofluorescence indicating the sub-cellular localisation of plectin (green) with keratin 8 & 18 (red) in colon carcinoma cell lines. Co-localisation of the two proteins is shown in the cells with arrows pointing to examples of strong co-localisation (yellow). (E) Keratin 8 & 18 expression in breast carcinoma cell line MCF7 showing a dense intermediate filament network with co-localisation of plectin, note the elevated plectin expression at the cell periphery (Arrow). Scale bars 20µm.

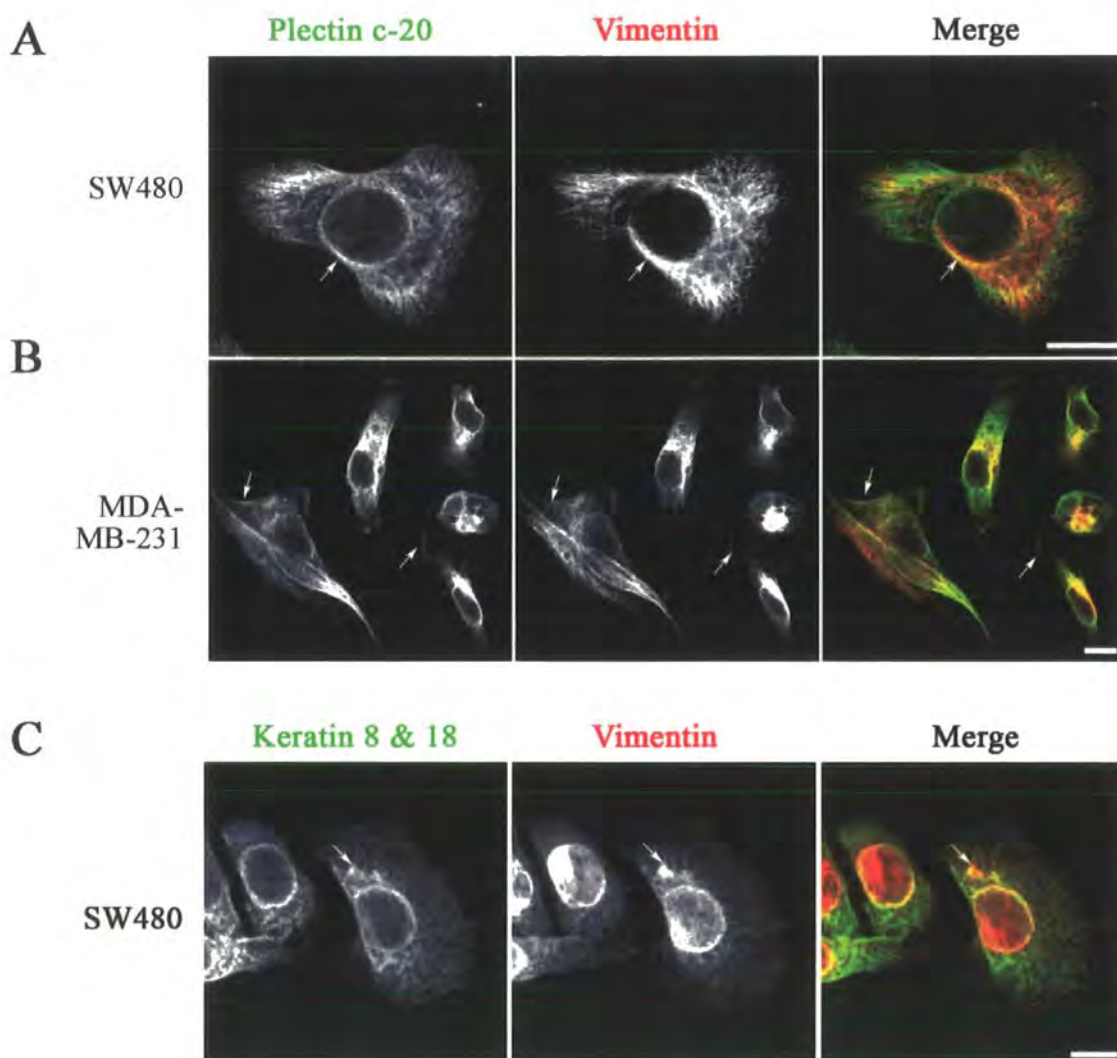
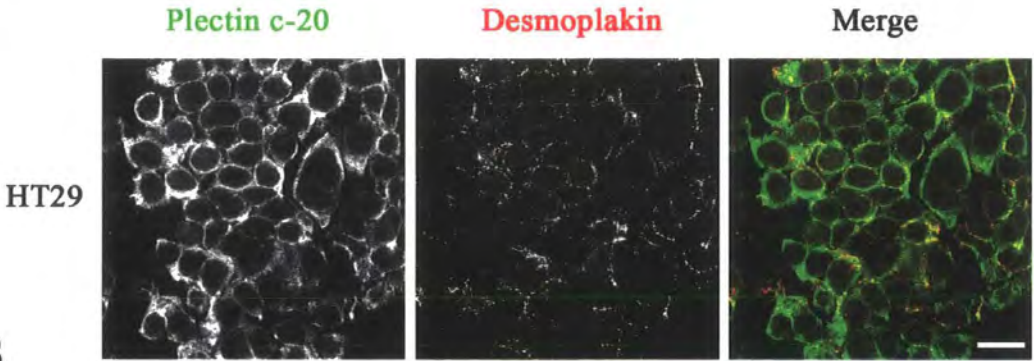


Figure 4.4. Subcellular expression of vimentin in SW480 and MDA-MB-231 cells. Single plane confocal images of immunofluorescence showing the vimentin network expression in the colon carcinoma SW480 and breast carcinoma MDA-MB-231 cells. (A) Partial co-localisation of plectin and vimentin expression is visible in SW480 cells with a dense network around the nucleus (arrow). (B) Co-expression of vimentin and plectin in MDA-MB-231 cells. Arrows points to co-localisation of filaments. (C) Co-expression of the keratin 8 & 18 and vimentin intermediate filament networks in SW480 cells showing partial co-localisation (arrow). Scale bars indicate 20 μ m.

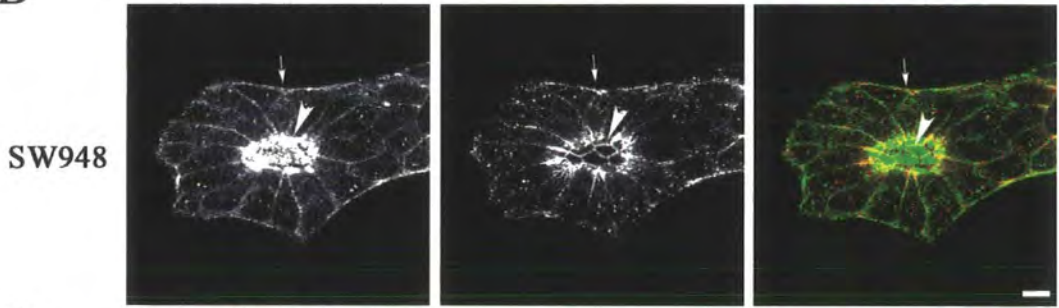
4.2.5. Invasive cell lines are not able to form a well-organised epithelial monolayer.

Desmoplakin is arranged in desmosomal-like junctions at the cell periphery of HT29 cells with plectin localising to the cell periphery and cell junctions (Figure 4.5A). The above finding is supported by the previous work that found plectin to be closely associated with the desmosomal plaques in Madin-Darby canine kidney (MDCK) cells, (Eger et al., 1997). Desmoplakin was found to be highly expressed in the SW948 cell line (Figure 4.2) compared to the other carcinoma cells, this result is also mirrored in immunofluorescence (Figure 4.5B). The SW948 cells were observed to grow in multilayered colonies formed around three days after passaging the cells. The cells in this arrangement are tightly packed and form dense desmosome-like junctions, evident from the elevated desmoplakin expression at the cell junctions (Figure 4.5B arrow head). Interestingly, the invasive SW480 cells were observed to form some epithelial-like islands with desmoplakin decorating cell borders (Figure 4.5C arrowhead). However, the majority of cells formed a disarranged monolayer of cells with sparse desmosomal-like adhesions and low desmoplakin expression. Furthermore, high-resolution confocal images of HT29 cells showed that desmoplakin is located to cell-cell contacts as dense cytoplasmic plaques (Figure 4.5D). This finding correlates with previous work that has shown desmoplakin-containing fluorescent bright dots associated with keratin IF in the cytoplasm of cells grown in low calcium conditions. The authors interpreted these “dots” as desmosome precursors that translocate to the membrane to assemble the plaque (Jones et al., 1985). More recently, live cell imaging experiments utilizing GFP-tagged forms of desmoplakin demonstrate the translocation of non-membrane bound cytoplasmic desmoplakin-containing dots to sites of desmosome assembly (Godsel et al., 2005). Interestingly, plectin is seen to colocalise to the cell junction but not specifically with the desmoplakin dots in the HT29 cells, speculating that plectin is not involved in desmosomal assembly but can localise to desmosomes at later stages.

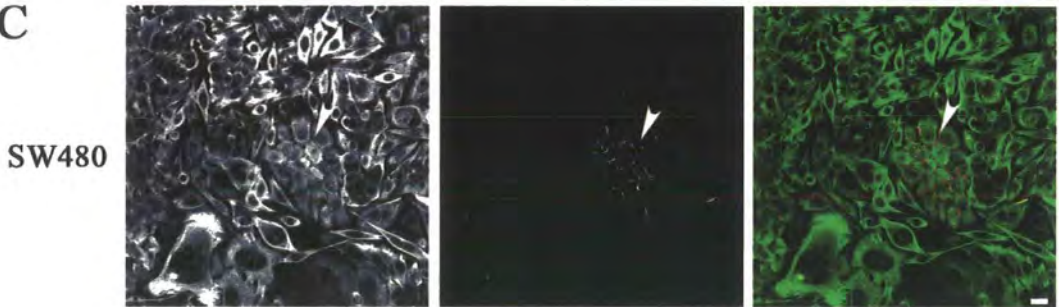
A



B



C



D

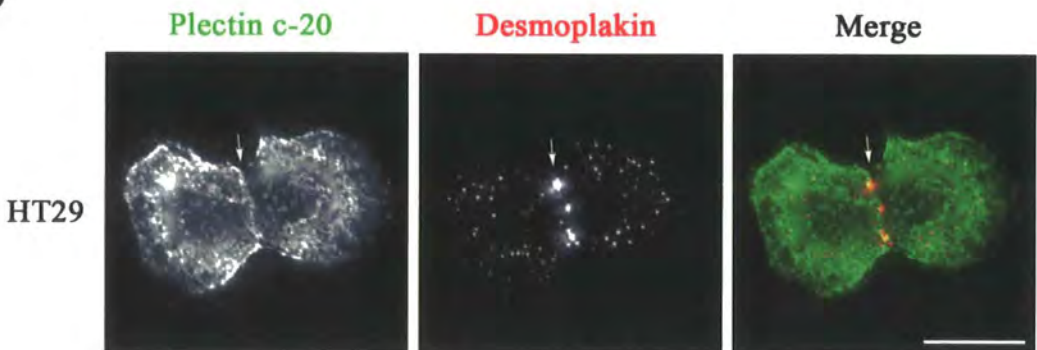


Figure 4.5. Desmoplakin and plectin immunofluorescence in colon carcinoma cells.

(A) Desmoplakin expression in HT29 cells decorating cell borders with plectin localised to the cytoplasm and at the cell periphery (scale bar 50 μm). (B) Desmoplakin and plectin expression in a colony of SW948 cells, arrow points to desmoplakin and plectin localisation at cell borders and arrow head points to tightly packed cells in the centre of the colony with desmoplakin decorating cell borders (scale bar 20 μm). (C) SW480 cells with occasional epithelial islands (arrow head) with desmoplakin localising to desmosome-like adhesions (scale bar 20 μm). Note plectin expression localising more to the cytoplasm and in perinuclear areas in SW480 cells compared to the lower grade HT29. (D) A larger resolution of the cell-cell junctions between HT29 cells with high expression of desmosome-like plaque areas, plectin is also localised at cell-cell contacts (arrow) along with expression at the cell periphery and in the cytoplasm (scale bar 20 μm).

4.2.6. Plectin co-localised with the actin cytoskeleton in cancer cell lines.

In the HT29 cells, that have a rounded morphology with small cytoplasm, the actin cytoskeleton is arranged at the cell periphery with thick bundles of fibers. The arrangement of plectin in the HT29 cells was found to interact primarily with intermediate filament network (as seen in Figure 4.3A) with partial actin co-localisation at the cell periphery (Figure 4.6A). Immunofluorescence analysis of SW948 cells show that within the multilayered cell colony, there is an elevated actin expression in the central cells, where the tightly packed filaments cannot be resolved with confocal microscopy. The cells at the edge of the colony show peripheral co-localisation of actin and plectin (Figure 4.6B). The invasive SW480 cell line has a tight basket actin network around the nucleus similar to that observed with vimentin. Figure 4.4C shows a section through the middle of SW480 cells showing plectin and actin co-localising in thick actin bundles, plectin can also be observed to localise to the fine actin meshwork at the leading edge of the cell (arrow). Further investigation of actively migrating SW480 cells revealed a third type of co-localisation of actin and plectin in round adhesion foci. These structures, which are investigated in Chapters 5 and 6, were abundant in scratch wound edge cells but rarely seen in resting cells of SW480 monolayer. In the T84 cells actin is localised to the cell periphery in long stress fibres and also elevated at the perinuclear region, actin plectin expression in these cells is not defined (Figure 4.6 D). The invasive MDA-MD-231 cells show expression of actin and plectin that is localised in the cells similar to the SW480 colon cancer cells. However, actin is arranged into more pronounced stress fibres in these cells (Figure 4.6E). These results show that plectin is able to colocalise with the actin cytoskeleton in carcinoma cells and it can suggested that the more invasive cell lines have more pronounced co-localisation of actin and plectin than the non-invasive cells and this may have a bearing on the migratory potential of these cells. Further elucidation of the role of the alternative N-terminal isoforms have on the localisation of plectin to actin will be investigated using GFP expressing alternative plectin N-terminal domains fused to a GFP tag and by isoform specific antibodies.



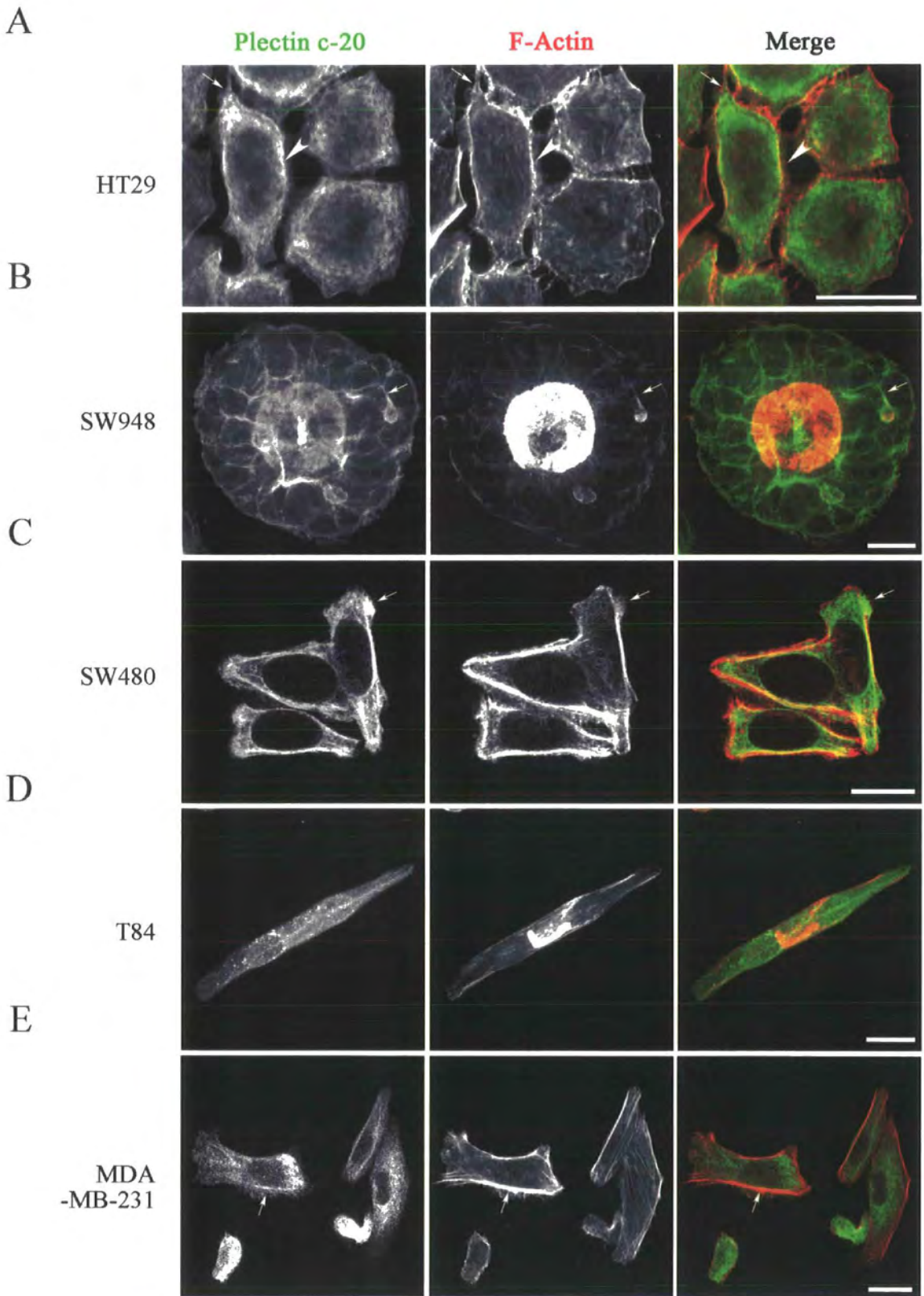


Figure 4.6. F-actin sub-cellular localisation in carcinoma cells.

Confocal single plane images of carcinoma cells showing F-actin (phalloidin staining) expression co-stained with plectin. (A) Thick actin bundles localise at the cell periphery of HT29 cells, with plectin co-localising at actin bundles (arrowhead). The arrow points to actin cytoskeleton extensions co-localising with plectin. (B) Colony of SW948 with high expression of F-actin in the cells located in the central of the colony, arrow shows actin and plectin co-localisation at cell periphery of cells of the outer layers of the colony. (C) SW480 cells with thick actin bundles co-localising with plectin, arrow shows co-localisation of filaments. (D) T84 cells expressing actin and plectin, note a plectin cytoskeleton networks are not defended in these spindle shaped cells. Actin is expressed perinuclear and at the cell periphery. (E) Stress fibres are visible in MDA-MB-231 cells throughout the cytoplasm with thick actin bundles at the periphery and plectin is localised as a network in the cytoplasm in this case. Scale bars indicate 20 μ m.

4.2.7. Expression of eGFP-tagged alternative plectin actin-binding domains in stable cell lines.

Alternative N-termini of the human plectin gene, including the actin-binding domain to exon 8, were tagged with C-terminal eGFP and transfected into SW480 cells (Figure 4.7A). Stable cell lines for each isoform were established using antibiotic selection (refer to Section 2.4.4) in order to obtain cultures of constitutively expressing N-terminal isoform-GFP protein. Due to the heterogeneous nature of the SW480 cell line, it was decided that stably selected mixed clones would be used, as single cell clones gave cultures of variable phenotypes that were difficult to compare. Use the heterogeneous cell lines allowed for a wide spectrum of subcellular localisation of the N-terminal GFP constructs to be validated. It should be noted that the short N-terminal constructs lack the C-terminal intermediate filament binding domain of plectin that can play a role in the localisation of the protein. However, the aim of these experiments was to investigate the effect the N-terminal exons have on localisation of plectin to actin-rich structures. The immunoblot (Figure 4.7B) shows the expression of GFP constructs in stable selected cells. Lane one shows the control cell line expressing GFP alone with a band at the expected size of 27 kDa. Plec-1-eGFP is seen as a higher molecular weight band compared to the other isoforms as expected. Note that the GFP-antibody used also recognised non-specific proteins in every lane and a star denotes the specific protein bands. Expression of the construct plec-1a-eGFP was not visible in transient transfections and no stable cell line could be established in these cells, although the cloned sequence was confirmed as correct using BLAST (NCBI) and the GFP-tag was in frame with the ATG start site.

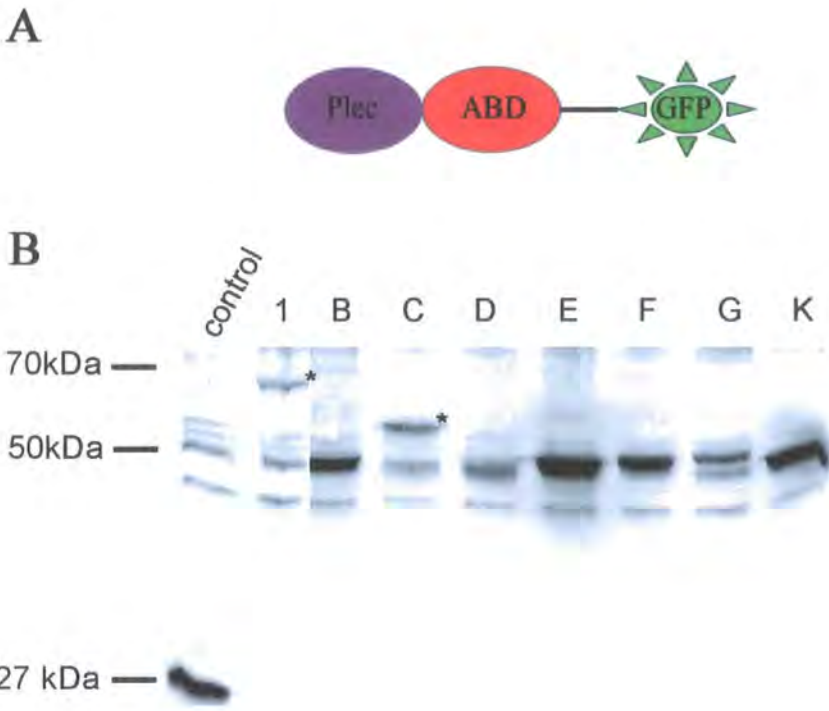


Figure 4.7. Expression of eGFP-tagged plectin N-terminal isoforms.

(A) Plectin alternative N-terminal exon-eGFP construct used to investigate how the alternative N-terminal exons targets the actin-binding domain of plectin in SW480 cells. Purple oval, N-terminus encoded by the alternative first exon. Red oval, calponin-homology actin binding domain. Green star, enhanced Green Fluorescent Protein. (B) Immunoblot showing the expression of the eGFP-tagged plectin N-terminal isoforms in stable transfected SW480 cells detected by an anti-GFP antibody. Note that some of the non-specific bands are close to the correct bands that are indicated by * marks. Control lane is eGFP alone. In the composite image one lane has been cut out between isoform 1 and 1b.

4.2.8. Alternative first exons target plectin actin binding domains to unique cytoskeletal structures.

Confocal microscopy was used to investigate the sub-cellular localisation of the alternative N-terminal plectin-GFP proteins. As expected, due to expression of only the actin-binding domain, these isoforms localised with sub-cellular actin structures. Differences in the subcellular and cytoskeletal localisation were observed with the alternative plectin isoforms similar to those found in the mouse (Rezniczek et al., 2003). For example, plectin-1 was found to be localised to actin microspikes and in the nucleus, plectin-1b to mitochondria and focal adhesions, 1c to actin stress fibres, 1d to adhesion like plaques and in the nucleus, 1e to focal adhesions and stress fibers, 1f to focal adhesion sites at the ends of stress fibers and focal complexes in lamellipodia and filopodia and finally 1g in membrane ruffles of lamellipodia (Figure 4.8). The novel isoform plectin-1k was shown to localise to dorsal ruffles and focal adhesion-like foci (Figure 6.5) that were later recognised as podosome-type adhesions (Chapter six). It was noted, that although the alternative isoforms had a preferential sub-cellular localisation these were not mutually exclusive as most of the N-terminal-GFP constructs (with the exception of 1b) could localise to the podosome like adhesion plaques. Three independent transfection experiments in SW480 cells were carried out and the localisation of the isoforms to podosome-like adhesions, membrane ruffles, focal adhesion sites, and thick actin stress fibres and finally to the nucleus was scored (summarised in Table 4.1). Additional images can be found in appendix III providing detailed sub-cellular expression using deconvoluted single plane images (Delta Vision 60x lens) of the N-terminal plectin-GFP proteins in the SW480 cells. In summary, these results reveal that human plectin N-terminal have the potential to influence isoform localisation as previously identified for the mouse alternative isoforms (Rezniczek et al., 2003).

4.2.9. Plectin-1b GFP colocalised with a transfected mitochondrial marker.

Plectin has previously been found to link desmin intermediate filaments to mitochondria at Z-disc in muscle (Reipert et al., 1999). Furthermore, an EBS-MD mutation in plectin close to the intermediate filament-binding domain was shown to cause severe mitochondrial dysfunction (Schröder et al., 2002). Appaix et al., 2003, showed that cytoskeletal proteins participate in the intracellular organization and control of mitochondrial function in vivo, where mitochondria are incorporated into

functional complexes with sarcomeres and sarcoplasmic reticulum. Interestingly, the mouse isoform plectin-1b has been described as the specific isoform that can localise to mitochondria (Rezniczek et al., 2003) and possibly link to desmin intermediate filaments. To confirm the above finding in human cells, SW480 cells were double transfected with pDsRed2-Mito vector (BD biosciences UK), containing a mitochondrial targeting sequence of human cytochrome c oxidase subunit VIII and plec-1B-eGFP. Plectin-1b-eGFP was found to co-localise with the transfected mitochondrial target sequence expressed protein (Figure 4.9). The mitochondria are rod shaped concentrated around the nucleus extending through the cytoplasm, plec-1b-eGFP can be seen to be expressed around these structures confirming the similarities to mouse plectin-1b (Rezniczek et al., 2003). These results further demonstrate the complexity of the N-terminal exons on sub-cellular localisation and that each isoforms could harbour a specific function.

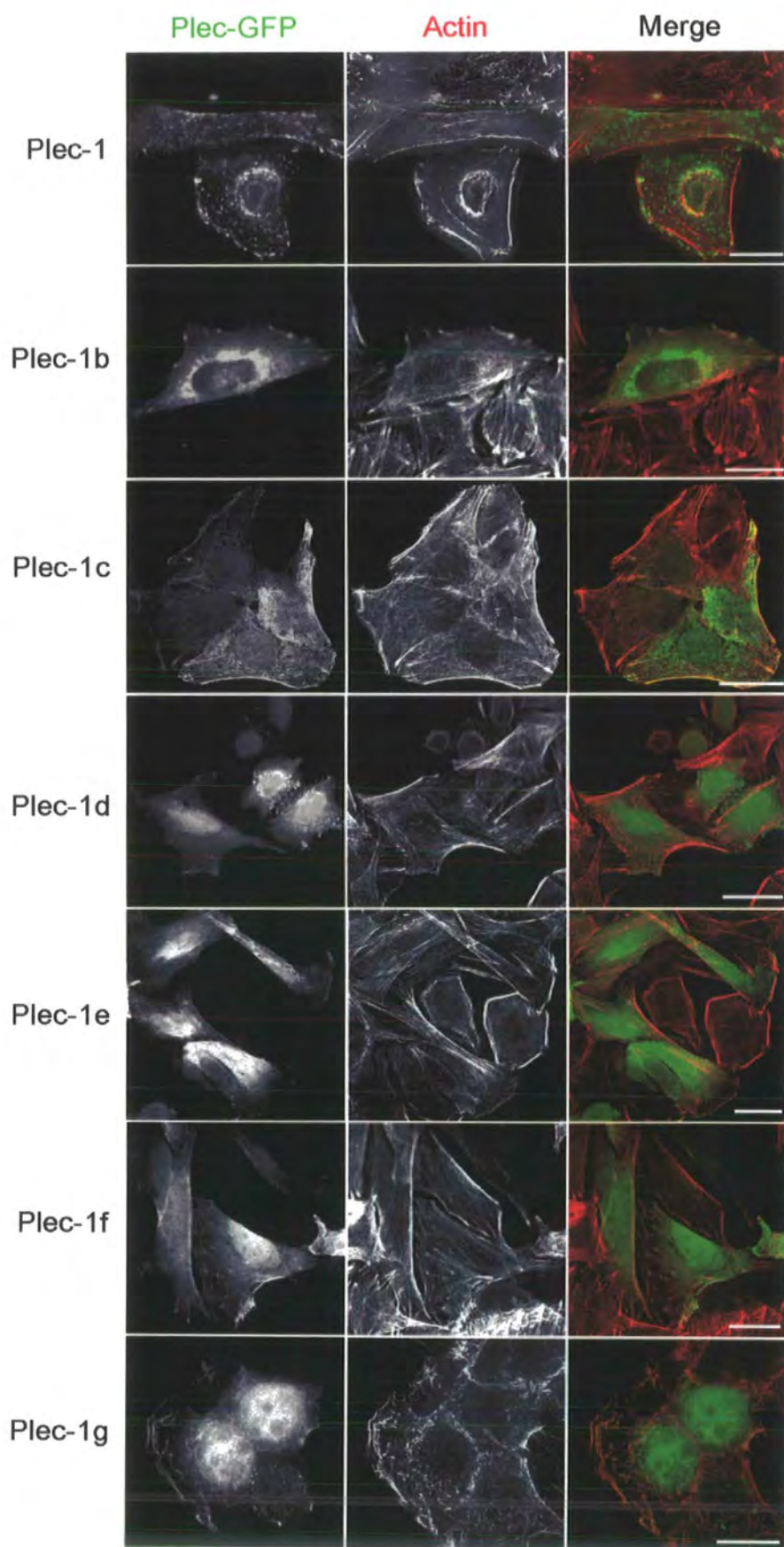


Figure 4.8. Subcellular localisation of alternative plectin N-terminal domains.

Representative examples of co-localisation of GFP fluorescence and actin cytoskeleton (red, phalloidin staining) in SW480 cells transfected with the indicated constructs. Plec-1 and plec-1g are single plane Delta Vision images, whilst the remaining images are single plane Zeiss confocal images. Note co-localisation of plectin with actin at focal adhesions and stress fibres. Scale bars represent 20 μm .

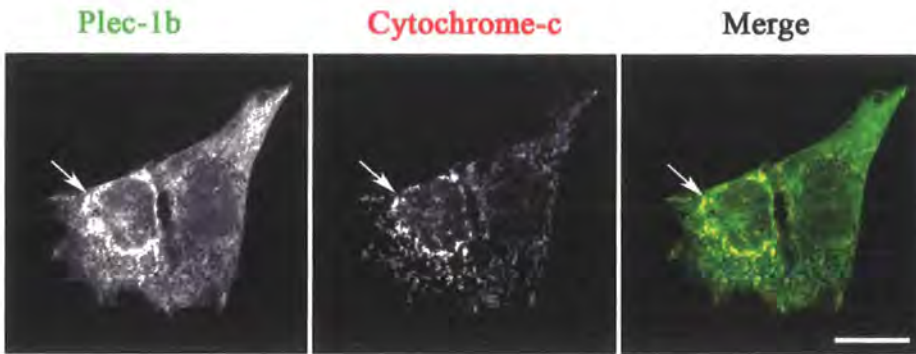


Figure 4.9. Co-localisation of plec-1b-GFP and mitochondria. Confocal single plane image of SW480 cells transfected with cytochrome-c (component of mitochondria) and plec-1b-GFP constructs. Arrows show co-localisation of mitochondria with plec-1b-GFP. Scale bar 20 μ m.

Table 4.1.

Summary of subcellular localisations of alternative plectin N-terminal eGFP constructs.

Isoform	Podosomes	Membrane ruffles	Focal Adhesions	Thick actin stress fibres	Nucleus
1	++	-	-	-	+
1B*	-	-	+	-	-
1C	+/-	+	-	+	-
1D	++	-	-	-	+
1E	+/-	+	++	+	-
1F	+/-	+	+	+	-
1G	+/-	++	-	+/-	-
1K	++	+	-	+/-	-

The table summarises observations from three independent transfection experiments. All indicated GFP-positive structures for each construct were not usually present in the same cells. (++) Major subcellular target in most transfected cells in all experiments. (+) Localisation seen in several cells in all transfection experiments. (+/-) Localisation seen only in a small number of cells. (-) Localisation not detected.

*Note, that majority of Plec-1b was localised at mitochondria.

4.2.10. Investigation of the human plectin isoforms using polyclonal antibodies raised to plectin isoforms 1, 1b, 1f, 1k.

To investigate the plectin alternative isoform proteins further, two polyclonal antibodies for each of plectin-1, -1b, -1f and -1k (named LM1-LM8 respectively) were raised to synthetic peptides corresponding to amino acids in each of the alternative first exons (Table 2.6). These isoforms were selected due to their interesting specific localisation as seen in the GFP transfection experiments with plec-1-eGFP localising to microspikes and the nucleus, plec-1b-eGFP to mitochondria and focal adhesions, plec-1f-eGFP also to focal adhesions and membrane ruffles and the novel isoform plec-1k-eGFP localising to podosome like structures. The antibodies were first characterised by immunoblotting to determine that they were specific for the isoform they were raised to.

4.2.11. Polyclonal plectin isoform antibodies recognise full-length plectin.

The antibodies recognise a band corresponding to a 500-kDa polypeptide in immunoblots of both SW480 colon carcinoma and MDA-MB-231 breast carcinoma cells (Figure 4.10). Plectin C-terminal antibody (c-20) was used as a positive control and High Molecular weight ladder from Invitrogen UK confirmed the 500-kDa sizes. This is the expected size of full-length plectin as, for example, mouse plectin isoforms have deduced range of molecular mass from 499 to 533 kDa (Rezniczek et al., 2003). The antibodies LM6 and LM8 recognised single clean protein bands on a gradient gel. LM2 antibody is more specific than LM1 with LM1 recognising an additional band at ~100 kDa. Antibodies LM3 antibody recognised a weak band at 500 kDa in the carcinoma cell lines but LM4 did not bind to 500 kDa proteins. Using a cell extract from BHK21 cells that express desmin, vimentin and keratin intermediate filaments (Schroder et al., 2003), LM3 recognised a strongly positive 500-kDa band, so it may be that expression of plectin-1b is low in the epithelial carcinoma cells. Subsequent immunoblots using lower dilutions of the antibodies resolved the non-specific binding seen for LM2 and LM7; however LM1 and LM5 continued to show non-specific bands and therefore would be unreliable for immunofluorescence or immunoprecipitation studies.

4.2.12. The specificity of plectin N-terminal human antibodies was further supported by siRNA transfection experiments with total plectin.

The peptide competition assay is the traditional method of determining specificity of polyclonal antibodies as described in section 2.9.2. However, after trial of this method it was found that use of a siRNA method, as described in section 2.9.2, was much more convincing. Depletion of all plectin isoforms in SW480 cells by siRNA transfection abolished the 500 kDa band both when LM 2,5,6,7,8 or a control antibody against plectin C-terminus (c-20) was used for immunoblotting, whereas the 500 kDa protein band was still present when the cells were transfected with a scrambled control siRNA (Fig. 4.11). These results confirm the specificity of the N-terminal plectin isoform antibodies. Note the LM3 specificity could not be evaluated in this assay due to low expression levels of this isoform in the plectin positive sample.

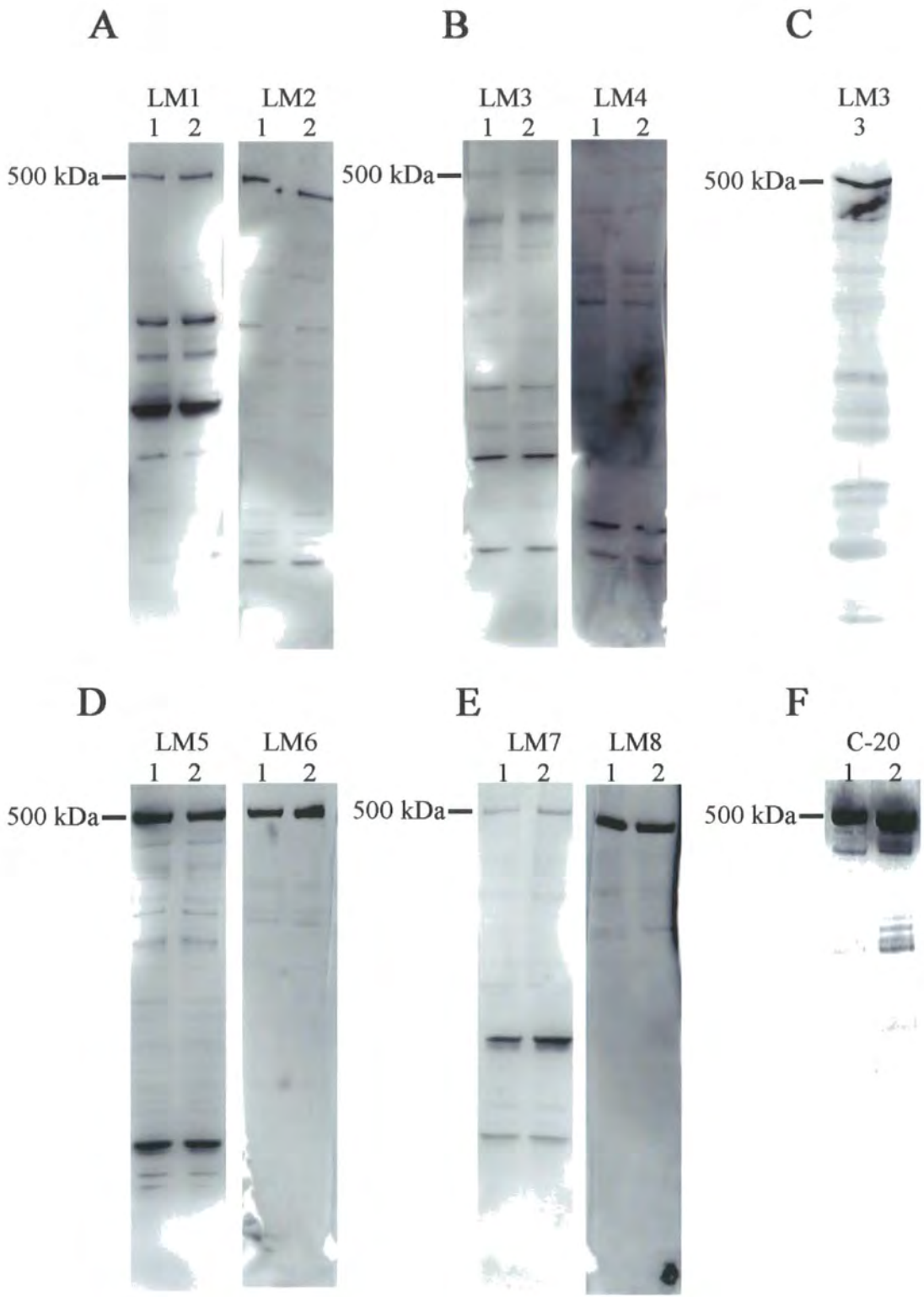


Figure 4.10. Detection of plectin-1, 1b, 1f and 1k with polyclonal antibodies.

Immunoblots of total cell extracts using plectin polyclonal antibodies recognising ~500 kDa band in SW480 (1) and MBA-MD-231 cells (2) or BHK21 cells (3). (A) LM1 and LM2 rabbit polyclonal anti-peptide antibody against exon 1. (B) LM3 and LM4 rabbit polyclonal anti-peptide antibody against exon 1b. (C) LM3 rabbit polyclonal anti-peptide antibody against exon 1b in BHK21 cells. (D) LM5 and LM6 rabbit polyclonal anti-peptide antibody against exon 1f. (E) LM7 and LM8 rabbit polyclonal anti-peptide antibody against exon 1k. (D) Positive control, c-20, goat polyclonal anti-peptide antibody against total plectin.

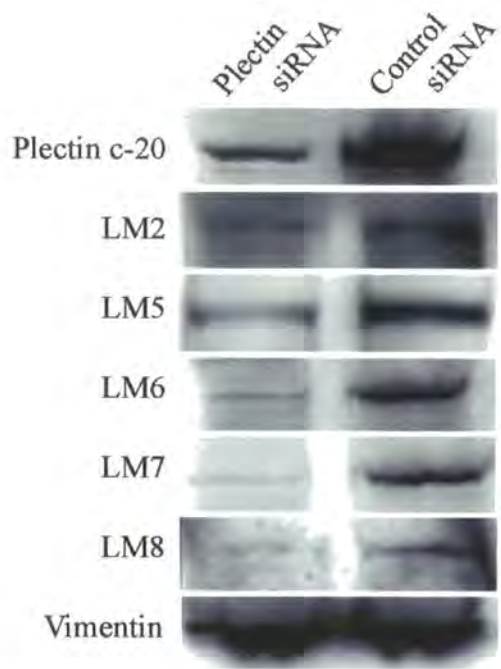


Figure 4.11. Confirmation of the specificity of polyclonal antibodies using siRNA. Plectin knock-down by siRNA transfection in SW480 cells ablates the 500 kDa protein detected by antibody against exons 1 (LM2), 1f (LM5 & LM6) and 1k (LM7 & LM8). Total plectin antibody against the C-terminus of plectin common to all isoforms (c-20; top panel) shows knockdown of the same 500 kDa band. Vimentin antibody (bottom panel) was used to confirm equal loading of plectin siRNA and control scrambled siRNA transfected samples in all experiments.

4.2.13. Expression of plectin isoforms 1, 1b, 1f and 1k in cancer cell lines.

Analysis of plectin isoform expression by immunoblotting revealed an increased expression in the invasive SW480 colon carcinoma cells compared to the non-invasive HT29 cells (Figure 4.12). Likewise MCF-7 cells had considerably lower expression of plectin isoforms compared to invasive MDA-MB-231 cells (Figure 4.12). Plectin-1 and plectin-1f were the dominantly expressed isoforms with plectin-1k expressed at extremely low levels in the non-invasive cell lines. Plectin-1b was detected in these extracts as a weak 500 kDa band. It was found that plectin-1b was constitutively expressed at low levels in all the cells, which correlates to the mRNA expression data (Figure 3.7). Actin was used as a reference for loading, but again Ponceau S and BCA assay is used to load accurate protein levels for each lane due actin being expressed at different levels in these cells.

4.2.14. Immunofluorescence using isoform specific antibodies in carcinoma cells.

Immunofluorescence staining of SW480 and MDA-MB-231 cells was used to map the sub-cellular localisation of plectin-1, 1b, 1f, and 1k (Figure 4.13 A B C D). Plectin isoforms were localised to the perinuclear regions and in a filamentous network in the cytoplasm. The antibodies LM1 and LM2 show expression to be localised to a cytoplasmic filament network with evidence of adhesion like structures at the cell periphery. Although immunoblotting using LM3 and LM4 showed low expression in these cells, immunofluorescence data contrast this and displays localisation of plectin-1b to focal adhesions along with elevated expression at perinuclear regions. It could be that the antibody does not have a high affinity for use in immunoblotting. Antibodies LM5 and LM6 could be seen to localise to focal adhesion like structures at the edges of migrating cells and finally LM7 and LM8 showed particular localisation to podosome-like adhesions in both cell types. Pre-immune serum was used as a negative control to confirm the specificity of the antibodies, no specific staining was observed in these samples (not shown). These antibodies were shown to correlate with the data obtained for the alternative N-terminal GFP constructs. A more detailed characterisation of the sub-cellular localisation and function of the novel isoform plectin-1k will be presented in Chapter 6. In summary, the generation of human isoform specific antibodies provides an excellent tool for the further study of the N-terminal plectin isoform and their binding partners and may lead to better understanding of the human plectin protein.

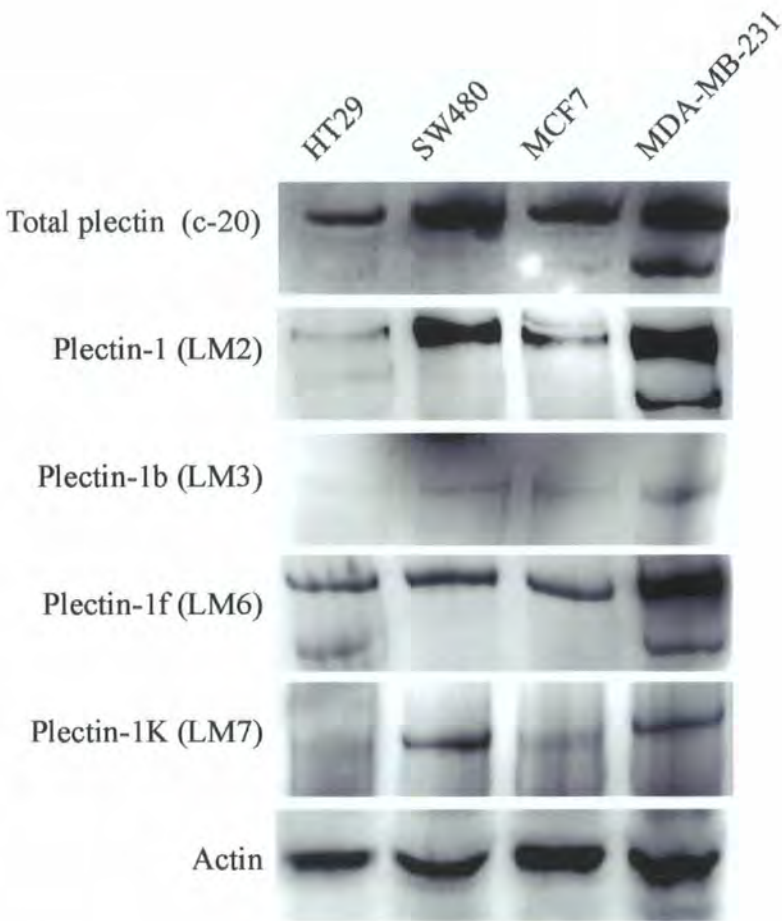


Figure 4.12. Expression of plectin isoforms in carcinoma cell lines.

Immunoblot of colon carcinoma cell lines; HT29 and SW480, and breast carcinoma cell lines; MCF7 and MDA-MB-231, using rabbit polyclonal antibodies for plectin isoforms 1, 1b, 1f and 1k. Total plectin is detected using plectin c-20 antibody and actin is used as a loading control. Note the detection of the lower molecular weight rodless isoform in plectin-1 and plectin 1-f as well as total plectin.

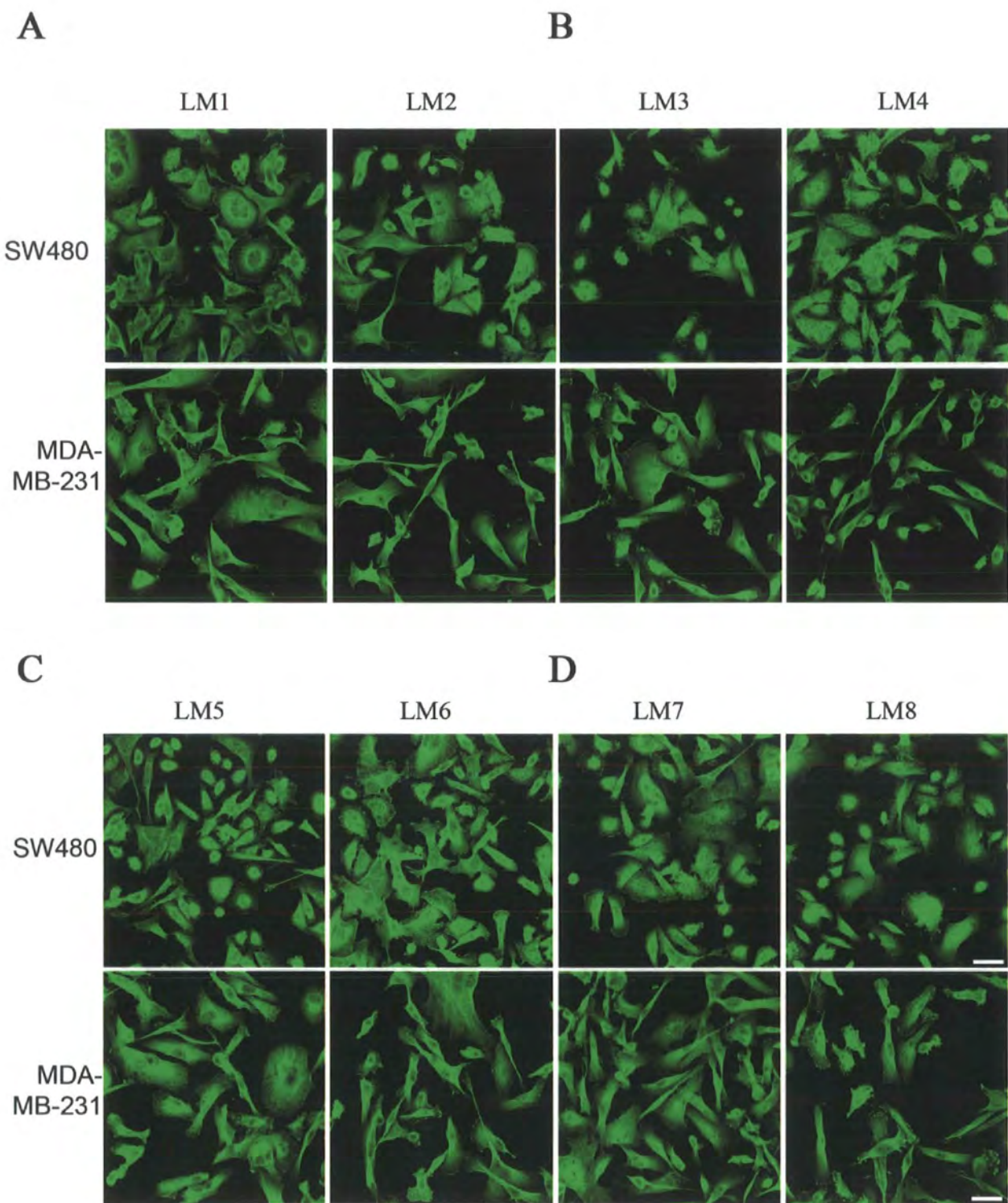


Figure 4.13. Subcellular localisation of plectin alternative first exon isoforms using polyclonal antibodies.

Immunofluorescence staining of SW480 cells and MDA-MB-231 of (A) plectin-1 (B) plectin-1b (C) plectin-1f (D) plectin-1k staining using both rabbit polyclonal anti-peptide antibodies against plectin alternative N-terminal isoforms. Alexa Fluor 488 (Invitrogen UK) anti-rabbit is used as the secondary antibody. Note expression at cell periphery and filamentous network throughout the cytoplasm. Scale bars represent 50 μm for all panels.

4.3. Discussion.

To study the role of plectin in the invasive potential of cancer we used a panel of colon and breast carcinoma cells, where high-grade colon SW480 and breast MDA-MB-231 carcinoma cells showed an increased invasive potential in a collagen gel invasion assay. Immunoblotting was used to identify possible cytoskeletal and related proteins that could play a role in the invasive potential. Surprisingly, plectin protein expression showed a marked increase in the more invasive cell lines, including also the cell line derived from colon metastasis to the lung (T84). Plectin, a cytoskeletal linker protein, is viewed traditionally as a hemidesmosomal protein involved in skin architecture and also in muscle where it predominantly resides at the Z-lines of striated muscles, dense plaques of smooth muscle cells and intercalated discs of cardiac muscles (Leung et al., 2002). However, it has never before been studied in depth in cancer. Other plakin family members have been studied in relation to cancer progression namely desmoplakin where a reduction in desmosomes associated with invasive behaviour. Previously, Alroy et al., 1981, and Davies et al., 1999, suggested that a loss of desmoplakin in breast cancer is likely to be important in the progression and metastasis of breast cancer. In the carcinoma panel presented here desmoplakin protein expression is also reduced in the higher-grade carcinoma cells correlating with the widely held view that decrease of cell-to-cell adhesion is associated with metastatic ability of cancer cells (Depondt et al., 1999 and Bankfalvi et al., 2002). Of interest, periplakin, vinculin, HSP27, talin, E-cadherin, keratin and vimentin expression were all altered in the carcinoma cell panel; with exception of periplakin, all these proteins have been widely studied in cancer cell progression showing altered expression levels (refer to previous references in Section 4.2.3). Loss of E-cadherin and its associated proteins α -catenin and β -catenin has been found in a wide range of cancers and correlates with increased metastatic potential (reviewed by Birchmeier et al., 1995 and Bosch et al., 2004). Vimentin is of particular interest as previous studies have found that in epithelial to mesenchymal transition, the intermediate filament cytoskeleton of epithelial carcinoma cells changes from a keratin-rich network, which connects to desmosomes and hemidesmosomes, to a vimentin-rich network connecting to focal adhesions (reviewed by Kokkinos et al., 2007), this will be visited in Chapter 5.

The characterisation of expression levels of these proteins will help to fully understand the role plectin plays in invasion and migration of the carcinoma cells in the chapters

to follow. These results indicate that the expression of cytoskeletal and related proteins may have a role in the invasive potential of these cell lines and could be implicated in the progression of cancer.

When the subcellular localisation of plectin was investigated in the invasive carcinoma cells, it was observed using an antibody for total plectin (c-20) the protein was recruited away from the hemidesmosomes and cell periphery as seen in the low invasive HT29 and MCF7 cells and localised in a dense actin/vimentin cage around the nucleus in the high invasive SW480 and MDA-MB-231 cell lines. Intriguingly, the observations also suggested that in the low invasive carcinoma cells plectin associated with mainly the intermediate filament cytoskeleton, whereas in the invasive cell lines plectin was associated more with the actin cytoskeleton.

To further investigate the localisation of plectin to the actin cytoskeleton and also the effect the plectin N-terminal isoforms have on recruitment of the protein to specific actin structures, Human plectin N-terminal sequences including the actin binding domains from the nine identified human isoforms were cloned into GFP expressing vector. The previous study on the murine alternative isoforms showed the alternative N-terminal exons yielded an effect on the sub-cellular localisation of plectin (Rezniczek et al., 2003). In the study the authors found plectin-1 to be localised in the nucleus and weakly throughout cells with faint staining of actin stress fibers in which they suggest that exon 1 contains a putative nuclear localization signal. Isoforms plectin-1a, 1c, 1d, 1e and 1g decorated actin stress fibers, although less so in the case of plectin 1d. Plectin-1b was concentrated at the perinuclear region encasing mitochondria. Plectin-1f was concentrated at stress fiber ends and at the cell periphery concentrated in vinculin-positive structures. These results were similar to the sub-cellular localisations observed for the human N-terminal exons (Figure 4.8 and Table 4.1) in the SW480 colon carcinoma cell lines. However, isoforms 1f, 1d and specifically 1k also localised to actin rich foci at the cell periphery that are later identified as podosomes (Chapter 6). The identification of plectin N-terminal isoforms that localise to migratory actin structures or actin stress fibers may provide a mechanism through which cancer cells could modulate adhesion migration and invasion by regulating expression of plectin isoforms.

The probability that full-length plectin isoform proteins may have a different sub-cellular localisation than the N-terminal GFP constructs in the carcinoma cells was recognised. This was observed previously in the murine plectin isoforms where the full-length proteins expressed in mouse keratinocytes showed plectin-1, unlike the N-terminal domain of the same protein, to be distributed throughout the cytosol with punctuated diffuse staining, but not in the nucleus. Additionally, only the full-length plectin-1a was concentrated in patchy structures that were suggested to be hemidesmosomes (Rezniczek et al., 2003). Thus, expression of full-length human plectin isoforms was investigated in the carcinoma cells by using polyclonal antibodies raised to plectin-1 1b 1f and 1k.

To start with, the relative expression levels of these isoforms were investigated using immunoblotting to identify if any of the four isoforms contributed to the increased expression observed in total plectin (Figure 4.12). The results show that plectin-1 and plectin-1f are strongly expressed in the carcinoma cells and upregulated in the more invasive cells. This is interesting considering that plectin-1 is the isoform prominently expressed in cells of mesenchymal origin (Fuchs et al., 1999) and ablation of this isoform caused reduced migration of T-lymphocytes and murine dermal fibroblasts (Abrahamsberg et al., 2005). Moreover, plectin-1f is localised to focal adhesion structures rather than hemidesmosomes (Rezniczek et al., 2003). Plectin-1b was constitutively expressed in these cell lines. Most interestingly, the novel isoform plectin-1k was expressed at significantly lower levels in the low-grade carcinoma cells than in SW480 and MDA-MB-231 cells, indicating the potential of plectin-1k to participate in cancer cell invasion.

In some cell lines two high-molecular weight proteins were detected using plectin antibodies. It is possible that the lower band observed in immunoblotting using the C-terminal plectin antibody could be the rodless plectin splice variant which lacks exon 31 (Elliott et al., 1997). The lower protein migrates at the expected size of 390 kDa (Steinboeck et al., 2005) and is depleted in a protein extract from plectin siRNA transfected cells. Interestingly, the lower band is more prevalent in the MDA-MB-231 cells and a corresponding band is expressed at lower levels within the carcinoma cell panel (Figure 4.2). Plectin-1 and 1f show positive expression of the lower band however plectin 1b and 1k do not. Previously exon 1c was identified as the first coding

exon of the rodless isoform in neuronal tissues (Steinboeck et al., 2005 and Fuchs et al., 2005). My results show that plectin-1 and 1f could possibly also code for the rodless domain.

Immunofluorescence in SW480 and MDA-MB-231 carcinoma cells, using isoform specific antibodies, demonstrates similar subcellular localisations as observed previously in murine keratinocytes (Rezniczek et al., 2003) and the human plectin GFP fusion proteins. Plectin-1 (antibodies LM1 and LM2) was expressed in a filamentous network around the nucleus, not in the nucleus and also at punctuated structures in the cytoplasm and at cell periphery. Plectin-1b (antibodies LM3 and LM4) showed localisation around the perinuclear area and to focal adhesions. Plectin-1f (LM5/LM6) was targeted to a filamentous network and at focal adhesions. Finally, the novel isoform, plectin 1k, was expressed at adhesion like foci at the basal surface of the cells and in the perinuclear cage around the nucleus (Figure 4.13). The sub-cellular localisation of plectin in the vimentin and actin-rich cage encasing the nucleus in the invasive colon and breast carcinoma cell lines is of interest as the mechanisms that maintain the nucleus in its proper position in the cell is not yet fully understood (Wilhelmsen et al., 2005). The expression of plectin in Sertoli cells was also observed to concentrate at the nuclear surface, suggested to link intermediate filaments centrally to the nucleus (Guttman et al., 1999). Importantly, the identification of nesprin-3 an outer nuclear membrane protein that binds to plectin and the demonstration that over expression results in a dramatic recruitment of plectin to the nuclear perimeter further adds to the versatility of plectin (Wilhelmsen et al., 2005).

There is an increasing interest in the function of up regulation of alternatively spliced plectin isoforms. Plectin is expressed at Z-disks and sarcolemma in skeletal muscle and the alternative plectin isoforms show differential regulation during myotube differentiation. It has been shown that plectin-1 and 1f associate with the sarcolemma whereas plectin-1d localises exclusively to Z-disks (Rezniczek et al., 2007). In epidermal keratinocytes, isoforms plectin-1a and 1c were shown to interact with integrin β 4, with isoform 1a suggested to be important for regulating the affinity of the ABD for β 4 and F-actin (Litjens et al., 2003). A subsequent study found that only the full-length isoform 1a, but not plectin-1c or 1, could restore hemidesmosomal

contacts in plectin deficient keratinocytes. These data suggest that plectin-1a is the isoform responsible for skin blistering in plectin related diseases (Andra et al., 2003). Plectin has been shown to interact with another plakin family member periplakin (Boczonadi et al., 2007) and this study shows that periplakin is upregulated in the more invasive cell types along with periplakin. In addition, immunofluorescence of mouse skin show plectin-1 staining to be low in the suprabasal layers, however both plectin-1f and 1k were present at the cell borders of differentiated epidermal cell layers similar to periplakin staining. Thus, it appears that only a subset of plectin splice isoforms co-localise with periplakin in differentiated epidermal keratinocytes in granular and cornified cell layers (Boczonadi et al., 2007).

To summarise it was demonstrated that higher-grade invasive carcinoma cells had a elevated expression of plectin protein along with periplakin and down regulation of desmoplakin implicating the plakin family members as possible modulators of cell migration and cancer progression. I also found that plectin is located away from hemidesmosomal plaques and intermediate filaments in the invasive carcinomas and shows a predominant expression in actin rich structures. Investigation of short plectin N-terminal GFP fusion proteins demonstrate the localisation of these isoforms at specific actin migratory structures and suggest that regulation of the plectin N-terminal isoforms could contribute to carcinoma cell migration. Polyclonal antibodies raised to four of the nine human plectin isoforms support the GFP data and show upregulation of isoforms 1, 1f and 1k but not 1b in the carcinoma cell lines. This study provides fundamental research on human plectin isoform expression including the expression cancer cells that could lead to a better understanding of the full versatility of this complex protein.

CHAPTER 5
ROLE OF PLECTIN AND VIMENTIN IN
INVASION AND MIGRATION OF
CARCINOMA CELLS.

5.1. Introduction.

Over 90% of human tumours are carcinomas where transformed epithelial cells grow uncontrollably, breaking through the basement membrane and invading the underlying mesenchyme. Moreover, the metastatic spread of tumour cells to distant organs via haematogenous routes represents the most important cause of morbidity and mortality in cancer (Chambers et al., 2002). Carcinomas are characterised by invasion of malignant cells into the underlying connective tissue and migration of malignant cells to form metastases at distal sites (Lyons et al., 2007). Cell migration is a highly complex and integrated process that involves the assembly and disassembly of adhesions initiated by signalling transduction pathways orchestrating the cytoskeleton. Plectin, a cytoskeletal linker protein and more recently as a recognised scaffolding protein for signal transduction pathways, was found to be up regulated in the more invasive cell lines that also express vimentin (Figure 4.2).

Ongoing elucidation of molecular interactions of vimentin gives clues of the potential functions of vimentin in migration and invasion. Unlike keratin intermediate filaments that are connected to cellular junctions promoting adherence and tissue integrity, hemidesmosomes and desmosomes, vimentin can be localised with transient, actin-rich adhesion sites that play a role in cell migration. For example, in macrophages vimentin co-localises with fimbrin (T-plastin) in podosomes (Corrêa et al., 1999) whereas in endothelial cells, vimentin filaments associate with $\alpha\beta 3$ -positive focal contacts. Finally, vimentin is phosphorylated by PKC ϵ on vesicles that recycle $\beta 1$ integrins in mouse embryonic fibroblasts and expression of mutant vimentin harbouring PKC targets that are replaced with phosphomimetic amino acid residues results in a rescue of cell migration in PKC ϵ null cells (Ivaska et al., 1999). The recently recognised role for vimentin in the recycling of integrin heterodimers (Ivaska et al., 2005) and reports demonstrating requirement of vimentin for focal adhesion complex stability in endothelial cells (Tsuruta et al., 2003) prompted the investigation into the consequences of vimentin ablation on cell-matrix adhesion. Intriguingly, the expression of vimentin in breast cancer cells has been shown to be downstream of several signalling proteins implicated in carcinogenesis. Smad-interacting protein1 (SIP1), a transcription factor implicated in epithelia-mesenchymal transition, up-regulates vimentin expression (Bindels et al., 2006). Likewise, β -Catenin/TCF complex can directly transactivate the vimentin promoter (Gilles et al., 2003). Finally,

over-expression of tiam-1, a guanine nucleotide exchange factor (GEF), results in an increased invasiveness and vimentin expression in colon carcinoma cells (Minard et al., 2006). However, none of the above studies have conclusively established, whether vimentin expression is only a marker of epithelial-mesenchymal transition (EMT) – like changes or if vimentin expression is required for the invasive behaviour of the cells.

The role of plectin in the migration of keratinocytes and fibroblast has recently been investigated. It has been shown that depletion of plectin (Andra et al., 1998), or plectin-1 isoform only (Abrahamsberg et al., 2005) leads to impaired migration of fibroblasts. However, plectin-null keratinocytes migrate faster than their wild-type counterparts (Osmanagic-Myers et al., 2006). In contrast to that ablation of plectin caused impaired migration of MCF-7 epithelial sheets (Boczonadi et al., 2007). The $\alpha 6\beta 4$ integrin, a direct interacting partner of plectin, has been implicated in carcinoma cell invasion and migration. Increased suprabasal expression of $\alpha 6\beta 4$ integrins correlated with poor prognosis in both mouse and human squamous cell carcinomas (Tennenbaum et al., 1993 and Van Waes et al., 1995). Furthermore, $\alpha 6\beta 4$ is relocated from hemidesmosomes to actin rich protrusions in invasive carcinomas (Rabinovitz et al., 1999). This integrin also has a significant impact on cell signalling pathways that are involved in cell migration and invasion, especially PI3-K, Rho GTPase (Mercurio et al., 2001). A recent study has also shown that in p53-deficient cells, $\alpha 6\beta 3$ can mediate a tumour-suppressive effect, dependant on its ability to recruit plectin to the plasma membrane (Raymond et al., 2007).

Although plectin has been well characterised for its role as a hemidesmosomal plaque protein, a link has also been shown for plectin at vimentin positive focal adhesions (Gonzales et al., 2001). In this chapter the effect plectin and vimentin ablation has on migration, invasion and attachment in colon and breast carcinoma cell lines will be addressed. In this chapter a summary of cancer cell migration is given with the results section following.

5.1.1. Cell migration.

Cell migration is important in many processes including embryogenesis, inflammation, tissue repair and regeneration, and cancer (Webb et al., 2002). A key event of migration involves the reorganisation of actin dynamics controlled by a large number of effectors. The small GTPases of the Rho family (Rho, Rac and Cdc42) are essential for both cell motility and cell-cell adhesion (Braga et al., 2000). Rac is required for new adhesions at the cell front and Rho is required for the maturation of existing contacts and disassembly of adhesions at the rear of cells and its effector Rho kinase promotes retraction of the tail by altering integrin nature (Kiosses et al., 1999; Chung et al., 1999). Increased motility and invasiveness is often associated with decreased cell adhesion, degradation of basement membranes and stroma, and enhanced growth of tumour cells (Grille et al., 2003). Thus, understanding cell migration and adhesion could lead to new therapeutic designs for various diseases.

5.1.1.1. Modes of cell migration.

Three distinct modes of cell migration have been described: amoeboid, mesenchymal and collective migration (Figure 5.1). Amoeboid movement is described in certain tumour cells that use fast crawling movement with weak substrate interactions. Mesenchymal cells on the other hand follow a series of events. First, cell polarisation and protrusion of actin structures such as pseudopodia, lamellipodia, next, the formation of adhesions to the extra cellular matrix, mediated by integrins at focal adhesions and podosomes with the recruitment of surface proteases such as MMPs that are thought to widen scaffolds. During this, actin engages with contractile proteins myosin and local cell contractions occur with disassembly of contacts at the rear (Friedl, 2004). In collective migration cells maintain contact at adherence junctions through cadherins and cortical actin reinforces collective integrity. At the leading edge the cells utilise actin mediated ruffles and integrins and drag adhering cells along established tracks. This movement is important in wound healing, and also in primary cancers, clusters of cells can disseminate through connective tissue (Perez-Moreno et al., 2003; Farooqui et al., 2005).

5.1.1.2. Cell-matrix attachments.

Focal adhesions are the main adhesive structures that are involved in cell-matrix attachment, consisting of a transmembrane component of clustering integrin molecules linked to the matrix, and a sub-membranous component made by complex of specific proteins such as vinculin, talin, focal adhesion kinase (Vasiliev et al., 2004). The definition of focal adhesions is often confused. Wozniak et al., 2004 defines four different structures focal complexes, focal adhesions, fibrillar adhesion and 3D matrix adhesions. Focal complexes are small focal adhesions at the periphery of spreading or migrating cells regulated by Rac and Cdc42 and that precede larger focal adhesions that are regulated by Rho activity (Wozniak et al., 2004). Under tension the small adhesions can mature into larger more organized adhesions called focal adhesions (Webb et al., 2002). Tyrosine phosphorylation is also an important signalling event and regulates focal adhesions; vinculin, focal adhesion kinase (FAK) and paxillin are all recruited to the complex preceding tyrosine phosphorylation (Kirchener et al., 2003). Focal adhesions mediated adhesion links to the actin cytoskeleton via integrins and proteoglycans (Wozniak et al., 2004) and are usually found associated with the ends of stress fibers, but it's not yet clear which components of a focal complex distinguish it from a focal adhesion (Zamir et al., 2001). Fibrillar adhesions form as an elongation of focal adhesions containing $\alpha 5\beta 1$ integrin and tensin (Pankov et al., 2000). The final adhesion arises from studies showing that cells form 3D matrix adhesions that are not the same as their 2D counterparts, suggesting that these different focal adhesions can alter signalling events to regulate cell behaviour and phenotype (reviewed in Wozniak et al., 2004).

5.1.1.3. Integrins.

Integrins are transmembrane glycoproteins that mediate cell adhesion to extracellular matrix components such as laminin, collagens, fibronectin, and vitonectin (Hynes, 2002). They form heterodimeric receptors in a non-covalent association that comprise of one α subunit and one β subunit. Eighteen α and eight β subunits combine with a partial overlap to form 24 integrins (Hynes, 2002; Guo et al., 2004). Integrins are mainly found coupled to actin cytoskeleton with the exception of the integrin $\alpha 6\beta 4$, and $\alpha V\beta 3$, which is linked to the intermediate filament cytoskeleton (as described in Chapter 1). The binding of integrins to their ligands and subsequent integrin-mediated cell adhesion is a tightly regulated process, which involves a change in affinity of the

receptor for its ligand (Kreis et al., 2005). Receptor binding and clustering of integrin at the cell surface appears to be a trigger of events that initiates interactions with cytoskeletal components (Yamada et al., 1995). Talin, a cytoskeletal linker protein is involved in the activation of integrins (Calderwood et al., 2004; Critchley et al., 2004) and in turn the integrins activate focal adhesion kinase (FAK), thus, initiating phosphorylation and modulation of signalling cascades such as the Src-family kinases (Guo et al., 2004). Vinculin, a binding partner of talin is one of the best-characterised focal adhesion proteins and cycles between active and inactive states. The crystal structure of vinculin displays an open or closed conformation, where C-terminal tail interacts with the N-terminal head masking the ligand binding sites in the closed conformation (Bakolitsa et al., 2004). Despite being well characterised, vinculin's precise role at focal adhesions is not known, although overexpression has been shown to reduce cell migration whereas downregulation can enhance cell motility (Zeigler et al., 2006). Altered integrin expression has been reported in many tumours (Lyons et al., 2007). Furthermore, there is also evidence that integrin trafficking pathways that recycle adhesion components can contribute to cell migration, and that integrin deregulation contributes to the pathogenesis of many diseases including cancer (Caswell et al., 2006). Therefore, the dynamic regulation of focal adhesion and the integrin cytoskeleton associations play a central role in balancing adhesion and migratory responses in the cell (Cohen et al., 2006).

5.1.1.4. Epithelial to mesenchymal transition.

Epithelial to mesenchymal transition (EMT) with a loss of cell adhesion is seen as an important step in cancer progression (Figure 5.2), allowing benign non-invasive tumour cells to metastasize (Depondt et al., 1999; Bankfalvi et al., 2002). During EMT, cells progressively redistribute or downregulate their apical and basolateral epithelial-specific proteins such as E-cadherin, catenins and re-express mesenchymal molecules such as vimentin, fibronectin and N-cadherin (Wicki et al., 2006). Several studies have also identified a “metastable cell” phenotype (termed defined by Pierre Savagner) that is able to express attributes of both epithelial and mesenchymal cells (reported in Lee et al., 2006). Vimentin expression is an important marker of EMT and could be an important target for drug development in cancer (Reviewed by Lee et al., 2006). Loss of E-cadherin by transcriptional repression and its associated proteins α -catenin and β -catenin has been found in a wide range of cancers and correlates with

increased metastatic potential (reviewed by Birchmeier et al 1995, Bosch et al., 2004; Cowin et al., 2005). E-cadherin is a transmembrane protein of the cadherin superfamily and forms cell-cell junctions through homotypic interactions, which results in the formation of stable junctions. The cadherin proteins dimerise in a calcium dependent manner, triggering β -catenin linkage to actin leading to the formation of stable adherence junctions. The loss of E-cadherin is contrasted with the gain of mesenchymal cadherins such as N-cadherin is described as the “cadherin switch” (Cavallaro et al., 2002). Interestingly, in human colorectal cancer, cells at the central tumour mass display polarised epithelial organisation with junctional localisation of β -catenin and E-cadherin whereas cells at the invasive front are characterised by a loss of cell surface E-cadherin nuclear localisation of β -catenin (Brabletz et al., 2001). Interestingly, there are arguments that EMT does not always occur in the progression of cancer, as in colon tumours loss of cell adhesion could not be correlated with poor prognosis and increase invasion (Bosch et al., 2004). Furthermore, continued expression and synthesis of junctional proteins in colon carcinomas was also reported supporting this result (Kartenbeck et al., 2005).

5.1.1.5. Matrix degradation.

Efficient tumour invasion requires partial degradation and remodelling of the ECM at the invasive front (Guo et al., 2004). Increased expression of multiple classes of extracellular matrix degrading enzymes are often up regulated and activated in cancer, such as the matrix metalloproteinases (MMPs), serine proteases and cathepsins (Birkedal-Hansen, 1995; Baker et al., 2006; Impola et al., 2004). MMPs are a family of related zinc containing proteases that have the ability to degrade the ECM (Brinckerhoff et al., 2002). Fibrillar collagen, the main constituent of the connective tissue is degraded by several proteases, including MMP-1, -2, -8 and 13 and membrane anchored MT1-MMP, MT3-MMP and cathepsin B, K and L (Wolf et al., 2003). Matrix metalloproteinases have been localised to podosomes and invadopodia described in Chapter 6, and were found to be involved in matrix degradation (Chen et al., 1989 reviewed in Linder, 2007). Fibroblast and tumour cells have been shown to tunnel through cross-linked type 1 collagen via a similar process that requires MMP activity (Sabeih et al., 2004). Furthermore, the significant role of MMPs in tumour cell invasion has led to the development of MMP inhibitory drugs (Lyons et al., 2007) highlighting the importance of cell invasion therapies for the treatment of cancer.

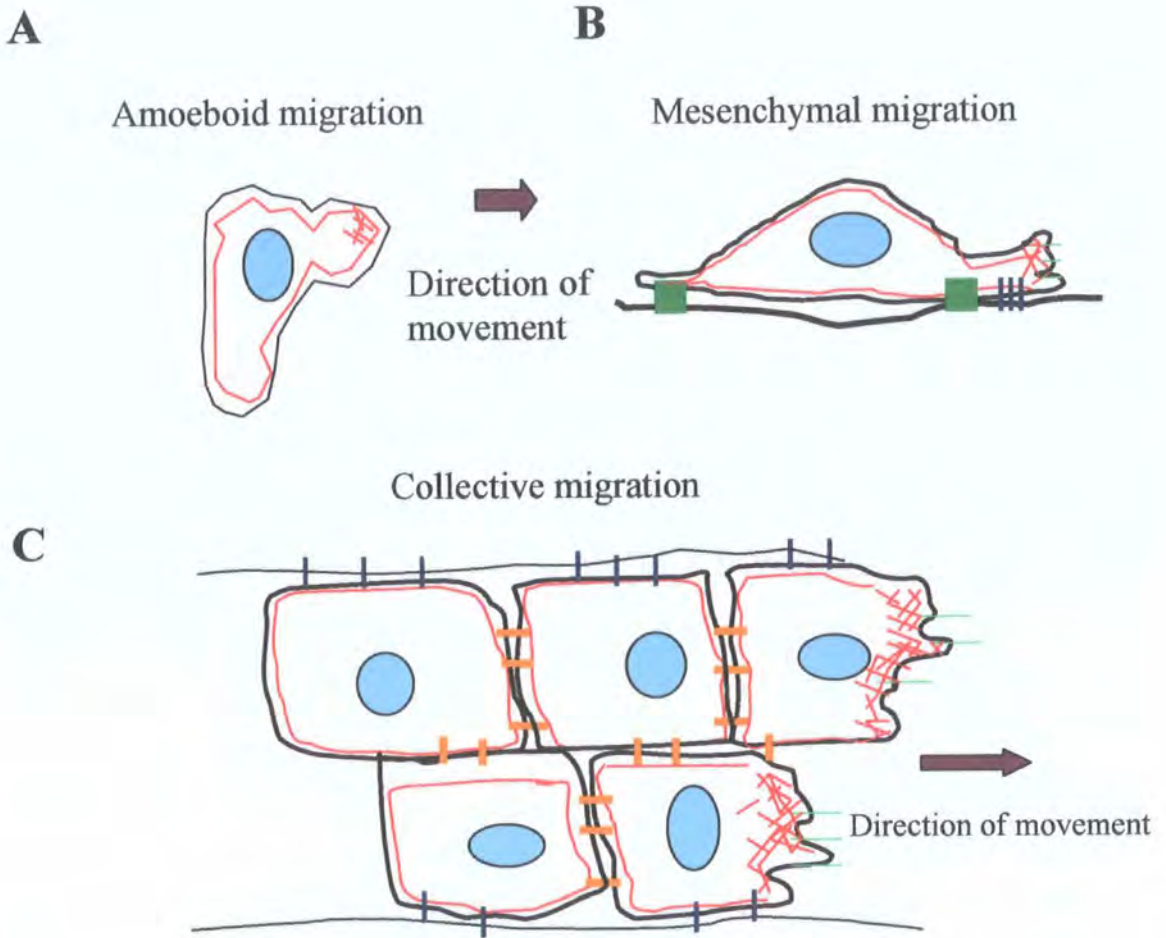


Figure 5.1. Modes of cancer cell migration.

(A) Amoeboid motility involves an irregular cell shape and rapid changes in direction. (B) Mesenchymal motility is dependant on substrate attachments with small integrin rich contacts at the leading edge where the matrix is degraded. Cells also are characterised by an elongated morphology. (C) Cell-cell attachments are retained in collective migration where groups of cells can disseminate through tissue. Red lines circumference the cells represent thick actin cables and short red lines represent actin polymerization at the leading edge. Orange dashes represent adherence junctions. Dark green squares are large integrin-rich focal adhesions that connect to the matrix and blue dashes are the small focal contacts. Light green lines represent receptors that sense chemokines. (Adapted from Sahai, 2005)

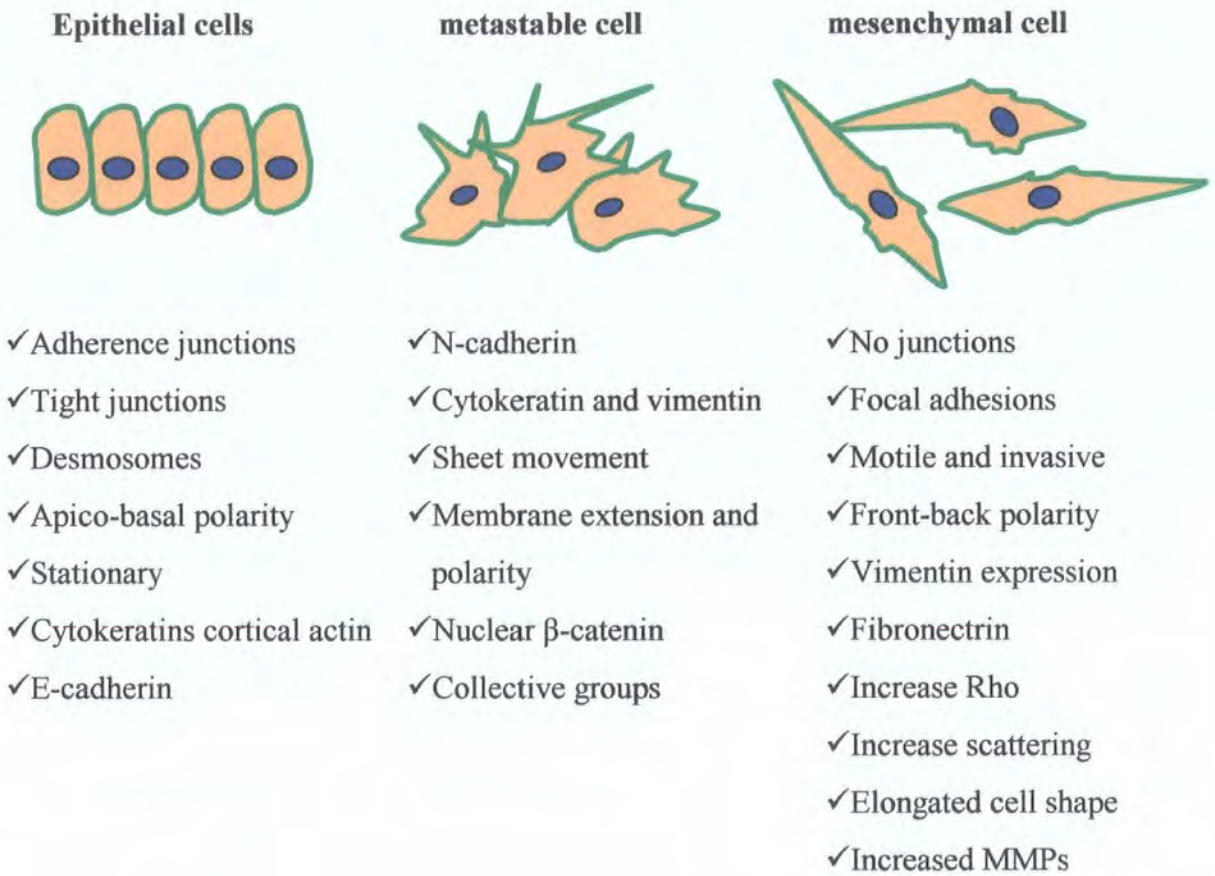


Figure 5.2. Summary of epithelial to mesenchymal transition.

The main characteristics of each cell type including a metastable intermediate that is a hybrid cell showing both epithelial and mesenchymal traits (Figure adapted from Lee et al., 2006).

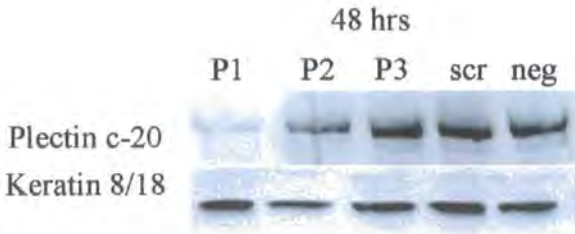
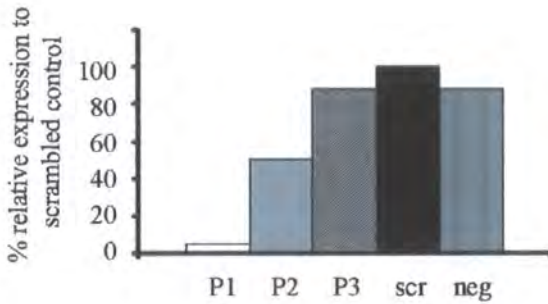
5.2. Results.

5.2.1. Transfection of short interfering RNA (siRNA) to down-regulate expression of plectin and vimentin proteins.

Prior to the invasion and migration assays, it was necessary to investigate the efficiency of siRNA to knock down protein expression in SW480 and MDA-MB-231 carcinoma cell lines. To target plectin and vimentin proteins we ordered three alternative siRNA oligonucleotides for each protein (Table 2.5). The validation of siRNA was carried out on the SW480 cells; which were transfected with the siRNA of interest and a scrambled control siRNA. The scrambled control contains a mixed sequence of nucleotides that does not correspond to any known human mRNA sequence and therefore provides a negative control for the experiments. After transfection, cells were harvested at either 48, 72 and 96 hours and the knock down efficiency was analysed by immunoblotting. A 95 % depletion of plectin expression was achieved 48 hours after the transfection with siRNA ID144451 compared to transfection of the scrambled siRNA control (Figure 5.3A). Plectin siRNA oligonucleotides ID 144452 and ID144453 showed a less efficient knock down of 50% and 12%, respectively. Furthermore, when the scrambled control siRNA was compared to a control transfections using water instead of any siRNAs plectin expression was not affected therefore confirming the scrambled siRNA as a suitable control. In later experiments, plectin siRNA transfection with ID144451 was analysed at time points up to 96 hours (Figure 5.11C) showing that a continued efficient knock down of plectin expression could be achieved. Each plectin siRNA targets a different exon and the efficiency of each siRNA is dependent on their ability to target the plectin RNA sequence which may be affected by conformation and specific binding properties of the RNAs. This result shows that siRNA ID144451, gives the most efficient knock down at the time points from 48 hours to 96 hours. These parameters for the ablation of plectin in epithelial cells were then used in subsequent assays.

To achieve vimentin ablation in SW480 and subsequently in MDA-MB-231 cells, three siRNAs targeted to vimentin (Table 2.5) were used to transfect SW480 cells that were harvested 96 hours after the transfections to determine the efficiency of each siRNA. Optimization of vimentin siRNA resulted in over 90% knock down after 96 hours using vimentin siRNAs, ID 138993 and ID 138995 (Figure 5.4A). However,

siRNA ID 138994 was less efficient with only a 48% knock down after 96 hours (Figure 5.2A). Actin was used as a loading control showing equal loading of total proteins from each sample. These samples were run simultaneously on the same gel in the adjacent lanes to ensure that the blotting conditions were constant. In order to investigate the optimum time point after transfection, the experiment was repeated with the cells harvested also at 48 and 72 hour time points. When the cells were harvested 48 hours after transfection, vimentin siRNAs ID 138993 and ID 138995 depleted vimentin expression by 60% and by about 80% after 72 hours. After 96 hours the knockdown efficiency was again over 90% (Figure 5.4B, 5.4C). The less efficient siRNA, ID 138994 showed 20%, 30% and 40% depletion of vimentin expression after 72, 48 and 96 hours, respectively (Figure 5.4B, 5.4C). Additionally, it was observed that siRNA transfections reached the greatest efficiency when the cells were transfected 12 hours after seeding at 40% confluency. Seeding cells at over 40% confluency resulted in increasingly less efficient vimentin depletion possibly due to stabilisation of the intermediate filament network (Figure 5.11C 5.12C). This extent of down-regulation of vimentin at 48 hours is similar to that seen in experiments with another intermediate filament, keratin 8 (Long et al., 2006). These results confirm that an efficient vimentin knock down can be achieved after 48 hours and up to 96 hours using two out of three of siRNA oligomers.

A**B****Figure 5.3. Comparison of plectin siRNA nucleotides.**

(A) Immunoblot using Plectin c-20 antibody on 48-hour total cell extractions from SW480 cells, after transfection with siRNAs ID144451 (P1), ID144453 (P2), ID 144453 (P3), a control with scrambled siRNA (scr) and a control transfected with water (neg). Keratin 8/18 bands from the same blot confirm equal loading. (B) The relative expression of plectin when compared to the siRNA control, measured by Image J software from raw tiff format images taken with FujiFilm Intelligent Dark Box II.

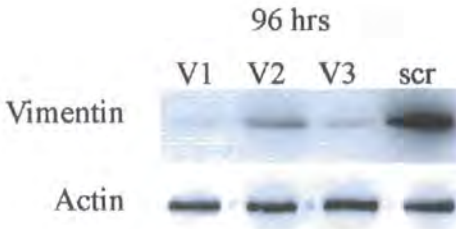
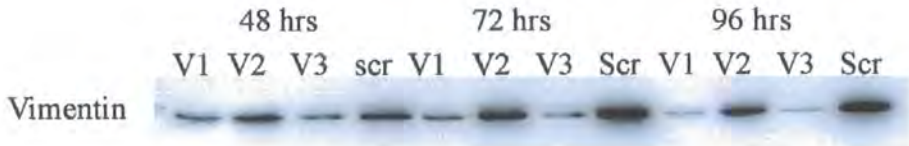
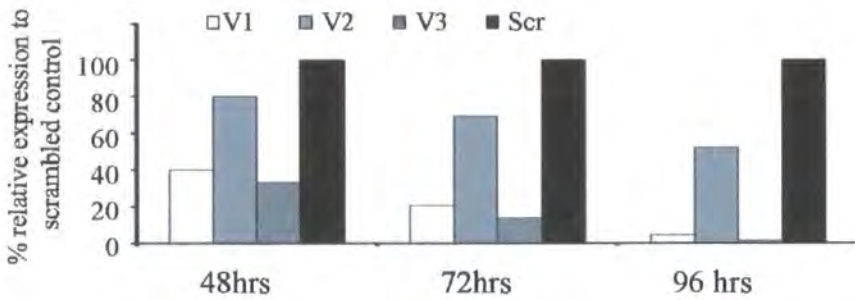
A**B****C**

Figure 5.4. Comparison of vimentin siRNA nucleotides.

(A) Immunoblot using vimentin polyclonal antibody on total protein extracts from SW480 cells transfected with siRNAs ID138993 (V1), ID138994 (V2), ID 138995 (V3) and a control with scrambled siRNA (scr). Actin bands act as a loading control from the same extract loaded in duplicate on a single 10% SDS page gel. (B) Repeat of above experiment (A) however, cells are harvested at 48, 72 and 96-hours before immunoblotting with vimentin polyclonal antibody. (C) The relative expression of vimentin when compared to the control siRNA, measured using Image J software from raw tiff format images taken with FujiFilm Intelligent Dark Box II.

5.2.2. Cell viability is not affected by either vimentin or plectin siRNA transfections.

To ensure that any changes observed in the assays to follow were not due to decreased cell survival after plectin or vimentin down regulation, the cell numbers were analysed after 72 hours. Both vimentin and plectin siRNA transfected cells had similar, only slightly lower survival compared with scrambled control transfected cells in the SW480 cells (Figure 5.5A). Moreover, the cell survival of breast carcinoma cells MDA-MB-231 gave similar results to the SW480 cells for both plectin and vimentin transfections (Figure 5.5B). Overall cell viability did not change more than 5% compare to the scrambled control for plectin or vimentin knock-down in these cells, therefore changes in cell viability should not have a significant effect in the migration and invasion assays used below. For the attachment assay and invasion assays, cell numbers were adjusted to the equal concentration of cells per ml prior to assay so the slight decrease in survival did not affect the assays. These results also confirm that the depletion of these proteins do not have a significant effect on cell proliferation after 72 hours and that none of these proteins are essential for cell survival. When comparing the scrambled siRNA control to a non-transfected control, in both cell types, a slight (<10%) cytotoxic effect was observed due to the transfection reagent (Figure 5.5A and Figure 5.5B). As the assays to follow will be compared to the scrambled control this will not affect the results.

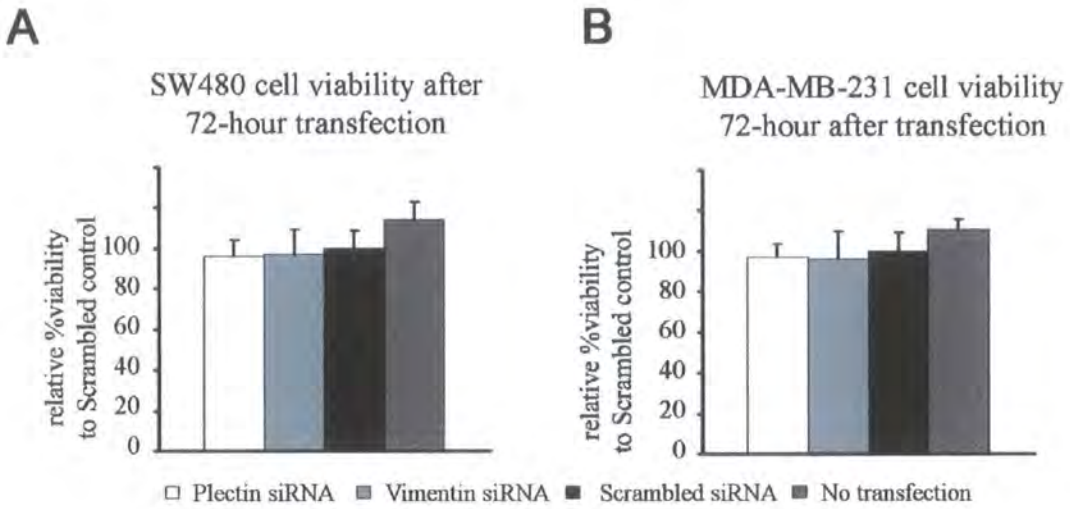


Figure 5.5. Cell survival after siRNA transfections.

Cell survival was measured using CellTiter cell proliferation kit (Promega UK). Mean and standard deviation of three measurements each, from three transfections are shown. (A) Cell survival of colon carcinoma SW480 cells after a 72-hour transfection. (B) MDA-MB-231 breast carcinoma cell survival.

5.2.3. Plectin depletion causes impairment of carcinoma cell invasion through collagen gels.

The ability of the plectin depleted carcinomas cells to migrate in a collagen gel invasion assay was investigated. Again, as in the invasion assays comparing the invasive potential of the carcinoma breast and colon cell panel, collagen was used instead of laminin, as the study was interested in the later stages of carcinoma cell invasion through the stroma. Serum starved cells were induced to migrate from cell culture inserts through collagen gel-coated filters using 10% Fetal Calf Serum (Sigma Aldrich UK) as a chemoattractant. Migrated cells were visualised by Dapi (Invitrogen UK) staining using randomised counting, where each insert was given a number at random that corresponds to the correct sample to ensure unbiased results. For each of the cell line the results were quantified from three independent experiments using triplicate filters for each transfection. Depleting SW480 cells of plectin caused a decrease of 72% in the number of invading cells compared to the control at twelve hours (Figure 5.6B). Figure 5.6A shows a representative filter from one of the assays demonstrating the marked decrease of invaded plectin depleted cells compared to the control. A similar decrease in invasion was not observed in the breast carcinoma MDA-MB-231 cells, where plectin-depleted cells showed a modest decrease of invasion at 14% compared to the control in six hours (Figure 5.7B). Figure 5.7A shows representative filters from one of the assays demonstrating the modest decrease. The degree of protein expression knockdown in both cell lines at the end of each assay was confirmed by immunoblotting showing at least an 84% down regulation of protein expression in both cell lines (Figure 5.6C, Figure 5.7C). The results presented above suggest that the degree of invasion in plectin depleted carcinoma cells is dependent on the cell type, although the observed trend is that plectin siRNA transfection causes a decrease in the invasion of carcinoma cell lines.

5.2.4. The depletion of vimentin dramatically reduces the ability of SW480 and MDA-MB-231 cells to invade through collagen gels.

A representative experiment illustrated by Dapi stained insert filters demonstrates a marked reduction in the invasion of both SW480 and MDA-MB-231 cells after vimentin siRNA transfection compared to a control siRNA transfection (Figure 5.8A and Figure 5.9A). Again, the results were quantified from three independent experiments using triplicate filters for each transfection, confirming significant

decrease in the number of vimentin-ablated SW480 (Figure 5.8B) and MDA-MB-231 (Figure 5.9B) cells migrating through collagen. The cells used in the experiment were analysed for vimentin depletion after the end point of each assay, Figure 5.9C shows that in SW480 cells vimentin was depleted by 82%. However, vimentin depletion in MDA-MB-231 cells demonstrates only a 58% knock down efficiency possibly due to the vimentin network having an increase stability or lower turnover in these cells that predominantly express vimentin but not keratins. The dramatically reduced invasion of the MDA-MD-231 cells after 58% depletion demonstrates the importance of vimentin in this process. The SW480 cells express a keratin network alongside the vimentin network (Figure 4.2) that may be able to circumvent the requirement of vimentin for integrin targeting which, in turn, could account for the differences observed between the two cell lines.

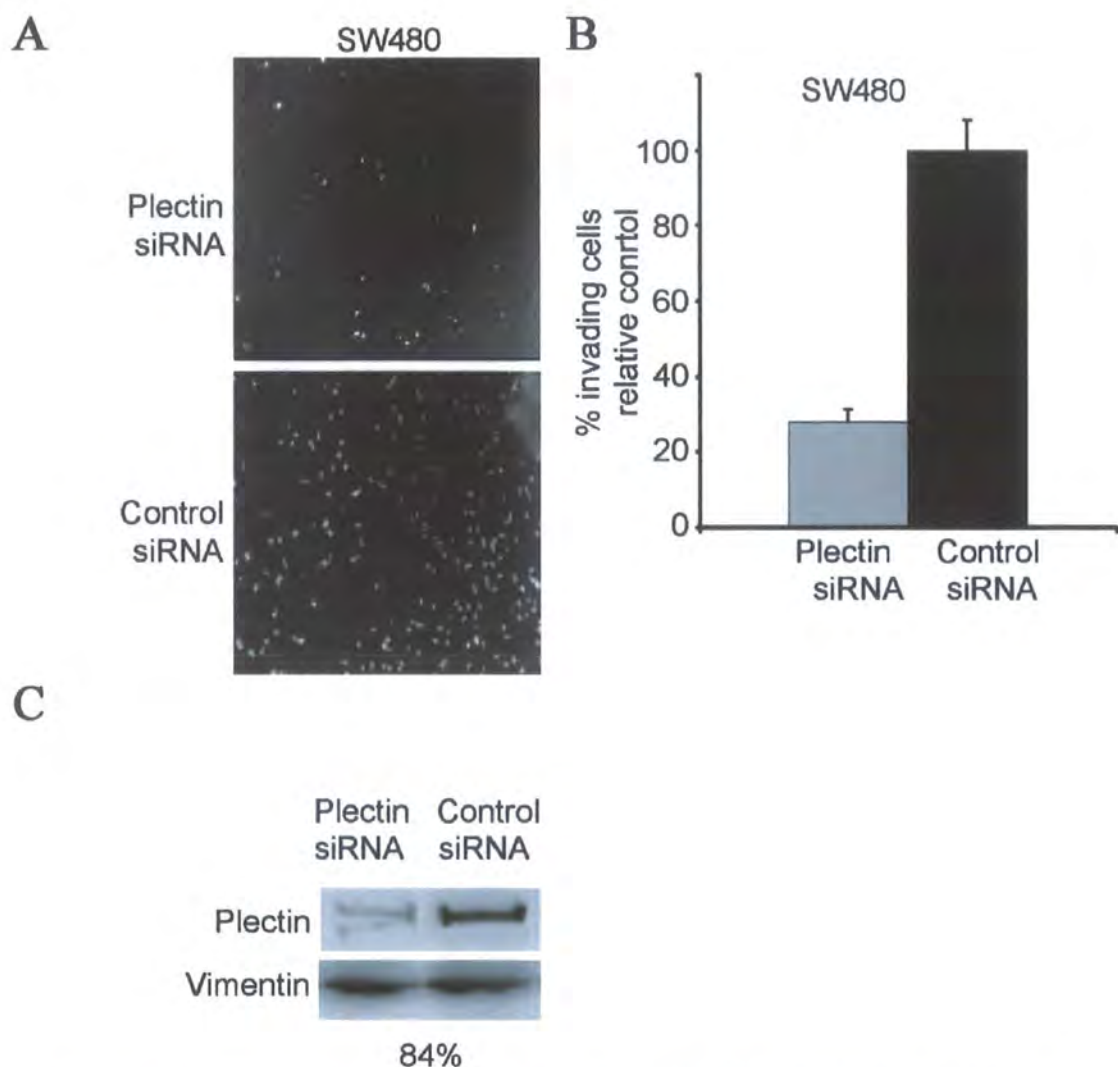


Figure 5.6. Impaired migration of plectin siRNA transfected SW480 cells.

(A) Dapi stainings to visualise cells migrated through collagen coated filters towards 10% FCS in a collagen invasion assay. Cells were transfected with control scrambled siRNA or plectin siRNA 72 hours prior to the assay. (B) Quantification of SW480 cell migration. Dapi stained nuclei were counted from three independent migration experiments at 12 hour time points, the graphs show average number of cells per microscopic field and standard error. (C) Immunoblot analysis of siRNA knockdown efficiency detected from same population of cells, extracted 96 hours after transfections.

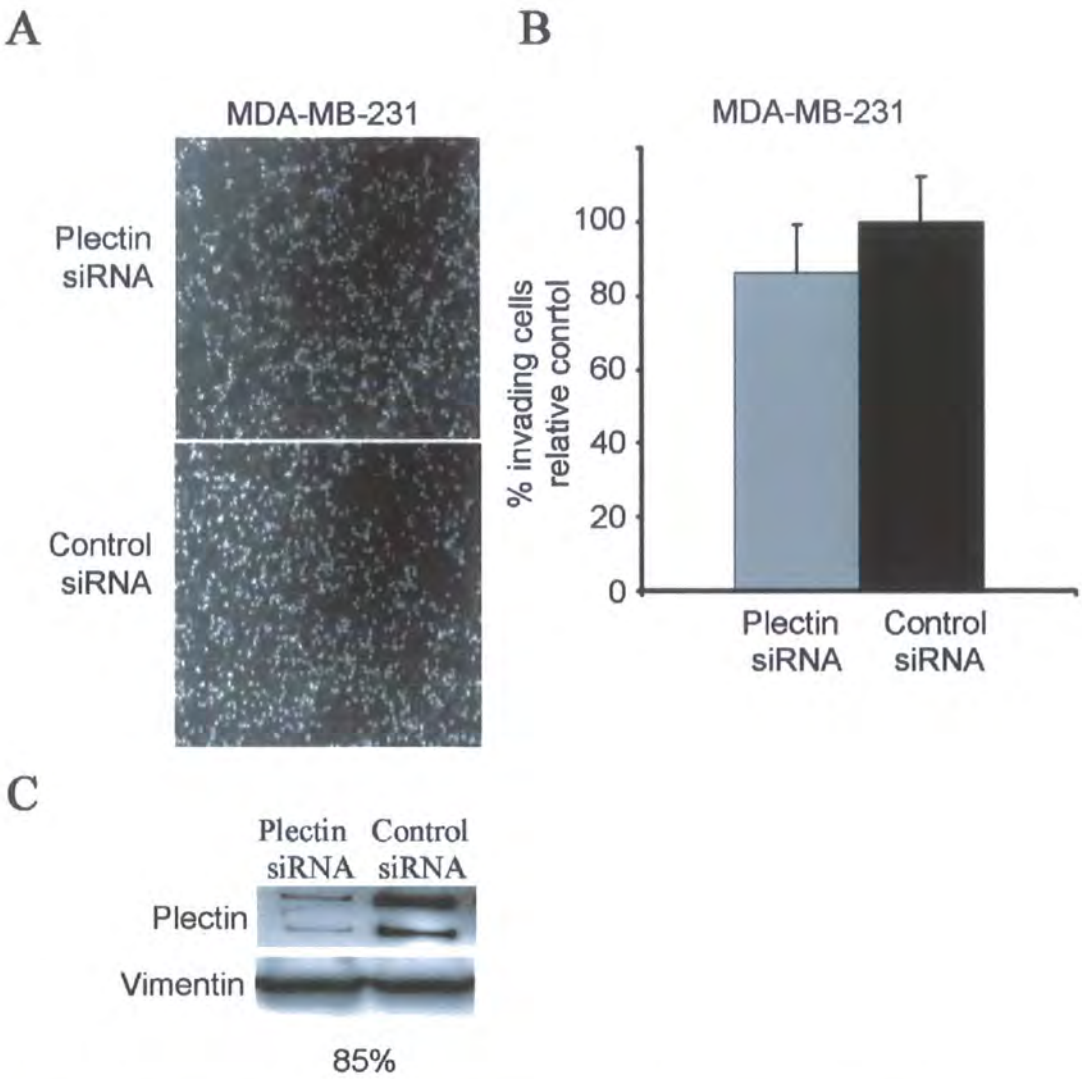


Figure 5.7. Invasion of plectin siRNA transfected MDA-MB-231 cells.

(A) Dapi stainings to visualise cells migrated through collagen coated filters towards 10% FCS in a collagen invasion assay. Cells were transfected with control scrambled siRNA or plectin siRNA 72 hours prior to the assay. (B) Quantification of MDA-MB-231 cell migration. Dapi stained nuclei were counted from three independent migration experiments at 6 hour time point, the graphs show average number of cells per microscopic field and standard error. (C) Immunoblot analysis of siRNA knockdown efficiency detected from same poulation of cells, extracted 78 hours after transfections.

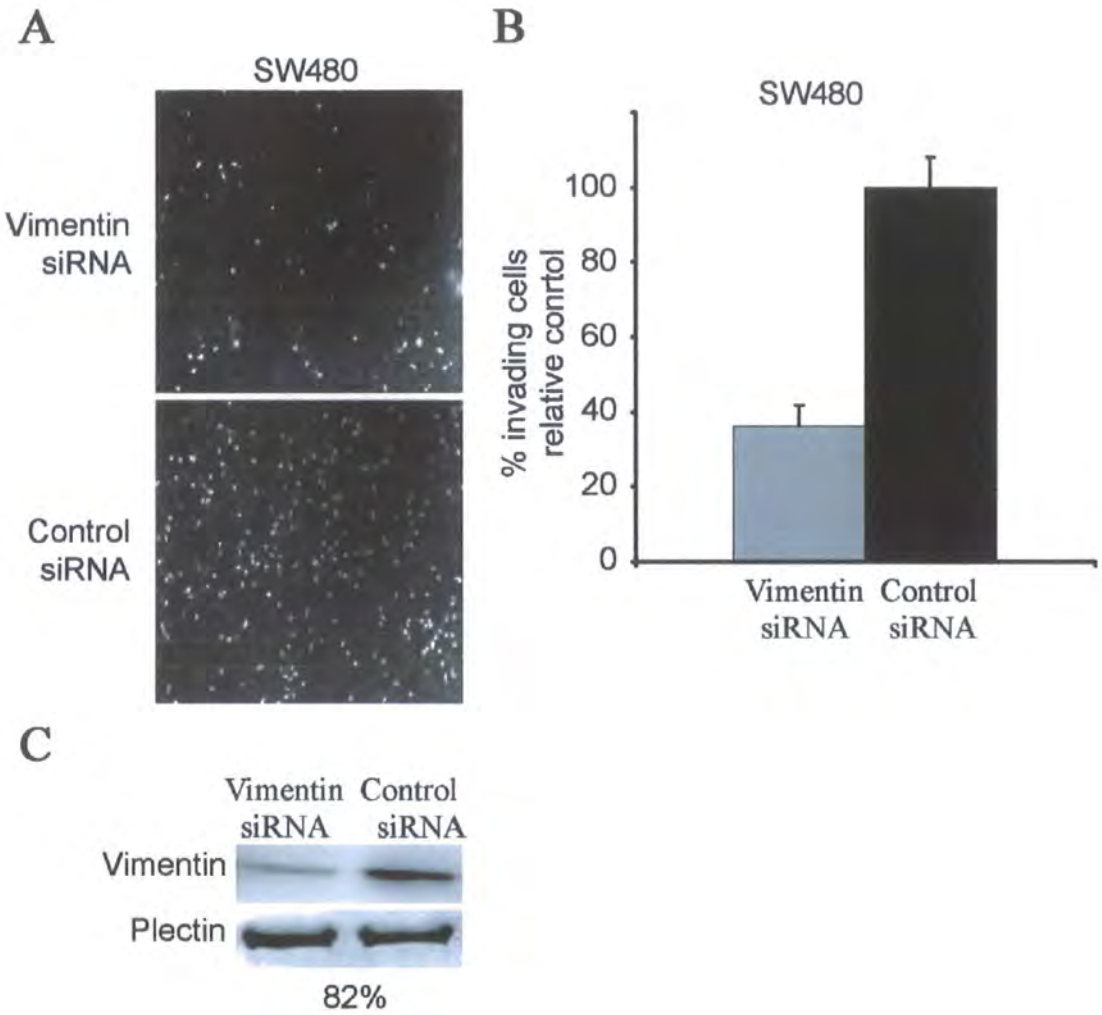


Figure 5.8. Impaired migration of vimentin siRNA transfected SW480 cells.

(A) Dapi stainings to visualise cells migrated through collagen coated filters towards 10% FCS in a collagen invasion assay. Cells were transfected with control scrambled siRNA or vimentin siRNA 72 hours prior to the assay. (B) Quantification of SW480 cell migration. Dapi stained nuclei were counted from three independent migration experiments at 12 hour time point, the graphs show average number of cells per microscopic field and standard error. (C) Immunoblot analysis of siRNA knockdown efficiency detected from same population of cells, extracted 96 hours after transfections.

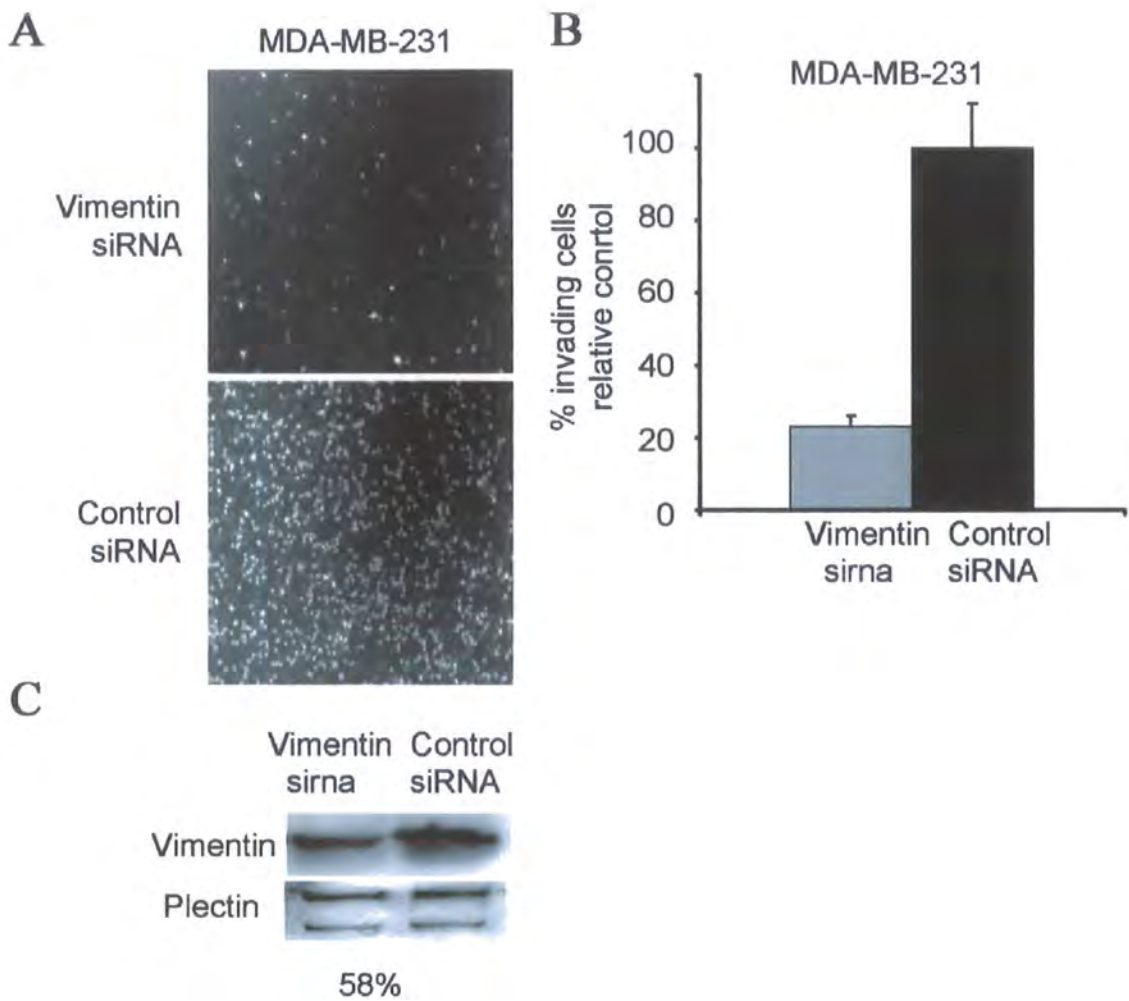


Figure 5.9. Impaired migration of vimentin siRNA transfected MDA-MB-231 cells. (A) Dapi stainings to visualise cells migrated through collagen coated filters towards 10% FCS in a collagen invasion assay. Cells were transfected with control scrambled siRNA or vimentin siRNA 72 hours prior to the assay. (B) Quantification of MDA-MB-231 cell migration. Dapi stained nuclei were counted from three independent migration experiments at 6 hour time point, the graphs show average number of cells per microscopic field and standard error. (C) Immunoblot analysis of siRNA knockdown efficiency detected from same population of cells, extracted 78 hours after transfection.

5.2.5. Plectin ablation decreases attachment to fibrillar collagen in both MDA-MB-231 and SW480 carcinoma cells.

The results obtained in the invasion assay prompted the study of the ability of the carcinoma cells to attach to a collagen surface to find out if cell attachment could account for the differences observed in the invasion experiments. The ability of the siRNA transfected cells to attach to fibrillar collagen was measured after 5, 10, 20 and 40 min of incubation. Depletion of plectin in SW480 colon carcinoma cells resulted in a significant decrease in adhesion to collagen (Figure 5.10A) at all time points, determined at T-test acceptance of $p < 0.05$. When plectin was depleted in the MDA-MB-231 attachment was also impaired although not to the same extent that was seen in the SW480 cells (Figure 5.10B). The efficiency of the knockdown was evaluated using immunoblotting after the assay had terminated showing similar results to the invasion assay (Figure 5.6 C and Figure 5.7C).

5.2.6. Vimentin ablation alters attachment to fibrillar collagen in both MDA-MB-231 and SW480 carcinoma cells.

In MDA-MB-231 breast cancer cells, siRNA ablation of vimentin resulted in a significant decrease in adhesion to fibrillar collagen (Figure 5.10D). Impaired adhesion was evident at 10 min time point and the difference in the adherent cells was even more pronounced in the later time points with more than 30% less cells attaching. On the contrary, vimentin ablation had only a modest effect on cell adhesion in SW480 cells with no clear trend observed in comparison with control siRNA transfected cells (Figure 5.10C). Thus, the effect of vimentin on cell adhesion is cell type specific. Again, it is possible that the expression of keratin in the SW480 cells unlike the MDA-MB-231 cells could account for the observed differences in this assay. The efficiency of the knockdown was evaluated using immunoblotting after the assay had terminated showing similar results to the invasion assay (Figure 5.8C Figure 5.9C).

5.2.7. Depletion of plectin and vimentin in SW480 cells reduce number of cells in suspension compared to scrambled control.

The colon carcinoma SW480 cell line is unusual compared to the other epithelial carcinoma cell lines used in this study as a subset of cells go through cycles of detaching and reattaching in culture (observed during routine cell maintenance and Dr Naomi Willis, personal communication). Interestingly, during experiments using

siRNA transfections it was observed that plectin or vimentin depletion decreased the number of cells growing in suspension. In order to quantify this, the media was collected after a 72-hour transfection and centrifuged to pellet the suspended cells that were then resuspended in equal volumes of media and counted discounting any dead cells with Trypan blue (Sigma Aldrich UK). The results confirm the observation demonstrating that plectin or vimentin depletion significantly reduced the number of cells in suspension by 66% and 54%, respectively (Figure 5.10E). Furthermore, when immunoblot analysis was performed on the detached cells it was found that they had the same degree of plectin depletion compared to the control as the adherent cells (Figure 5.10F). It should be pointed out that in the attachment assays described above all cells were suspended by trypsinization, which strips the cell surface of integrin attachments. However, it can be speculated that the decreased level of the cells in suspension is not due to an inability of plectin and vimentin depleted cells to detach and reattach. Instead, knockdown of these proteins may result in a slower kinetics of adhesion possibly by interfering with the ability of the cell to remodel the cytoskeleton. This is further supported by the observation that in longer cell attachment assays lasting 2 hours the plectin and vimentin depleted SW480 and MDA-MD-321 cells had all attached to the same degree as the control cells.

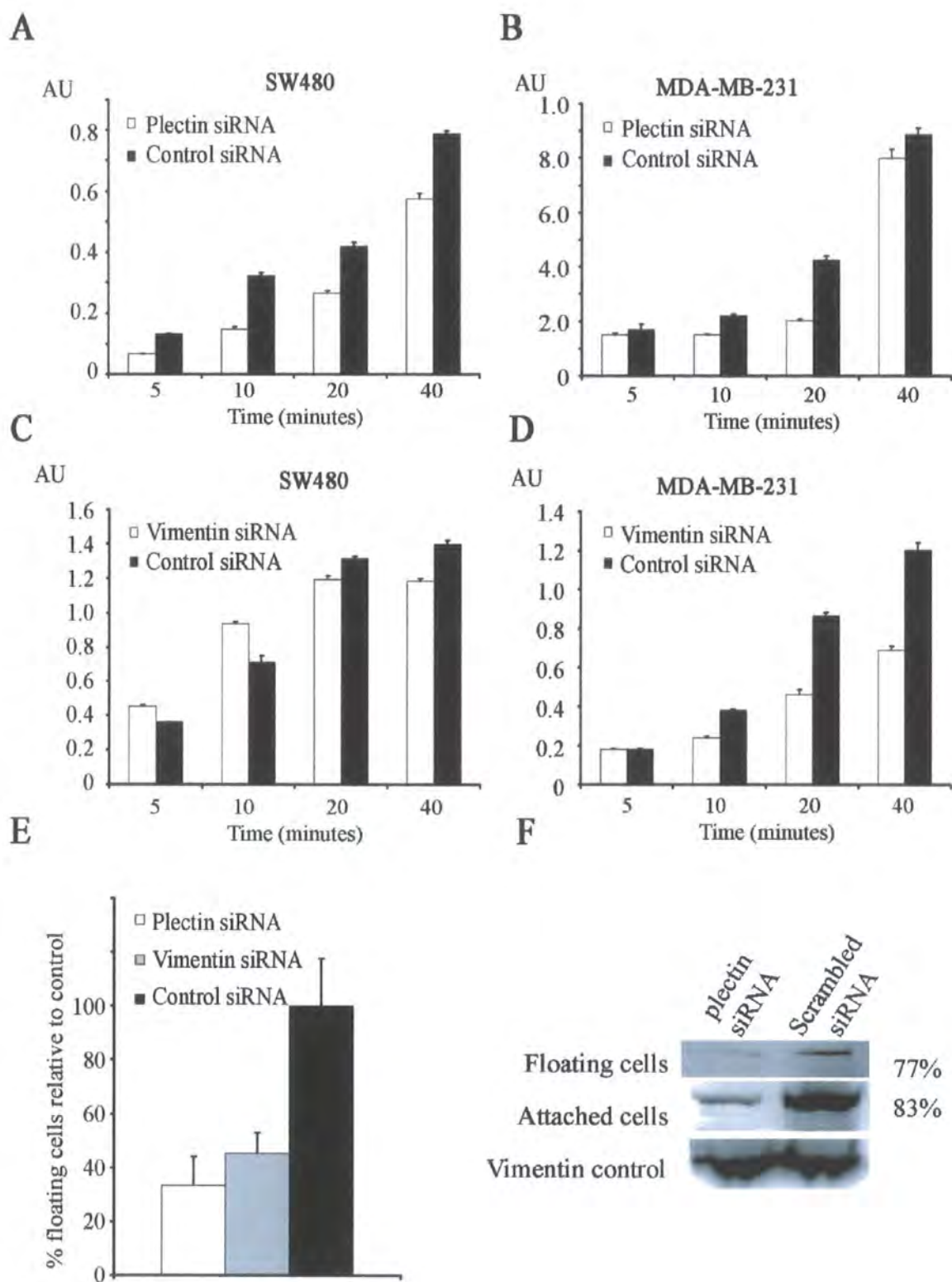


Figure 5.10. Adhesion of carcinoma cells to fibrillar collagen.

Cell attachment assay of plectin siRNA (white bars) or control siRNA (black bars) transfected SW480 cells (A) and MDA-MB-231 cells (B). Cell attachment assay of vimentin siRNA (white bars) or control siRNA (black bars) transfected SW480 cells (C) and MDA-MB-231 cells (D). Cells were suspended 72 hours after transfection and left to attach to collagen coated tissue-culture wells. Non-adherent cells were washed away at indicated time points and the adherent cells were quantified by colorimetric cell viability kit (measured by absorbance units (AU) at 490 nm). Mean and standard error of mean of three independent experiments (Three repeats each) are shown. The difference between control and vimentin or plectin siRNA transfected cells was statistically significant (T-test, $p < 0.05$) at 10, 20 and 40 minutes time points for (C). (D) Percentage of plectin and vimentin siRNA transfected SW480 cells in suspension after 96-hour transfection with a 48-hour media change compared to control transfected cells. (E) Immunoblot analysis of protein extracted from siRNA plectin and control transfected suspended cells compared to adherent cells, with vimentin as a loading control.

5.2.8. Scratch wound assay as a tool to measure wound closure rates in epithelial cells.

Scratch-wound assays on confluent monolayers were utilised as an additional way of investigating cell migration. Growing cells to a confluent monolayer and scratching with a pipette tip to produce a wound is a widely used classical method to measure migration rates of epithelial cells (Wong et al., 1988; Yarrow et al., 2005; Valster et al., 2005 and recently Long et al., 2006). Cell monolayers were wounded in triplicate and the closure was measured at 2, 4, 6, hours after wounding using phase contrast imaging of exactly the same area of the wounds. Control transfected MDA-MB-231 cells migrated particularly rapidly in this assay filling the empty wound space within the 6 hours, whereas the control transfected SW480 cells migrated at a slower rate of only 80% wound closure after the 6 hours. This correlates with the invasion assay where the MDA-MB-231 cell had a high invasive potential. Moreover, after 6 hours the floating SW480 cells started to re-attach and fill the wound space making measurement of wound edge closure in the subsequent time points difficult. The 6-hour time point was, therefore, chosen to provide a fair and representative assay of wound closure. It is noted that in this case the cells do not form coherent epithelial sheets, have sparse cell-cell contacts and are able to detach from the wound edge. Thus, the measurements here are an indication of migration of cells to fill a wound space.

5.2.9. The ability of cells to close a wound in vitro was impaired by plectin siRNA in SW480 carcinoma cells but not in MDA-MB-231 carcinoma cells.

Scratch wound assays indicated that plectin contributes to SW480 carcinoma cell migration as plectin knockdown wounds started to close more slowly than control scrambled siRNA transfected wounds (Figure 5.11A). Moreover, plectin depleted wounds remained open up to 24 hour time point when control transfected scratch wounds were completely closed (Figure 5.11D). On the contrary, plectin depletion in MDA-MB-231 cells demonstrated a slight increase in the rate of wound closure at 2 and 4 hours compared to control cells. Both control and plectin depleted wounds were completely closed after the six hours in two out of three wounds (Figure 5.12B). The extent of the down-regulation of plectin was confirmed by immunoblot analysis of an extract from the scratch wound after the 6 hours showing depletion of 83% in SW480 cells and 80% in MDA-MB-231 cells (Figure 5.11C and Figure 5.12C). The above

results indicate that the down regulation of plectin affects the ability of epithelial cells to close a wound in a cell-dependent manner.

5.2.10. The ability of cells to close a wound in vitro is significantly impaired by vimentin depletion in both colon and breast carcinoma cells.

Wound closure was also investigated in vimentin siRNA transfected SW480 and MDA-MB-231 monolayers. Control transfected MDA-MB-231 cells migrated to fill the empty wound space in about 6 hours, whereas the vimentin knock-down wounds remained largely open at that time point (Figure 5.14B). SW480 cells migrated more slowly than MDA-MB-231 cells (Figure 5.13A), but the difference between control transfected and vimentin siRNA transfected cells was evident at the 6 hour time point and was confirmed by measurements of the relative closure of the wound in three independently transfected wounds. Closure of vimentin ablated MDA-MB-231 wounds was quantified at 2, 4 and 6 hour time points demonstrating significantly slower closure at all studied time points compared to control transfected cells. Notably, two out of three control wounds were completely closed after 6 hours, whereas all vimentin siRNA transfected wounds remained almost 80% open (Figure 5.14 A). The down regulation of vimentin was confirmed by immunoblot analysis of an extract after the 6 hours showing depletion of 72% in SW480 cells and only 48% in MDA-MB-231 cells (Figure 5.13C and Figure 5.14C). The low efficiency of vimentin depletion in the MDA-MB-231 cell line is possibly due to transfection of the cells at a higher density of 50-60% that was needed for the cells to form a monolayer at the 96 hour time point. The decrease in knockdown efficiency could be possibly due to the stabilisation of vimentin networks in confluent monolayers. This result further demonstrates the dramatic impairment of migration that even a partial loss of vimentin causes in this cell line.

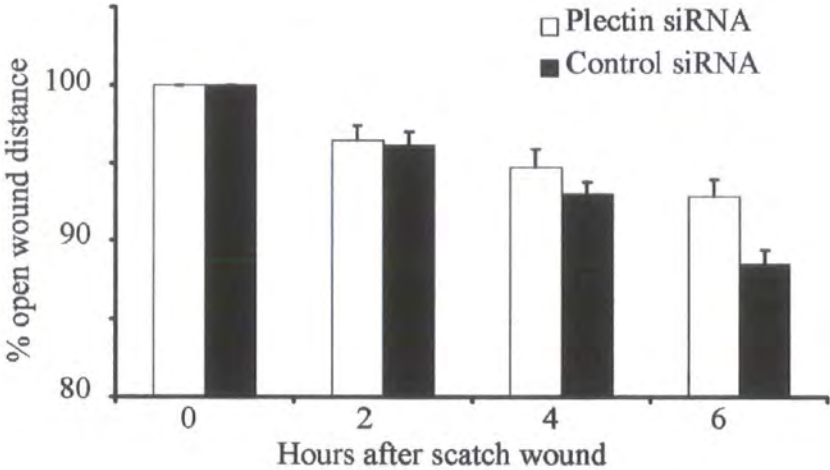
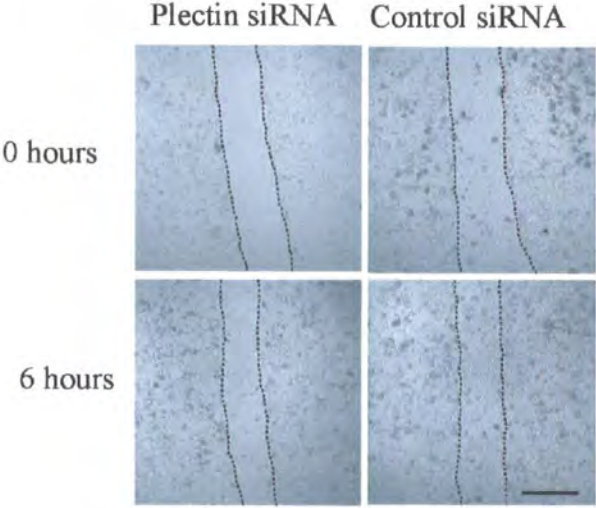
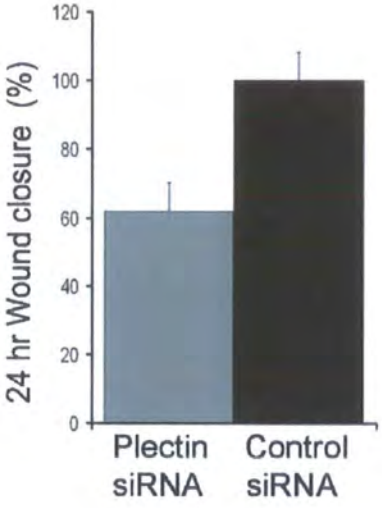
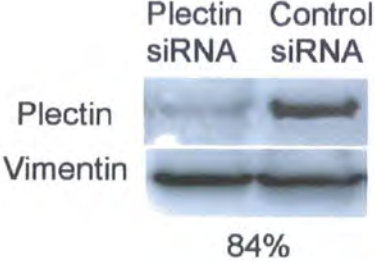
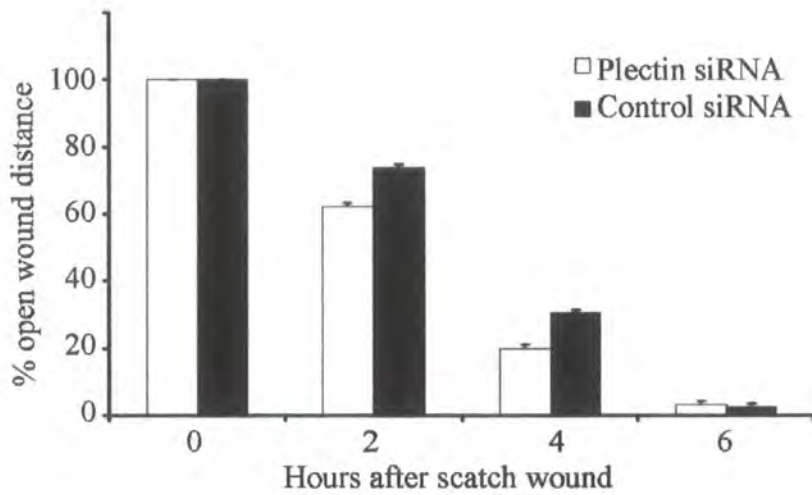
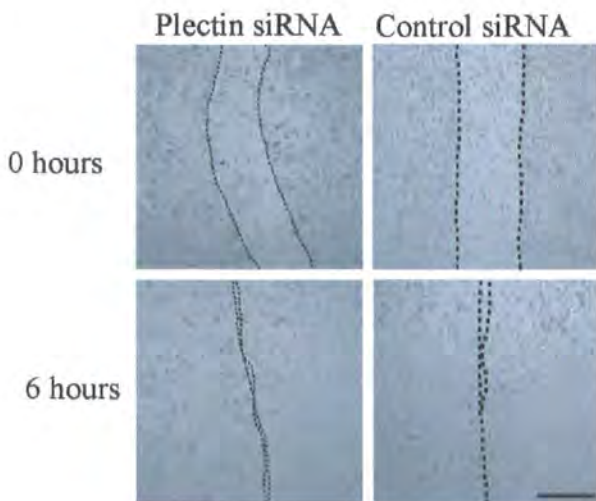
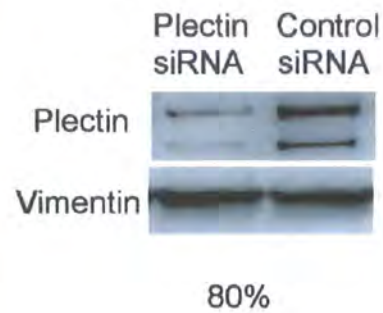
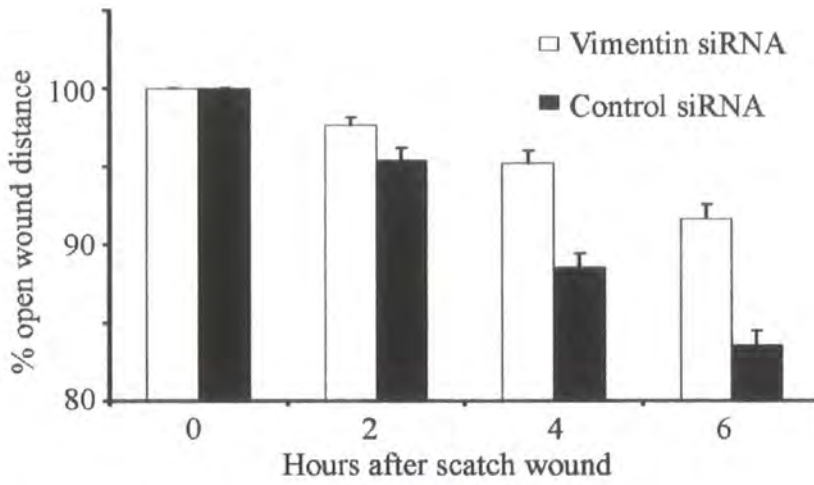
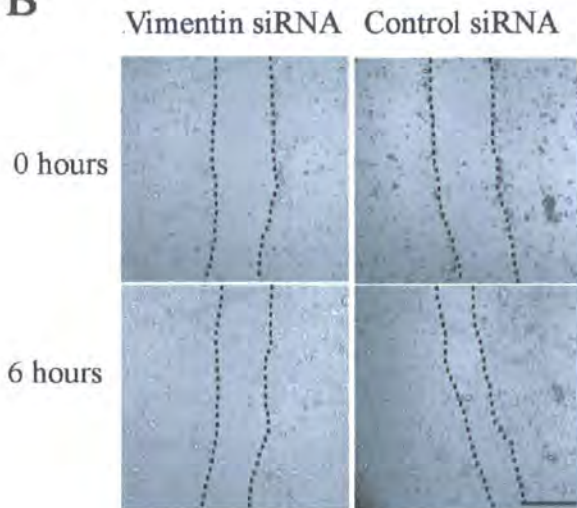
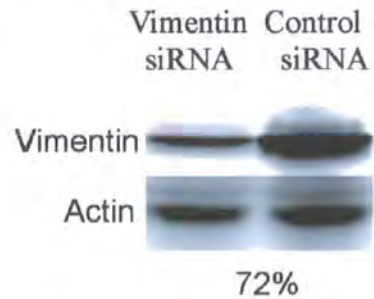
A**SW480 Scratch wound****B****C****D**

Figure 5.11. Wound migration properties of plectin depleted SW480 cells.

(A) Open wound distance of SW480 wounds. Three locations of three independent control and plectin siRNA transfected wounds were photographed at 0, 2, 4 and 6 hours. Open wound distance at the start of the experiment designated as 100% and closure of the wounds is shown relation to that. Error bars denote standard error. (B) Representative phase contrast micrographs of closure of scratch-wounded confluent cultures of control siRNA or plectin siRNA transfected SW480 cells at time point immediately after wounding and six hours post wounding. Scratch wound edges are marked by dotted lines. Scale bar represents 500 μm . (B) Closure of the control (black) and plectin (grey) siRNA transfected scratch wounds at 24 hours after wounding was measured from photomicrographs. 100% indicates a completely closed wound. The bars represent mean and standard deviation of three measurements. (C) Immunoblot analysis of knockdown efficiency of cell extracted from representative wound shown after assay termination. Vimentin expression is shown as a loading control.

A**MDA-MB-231 Scratch wound****B****C****Figure 5.12. Open wound migration distance of plectin depleted MDA-MB-231.**

(A) Open wound distance of MDA-MB-231 wounds. Three locations of three independent control and plectin siRNA transfected wounds were photographed at 0, 2, 4 and 6 hours. Open wound distance at the start of the experiment designated as 100% and closure of the wounds is shown relation to that. Error bars denote standard error. (B) Representative phase contrast micrographs of closure of scratch-wounded confluent cultures of control siRNA or plectin siRNA transfected MDA-MB-231 cells at time point immediately after wounding and six hours post wounding. Scratch wound edges are marked by dotted lines. Scale bar represents 500 μm . (C) Immunoblot analysis of knockdown efficiency of cell extract from representative wound shown after assay termination. Vimentin is shown as a loading control.

A**SW480 Scratch wound****B****C****Figure 5.13. Open wound migration distance of vimentin depleted SW480 cells.**

(A) Open wound distance of SW480 wounds. Three locations of three independent control and vimentin siRNA transfected wounds were photographed at 0, 2, 4 and 6 hours. Open wound distance at the start of the experiment designated as 100% and closure of the wounds is shown relation to that. Error bars denote standard error. (B) Representative phase contrast micrographs of closure of scratch-wounded confluent cultures of control siRNA or vimentin siRNA transfected SW480 cells at time point immediately after wounding and six hours post wounding. Scratch wound edges are marked by dotted lines. Scale bar represents 500 μm . (C) Immunoblot analysis of knock-down efficiency of cell extract from representative wound shown after assay termination. Actin is shown as a loading control.

A

MDA-MB-231 Scratch wound

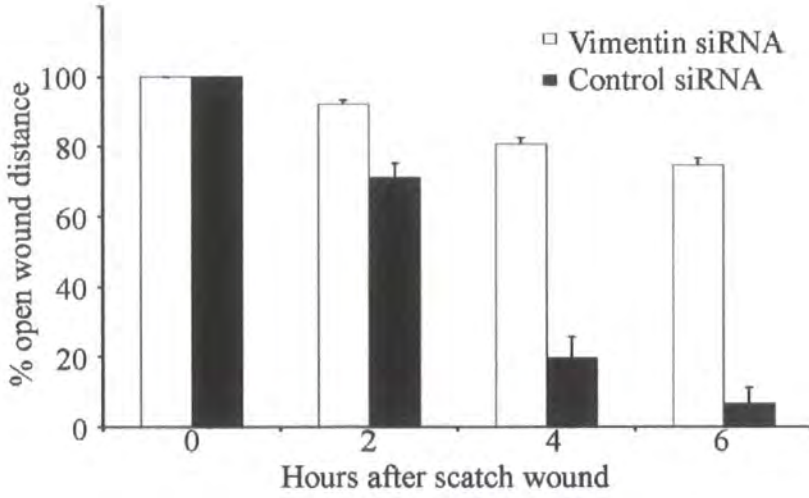
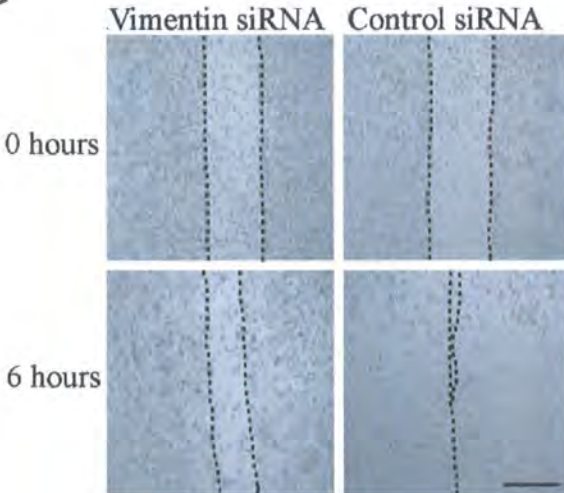
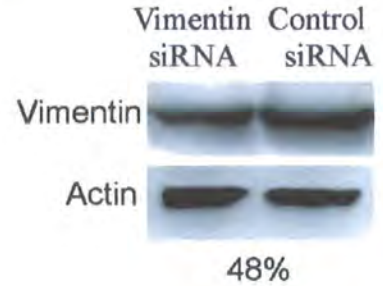
**B****C**

Figure 5.14. Open wound migration distance of vimentin depleted MDA-MB-231 cells. (A) Open wound distance of MDA-MB-231 wounds. Three locations of three independent control and vimentin siRNA transfected wounds were photographed at 0, 2, 4 and 6 hours. Open wound distance at the start of the experiment designated as 100% and closure of the wounds is shown relation to that. Error bars denote standard error. (B) Representative phase contrast micrographs of closure of scratch-wounded confluent cultures of control siRNA or vimentin siRNA transfected MDA-MB-231 cells at time point immediately after wounding and six hours post wounding. Scratch wound edges are marked by dotted lines. Scale bar represents 500 μ m. (C) Immunoblot analysis of knockdown efficiency of cell extract from representative wound shown after assay termination. Actin is shown as a loading control.

5.2.11. Vimentin depletion is confirmed by immunofluorescence on scratch wound monolayers.

Confocal microscopy using immunofluorescence confirms that vimentin is uniformly down regulated in the scratch wound migration experiments in both SW480 and MDA-MB-231 cells (Figure 5.15A/B). Vimentin expression in these cells was visualised using Cy3-conjugated antibody that gives a very bright fluorescent signal especially around the nucleus where the vimentin cytoskeleton is organised into a dense cage-like network. The confocal settings for detection of fluorescent signal were unchanged for vimentin-depleted cells as control cells to demonstrate the difference in fluorescent signal. These results confirm that siRNA transfections were efficient in causing a consistent and reproducible downregulation of vimentin expression. Immunofluorescence analysis with antibodies against plectin demonstrated that vimentin ablation did not cause major changes in cell morphology (Figure 5.15). However, it was noted that in scratch-wound experiments, there were markedly less SW480 cells that quickly escaped the wound edge and started to fill in the wound space (Figure 5.15A). This observation was a further indication that cell migration is affected by absence of vimentin.

5.2.12. Plectin depletion alters actin dynamics at the wound edge.

In order to investigate the possible causes for the decrease of migration in plectin depleted SW480 cells, confocal microscopy was used to characterise the appearance at the wound edge using co-staining with the cytoskeletal protein actin. In control-transfected monolayers, wound edge cells were actively migrating away from the edge, whereas plectin knockdown cells retained a flattened morphology and remained tightly packed at the wound edge (Figure 5.16A). Actin staining of the control transfected cells demonstrated the presence of round adhesion structures at the cell periphery that were absent in plectin knockdown cells (Figure 5.16B). These results show that plectin is involved in actin dynamics at the wound edge and support previous work showing plectin to be involved in the regulation of actin organisation (Andra et al., 1998).

5.2.13. Plectin depletion alters the appearance of actin in confluent monolayers in SW480 cells.

Further evidence to support that plectin is involved in the remodelling of actin was provided by confocal microscopy of plectin depleted unwounded SW480 monolayers (Figure 5.17). Actin and plectin staining in control layers show cells to be irregularly shaped with areas in the monolayer where cells do not form cell-cell junctions (arrow). Furthermore, actin is arranged at the cell periphery and at a dense cage around the nucleus where it co-localises with plectin. In contrast, plectin depleted monolayers resemble an epithelial sheet as observed in the less aggressive cell lines (HT29, Figure 4.5) where the cells are arranged in a regular array and are tightly packed. In the plectin depleted cells there was also an observed increase in actin stress fibers in these cells that also display flattened cell morphology, with loss of the dense actin cage around the nucleus (Figure 5.17). In conclusion depletion of plectin causes an alteration of actin dynamics in colon carcinoma cells and leads to a flattened cell morphology.

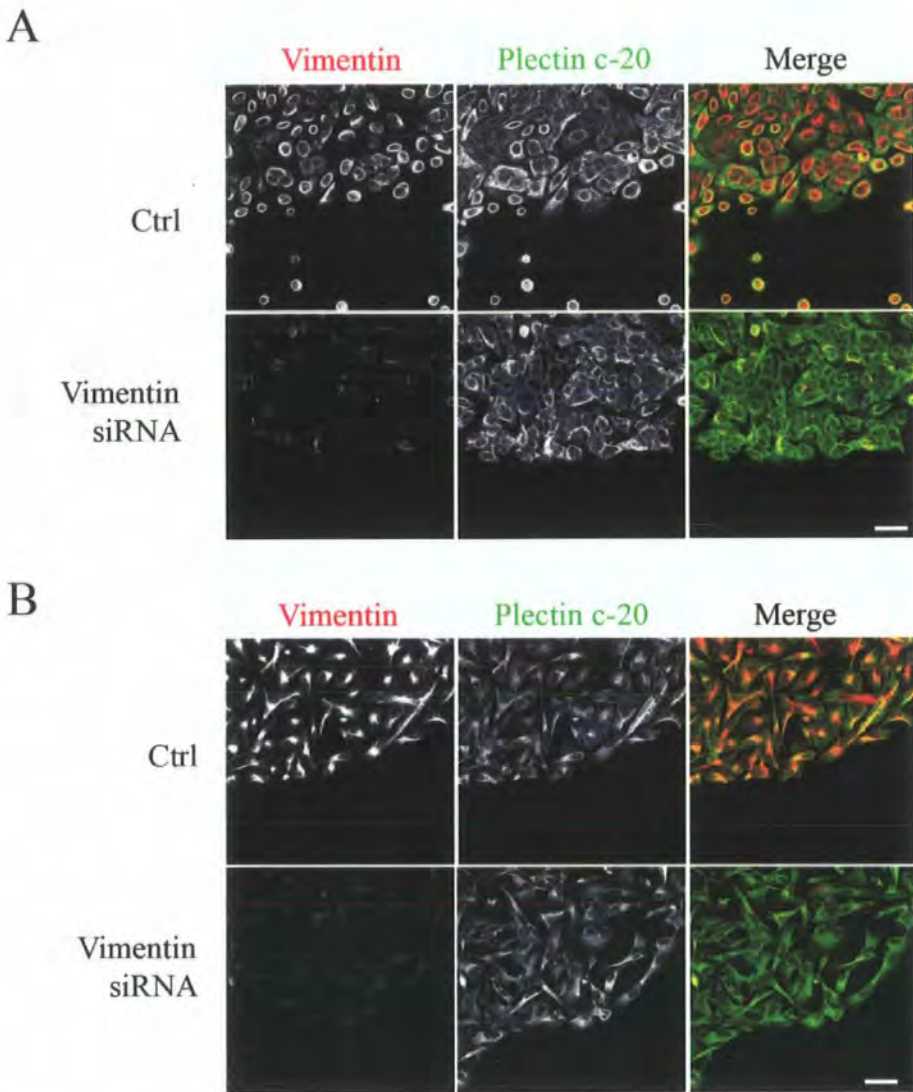


Figure 5.15. Immunofluorescence analysis of vimentin ablation in carcinoma cell monolayers.

(A) Vimentin (red channel) and plectin (green channel) and merged image (on the right) immunofluorescence staining of vimentin siRNA or control siRNA transfected SW480 monolayers, that were scratch-wounded 72 hours after transfection. (B) Vimentin and plectin immunostainings of siRNA transfected and scratch wounded MDA-MB-231 cell monolayers. Note in both panel A and B that vimentin siRNA transfection leads to uniform downregulation of vimentin expression. Scale bars corresponds to 20 μm for all panels.

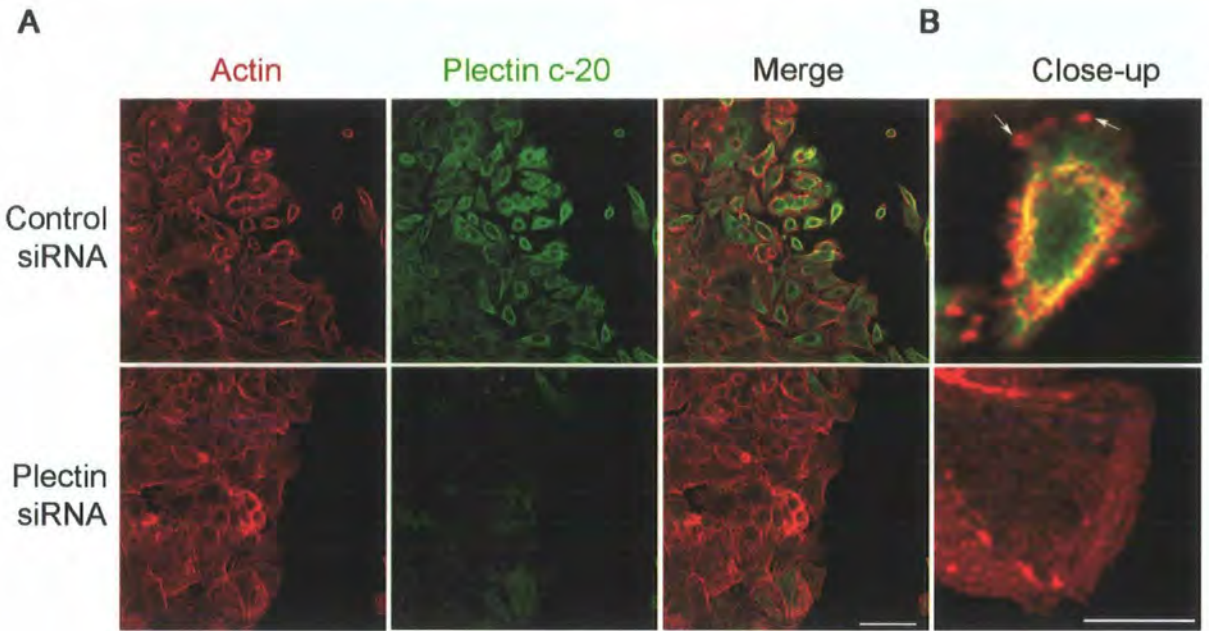


Figure 5.16. Plectin knock-down inhibits actin dynamics at the wound edge of SW480 cells.

(A) SW480 cell monolayers were transfected with either scrambled control siRNA (top row) or plectin siRNA (bottom row) and scratch wounded. The panels show immunofluorescence analysis of actin organisation and expression of plectin two hours after wounding. (B) Magnified detail: Arrows point at podosome-like actin foci that are absent in plectin siRNA transfected migrating wound edge cells. Scale bar corresponds to 50 μm panel A and 10 μm in panel B.

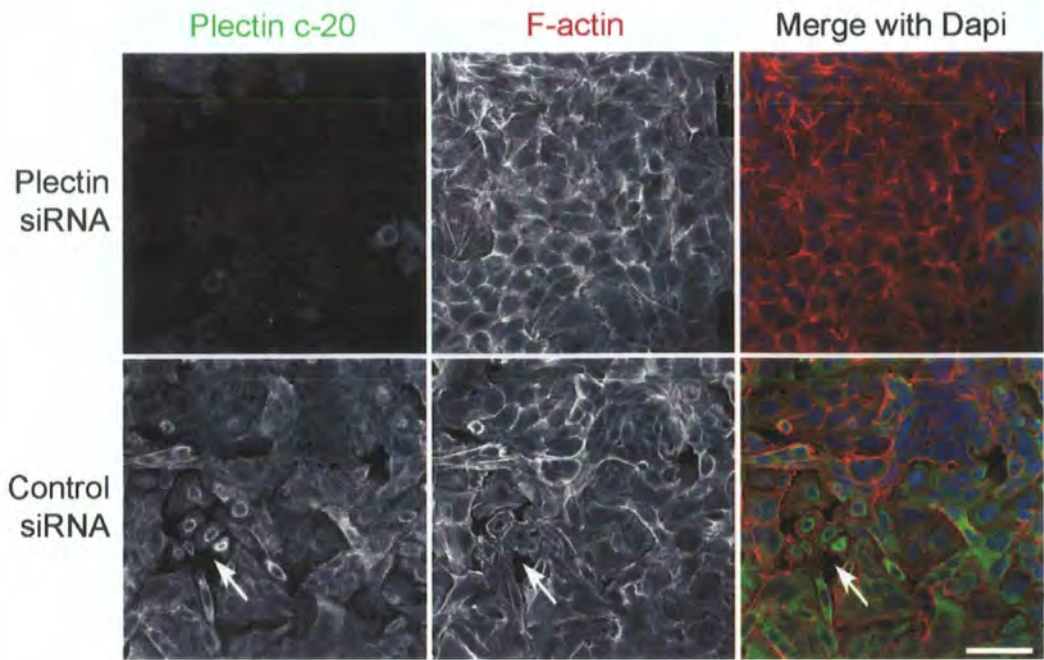


Figure 5.17. Plectin knock-down alters monolayer characteristics of SW480 cells. SW480 cell monolayers were transfected with either plectin siRNA (top row) or scrambled control siRNA (bottom row). The panels show immunofluorescence analysis of actin organisation and expression of plectin. Scale bar represents 50 μ m. Control monolayers expressing high levels of plectin show a more disordered monolayer with heterogeneous cell morphologies.

5.3. Discussion.

In order to investigate the role of the intermediate filament protein vimentin and its associated linker protein plectin in carcinoma cell migration, vimentin expressing SW480 and MDA-MB-231 cell lines were used. From previous results it can be seen that these cell lines were the most invasive in the investigated carcinoma cell panel. Furthermore, these cells were vimentin positive and had significantly elevated protein expression of plectin compared to the lower grade carcinoma cells HT29 and SW480 (Figure 4.2). The SW480 cells had also retained relatively high expression of keratin 8/18 intermediate filaments and desmoplakin, the major cytolinkers protein connecting keratin intermediate filaments to desmosomes (Leung et al., 2002). Thus, these cell lines provide a model where the effect of vimentin ablation could be investigated in the presence or absence of an intact keratin cytoskeleton. Co-expression of vimentin and keratin intermediate filaments in the same cells is intriguing, as previous experiments have shown increased motility in vimentin positive melanoma cells that were transfected with keratin 8 and 18 constructs (Chu et al., 1996). Vimentin and keratin intermediate filament expression is also associated with recurrent and metastatic disease in melanoma (Hendrix et al., 1992). The relative increased expression of plectin in both the high-grade breast and colon carcinoma cell lines is interesting, as plectin has previously been found to link to vimentin via the C-terminal plectin repeat domain (Wiche et al., 1993). Plectin has also been shown to localise with vimentin positive focal adhesions in endothelial cells (Gonzales et al., 2001) and also to link intermediate filaments to hemidesmosomes via $\alpha 6\beta 4$ integrin (Foisner et al., 1988; Reznicek et al., 1998; Schaapveld et al., 1998). Moreover, an additional vimentin-binding site in plectin residing within the CH1 subdomain of its ABD has been identified. Vimentin has been shown to bind to this site via the amino-terminal part of its rod domain (Sevcik et al., 2004). The authors speculate that this additional amino-terminal intermediate filament protein-binding site of plectin may have a function in intermediate filament dynamics and assembly, rather than in linking and stabilizing intermediate filament networks (Sevcik et al., 2004). All these previous findings above prompted the investigation of the role of plectin and vimentin in the migration and invasion of SW480 and MDA-MB-231 cells that express these proteins in high levels. Table 5.1 at the end of this discussion summarises the main results of migration invasion and adhesion assays of carcinoma cells used in this study.

To first investigate the role of plectin in these cell lines, down regulation of plectin expression was carried out using transient siRNA transfection in SW480 cells. The stability or the turnover of a plectin is relatively fast showing over 95% knockdown using plectin siRNA ID144451 in 48 hours and a continued knockdown to the same efficiency still after 102 hours. Transfection of plectin siRNA into the MDA-MB-231 cell line showed similar levels of depletion as in the colon carcinomas cells. The use of transient transfection of siRNA to knockdown plectin was found to be a suitable tool for migration, invasion and attachment assays.

Since plectin is involved in remodelling of the cytoskeleton (Wiche et al., 1998), knocking down plectin may affect the ability of the cell to do this efficiently. It was found that the plectin depleted SW480 cells invaded 72% (Figure 5.6) less than the control transfected cells in an invasion assay. However, the MDA-MB cell line showed a modest decrease of only 14% less cell invasion in the collagen invasion assay (Figure 5.7). This result indicates that plectin is involved in the invasion of carcinoma cells in a cell type specific manner. This is further supported by the finding that in a scratch wound assay, plectin-depleted SW480 cells show impairment in the ability to close a wound (Figure 5.11), whereas plectin depletion of the MDA-MB-231 cells results in a modest increased rate of wound closure compared to control cells (Figure 5.12). The above results suggest that the breast carcinoma and colon carcinoma cells use different modes of migration and invasion and plectin plays a key role in modulating these processes in a regulatory manner in both cell lines. In other previous studies of plectin depletion impaired migration was displayed in fibroblasts, and epithelial cells (Andra et al., 1998; Boczonadi et al., 2007; Abrahamsberg et al., 2005). These results are contrasted by the finding of plectin-depleted keratinocytes that migrate faster than the control (Osmanagic-Myers et al., 2006). One possible explanation for the contrasting effects of plectin on cell migration could be that different cell lines exhibit cell-specific expression of plectin N-terminal isoforms as seen in the mRNA expression (Figure 3.6) where the MDA-MB-231 cells had a high expression of isoform 1a and 1d compared to SW480 cells. Also plectin-1a is a major isoform expressed in keratinocytes where the primary function of plectin is in hemidesmosomes (Rezniczek et al., 2003), whereas in fibroblasts it is likely that plectin isoforms associated with actin stress fibers or focal adhesion complexes play a more important role. It would, therefore, be of interest to investigate the effect on carcinoma cell migration and

invasion of specific plectin isoforms by knocking down each isoform individually. However, due to the short length of most of the alternative exons finding suitable siRNA targets is challenging. The generation of plectin isoform specific null mice (Abrahamsberg et al., 2005) will provide a tool for investigation of the specific isoforms in cell migration and invasion.

When the ability of plectin-depleted cells to attach to fibrillar collagen was investigated, the attachment was impaired in MDA-MB-231 cells and to a greater extent in the SW480 cells (Figure 5.10). Interestingly, after two hours all the cells had attached demonstrating that plectin was not essential for the attachment of cells to a substrate but increased the rate in which cells could attach. Furthermore, in the SW480 cell line where cells in culture cycle through attaching and reattaching it was found that plectin depleted cells had fewer cells in suspension and therefore decreased the ability of the cells to carry out this process. Previously, the attachment of keratinocytes from a patient with plectin deficiency was found to unexpectedly have increased adhesion compared to normal keratinocytes. However, it was found that these cells could be detached from a matrix-coated surface much easier than the normal keratinocytes (Kurose et al., 2000). In this case, the authors suggested that plectin depletion could cause an increased expression of other cell adhesion molecules in keratinocytes and plectin may then be involved in stabilising long-term adhesions. The differences in the matrix attachment of plectin-depleted cells lead to the suggestion of cell-type specific roles possibly again due to the difference in plectin N-terminal isoform expression between cell types.

To investigate the role of vimentin expression on carcinoma cell migration and invasion, siRNA transfections were used to deplete the protein in SW480 cells. After a 48 hour transfection vimentin was depleted by around 60% and by 90% after 96 hours. Compared to plectin, vimentin is more stable in these cells possibly due to stabilisation of the intermediate filament network. This is further supported by scratch wound assays of MDA-MB-231 cells, where the cells were transfected at a higher confluency of over 40% and subsequently showed only 58% depletion of vimentin expression.

The results presented in this chapter indicate that siRNA down-regulation of vimentin can inhibit migration of epithelial carcinoma cells that have acquired vimentin

expression as a part of epithelial–mesenchymal transition. These results correlate with previous findings that showed that vimentin was involved in the migratory status of human epithelial cells by expressing vimentin in MCF10A cells (Gilles et al., 1999). Furthermore, impaired wound healing in embryonic and adult mice lacking vimentin has been reported (Eckes et al., 2000). This inhibition of migration can be observed both in MDA-MB-231 cells and in the SW480 cells that co-express vimentin and keratin. These results also support other recent functional studies on vimentin. Reduced migration and invasion is consistent with a role for vimentin in controlling recycling of β 1 integrins (Ivaska et al., 2005) and reduced size of focal contacts in vimentin-ablated endothelial cells (Tsuruta et al., 2003). Vimentin-depleted MDA-MB-231 cells also showed a significant decrease in the rate of attachment to fibrillar collagen compared to the control. However, this was not observed in the SW480 cell line, where no clear trend was observed. It is possible that carcinoma cells that, like SW480 cells, have retained expression of keratin intermediate filaments are able to compensate for the requirement of vimentin for integrin targeting.

The importance of vimentin in cancer progression is underlined by the recent finding that expression of vimentin in the tumour stroma of colorectal cancer was associated with shorter survival suggesting a higher malignant potential (Ngan et al., 2007). Furthermore, an increase of over 20-fold vimentin cDNA expression was found in a prostate cancer model in which subsequent depletion of plectin led to a significant decrease in the invasive potential (Singh et al., 2003). Notably, a 58% inhibition of vimentin expression is sufficient to impair migration in MDA-MB-231 cells, which suggests that it could be plausible to investigate strategies to reduce vimentin expression *in vivo*. In future studies it would be of interest to elucidate molecular interactions of vimentin that are required for invasion and migration. Based on the results of this study a putative candidate for mediating the effects of vimentin could be plectin and further investigation into the interaction of these proteins in cell migration and invasion may yield interesting results.

The impaired adhesion observed in plectin-deficient SW480 and MDA-MB-231 cells and vimentin-deficient MDA-MB-231 cells is intriguing as a loss of cell adhesion is often correlated with increased invasion and progression of cancer, which had been studied extensively in E-cadherin mediated adhesion (see reviews by Wijnhoven et al.,

2000; Bremnes et al., 2002). However, in colorectal tumours loss of cell adhesion could not be correlated with poor prognosis and increased invasion (Bosch et al., 2004) and a subsequent study in metastasising colon carcinoma cells concluded that continued expression and synthesis of junctional proteins do not necessarily contribute to the suppression of tumour invasion and metastasis of colon cancer (Kartenbeck et al., 2005). Therefore, it is clear that the regulation of adhesions in cancer cell progression is a complicated process that is governed by cell-type and cancer cell environment.

Interestingly, depletion of vimentin did not show any obvious morphological changes in the MDA-MB-231 and SW480 cells at the wound edges or monolayers compared to the control. Plectin subcellular localisation was also unaltered by vimentin depletion suggesting that vimentin does not have a regulatory role in plectin localisation. In contrast to this, plectin depleted SW480 colon carcinoma cells showed a flattened morphology and rearrangement of actin at the wound edge. Monolayers of plectin-depleted SW480 cells resembled the lower grade HT29 cells observed in Chapter 4 (Figure 4.5), which have a relatively lower plectin expression. In control wound edge - actin positive foci were abundant at the leading edge of the cells, however these structures were mostly absent in plectin-depleted cells. These results further support involvement of plectin in actin remodelling and regulation (Andra et al., 1998, Fontao et al., 2001). The adhesion structures observed were similar to those observed using the plectin N-terminal GFP fusion proteins (Chapter 4) that were more prevalent for the plectin-1k GFP fusion protein-transfected cells. This prompted an in depth investigation of this novel isoform and the characterisation of the observed adhesive foci, the results of this study will be presented in the Chapter 6.

	Plectin depletion		Vimentin depletion	
	SW480	MDA-MB-231	SW480	MDA-MB-231
Collagen gel invasion	↓↓↓	↓	↓↓	↓↓↓
Wound migration	↓	↑	↓↓	↓↓↓
Collagen attachment	↓	↓	↑↓	↓↓

Table 5.1. Summary of cell migration assays.

Table depicts a summary of the SW480 and MDA-MB-31 cells lines ability to invade, migrate and attach when depleted of plectin or vimentin. Arrows indicate a (↓) decrease in ability or (↑) increase ability.

CHAPTER 6
CHARACTERISATION OF SUBCELLULAR
LOCALISATION AND FUNCTION OF
PLECTIN-1K

6.1. Introduction.

One unanswered question in plectin biology is whether any of the plectin isoforms are involved not only in the assembly of hemidesmosomes and focal adhesions, but also in the formation of invasive cell junctions such as podosomes and invadopodia. These podosome-type adhesions are found in cells of macrophage/monocyte lineage and in invasive carcinoma cell lines (reviewed by Linder, 2007; Buccione et al., 2004; Linder and Aepfelbacher, 2003) and were originally identified and named in RSV transformed fibroblasts (Tarone et al., 1985). They contain an F-actin rich core surrounded by a ring of proteins that are also constituents of focal adhesion complexes, such as vinculin, talin and Src. However, unlike focal complexes, podosomes and invadopodia are also enriched in proteins regulating actin dynamics such as N-WASP, cortactin, gelsolin, T-plastin (fimbrin) and Arp2/3 complex (see reviews by Buccione et al., 2004; Linder and Aepfelbacher, 2003, Linder, 2007). The Arp2/3 complex is activated by Wiskott/Aldrich-syndrome protein (WASP) and this complex nucleates a branched actin network (Amann et al., 2001). Interestingly, both podosomes and invadopodia have been recognised as sites of accumulation and activation of matrix metalloproteinases, which may have further implications for the role of these structures in carcinoma invasion. Podosome-like structures have also recently been described in epithelial cells where they are proposed to participate in hemidesmosome assembly (Spinardi et al., 2004).

Recent mapping of the protein-protein interactions of plectin has identified binding sites for several signalling molecules, such as AMP-activated protein kinase (Gregor et al., 2006), RACK-1 receptor for activated protein C kinase 1, (Osmanagic-Myers and Wiche, 2004) and Fer Kinase (Lunter and Wiche, 2002). The data collectively strengthens the case for plectin as a regulatory scaffolding protein in actin mediated processes.

In this chapter isoform, plectin-1k is demonstrated to be localised to podosome-type adhesions in SW480 colon carcinoma cells. siRNA knockdown of plectin inhibited podosome assembly that was rescued by transfection of Plectin-1k N-terminus. Thus, plectin-1k is a novel cytoskeletal linker protein that regulates actin dynamics in migrating cells.

6.2. Results.

6.2.1. Partial co-localisation of plectin-1k and total plectin in SW480 cells.

Immunofluorescence staining of SW480 cells was used to map the subcellular localisation of plectin-1k (LM-7) and total plectin (c-20) (Figure 6.1A). Plectin-1k co-localised with the C-20 staining in some but not all plectin-positive subcellular structures. Notably, plectin-1k was found in round adhesion sites similar to those found in Figure 5.16B that were most prevalent in cells at edges of scratch wounds made to confluent monolayers and in single migrating cells. In contrast, LM-7 antibody did not stain some of the cytoskeletal structures that were positive for total plectin antibody, such as apparent stress fibers along cell edges and the vimentin intermediate filament network. However, plectin-1k and total plectin antibodies could co-localise in the cytoskeletal cage surrounding the nucleus.

6.2.2 Plectin-1k localisation in MDA-MB-231 cells.

To investigate, if the localisation of plectin-1k to similar adhesion structures is observed in other carcinoma cells, MDA-MB-231 cells were stained with LM7 and plectin c-20 antibodies and found that plectin-1k is localised at round actin foci at basal aspect of MDA-MB-231 cells (Figure. 6.1B). The plectin foci were reminiscent of podosomes that have previously been described in MDA-MB-231 breast cancer cells, where they are implicated in the invasiveness of the cells (Seals et al., 2005).

6.2.3 Plectin-1k is localised in podosome-type adhesions

To investigate if the plectin-1k rich foci in scratch wound edge cells were involved in cell adhesion and migration, co-immunofluorescence staining of plectin-1k with antibodies against integrin subunits $\alpha 3$, $\alpha 6$, $\beta 1$ and $\beta 4$ was used. Previously, SW480 cells have been shown to express also $\alpha 1$, $\alpha 2$ and $\alpha 5$ subunits as well as $\beta 5$ integrin subunit (Koretz et al., 1994, Agrez et al., 1994), but this study concentrated on epithelial integrins as redistribution of both $\alpha 3\beta 1$ and $\alpha 6\beta 4$ has been implicated in epithelial migration and carcinoma invasion (Goldfinger et al., 1999; Lotz et al., 2000; Rabinovitz et al., 1999). Moreover, $\alpha 3\beta 1$ integrin has been shown to participate in the regulation of degradation and phagocytosis of extracellular matrix by breast carcinoma cells (Coopman et al., 1996).

Confocal microscopy of slices at cell-substratum attachment level revealed that plectin-1k co-localises with both $\beta 1$ and $\beta 4$ integrins (Figure 6.2A). Close-up views of the double immunofluorescence staining of integrin subunits and plectin-1k revealed apparent internal structure in the plectin-rich foci. The strongest immunofluorescence staining for integrin subunits formed ring-like structures that seemed to surround punctae with strong plectin-1k immunofluorescence (Figure 6.2B arrows). Some smaller integrin foci at edge of lamellipodial extensions (arrow in Figure 6.2B) were negative for plectin-1k staining suggesting that the initial focal contacts do not contain plectin-1k. Likewise, immunofluorescence staining of phalloidin-labelled actin and $\alpha 6$ integrin subunit demonstrated an integrin-containing ring that surrounded dense core of actin (Figure 6.2C). Finally, unlike the non-invasive HT29 cells (Chapter 4, Figure 4.3), there were no hemidesmosomal-like structures observed in SW480 cells.

6.2.4. Co-localisation of plectin-1k with podosome components.

In order to further characterise the plectin-1k foci observed in the previous experiments double immunofluorescence was carried out with previously published podosome components. Co-staining with phalloidin (filamentous actin) showed that plectin-1k did not co-localise with actin stress fibres or the meshwork at lamellipodial cell edges. Instead, plectin-1k and actin co-localised at adhesion foci at the basal surface of the cells (Figure 6.3A). Immunofluorescence staining of plectin-1k in cells transfected with eGFP-tagged N-WASP (Figure 6.3B) was undertaken to provide further confirmation that plectin-1k was located to podosome structures. WASP is required for podosome formation in haematopoietic cells (Linder et al., 1999) and the ubiquitously expressed N-WASP has been shown to be essential for podosome assembly in src-transformed fibroblasts (Mizutani et al., 2002) and in metastatic mammary carcinoma cells (Lorenz et al., 2004; Yamaguchi et al., 2005). Thus, the co-localisation of N-WASP and plectin-1k confirmed the identification of plectin-1k containing adhesive foci as podosome-type adhesions. This identification was supported by co-localisation of plectin-1k with dynamin (Figure 6.3C) and cortactin (Figure 6.3D). The large GTPase dynamin is involved in membrane organisation, which involves tubulations or invagination of membranes and is required for podosome formation in osteoclasts and carcinoma cells (Ochoa et al., 2000). Cortactin, an actin organising protein, is also required for assembly of podosomes and invadopodia (Webb et al., 2006). Likewise, there was a partial co-localisation of

plectin-1k and vinculin. Both vinculin and plectin-1k were found in podosome-type adhesions but only vinculin was present in focal adhesion sites or, uniformly, at lamellipodia (Figure 6.3E arrow head). At podosomes, vinculin was mostly localised as small rings with a diameter of 0.5-1 μm (Figure 6.3E), which is characteristic to these structures (Gavazzi et al., 1989). Finally vimentin has been previously described as a component of podosomes where it binds T-plastin (T-fimbrin) an actin bundling protein (Correia et al., 1999). Plectin-1k was able to co-localise with both vimentin (Figure 6.3F) and T-plastin (Figure 6.3G) in podosomes (arrows). To summarise the results above demonstrate that plectin-1k is a novel component of podosome-type adhesions in the SW480 colon carcinoma cell line.

6.2.5. Plectin-1k is localised to podosomes in macrophages.

Localisation of plectin in podosomes has not been described previously, although a review by Gimona et al., 2006 includes plectin in a list of proteins involved in the formation of podosomes and invadopodia. However podosomes/invadopodia of epithelial carcinoma cells have not been characterised as extensively as cells of macrophage/monocyte lineage or RSV transformed fibroblasts. Therefore, localisation of plectin-1k in THP-1 cell line that was differentiated towards macrophage lineage by PMA and allowed to adhere to collagen was examined. Double immunofluorescence staining demonstrated that plectin-1k co-localised with N-WASP in podosomes in THP1 cells (Figure 6.4). Thus, plectin is also a constituent of podosomes in cells of macrophage/monocyte origin.

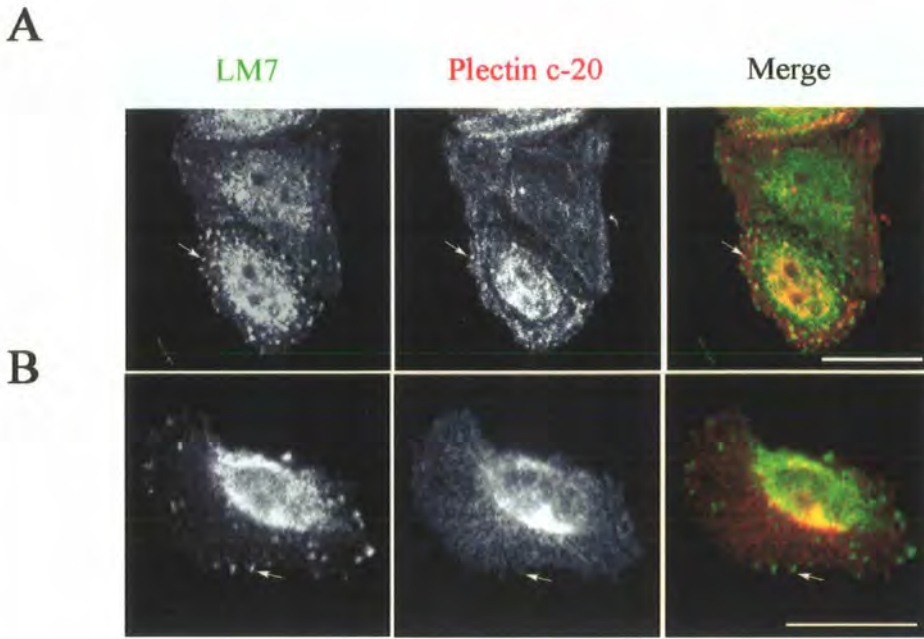


Figure 6.1. Plectin-1k localised to podosome-like foci.

Immunofluorescence staining of (A) SW480 cells and (B) MDA-MB-231 cells with plectin-1k (LM-7 staining, anti-rabbit secondary in green channel) and total plectin antibodies (c-20 staining, anti-goat secondary in the red channel). The arrows point at examples of podosome-like plectin foci. Scale bars equal 20 μm .

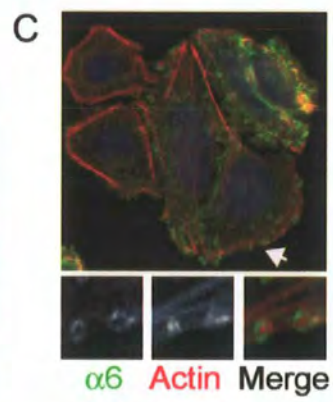
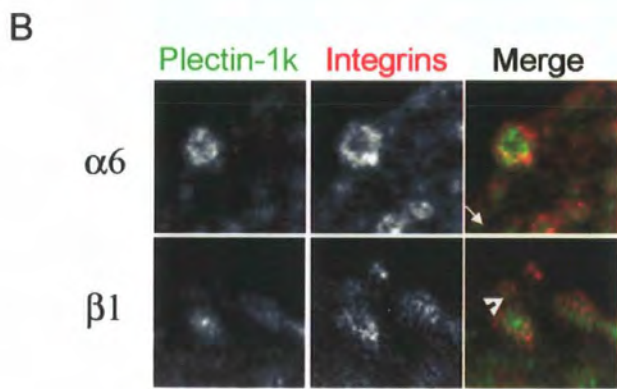
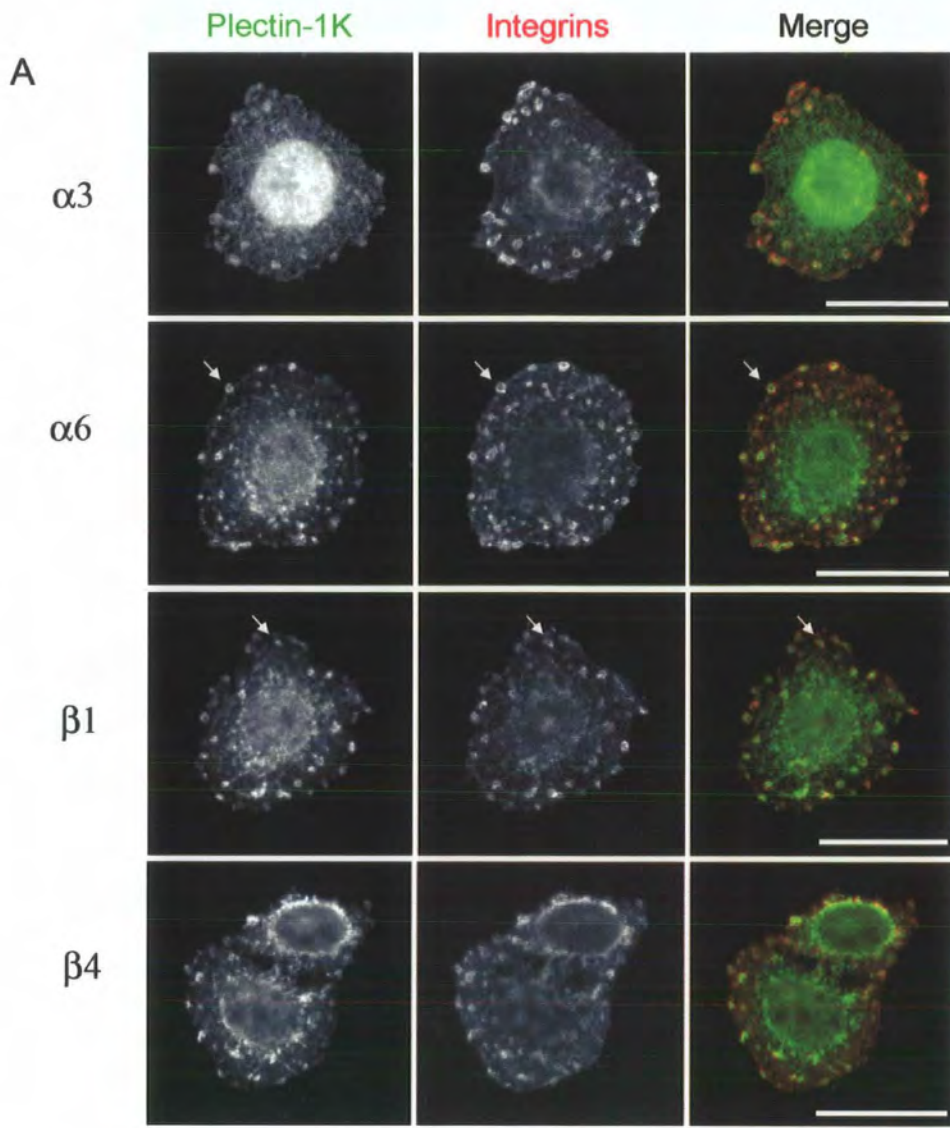
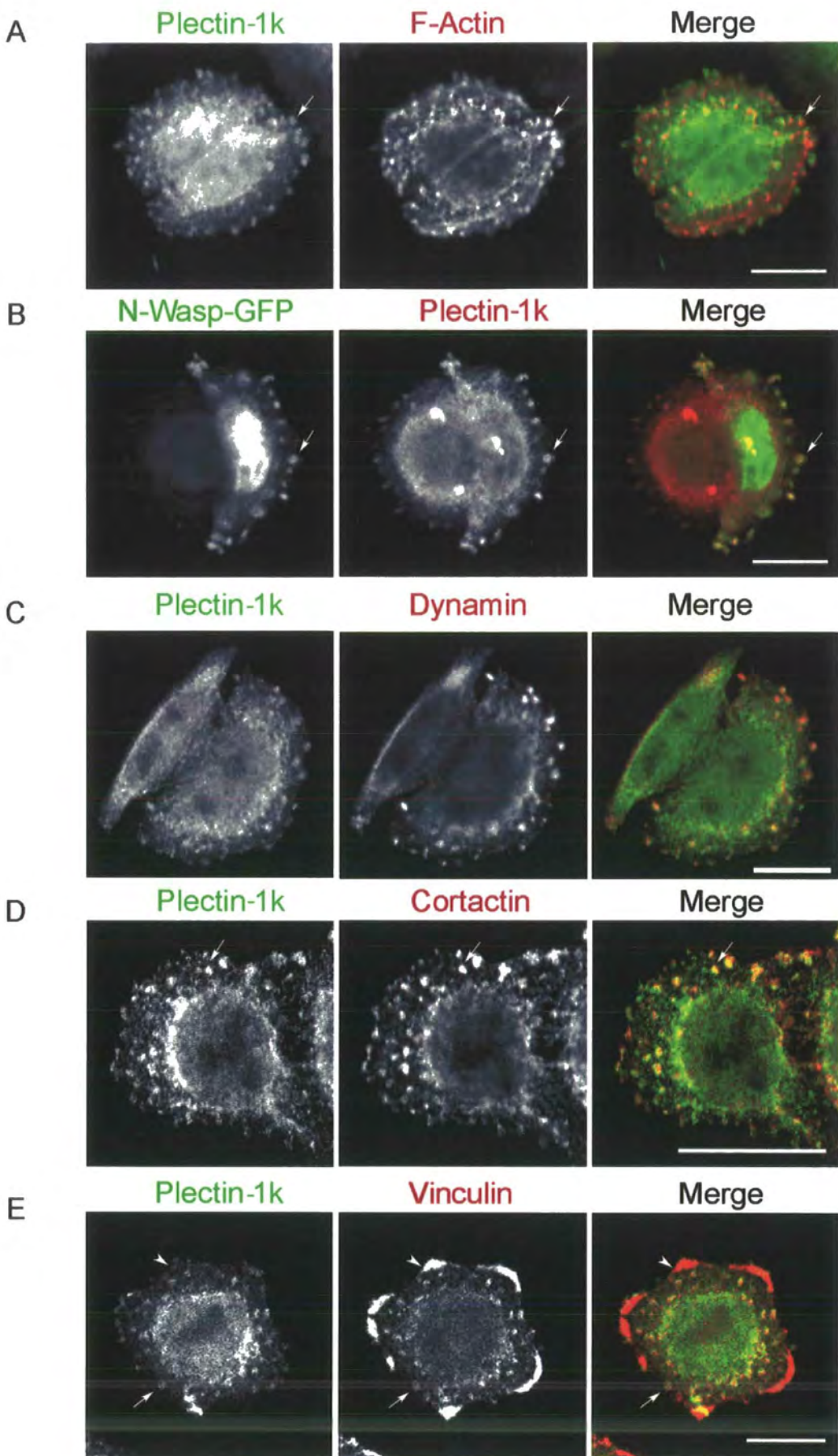


Figure 6.2. Co-localisation of plectin 1k with integrin subunits.

(A) SW480 cells were double immunofluorescence stained with plectin-1k (Green channel) and monoclonal antibodies against integrin subunits (order from top row to bottom row) $\alpha 3$, $\alpha 6$, $\beta 1$ and $\beta 4$. Scale bars equal 20 μm . Arrows in merged panels of $\alpha 6$ and $\beta 1$ rows indicate regions shown in detail in close-up images in panel (B). In the merged panel of $\beta 1$ integrin and plectin-1k staining in panel B, the arrow indicates small integrin focal contacts at the edge of the cell that are negative for plectin-1k and the arrowhead points at larger, podosome-type adhesion. (C) Double immunofluorescence staining of actin (red) and $\alpha 6$ integrin (green). Arrow in the top panel indicates the region that is shown in detail below.



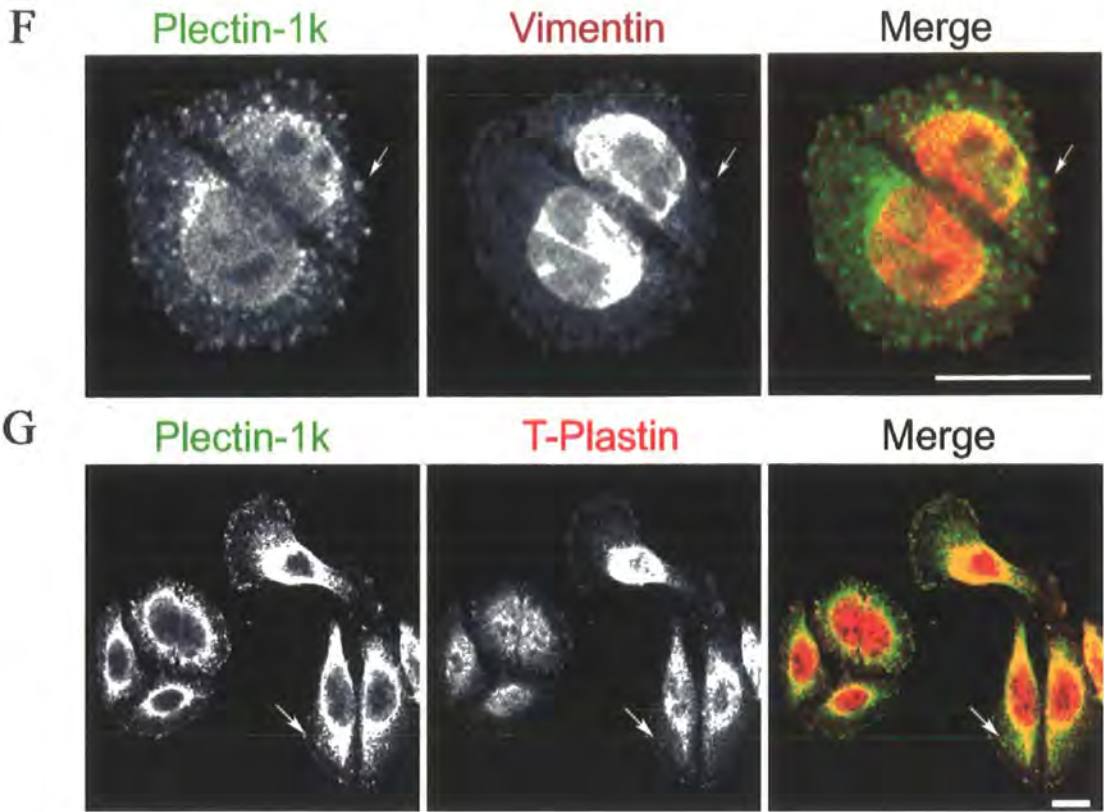


Figure 6.3. Subcellular localisation of Plectin-1k in SW480 cells.

(A) Confocal optical slice close to the basal surface of SW480 cells double stained for plectin-1k (LM-7 antibody, green channel) and actin (Phalloidin, red channel). Arrows point to a podosome positive for actin and plectin-1k in all panels. (B) Immunofluorescence staining of plectin-1k (red) in cells expressing GFP-tagged N-Wasp (green channel). (C) Double immunofluorescence staining of plectin-1k (green) and dynamin (red). (D) Double immunofluorescence staining of plectin-1k (green) and cortactin (red). (E) Double immunofluorescence staining of plectin-1k (green) and vinculin (red). The arrow points at a podosome where plectin-1k and vinculin co-localise. The arrowhead points at broad lamellipodial vinculin staining. (F) Co-localisation of plectin-1k (green) and Vimentin (red). (G) Double immunofluorescence staining of plectin-1k (green) and T-plastin (red). Arrow indicates co-localisation of plectin-1k and vimentin in podosomes. The scale bars corresponds to 20 μm in all panels. N-wasp construct was kindly provided by Dr. Michael Way (Cancer Research UK, London Institute).

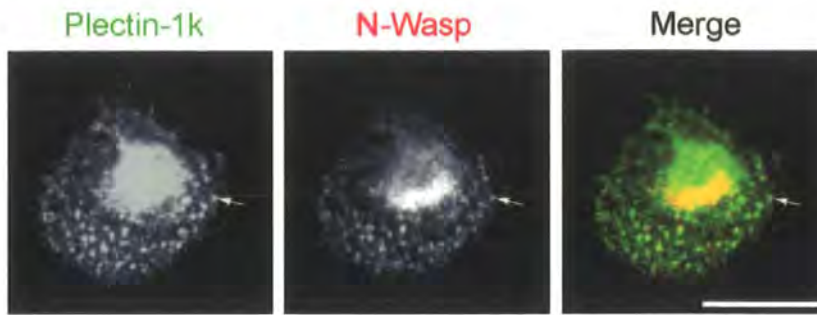


Figure 6.4. Plectin-1k co-localised with N-Wasp in macrophages.

THP-1 cells, differentiated towards macrophage lineage by PMA and attached to collagen-coated coverslips, were double immunofluorescence stained for plectin-1k (green channel) and N-Wasp (red). Confocal section shown is from the basal aspect of the cells, with arrows pointing to podosome foci. Scale bar indicates 20 μm .

6.2.6. Plectin-1k -Actin Binding Domain -GFP construct is targeted to podosomes.

Plectin-1k-eGFP construct was observed to be targeted mostly to podosomes in transfected SW480 cells (Figure 6.5BCD), the eGFP construct co-localised with the plectin C-terminal antibody in actin structures, but not at IF-network (Figure 6.5A). Analysis of XY and XZ confocal sections (Figure 6.5B) demonstrated that plectin-1k-eGFP construct localised to the actin core but also partially surrounded the core. The podosome-like adhesions were not restricted to ventral surface of the cells but extended upwards almost throughout the cell as shown by the co-localisation of F-actin and GFP fluorescence in the XZ-section (Figure 6.5B panel b). Over-expression of the plectin-1k ABD was observed to cause a re-organisation of actin in podosomes with more actin present in podosome ring compared to untransfected cells (compare Figure 6.5B and Figure 6.3A). Double staining with cortactin was used to confirm the identity of the Plectin-1k-eGFP - positive structures as podosome-type adhesions (Figure 6.5C). Finally, analysis of vimentin cytoskeleton in transfected cells demonstrated that plectin-1k N-terminus is targeted only to actin-rich structures as the vimentin-cage surrounding the nucleus was not GFP positive whereas podosomes contained both vimentin and plectin-1k-eGFP construct (Figure 6.5D). Taken together, the exon 1k was sufficient to target the plectin ABD to podosome-type adhesions and the localisation does not require the intermediate-filament binding domain of plectin.

6.2.7. Inhibition of ROCK activity impairs podosome assembly and alters plectin-1k localisation.

Podosomes and invadopodia are a characteristically found in Src-transformed cells (Buccione et al., 2004; Linder and Aepfelbacher, 2003) and Rho GTPase activity has been implicated as a downstream mediator of Src in podosome formation (Berdeaux et al., 2004). Rho-activation can also re-organise the vimentin cytoskeleton (Inada et al., 1999) and could therefore influence the localisation of vimentin-binding proteins such as plectin. In order to investigate the possible role of signalling pathways downstream of active Rho in targeting plectin-1k to podosomes, we scratch-wounded a stably transfected SW480 cell line expressing the plectin-1k-GFP construct and then treated the culture with Rho-kinase inhibitors (Figure 6.6). Control wound edge cells assembled several podosomes, two hours after wounding. In addition, the cells at the wound edge did not behave like an epithelial sheet, but the cells were seen to frequently escape from the wound edge and migrate individually or in small clusters into the wound

space (Figure 6.6A). Treatment of the cells with a Rho-kinase inhibitors prevented formation of circular podosome-type structures. Instead, the cells had smooth and wide lamellipodia-like edges with a dense actin staining along the cell edge (Figure 6.7AB bottom rows). Plectin-1k was co-localised with actin at the leading edge, but did not form regular circular podosome structures or focal-adhesion complexes. Compared to control cells, Rho-kinase inhibited cells were much less likely to escape from the wound edge and behaved like collectively migrating epithelial sheet (Figure 6.6A). These results indicate that podosome formation and plectin-1k localisation in SW480 cells are dependent on Rho-kinase activity.

6.2.8. The N-terminal Actin-binding domain of plectin-1k rescues podosome formation in plectin knockdown cells.

The observations that plec-1k-GFP transfected cells appeared to have more podosome like adhesions than control transfected cells prompted the study of, whether the N-terminus of plectin-1k alone was sufficient to induce podosome formation. Stably transfected SW480 cells were used that were expressing either plec-1k-eGFP construct (Figure 6.7A) or GFP alone (Figure 6.7B). Depletion of plectin expression in these cell lines was carried out with siRNA targeted to the C-terminus of the full-length plectin mRNA leading to downregulation of the endogenous plectin but not plec1k-eGFP (Figure 6.7D). The results show that podosome-type adhesions were abundant at wound edges of both control siRNA and plectin siRNA transfected plec-1k-eGFP cells (Figure 6.8A) whereas podosomes were almost completely absent in a control GFP cell line transfected with plectin siRNA (Figure 6.8B). Counting of podosome positive cells at scratch wound edges confirmed these observations and demonstrated that the N-terminus of plectin-1k was sufficient for promoting assembly of podosome-type adhesions (Figure 6.7C).

6.2.9. Plectin-1k is shown localising to actin adhesive structures in cells attaching to collagen.

In order characterise the participation of plectin-1k in adhesive actin structures, immunofluorescence Z-projection microscopy of plec-1k-GFP cells and actin was carried out on cells attaching to a collagen substrate. Cells were fixed at 10, 20, 40 and 80 minutes after being allowed to attached to collagen coated glass coverslips. In all instances as expected, plectin co-localised with actin in the attaching cells. At 10

minutes (Figure 6.8A) the cells have a rounded appearance where actin is localised to a dense ring around the nucleus. At the 20-minute time point the cells have started to spread and the actin cage around the nucleus is forming with dense actin staining at the cell periphery where plectin-1k colocalise. At 40 minutes the actin and plectin staining is similar to the 20-minute time point except that changes in cell polarity is starting to take place. The 80-minute time point is where we find the majority of cells forming podosome like adhesive structures although a proportion of cells at the earlier 20-40 minutes are able to do this. These results show that during attachment to collagen, actin is actively reorganised in adhesive structures with co-localisation of plectin-1k. This observation provides further evidence that plectin-1k interacting with actin is involved in the formation of adhesive structures.

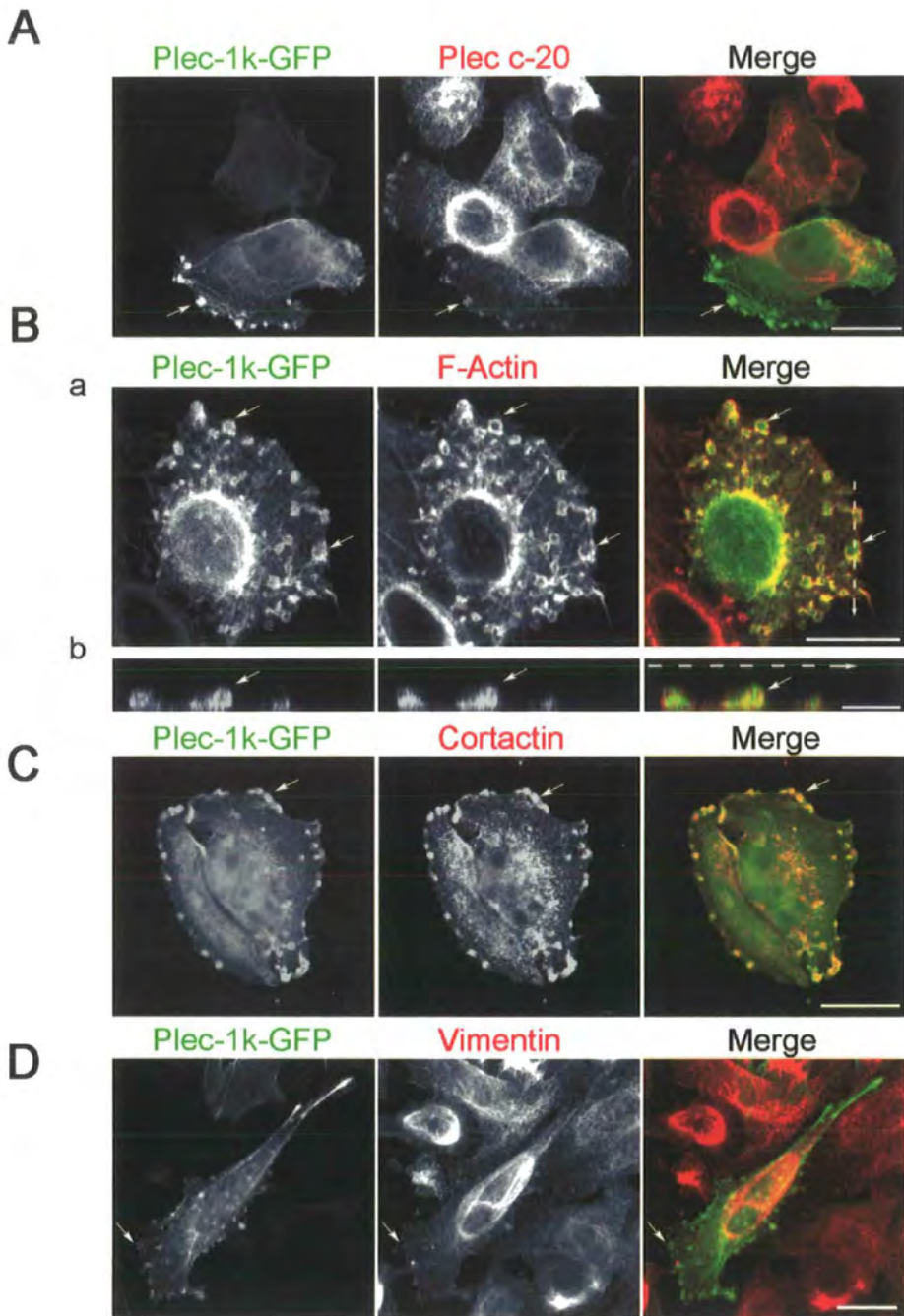
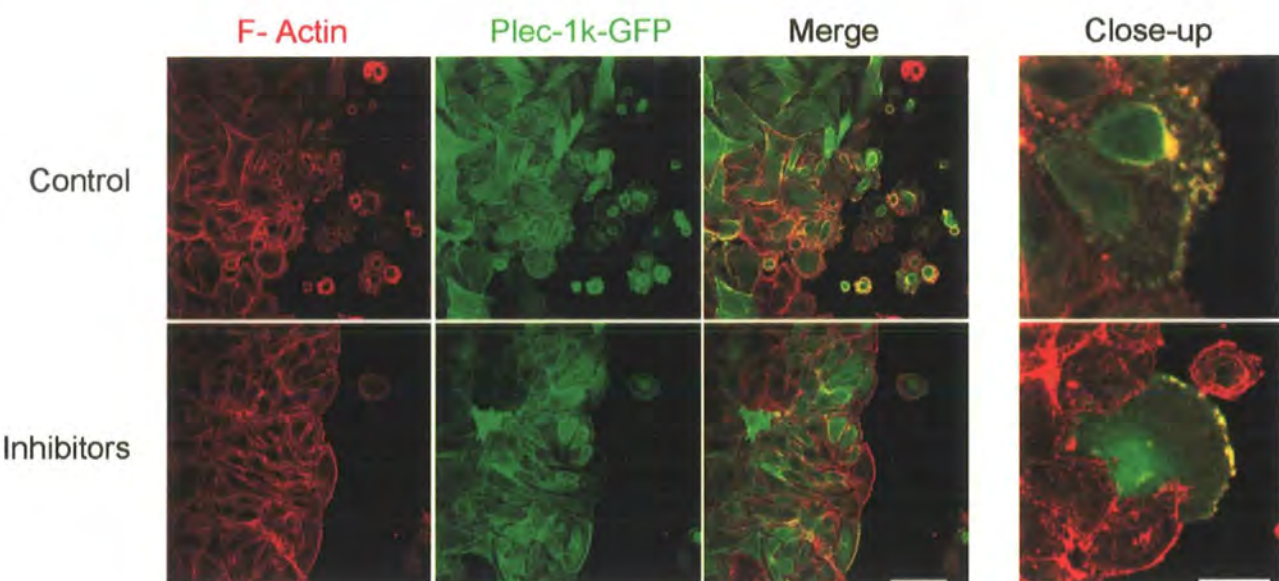


Figure 6.5. Exon 1k targets plectin actin-binding domain to podosomes and dorsal actin ruffles.

(A) Plec-1k-eGFP and endogenous plectin (red channel, c-20 antibody) co-localise in podosomes (example indicated by an arrow). (B) Plec-1k-eGFP fluorescence (green) and phalloidin-stained filamentous actin (red). Top panel (a) show an optical slice taken from the basal surface of the cells. The white dotted line in the merged image indicates the location of the XZ section shown below in (b); the arrow points at the edge one podosome-type junction. Both actin staining and eGFP fluorescence extend inwards in the cell from the basal surface. Scale bar 20 μm in (a) and 5 μm in (b). (C) GFP fluorescence (green) and cortactin staining (red). (D) Plec-1k-eGFP construct (Green) does not co-localise with vimentin (red) in the intermediate filament cage surrounding nucleus but only in podosomes (arrow). The scale bar represents 20 μm in panels A, C and D.

A



B

Figure 6.6. Rho-ROCK signalling regulates podosome assembly and plectin-1k localisation.

(A, B) Stably transfected SW480 cell monolayers expressing the plec-1k-EGFP construct were scratch wounded in the presence or absence of Rho-kinase inhibitors. Two different inhibitors (compounds Y-27632 and Rho-Kinase inhibitor, H-1152) were used separately or together with identical results. Top row, control cells, bottom row Rho-kinase inhibitor-treated cells. (B) Close-up detail of the wound edge. Note the lack of circular podosomes in the cells with ROCK inhibition. Scale bar is 50 μm in A and 20 μm in B.

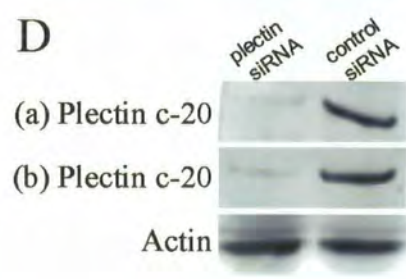
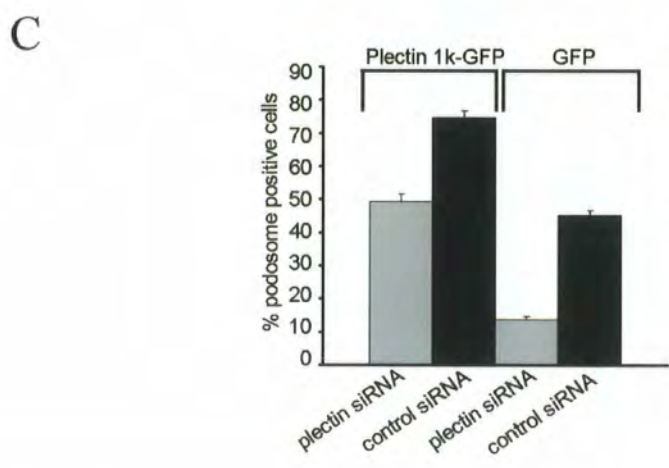
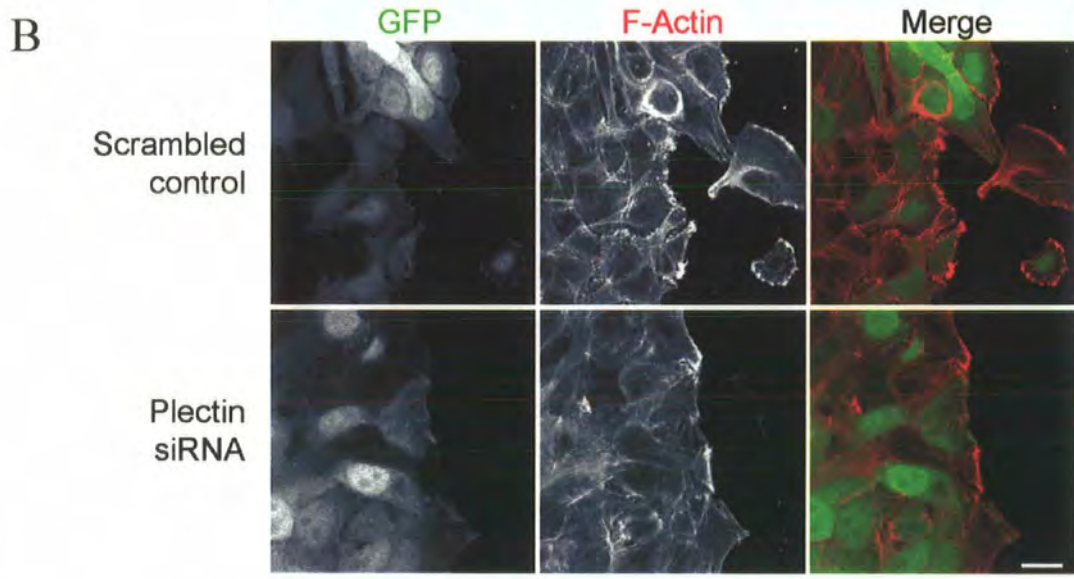
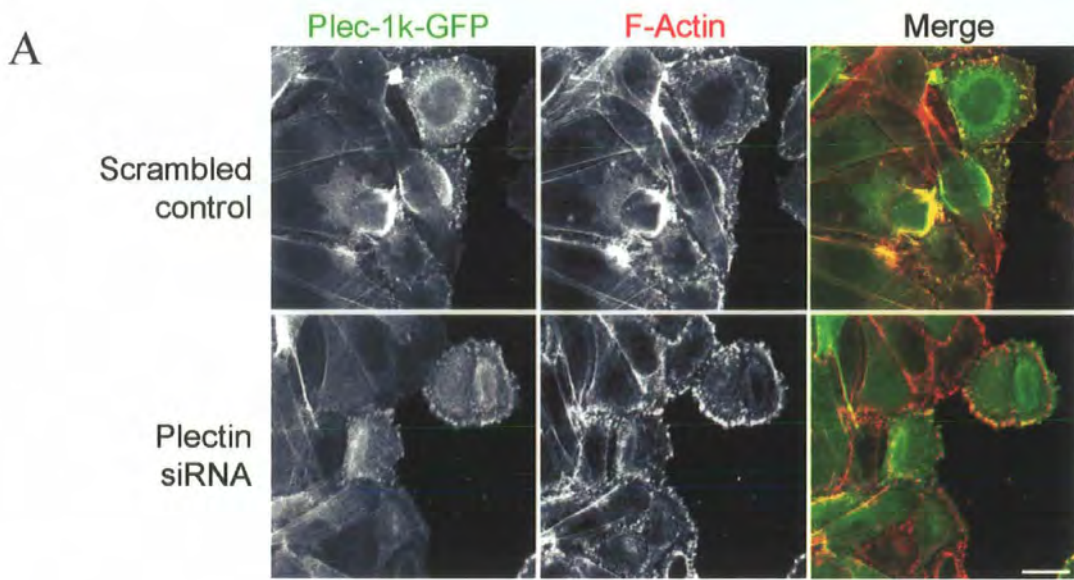


Figure 6.7. Plectin-1k N-terminus rescues podosome assembly in plectin knockdown cells.

(A) Stably transfected SW480 cells expressing plec-1k-eGFP construct were scratch wounded and subsequently transfected transiently with control siRNA (top row) or plectin siRNA (bottom row). Confocal imaging of eGFP fluorescence and phalloidin stained F-actin show the presence of podosome-type adhesions in plectin knockdown cells. (B) SW480 cells were stably transfected with eGFP alone, scratch wounded and siRNA transfected as in panel A. Note, that plectin siRNA transfection (Bottom row) inhibits podosome assembly in eGFP expressing cells. Scale bar is 20 μm in A and B (C) Wound edge cells containing podosome-type adhesion structures were counted from three independent experiments of plectin or control siRNA transfected cells expressing either plec-1k-eGFP construct or eGFP alone error bars indicate average deviation. (D) Immunoblot showing plectin siRNA depletion in (a) plec-1k-eGFP stable transfected cells and (b) control eGFP stable transfected cells. Total plectin is detected with plectin c-20 antibody and actin is shown as a loading control.

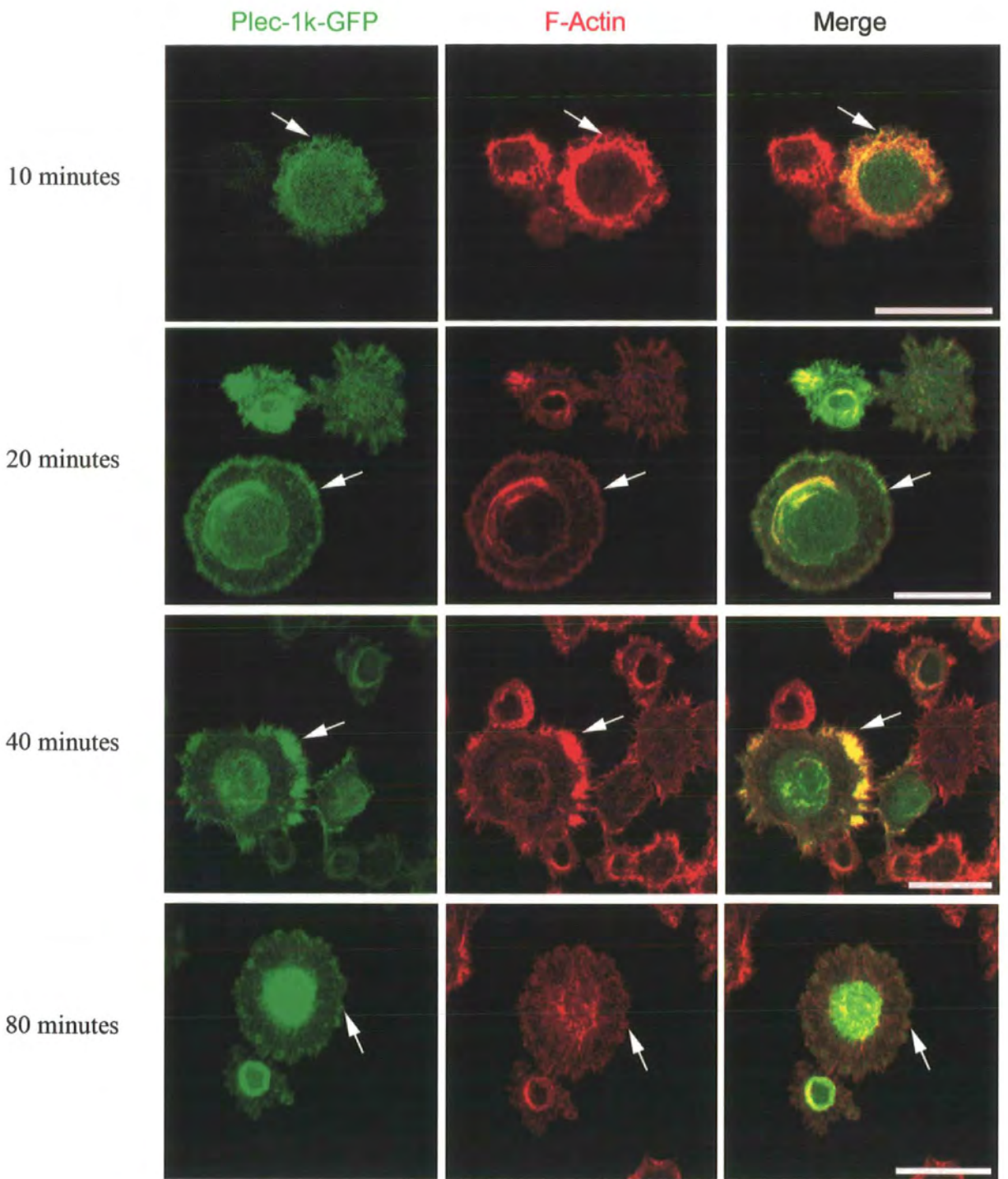


Figure 6.8. Plectin-1k localisation of cells attaching to collagen.

Confocal Z-projection images show stably transfected plect-1k-eGFP expression in SW480 cells that are stained with phalloidin (to show actin localisation). Cells were fixed at 10, 20 40 and 80 minutes on attachment to fibrillar collagen before processing for staining. Note the plec-1k-eGFP localisation at the cell periphery (arrows) co-localising with actin. In the 80 min panel the formation of podosome like adhesion structures are visible (arrow). Scale bars indicate 20 μ m in all panels.

6.3. Discussion.

The results presented in this chapter show that the novel isoform plectin-1k is localised to podosome-like adhesions in invasive SW480 and MDA-MB-231 cell lines. This provides a previously uncharacterised subcellular localisation for plectin and further implicates the role of plectin in carcinoma cell adhesion and invasion.

The localisation of the novel plectin isoform 1k to podosome like adhesions was particularly obvious in the wound edge cells of SW480 colon carcinoma monolayers. In accordance with described criteria (Linder and Aepfelbacher, 2003), I classified the observed actin structures as podosomes since they were found in the basal aspect of cells, contained a round actin core surrounded by a vinculin-positive ring and were positive for N-WASP, cortactin, dynamin, vinculin and vimentin. The carcinoma cell podosomes were between 0.5 and 1 μm in diameter and, when observed in XZ dimension by confocal microscope were not restricted to a flat adhesive plaque but extended inwards into the cytoplasm. It was demonstrated that plectin-1k colocalised with N-WASP in podosomes of THP-1 macrophages indicating that plectin is a component of podosomes in macrophage/monocyte lineage in addition to epithelial carcinoma cells. The nomenclature of podosome-type adhesions is not completely resolved, with more persistent and larger actin-rich foci in carcinoma cells often named as invadopodia, as opposed to more transient and smaller podosomes in macrophages, smooth muscle cells and endothelial cells (reviewed in Gimona et al., 2007 and Linder, 2007). However, in line with Seals et al., 2005 who show podosomes in invasive cancer cells I called the podosome-type adhesions, in both MDA-MB 231 and SW480 cells, podosomes.

The localisation of plectin-1k to podosomes was supported by immunofluorescence staining of plectin-1k specific antibody, plectin C-terminal antibody and by localisation of transfected plec-1k-eGFP fusion protein. By investigating the subcellular distribution of other plectin N-terminal isoforms as eGFP-fusion proteins, we also found that also isoforms plectin-1 and, to a lesser extent, 1d and 1g are localised to podosomes (see Chapter 4, Table 4.1). It is likely that different plectin isoforms function at these sites as heterodimers via their coiled-coil rod domains.

In the previous chapter it was observed that knockdown of plectin expression by siRNA inhibited both podosome assembly at scratch wound edge cells and SW480 cell migration and invasion (Figure 5.14). The inhibition of podosome assembly was rescued by the N-terminal domain of plectin-1k (Figure 6.7) suggesting plectin is required for podosome assembly in invasive carcinoma cells. Previous studies have identified instrumental roles for other cytoskeletal proteins, such as dynamin and cortactin, in podosome assembly (Ochoa et al., 2000; Bruzzaniti et al., 2005). Dynamin binds cortactin and both proteins can regulate actin assembly. Another actin-binding protein, l-caldesmon, has been shown to play an important role in podosome assembly in smooth muscle cells (Eves et al., 2006). Finally, a scaffolding protein, Tsk5/Fish that contains several SH3-domains is implicated in podosome assembly in invasive carcinoma cell lines (Seals et al., 2005). Plectin is both an actin binding protein and a scaffolding protein for protein kinases and could be considered in the same functional category as, cortactin, caldesmon and Tsk5.

Podosome-like actin rings in epithelial carcinoma cells have been suggested to be related to hemidesmosome assembly (Spinardi et al., 2004). As previously mentioned plectin interacts with $\beta 4$ integrin in assembly of hemidesmosomes (Chapter 1). It could be possible that invasive cell-matrix junctions, such as podosomes and invadopodia utilise existing components of epithelial cell-matrix adhesion sites. However, the results suggest that plectin isoforms that are not involved in hemidesmosome assembly *in vivo*, such as plectin-1, are targeted to podosomes. It is possible that epithelial carcinogenesis involves selective expression or activation of a subset of plectin isoforms. This is supported by the finding that plectin-1k is over-expressed in invasive colon and breast cancer cell lines (Chapter 4, Figure 4.12.).

Plectin siRNA transfection leading to ablation of plectin protein expression reduced invasiveness of SW480 cells through collagen gels (Chapter 5, Figure 5.4). In addition depletion of vimentin also slows down invasion and migration (Chapter 5, Figure 5.6). Since vimentin participates in PKC ϵ -mediated recycling of integrins (Ivaska et al., 2005) and vimentin has been identified as a component of podosomes (Correia et al., 1999), it appears possible that the protein complex between vimentin and plectin plays a role in the assembly of podosome-type adhesions. This suggestion is also supported

by impaired migration of immune cells in isoform specific plectin-1 null mice (Abrahamsberg et al., 2005).

Rho signalling plays an important role in podosome assembly (Berdeaux et al., 2004; Osiak et al., 2005). I found that formation of podosomes and dorsal actin ruffles in SW480 cells is sensitive to Rho kinase (ROCK) inhibitors (Figure 6.6). ROCK activity has previously been shown to be important in amoeboid mode of cancer cell invasion (Sahai and Marshall, 2003), but has not been implicated in podosome assembly. In fact, it appears that several Rho-dependent pathways can regulate podosome assembly. In Src transformed fibroblasts, C3 exotoxin, a Rho-inhibitor, blocks podosome formation, whereas Rho-kinase inhibitors do not affect podosome assembly (Berdeaux et al., 2004). In mouse osteoclasts, Rho acts upstream of PI4-P-5 and PI3 kinases to promote podosome assembly (reviewed by Chellaiah, 2006) and in HUVEC endothelial cells treated with phorbol esters a linear signalling pathway involving PKC, Src and Cdc42 leads to podosome assembly (Tatin et al., 2006). Thus, signalling events leading to podosome formation can be cell-type specific and it is possible that podosome-like structures and invadopodia in epithelial carcinomas are regulated by different mechanisms than 'physiological' podosomes in osteoclasts and macrophages.

Finally, further evidence that plectin-1k is localised to actin rich adhesion structures was demonstrated by investigation of plec-1k-GFP transfected SW480 cells attaching to collagen (Figure 6.8). Interestingly, at the early stages of attachment plec-1k-eGFP colocalised with actin at short filopodia like structures at the cell periphery. At later stages of attachment, upon possible polarisation of the cell, the appearances of podosomal-like adhesions were apparent. It is possible that this is the stage when SW480 cells are becoming polarised and matrix remodelling takes place. Podosomes were also most abundant in wound assays two hours after wounding. It would be of interest to investigate what signalling pathways in this cell trigger the formation of podosomes in single cells and at the wound edge. On another note, further investigation using live cell imaging may provide answers on the regulation of turnover of the carcinoma cell podosomes after their appearance in the SW480 cells. In summary localisation of plectin isoforms, including plectin-1k, to actin structures involved in carcinoma invasion suggests that plectin could play a role in the regulation of invasive and metastatic behaviour of colon cancer cells.

CHAPTER 7
CONCLUSIONS AND FUTURE OUTLOOK

Discussion and future outlooks.

Approximately 90% of all cancer deaths arise from the metastatic spread of primary tumours (Chambers et al., 2002, Christofori et al., 2006). Thus, understanding cell migration and invasion is invaluable in cancer cell biology research. Furthermore, 90% of cancers originate from epithelial tissues and show characteristics of epithelial to mesenchymal transition (Christofori et al., 2006). Current anti-cancer therapies are targeted to the ability of a cancer cell to proliferate. However, many tumours are resistant to this treatment. Furthermore, migrating cells are known to show a decreased proliferation rate and tend to be less sensitive to standard chemotherapy (reviewed in Hayote et al., 2006). The cytoskeletal networks (microfilaments, microtubules and intermediate filaments) along with the numerous cytoskeletal-associated proteins are intrinsically involved in cell migration. Additionally, alterations in cell-cell and cell-matrix adhesion have been shown to have a central role in facilitating tumour cell migration, invasion and metastatic dissemination (Kartenbeck et al., 2005; Christofori et al 2006; Lyons et al 2007). With the above in mind, I set out to investigate the role of the plakin family members, particularly plectin, in carcinoma cell migration, invasion and attachment with the hypothesis that plectin could act as a mediator in the regulation of these processes.

Plectin, a versatile cytoskeletal linker protein, has been implicated in many cellular functions. Firstly, plectin was recognised as a component of hemidesmosomes and a linker of intermediate filaments and actin. More recently, plectin has been shown to act as a scaffolding protein for signalling events (reviewed in Sonnenberg et al., 2007). Previous studies have focused on the role of plectin in skin and muscle integrity due to the defects found in plectin deficient mice and patients. Plectin mutations result in EBS-MD, epidermolysis bullosa simplex with muscular dystrophy (Pfender et al., 2005). In addition to the role of plectin in skin architecture, it has also been widely studied in striated muscle where it's a component of the Z-line associated with desmin (Andra et al., 1997; Hijikata et al., 1999). Plectin null mice show skin and tissue fragility with reduced desmosomes and hemidesmosomes resulting in blisters. Moreover, the revealed abnormalities were reminiscent of minicore myopathies in skeletal muscle and disintegration of intercalated discs in heart (Andra et al., 1997). Plectin has also been shown to be a modulator of intermediate filament and actin

dynamics (Wiche et al., 1998; Andra et al., 1998). Additionally, plectin may have a possible role in reorganisation of the actin cytoskeleton during death receptor-mediated apoptosis as an early substrate for caspase 8 (Stegh et al., 2000). The emerging data, implicating plectin in various signal transduction pathways (Lunter et al., 2002; Osmanagic-Meyers et al., 2004; Osmanagic-Meyers et al., 2006; Gregor et al., 2006) further emphasises the dynamic and versatile properties of plectin and the role that it may play in the regulation of cell migration adhesion and attachment.

Plectin was shown to have a complex N-terminal gene organisation, where there were eight possible first exons and two possible 2nd and 3rd exons found in the murine gene (Fuchs et al., 1999). I demonstrated in Chapter 3 that the human gene also contains a similar diversity of alternative first exons. I identified an additional N-terminal alternative first exon that encoded for a novel isoform that I named plectin-1k. The plectin isoform mRNAs were widely expressed in human tissue with a subset of N-terminal isoforms displaying a variable expression (specifically isoforms plec-1, 1a, 1d, 1f and 1k). Interestingly, plectin-1k showed variable expression across the tissue panel with up regulation in colon tissue. Plectin-1k was also found to have an elevated mRNA expression in the invasive SW480 colon carcinoma cell lines compared to the low invasive HT29 colon carcinoma cells but was not elevated in the invasive breast carcinoma cell lines. This result is of particular significance, as further in this study, plectin-1k is identified as a constituent of podosome like adhesions that are involved in carcinoma cell migration.

Using a panel of colon and breast carcinoma cells lines, which were shown to have variable invasive potential through collagen gels, I demonstrated plectin to have altered expression at the mRNA, protein and subcellular localisation levels. Strikingly, plectin protein expression was elevated in the more invasive cell types (SW480 and MDA-MB-231) compared to their low invasive counterparts (HT29, MCF7). Immunofluorescence data of the invasive carcinoma cells show the sub-cellular expression of plectin to be recruited away from hemidesmosomes (as observed in the low invasive carcinoma cells and other previously studied epithelial cells) and to be relocated at an actin/vimentin rich cage around the nucleus, to focal adhesions and actin rich foci that are later identified as podosomes in Chapter 6. I also confirm that similar to the murine data (Rezniczek et al., 2003), the expression of N-terminal exons

and the sequence encoding actin binding domain alone show preferences in subcellular localisation to the actin cytoskeleton. Thus, the alternative first exons could determine the subcellular localisation of the human plectin isoforms. Isoform specific antibodies raised to plectin-1, 1b, 1f and 1k provided an invaluable tool to understand the expression of the full length plectin isoforms. These isoforms were of particular interest as expression of the alternative first exons tagged to GFP showed preferential subcellular location at focal adhesions, actin adhesion structures or actin rich foci. The antibodies confirmed the localisation of plectin isoforms in the carcinoma cells to specific preferential subcellular localisation as observed using N-terminal plectin-GFP truncated proteins and the previous murine data (Rezniczek et al., 2003). The results also suggest that as the majority of the isoforms can be found at similar localisation a possible role of heterodimerisation of plectin isoforms may exist. Finally, a cancer cell may be able to regulate the expression levels of specific plectin N-terminal isoforms compared to each other, with the outcome of modulating invasion, migration and cell attachment.

Plectin depletion in invasive cells caused impairment in colon carcinoma cell migration, invasion and attachment. However, the severity of the impairments was cell type specific as the breast carcinoma cells exhibited defects in attachment only, with migration and invasion not significantly altered. On analysis of the cytoskeletal related protein expression profile, possible explanations as to why plectin ablation is shown to have a different effect in the breast and colon invasive cell lines are revealed. The invasive breast carcinoma cells predominantly express a vimentin intermediate cytoskeleton with an increase in focal adhesion proteins vinculin and talin, whereas the invasive colon carcinoma cells express a keratin and vimentin intermediate cytoskeleton. Both SW480 and MDA-MB-231 carcinoma cells show a loss of E-cadherin characteristic of epithelial to mesenchymal transition and also desmoplakin a component of desmosomes that mediate cell-cell attachment. Plectin was found to interact with vimentin as a linker protein and at vimentin positive focal adhesions and several previous studies show that vimentin is involved in migration and invasion in many cell types, including breast cancer derived cell lines (see Chapter 5). However, none of the previous studies conclusively established whether vimentin expression is only a marker of epithelial to mesenchymal transition changes or if vimentin expression is required for the invasive behaviour of the cells. I show that siRNA

mediated knockdown of vimentin results in impaired migration and adhesion of breast carcinoma cells that have acquired vimentin expression as a part of the epithelial to mesenchymal transition. However, in the SW480 colon carcinoma cells, depletion of vimentin caused only a modest effect on cell adhesion. This is possibly due to the ability of the retained keratin intermediate filaments to circumvent the requirement of vimentin for integrin targeting. Vimentin was shown to have role in controlling recycling of $\beta 1$ integrins (Ivaska et al., 2005) moreover there was reduced size of focal contacts in vimentin ablated cells (Tsuruta et al., 2003) which is consistent with the migration, invasion and attachment defects found in the vimentin ablated MDA-MB-231 cells. In future studies, it would be of interest to investigate the molecular interactions of vimentin that are required for migration and invasion and whether plectin is involved in mediating these effects. This could be investigated using double siRNA transfections in these cells for simultaneous depletion of vimentin and plectin and also transfection of specific plectin isoforms to demonstrate any defects of cancer cell migration, invasion and attachment that are dependent on specific N-terminal isoform expression.

Protein constructs with alternative plectin N-termini demonstrated that the first exons of isoforms 1k, 1 and 1d target the actin-binding domain of plectin to podosomes. The plectin 1k isoform was observed to be preferentially located to podosomes more than the other isoforms. Both the localisation of plectin-1k and podosome assembly was disrupted with Rho-kinase (ROCK) inhibitors. Down regulation of plectin expression by siRNA inhibited podosome assembly at wound edge cells of scratch wounded SW480 monolayers, impaired cell migration and inhibited invasion through collagen. Most strikingly, only the plectin-1k N-terminus was needed to rescue podosome formation in plectin knockdown cells. Thus, plectin was shown to participate in podosome assembly and invasiveness in carcinoma cells. Identification of plectin-1k adds to a growing list of cytoskeletal linkers that can be targeted to specific organelles or subcellular structures. Plectin has recently been shown that alternatively spliced MACF1b localizes to the Golgi complex (Lin et al., 2005). The plakin family members can have remarkably versatile effects on both architecture and function of various cell types and tissues. Furthermore, the results presented in this thesis suggest that plectin could play a role in the regulation of invasive and metastatic behaviour of colon cancer cells.

In addition to the involvement of plectin in migration, invasion and adhesion of carcinoma cells, many interesting areas have arisen during this study. The localisation of plectin in a network surrounding the nucleus in migrating cells and the interaction of plectin with nesprin-3 implicate plectin as a linker to the cell nuclear membrane could provide enlightenment on the function of the nuclear envelope during mitosis and proper nuclear positioning during quiescence and cell migration (Wilhelmsen et al., 2003). The possible role that plectin may play in the positioning mitochondria is starting to be addressed (Reipert et al., 1999; Appaix et al., 2003) and may yield further insight into the treatment and understanding of myofibrillar myopathies (Vita et al., 2003; Reimann et al., 2003). Plectin has been previously shown to have numerous interacting partners with the newly identified interaction with periplakin showing that interactions may be isoform specific (Boczonadi et al., 2007). It would be of high interest to investigate the molecular interacting partners of each of the alternative N-terminal plectin isoforms and what effect this interaction has on signal transduction pathways. The unlocking of the human alternative first exons with the generation N-terminal GFP expression proteins, along with the generation of isoforms specific antibodies will provide vital tools in the discovery of the specific molecular interactions of the human plectin N-terminal isoforms. The numerous interactions of plectin and the implication in pathogenesis continues to be an expanding area of cell biology, yielding surprising and exciting results, highlighting the importance of plectin in the integrity of the cell.

APPENDIX I. SEQUENCES OF PLECTIN ALTERNATIVE N-TERMINAL FIRST EXONS

PLEC 1X

HUMAN

**ATGGTGGCCGGCATGCTCATGCCACGGGACCAGCTGCGGGCCATCTATGAGGTGCTCT
TCCGCGAGGGCGTGATGGTGGCCAAGAAGGACCGGGCGCCCCGCAGCTTGCACCCCCA
TGTGCCCCGGCGTCACCAACCTGCAGGTCATGCGTGCCATGGCGTCCCTGCGGGCACGG
GGCCTGGTCCGCGAGACCTTTGCCTGGTGCCACTTTTACTGGTACCTCACCAATGAAG
GCATCGCCACCTCCGCCAGTACCTGCACCTGCCGCCAGAGATCGTGCCCCGCCTCTCT
GCAGCGCGTGCGCCGCCCCGTCGCCATGGTGTATGCCCGCACGCCGCACCCCCACGTG
CAGGCTGTGCAGGGTCCCCTGGGCTCCCCACCAAGCGGGGGCCGCTGCCGACGGAGG
AGCAGCGGGTCTACCGTCGGAAGGAGCTTGAGGAGGTGTCACCTGAGACCCCTGTGGT
GCCTGCTACCACCCAGCGGACCCTGGCCAGGCCAGGCCCGGAGCCTGCCCCAGCCACA
G**

MOUSE

**ATGGTGGCTGGCATGCTCATGCCGCTGGACCGGCTACGGGGCCATCTATGAGGTGCTCT
TCCGTGAGGGGGTGATGGTTGCCAAGAAGGACCGGGCGACCCCGCAGCCTGCATCCCCA
TGTGCCCCGGCGTCACCATTCTACAGGTCATGCGTGCCATGGCTTCACTGAAAGCTCGG
GGCCTGGTGCGGGAGACCTTTGCCTGGTGCCACTTCTACTGGTACCTGACCAACGAGG
GCATTGACCACCTACGCCAGTACTTACACCTGCCACCGGAGATTGTACCTGCCTCTCT
GCAGCGTGTGCGCCGCCCTGTCGCCATGGTGTATACCTGCACGTCGTCGCTCCCCCAT
GTGCAGACCATGCAAGGTCCCCTAGGCTGCCACCAAAGAGGGGGCCCTCTGCCAGCTG
AGGACCCTGCCCCTGAGGAGCGGCAGGTCTATCGCAGGAAGGAGCGTGAGGAGGGGGC
ACCTGAAACCCCTGTGGTGTCTGCCACCACCGTGGGGACCCTGGCCAGACCAGGTCCG
GAGCCTGCCCCAGCCACAG**

RAT

**ATGGTGGCTGGCATGCTCATGCCACTGGACCAGCTTCGGGGCCATCTATGAGGTGCTCT
TTCGTGAGGGGGTGATGGTTGCCAAGAAGGACCGGGCGACCCCGAAGCCTGCATCCCCA
TGTGCCCCGGCGTCACCAATCTACAGGTCATGCGTGCCATGACCTCGTGAAAGCTCGG
GGCCTGGTGCGGGAGACCTTTGCCTGGTGCCACTTCTACTGGTACCTGACCAACGAGG
GCATCGACCACCTACGCCAGTACCTACACCTGCCACCGGAGATCGTACCTGCCTCTCT
GCAGCGTGTGCGCCGCCCTGTTGCCATGGTGTATGCCTGCACGTCGTCGCTCCCCCAT
GTGCAGACCATGCAAGGTCCCCTTAGGCTGTCCACCAAAGAGGGGGCCCTCTGCCAGCTG
AGGACCCTGCCCCTGAGGAGCGGCAGGTCTATCGCAGGAAGGAGCGTGAGGAAGGGGC
ACCTGAAACCCCTGTGGTGTCTGCCACCATCGTGGGGACCCTGGCCAGGCCAGGCCCA
GAGCCACCCAGCCACAG**

PLEC 1A

HUMAN

ATGTCTCAGCACCAGCTCCGCGTGCCGCAGCCCGAGGGCCTGGGCCGAAAGAGAACCA
GCTCGGAGGACAACCTGTACCTGGCTGTGCTCAGGGCCTCTGAGGGCAAGAAAG

MOUSE

ATGTCTCAGCACC GGCTCCGTGTGCCCCGAGCCGGAAGGCCTGGGTAGCAAGAGAACCA
GCTCAGAGGACAACCTCTACCTGGCTGTGCTCAGAGCCTCCGAGGGCAAGAAAG

RAT

ATGTCTCAGCAACGGCTCCGTGTGCCCCGAGCCTGAAGGCCTGGGTAGCAAGAGAACCA
GCTCAGAGGACAACCTCTACCTGGCTGTGCTCAGGGCCTCCGAGGGCAAGAAAG

PLEC 1B

HUMAN

ATGGAGCCCTCGGGCAGCCTGTTTCCCTCCCTGGTGGTTGTGGGTCACGTTGTCACCC
TGGCCGCTGTGTGGCACTGGCGCAGGGGACGTCGGTGGGCGCAGGACGAGCAAG

MOUSE

ATGGAGCCGTGCGGGCAGCCTGTTTCCCTCCCTGGTAGTCGTGGGTCATGTTGTCACTC
TGGCTGCCGTATGGCACTGGCGTAAGGGGCATCGGCAGGCAAAGGATGAGCAAG

RAT

ATGGAGCCGTGCGGGCAGCCTGTTTCCCTCTCTGGTAGTCGTGGGTCATGTTGTCAGTC
TGGCTGCTGTATGGCACTGGCGTAAGGGGCATCGGCAGGCACAGGATGAGCAAG

PLEC 1C

HUMAN

ATGTCGGGTGAGGACGCTGAGGTCCGGGCAGTCTCTGAAGATGTCTCCAATGGAAGCA
GTGGCTCGCCAGCCCTGGGGACACACTGCCCTGGAACCTTGGGAAAACGCAGCGGAG
CCGGCGCAGCGGGGTGGCGCTGGGAGCAACGGGAGTGTCTGGACCCAGCTGAGCGG
GCGGTCATTTCGCATCGCAG

MOUSE

ATGTCAGGGGAGGATTCTGAGGTCCGGCCAGTGGCAGTGGCTGAAGGTAGTTCCAATG
GAAGCAGTGGCTCACCCAGCCCCGGGGACACACTGCCCTGGAACCTTGGGAAAACACA
GAGAAGTCGGCGAAGTGGAGGTGGTTCTGTGGGCAATGGGAGCGTCTTGGACCCTGCA
GAGCGGGCCGTCATCCGCATTGCAG

RAT

ATGTCAGGGGAGGACTCCGAGGTACGGCCAGTGGCAGTGGCTGAAGGTAGTTCCAATG
GAAGCAGTGGTTCACCCAGCCCCGGGGACACACTGCCCTGGAACCTTGGGAAAACACA
GAGAAGCCGGCGGAGTGGAGGTGGTTCTGTGGGCAATGGGAGCGTCTTGGATCCTGCA
GAGCGGGCCGTCATCCGCATTGCAG

PLEC 1D

HUMAN

ATGAAGATCGTGCCCCG

MOUSE

ATGAAGATCGTGCCCCG

RAT

ATGAAGATCGTGCCCCG

PLEC 1E

HUMAN

ATGGACCCCTCGCGAGCCATCCAGAACGAGATCAGCTCCCTCAAAG

MOUSE

ATGGACCCCTCAAGAGCCATCCAGCACGAGATCAGCTCCCTCAAAG

RAT

ATGGACCCCTCGAGAGCCATCCAGCATGAAATCAGCTCCCTCAAAG

PLEC 1F

HUMAN

**ATGGCCGGCCCGCTGCCCCGACGAGCAGGACTTCATCCAGGCCTACGAGGAGGTGCGCG
AGAAGTACAAAG**

MOUSE

**ATGGCCCATCTGCTGACGTCTGGCCCACCACCCGACGAACAGGATTCATCCAGGCCT
ACGAGGAGGTGCGGGAGAAGTACAAAG**

RAT

**ATGGCCCATCTGCTGACGTCCGGCCCACCACCCGACGAACAGGACTTCATCCAGGCC
TACGAGGAGGTGCGGGAGAAGTACAAAG**

PLEC 1G

HUMAN

ATGTCGGGGGCGGGGGGCGCCTTTGCCTCGCCGAGGGAGGTCTTGCTGGAGCGGCCGT
GCTGGCTGGACGGGGGCTGCGAGCCGGCCCGCAGGGGCTACCTCTACCAGCAGCTGTG
CTGCGTAG

MOUSE

ATGGGCTGGGGCGCGGCTTCCTGGCCACACTGGGCGGGGCGCTTGCTGCAGGGGCAG
GTTCTCCGGGTCTGGGTATTGCGTCCGATGGGCGGGGGCGAACGTGGAAGCCAGGGCC
TTCAGCCTTCAACACAAGCACGGCTTTCGTGTGCTCTGCGAGCAGCCCAGGGCACTCG
GGGCTCCTGGCA**ATG**GCAGGGACGTGGGCGGCGAAGGGAGTCTTCACTTCGCAGAGGG
AGGTCCTGGAGCGTCCCYCGTGGCTGGATGGGGGCTGCGAGCAGGTCCGCAGGGGCTA
CCTCTACGGGCAACTCTGTTGTGTAG

RAT

ATGGCAGGGACGTGGGCAGCGAAGGGCGTCTTCACTTCGCAGAGGGAGGTCTGTTGG
AGCGGCCCTGCTGGCTGGATGGGGGCTGTGAGCAGATTTCGCAGGGGCTATCTCTACGG
GCAACTGTGTTGTGTAG

PLEC 1K

HUMAN

ATGGACAGGTACAGCATGGAGGAGCTGATTCAGCTGGGCCAAG

MOUSE

ATGGATAGGTACAGCATGGAGGAGCTGATCCAGCTGGGCCAAG

RAT

ATGGATATGTACAGCATGGAGGAGCTGATCCAGCTGGGCCAAG

PLEC 1L (POSSIBLE)

HUMAN

ATGGATCAGGTGAGAAGCCTCTCCACAGAGGCCTGGCGAGGTCCACCCTGCTGCAGCA
GAGCAGGTGCCTGCGTGAGGAGGGCCTCCAGAGGGCAGCGGCAGGGCTGTGGTGGGAC
CTGCTTGTGCTCGGAGAGCACTGGCTGCTGTTGTCCAGTGCTTGGAG

APPENDIX II. PREDICTED AMINO ACID SEQUENCES OF PLECTIN
ALTERNATIVELY SPLICES N-TERMINAL EXONS

PLECTIN 1

HUMAN

MET V A G **MET** L **MET** P R D Q L R A I Y E V L F R E G V **MET**
V A K K D R R P R S L H P H V P G V T N L Q V **MET** R A **MET**
A S L R A R G L V R E T F A W C H F Y W Y L T N E G I A H
L R Q Y L H L P P E I V P A S L Q R V R R P V A **MET** V **MET**
P A R R T P H V Q A V Q G P L G S P P K R G P L P T E E Q
R V Y R R K E L E E V S P E T P V V P A T T Q R T L A R P
G P E P A P A T

MOUSE

MET V A G **MET** L **MET** P L D R L R A I Y E V L F R E G V **MET**
V A K K D R R P R S L H P H V P G V T I L Q V **MET** R A **MET**
A S L K A R G L V R E T F A W C H F Y W Y L T N E G I D H
L R Q Y L H L P P E I V P A S L Q R V R R P V A **MET** V I P
A R R R S P H V Q T **MET** Q G P L G C P P K R G P L P A E D
P A R E E R Q V Y R R K E R E E G A P E T P V V S A T T V
G T L A R P G P E P A P A T

RAT

MET V A G **MET** L **MET** P L D Q L R A I Y E V L F R E G V **MET**
V A K K D R R P R S L H P H V P G V T N L Q V **MET** R A **MET**
T S L K A R G L V R E T F A W C H F Y W Y L T N E G I D H
L R Q Y L H L P P E I V P A S L Q R V R R P V A **MET** V **MET**
P A R R R S P H V Q T **MET** Q G P L G C P P K R G P L P A E
D P A R E E R Q V Y R R K E R E E G A P E T P V V S A T I
V G T L A R P G P E P T P A T

PLECTIN 1A

HUMAN

MET S Q H Q L R V P Q P E G L G R K R T S S E D N L Y L A
V L R A S E G K K

MOUSE

MET S Q H R L R V P E P E G L G S K R T S S E D N L Y L A
V L R A S E G K K

RAT

MET S Q Q R L R V P E P E G L G S K R T S S E D N L Y L A
V L R A S E G K K

PLECTIN 1B

HUMAN

MET E P S G S L F P S L V V V G H V V T L A A V W H W R R
G R R W A Q D E Q

MOUSE

MET E P S G S L F P S L V V V G H V V T L A A V W H W R K
G H R Q A K D E Q

RAT

MET E P S G S L F P S L V V V G H V V S L A A V W H W R K
G H R Q A Q D E Q

PLECTIN 1C

HUMAN

MET S G E D A E V R A V S E D V S N G S S G S P S P G D T
L P W N L G K T Q R S R R S G G G A G S N G S V L D P A E
R A V I R I A

MOUSE

MET S G E D S E V R P V A V A E G S S N G S S G S P S P G
D T L P W N L G K T Q R S R R S G G G S V G N G S V L D P
A E R A V I R I A

RAT

MET S G E D S E V R P V A V A E G S S N G S S G S P S P G
D T L P W N L G K T Q R S R R S G G G S V G N G S V L D P
A E R A V I R I A

PLECTIN 1D

HUMAN

MET K I V P

MOUSE

MET K I V P

RAT

MET K I V P

PLECTIN 1E

HUMAN

MET D P S R A I Q N E I S S L K

MOUSE

MET D P S R A I Q H E I S S L K

RAT

MET D P S R A I Q H E I S S L K

PLECTIN 1F

HUMAN

MET A G P L P D E Q D F I Q A Y E E V R E K Y K

MOUSE

MET A H L L T S G P P P D E Q D F I Q A Y E E V R E K Y K

RAT

MET A H L L T S G P P P D E Q D F I Q A Y E E V R E K Y K

PLECTIN 1G

HUMAN

MET S G A G G A F A S P R E V L L E R P C W L D G G C E P A R R
G Y L Y Q Q L C C V

MOUSE

MET A G T W A A K G V F T S Q R E V L E R P X W L D G G C E Q V
R R G Y L Y G Q L C C V

RAT

MET A G T W A A K G V F T S Q R E V L L E R P C W L D G G C E Q
I R R G Y L Y G Q L C C V

PLECTIN 1K

HUMAN

MET D R Y S **MET** E E L I Q L G Q

MOUSE

MET D R Y S **MET** E E L I Q L G Q

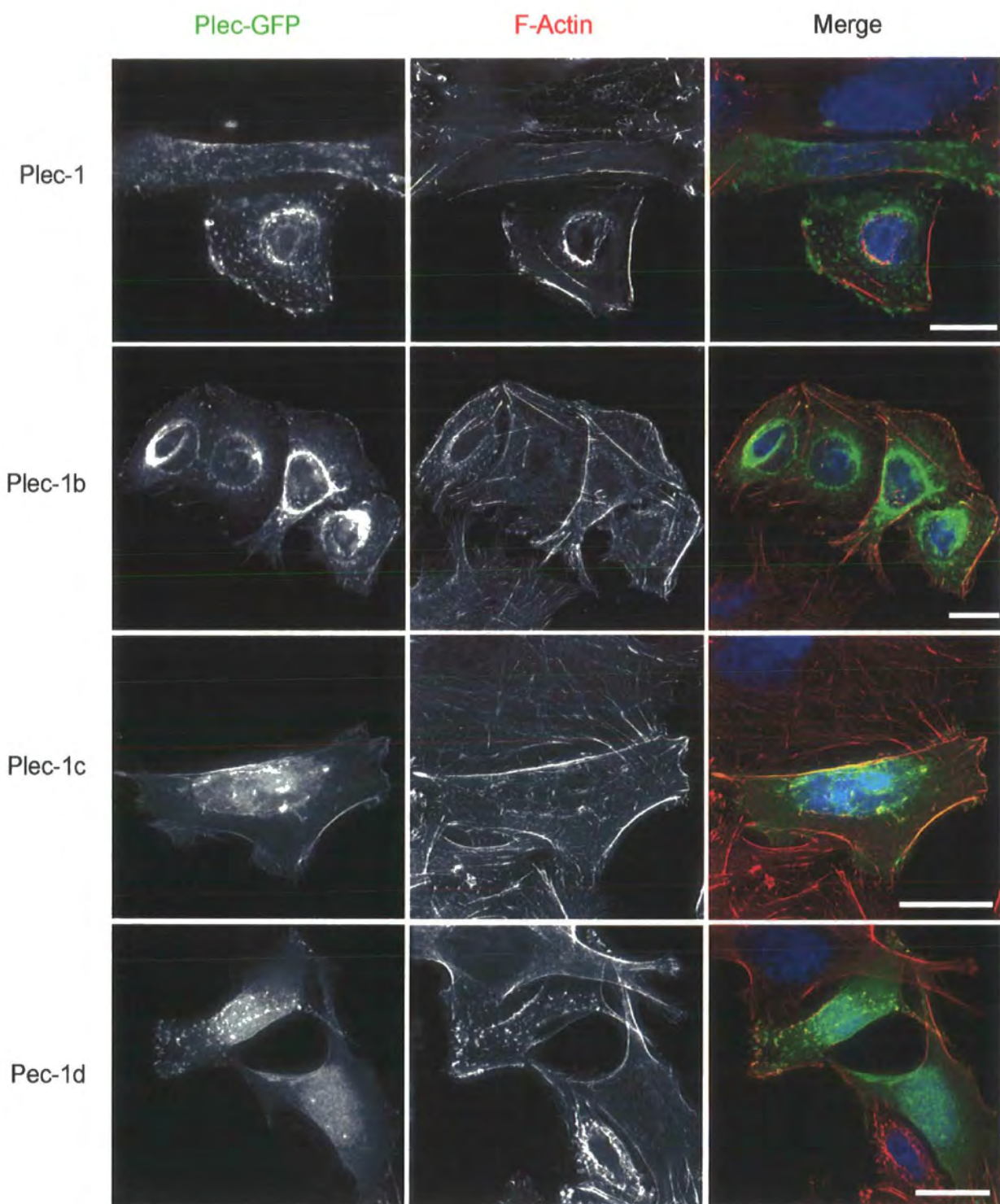
RAT

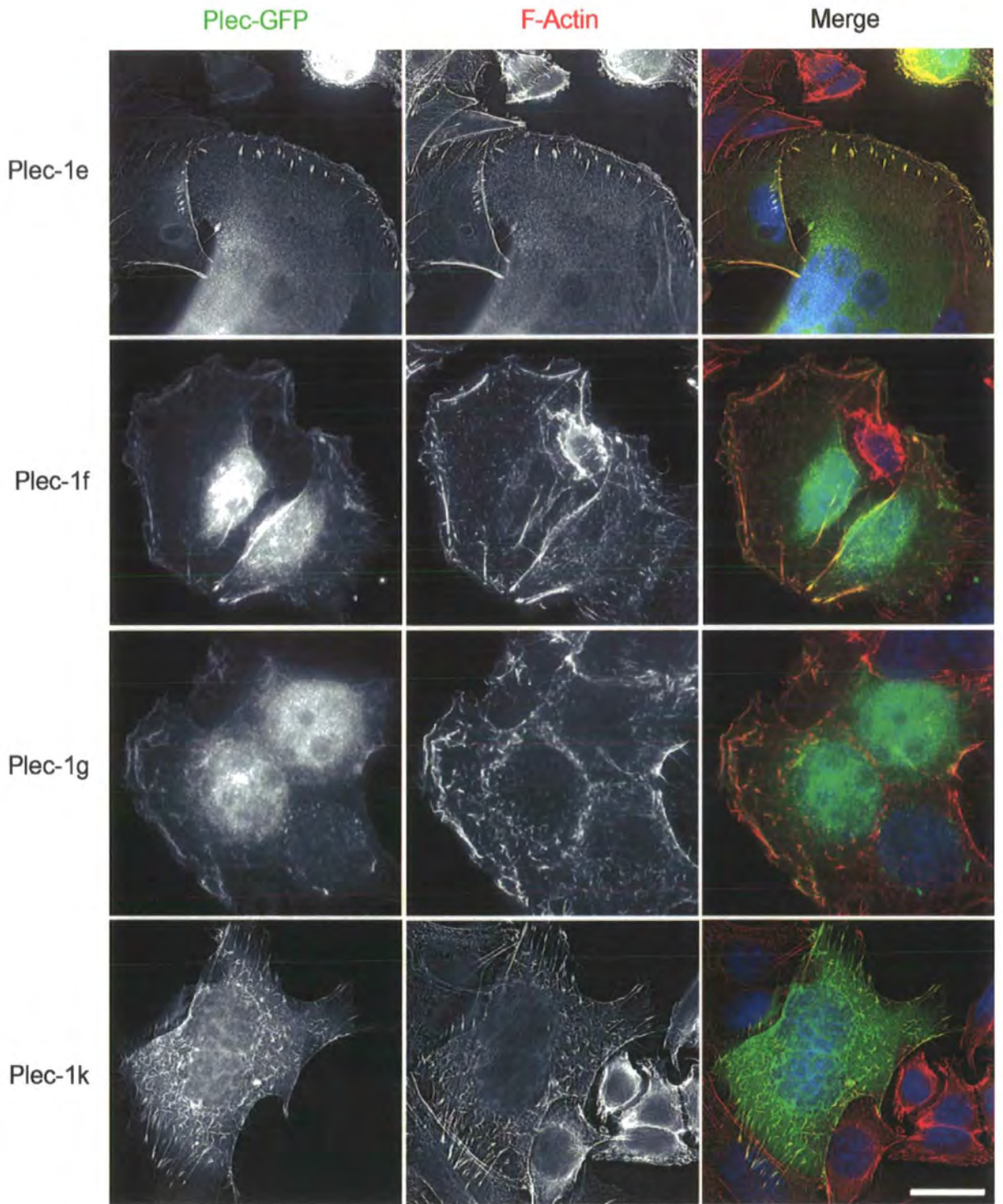
MET D **MET** Y S **MET** E E L I Q L G Q

PLECTIN 1L (POSSIBLE)

HUMAN

MET D Q V R S L S T E A W R G P P C C S R A G A C V R R A S R G
Q R Q G C G G T C L C S E S T G C C C P V





Appendix III. Subcellular localisation of alternative plectin N-terminal domains.

Representative examples of co-localisation of eGFP fluorescence and actin cytoskeleton (red, phalloidin staining) in SW480 cells transfected with the indicated constructs. Dapi staining of cell nucleus is included in the merged image (blue). Images are taken with Delta Vision deconvolution microscope with x 60 oil immersion lense. Note, co-localisation of plectin with actin at focal adhesions and stress fibers. Scale bars represent 20µm.

- Abrahamsberg, C., P. Fuchs, S. Osmanagic-Myers, I. Fischer, F. Propst, A. Elbe-Burger, and G. Wiche. 2005. Targeted ablation of plectin isoform 1 uncovers role of cytolinker proteins in leukocyte recruitment. *Proc Natl Acad Sci U S A.* 102:18449-54.
- Agrez, M., A. Chen, R.I. Cone, R. Pytela, and D. Sheppard. 1994. The alpha v beta 6 integrin promotes proliferation of colon carcinoma cells through a unique region of the beta 6 cytoplasmic domain. *J Cell Biol.* 127:547-56.
- Agrez, M.V., and R.C. Bates. 1994. Colorectal cancer and the integrin family of cell adhesion receptors: current status and future directions. *Eur J Cancer.* 30A:2166-70.
- Aho, S. 2004. Many faces of periplakin: domain-specific antibodies detect the protein throughout the epidermis, explaining the multiple protein-protein interactions. *Cell Tissue Res.* 316:87-97.
- Aho, S., M.G. Mahoney, and J. Uitto. 1999. Plectin serves as an autoantigen in paraneoplastic pemphigus. *J Invest Dermatol.* 113:422-3.
- Aho, S., W.H. McLean, K. Li, and J. Uitto. 1998. cDNA cloning, mRNA expression, and chromosomal mapping of human and mouse periplakin genes. *Genomics.* 48:242-7.
- Alroy, J., B.U. Pauli, and R.S. Weinstein. 1981. Correlation between numbers of desmosomes and the aggressiveness of transitional cell carcinoma in human urinary bladder. *Cancer.* 47:104-12.
- Amann, K.J., and T.D. Pollard. 2001. The Arp2/3 complex nucleates actin filament branches from the sides of pre-existing filaments. *Nat Cell Biol.* 3:306-10.
- Andra, K., I. Kornacker, A. Jorgl, M. Zorer, D. Spazierer, P. Fuchs, I. Fischer, and G. Wiche. 2003. Plectin-isoform-specific rescue of hemidesmosomal defects in plectin (-/-) keratinocytes. *J Invest Dermatol.* 120:189-97.
- Andra, K., H. Lassmann, R. Bittner, S. Shorny, R. Fassler, F. Propst, and G. Wiche. 1997. Targeted inactivation of plectin reveals essential function in maintaining the integrity of skin, muscle, and heart cytoarchitecture. *Genes Dev.* 11:3143-56.
- Andra, K., B. Nikolic, M. Stocher, D. Drenckhahn, and G. Wiche. 1998. Not just scaffolding: plectin regulates actin dynamics in cultured cells. *Genes Dev.* 12:3442-51.
- Angst, B.D., L.A. Nilles, and K.J. Green. 1990. Desmoplakin II expression is not restricted to stratified epithelia. *J Cell Sci.* 97 (Pt 2):247-57.
- Auwerx, J.H., S. Deeb, J.D. Brunzell, R. Peng, and A. Chait. 1988. Transcriptional activation of the lipoprotein lipase and apolipoprotein E genes accompanies differentiation in some human macrophage-like cell lines. *Biochemistry.* 27:2651-5.
- Baker, E.A., D.J. Leaper, J.P. Hayter, and A.J. Dickenson. 2006. The matrix metalloproteinase system in oral squamous cell carcinoma. *Br J Oral Maxillofac Surg.* 44:482-6.

Bankfalvi, A., M. Krassort, I.B. Buchwalow, A. Vegh, E. Felszeghy, and J. Piffko. 2002. Gains and losses of adhesion molecules (CD44, E-cadherin, and beta-catenin) during oral carcinogenesis and tumour progression. *J Pathol.* 198:343-51.

Bankfalvi, A., M. Krassort, A. Vegh, E. Felszeghy, and J. Piffko. 2002. Deranged expression of the E-cadherin/beta-catenin complex and the epidermal growth factor receptor in the clinical evolution and progression of oral squamous cell carcinomas. *J Oral Pathol Med.* 31:450-7.

Bantounas, I., L.A. Phylactou, and J.B. Uney. 2004. RNA interference and the use of small interfering RNA to study gene function in mammalian systems. *J Mol Endocrinol.* 33:545-57.

Bakolitsa, C., D.M. Cohen, L.A. Bankston, A.A. Bobkov, G.W. Cadwell, L. Jennings, D.R. Critchley, S.W. Craig, and R.C. Liddington. 2004. Structural basis for vinculin activation at sites of cell adhesion. *Nature.* 430:583-6.

Brabletz, T. 2001. [The Rudolf Virchow Prize 2001. The role of the oncoprotein beta-catenin in the progression of colorectal cancers]. *Verh Dtsch Ges Pathol.* 85:243-9.

Brabletz, T., A. Jung, S. Reu, M. Porzner, F. Hlubek, L.A. Kunz-Schughart, R. Knuechel, and T. Kirchner. 2001. Variable beta-catenin expression in colorectal cancers indicates tumor progression driven by the tumor environment. *Proc Natl Acad Sci U S A.* 98:10356-61.

Beekman, J.M., J.E. Bakema, J. van der Linden, B. Tops, M. Hinten, M. van Vugt, J.G. van de Winkel, and J.H. Leusen. 2004. Modulation of FcgammaRI (CD64) ligand binding by blocking peptides of periplakin. *J Biol Chem.* 279:33875-81.

Berdeaux, R.L., B. Diaz, L. Kim, and G.S. Martin. 2004. Active Rho is localized to podosomes induced by oncogenic Src and is required for their assembly and function. *J Cell Biol.* 166:317-23.

Bernier, G., M. Mathieu, Y. De Repentigny, S.M. Vidal, and R. Kothary. 1996. Cloning and characterization of mouse ACF7, a novel member of the dystonin subfamily of actin binding proteins. *Genomics.* 38:19-29.

Bershadsky, A.D., I.S. Tint, and T.M. Svitkina. 1987. Association of intermediate filaments with vinculin-containing adhesion plaques of fibroblasts. *Cell Motil Cytoskeleton.* 8:274-83.

Bindels, S., M. Mestdagt, C. Vandewalle, N. Jacobs, L. Volders, A. Noel, F. van Roy, G. Berx, J.M. Foidart, and C. Gilles. 2006. Regulation of vimentin by SIP1 in human epithelial breast tumor cells. *Oncogene.* 25:4975-85.

Birchmeier, C., D. Meyer, and D. Riethmacher. 1995. Factors controlling growth, motility, and morphogenesis of normal and malignant epithelial cells. *Int Rev Cytol.* 160:221-66.

- Birchmeier, W., and C. Birchmeier. 1995. Epithelial-mesenchymal transitions in development and tumor progression. *Exs.* 74:1-15.
- Birchmeier, W., J. Hulsken, and J. Behrens. 1995. Adherens junction proteins in tumour progression. *Cancer Surv.* 24:129-40.
- Birchmeier, W., J. Hulsken, and J. Behrens. 1995. E-cadherin as an invasion suppressor. *Ciba Found Symp.* 189:124-36; discussion 136-41, 174-6.
- Birkedal-Hansen, H. 1995. Matrix metalloproteinases. *Adv Dent Res.* 9:16.
- Birkedal-Hansen, H. 1995. Proteolytic remodeling of extracellular matrix. *Curr Opin Cell Biol.* 7:728-35.
- Black, D.L. 2003. Mechanisms of alternative pre-messenger RNA splicing. *Annu Rev Biochem.* 72:291-336.
- Boczonadi, V., L. McInroy, and A. Maatta. 2007. Cytolinker cross-talk: Periplakin N-terminus interacts with plectin to regulate keratin organisation and epithelial migration. *Exp Cell Res.* 313:3579-91.
- Boguski, M.S. 1995. Hunting for genes in computer data bases. *N Engl J Med.* 333:645-7.
- Boguski, M.S., T.M. Lowe, and C.M. Tolstoshev. 1993. dbEST--database for "expressed sequence tags". *Nat Genet.* 4:332-3.
- Boguski, M.S., and G.D. Schuler. 1995. ESTablishing a human transcript map. *Nat Genet.* 10:369-71.
- Borradori, L., P.J. Koch, C.M. Niessen, S. Erkeland, M.R. van Leusden, and A. Sonnenberg. 1997. The localization of bullous pemphigoid antigen 180 (BP180) in hemidesmosomes is mediated by its cytoplasmic domain and seems to be regulated by the beta4 integrin subunit. *J Cell Biol.* 136:1333-47.
- Borradori, L., and A. Sonnenberg. 1996. Hemidesmosomes: roles in adhesion, signaling and human diseases. *Curr Opin Cell Biol.* 8:647-56.
- Borradori, L., and A. Sonnenberg. 1999. Structure and function of hemidesmosomes: more than simple adhesion complexes. *J Invest Dermatol.* 112:411-8.
- Bosch, F.X., C. Andl, U. Abel, and J. Kartenbeck. 2005. E-cadherin is a selective and strongly dominant prognostic factor in squamous cell carcinoma: a comparison of E-cadherin with desmosomal components. *Int J Cancer.* 114:779-90.
- Bosher, J.M., B.S. Hahn, R. Legouis, S. Sookhareea, R.M. Weimer, A. Gansmuller, A.D. Chisholm, A.M. Rose, J.L. Bessereau, and M. Labouesse. 2003. The *Caenorhabditis elegans* vab-10 spectraplakins isoforms protect the epidermis against internal and external forces. *J Cell Biol.* 161:757-68.

- Braga, V. 2000. Epithelial cell shape: cadherins and small GTPases. *Exp Cell Res.* 261:83-90.
- Braga, V. 2000. The crossroads between cell-cell adhesion and motility. *Nat Cell Biol.* 2:E182-4.
- Braga, V.M. 2002. Cell-cell adhesion and signalling. *Curr Opin Cell Biol.* 14:546-56.
- Braga, V.M., M. Betson, X. Li, and N. Lamarche-Vane. 2000. Activation of the small GTPase Rac is sufficient to disrupt cadherin-dependent cell-cell adhesion in normal human keratinocytes. *Mol Biol Cell.* 11:3703-21.
- Bremnes, R.M., R. Veve, F.R. Hirsch, and W.A. Franklin. 2002. The E-cadherin cell-cell adhesion complex and lung cancer invasion, metastasis, and prognosis. *Lung Cancer.* 36:115-24.
- Brinkley, W. 1997. Microtubules: a brief historical perspective. *J Struct Biol.* 118:84-6.
- Bruzzaniti, A., L. Neff, A. Sanjay, W.C. Horne, P. De Camilli, and R. Baron. 2005. Dynamin forms a Src kinase-sensitive complex with Cbl and regulates podosomes and osteoclast activity. *Mol Biol Cell.* 16:3301-13.
- Buccione, R., J.D. Orth, and M.A. McNiven. 2004. Foot and mouth: podosomes, invadopodia and circular dorsal ruffles. *Nat Rev Mol Cell Biol.* 5:647-57.
- Burgeson, R.E., and A.M. Christiano. 1997. The dermal-epidermal junction. *Curr Opin Cell Biol.* 9:651-8.
- Byers, T.J., A.H. Beggs, E.M. McNally, and L.M. Kunkel. 1995. Novel actin crosslinker superfamily member identified by a two step degenerate PCR procedure. *FEBS Lett.* 368:500-4.
- Calderwood, D.A. 2004. Talin controls integrin activation. *Biochem Soc Trans.* 32:434-7.
- Calderwood, D.A. 2004. Integrin activation. *J Cell Sci.* 117:657-66.
- Camargo, L.M., V. Collura, J.C. Rain, K. Mizuguchi, H. Hermjakob, S. Kerrien, T.P. Bonnert, P.J. Whiting, and N.J. Brandon. 2007. Disrupted in Schizophrenia 1 Interactome: evidence for the close connectivity of risk genes and a potential synaptic basis for schizophrenia. *Mol Psychiatry.* 12:74-86.
- Caswell, P.T., and J.C. Norman. 2006. Integrin trafficking and the control of cell migration. *Traffic.* 7:14-21.
- Cavallaro, U., Schaffhauser, B., Cristofori, G. 2002. Cadherins and the tumour progression: is it all in a switch. *Cancer lett.* 25;176(2);123-8

- Chambers, A.F., A.C. Groom, and I.C. MacDonald. 2002. Dissemination and growth of cancer cells in metastatic sites. *Nat Rev Cancer*. 2:563-72.
- Chellaiah, M.A. 2006. Regulation of podosomes by integrin alphavbeta3 and Rho GTPase-facilitated phosphoinositide signaling. *Eur J Cell Biol*. 85:311-7.
- Chen, H.J., C.M. Lin, C.S. Lin, R. Perez-Olle, C.L. Leung, and R.K. Liem. 2006. The role of microtubule actin cross-linking factor 1 (MACF1) in the Wnt signaling pathway. *Genes Dev*. 20:1933-45.
- Choi, H.J., S. Park-Snyder, L.T. Pascoe, K.J. Green, and W.I. Weis. 2002. Structures of two intermediate filament-binding fragments of desmoplakin reveal a unique repeat motif structure. *Nat Struct Biol*. 9:612-20.
- Christofori, G. 2006. New signals from the invasive front. *Nature*. 441:444-50.
- Chu, P.G., and L.M. Weiss. 2002. Keratin expression in human tissues and neoplasms. *Histopathology*. 40:403-39.
- Chu, Y.W., R.B. Runyan, R.G. Oshima, and M.J. Hendrix. 1993. Expression of complete keratin filaments in mouse L cells augments cell migration and invasion. *Proc Natl Acad Sci U S A*. 90:4261-5.
- Chu, Y.W., E.A. Seftor, L.H. Romer, and M.J. Hendrix. 1996. Experimental coexpression of vimentin and keratin intermediate filaments in human melanoma cells augments motility. *Am J Pathol*. 148:63-9.
- Chung, W., and J.T. Campanelli. 1999. WW and EF hand domains of dystrophin-family proteins mediate dystroglycan binding. *Mol. Cell. Biol. Res. Commun*. 2;162-171.
- Chung, C.Y., and R.A. Firtel. 1999. PAKa, a putative PAK family member, is required for cytokinesis and the regulation of the cytoskeleton in *Dictyostelium discoideum* cells during chemotaxis. *J Cell Biol*. 147:559-76.
- Ciocca, D.R., and S.K. Calderwood. 2005. Heat shock proteins in cancer: diagnostic, prognostic, predictive, and treatment implications. *Cell Stress Chaperones*. 10:86-103.
- Cochard, P., and D. Paulin. 1984. Initial expression of neurofilaments and vimentin in the central and peripheral nervous system of the mouse embryo in vivo. *J Neurosci*. 4:2080-94.
- Cohen, D.M., B. Kutscher, H. Chen, D.B. Murphy, and S.W. Craig. 2006. A conformational switch in vinculin drives formation and dynamics of a talin-vinculin complex at focal adhesions. *J Biol Chem*. 281:16006-15.
- Coopman, P.J., D.M. Thomas, K.R. Gehlsen, and S.C. Mueller. 1996. Integrin alpha 3 beta 1 participates in the phagocytosis of extracellular matrix molecules by human breast cancer cells. *Mol Biol Cell*. 7:1789-804.

- Correia, I., D. Chu, Y.H. Chou, R.D. Goldman, and P. Matsudaira. 1999. Integrating the actin and vimentin cytoskeletons. adhesion-dependent formation of fimbrin-vimentin complexes in macrophages. *J Cell Biol.* 146:831-42.
- Coulombe, P.A., L. Ma, S. Yamada, and M. Wawersik. 2001. Intermediate filaments at a glance. *J Cell Sci.* 114:4345-7.
- Coulombe, P.A., and M.B. Omary. 2002. 'Hard' and 'soft' principles defining the structure, function and regulation of keratin intermediate filaments. *Curr Opin Cell Biol.* 14:110-22.
- Cowin, P., T.M. Rowlands, and S.J. Hatsell. 2005. Cadherins and catenins in breast cancer. *Curr Opin Cell Biol.* 17:499-508.
- Critchley, D.R. 2004. Cytoskeletal proteins talin and vinculin in integrin-mediated adhesion. *Biochem Soc Trans.* 32:831-6.
- Culligan, K.G., A.J. Mackey, D.M. Finn, P.B. Maguire and K. Ohlendieck. 1998. Role of dystrophin isoforms and associated proteins in muscular dystrophy. *Int. J. Mol. Med.* 2:639-648.
- Davies, E.L., J.M. Gee, R.A. Cochrane, W.G. Jiang, A.K. Sharma, R.I. Nicholson, and R.E. Mansel. 1999. The immunohistochemical expression of desmoplakin and its role in vivo in the progression and metastasis of breast cancer. *Eur J Cancer.* 35:902-7.
- Depondt, J., A.H. Shabana, S. Florescu-Zorila, P. Gehanno, and N. Forest. 1999. Down-regulation of desmosomal molecules in oral and pharyngeal squamous cell carcinomas as a marker for tumour growth and distant metastasis. *Eur J Oral Sci.* 107:183-93.
- DiColandrea, T., T. Karashima, A. Maatta, and F.M. Watt. 2000. Subcellular distribution of envoplakin and periplakin: insights into their role as precursors of the epidermal cornified envelope. *J Cell Biol.* 151:573-86.
- Drabek, K., M. van Ham, T. Stepanova, K. Draegestein, R. van Horssen, C.L. Sayas, A. Akhmanova, T. Ten Hagen, R. Smits, R. Fodde, F. Grosveld, and N. Galjart. 2006. Role of CLASP2 in microtubule stabilization and the regulation of persistent motility. *Curr Biol.* 16:2259-64.
- Eckert, K.A., and T.A. Kunkel. 1990. High fidelity DNA synthesis by the *Thermus aquaticus* DNA polymerase. *Nucleic Acids Res.* 18:3739-44.
- Eckes, B., E. Colucci-Guyon, H. Smola, S. Nodder, C. Babinet, T. Krieg, and P. Martin. 2000. Impaired wound healing in embryonic and adult mice lacking vimentin. *J Cell Sci.* 113 (Pt 13):2455-62.
- Eckes, B., D. Dogic, E. Colucci-Guyon, N. Wang, A. Maniotis, D. Ingber, A. Merckling, F. Langa, M. Aumailley, A. Delouvee, V. Koteliensky, C. Babinet, and T. Krieg. 1998. Impaired mechanical stability, migration and contractile capacity in vimentin-deficient fibroblasts. *J Cell Sci.* 111 (Pt 13):1897-907.

Eger, A., A. Stockinger, G. Wiche, and R. Foisner. 1997. Polarisation-dependent association of plectin with desmoplakin and the lateral submembrane skeleton in MDCK cells. *J Cell Sci.* 110 (Pt 11):1307-16.

Elbashir, S.M., J. Harborth, W. Lendeckel, A. Yalcin, K. Weber, and T. Tuschl. 2001. Duplexes of 21-nucleotide RNAs mediate RNA interference in cultured mammalian cells. *Nature.* 411:494-8.

Elliott, C.E., B. Becker, S. Oehler, M.J. Castanon, R. Hauptmann, and G. Wiche. 1997. Plectin transcript diversity: identification and tissue distribution of variants with distinct first coding exons and rodless isoforms. *Genomics.* 42:115-25.

Ellsworth, D.L., K.D. Rittenhouse, and R.L. Honeycutt. 1993. Artifactual variation in randomly amplified polymorphic DNA banding patterns. *Biotechniques.* 14:214-7.

Engel, J., H. Fasold, F.W. Hulla, F. Waechter, and A. Wegner. 1977. The polymerization reaction of muscle actin. *Mol Cell Biochem.* 18:3-13.

Errante, L.D., G. Wiche, and G. Shaw. 1994. Distribution of plectin, an intermediate filament-associated protein, in the adult rat central nervous system. *J Neurosci Res.* 37:515-28.

Eves, R., B.A. Webb, S. Zhou, and A.S. Mak. 2006. Caldesmon is an integral component of podosomes in smooth muscle cells. *J Cell Sci.* 119:1691-702.

Fawcett, D. W. and Porter, K. R. 1954. A study of the fine structure of ciliated epithelia. *J. Morphol.* 94 pp. 221–281.

Foisner, R., B. Feldman, L. Sander, G. Seifert, U. Artlieb, and G. Wiche. 1994. A panel of monoclonal antibodies to rat plectin: distinction by epitope mapping and immunoreactivity with different tissues and cell lines. *Acta Histochem.* 96:421-38.

Foisner, R., F.E. Leichtfried, H. Herrmann, J.V. Small, D. Lawson, and G. Wiche. 1988. Cytoskeleton-associated plectin: in situ localization, in vitro reconstitution, and binding to immobilized intermediate filament proteins. *J Cell Biol.* 106:723-33.

Foisner, R., P. Traub, and G. Wiche. 1991. Protein kinase A- and protein kinase C-regulated interaction of plectin with lamin B and vimentin. *Proc Natl Acad Sci U S A.* 88:3812-6.

Fontao, L., S. Dirrig, K. Owaribe, M. Kedinger, and J.F. Launay. 1997. Polarized expression of HD1: relationship with the cytoskeleton in cultured human colonic carcinoma cells. *Exp Cell Res.* 231:319-27.

Fontao, L., B. Favre, S. Riou, D. Geerts, F. Jaunin, J.H. Saurat, K.J. Green, A. Sonnenberg, and L. Borradori. 2003. Interaction of the bullous pemphigoid antigen 1 (BP230) and desmoplakin with intermediate filaments is mediated by distinct sequences within their COOH terminus. *Mol Biol Cell.* 14:1978-92.

- Fontao, L., D. Geerts, I. Kuikman, J. Koster, D. Kramer, and A. Sonnenberg. 2001. The interaction of plectin with actin: evidence for cross-linking of actin filaments by dimerization of the actin-binding domain of plectin. *J Cell Sci.* 114:2065-76.
- Fontao, L., J. Stutzmann, P. Gendry, and J.F. Launay. 1999. Regulation of the type II hemidesmosomal plaque assembly in intestinal epithelial cells. *Exp Cell Res.* 250:298-312.
- Franke, W.W., M. Hergt, and C. Grund. 1987. Rearrangement of the vimentin cytoskeleton during adipose conversion: formation of an intermediate filament cage around lipid globules. *Cell.* 49:131-41.
- Franke, W.W., E. Schmid, C. Grund, H. Muller, I. Engelbrecht, R. Moll, J. Stadler, and E.D. Jarasch. 1981. Antibodies to high molecular weight polypeptides of desmosomes: specific localization of a class of junctional proteins in cells and tissue. *Differentiation.* 20:217-41.
- Franke, W.W., E. Schmid, M. Osborn, and K. Weber. 1978. Different intermediate-sized filaments distinguished by immunofluorescence microscopy. *Proc Natl Acad Sci U S A.* 75:5034-8.
- Franke, W.W., E. Schmid, D.L. Schiller, S. Winter, E.D. Jarasch, R. Moll, H. Denk, B.W. Jackson, and K. Illmensee. 1982. Differentiation-related patterns of expression of proteins of intermediate-size filaments in tissues and cultured cells. *Cold Spring Harb Symp Quant Biol.* 46 Pt 1:431-53.
- Friedl, P. 2004. Prespecification and plasticity: shifting mechanisms of cell migration. *Curr Opin Cell Biol.* 16:14-23.
- Fuchs, E., and D.W. Cleveland. 1998. A structural scaffolding of intermediate filaments in health and disease. *Science.* 279:514-9.
- Fuchs, P., M. Zorer, G.A. Rezniczek, D. Spazierer, S. Oehler, M.J. Castanon, R. Hauptmann, and G. Wiche. 1999. Unusual 5' transcript complexity of plectin isoforms: novel tissue-specific exons modulate actin binding activity. *Hum Mol Genet.* 8:2461-72.
- Fujiwara, S., K. Kohno, A. Iwamatsu, I. Naito, and H. Shinkai. 1996. Identification of a 450-kDa human epidermal autoantigen as a new member of the plectin family. *J Invest Dermatol.* 106:1125-30.
- Fujiwara, S., H. Shinkai, S. Takayasu, K. Owaribe, S. Tsukita, and T. Kageshita. 1992. A case of subepidermal blister disease associated with autoantibody against 450 kD protein. *J Dermatol.* 19:610-3.
- Fujiwara, S., N. Takeo, Y. Otani, D.A. Parry, M. Kunimatsu, R. Lu, M. Sasaki, N. Matsuo, M. Khaleduzzaman, and H. Yoshioka. 2001. Epiplakin, a novel member of the Plakin family originally identified as a 450-kDa human epidermal autoantigen. Structure and tissue localization. *J Biol Chem.* 276:13340-7.

- Furst, D.O., M. Osborn, and K. Weber. 1989. Myogenesis in the mouse embryo: differential onset of expression of myogenic proteins and the involvement of titin in myofibril assembly. *J Cell Biol.* 109:517-27.
- Gache, Y., S. Chavanas, J.P. Lacour, G. Wiche, K. Owaribe, G. Meneguzzi, and J.P. Ortonne. 1996. Defective expression of plectin/HD1 in epidermolysis bullosa simplex with muscular dystrophy. *J Clin Invest.* 97:2289-98.
- Galarneau, L., A. Loranger, S. Gilbert, and N. Marceau. 2007. Keratins modulate hepatic cell adhesion, size and G1/S transition. *Exp Cell Res.* 313:179-94.
- Gallant, N.D., K.E. Michael, and A.J. Garcia. 2005. Cell adhesion strengthening: contributions of adhesive area, integrin binding, and focal adhesion assembly. *Mol Biol Cell.* 16:4329-40.
- Gallicano, G.I., C. Bauer, and E. Fuchs. 2001. Rescuing desmoplakin function in extra-embryonic ectoderm reveals the importance of this protein in embryonic heart, neuroepithelium, skin and vasculature. *Development.* 128:929-41.
- Gallicano, G.I., P. Kouklis, C. Bauer, M. Yin, V. Vasioukhin, L. Degenstein, and E. Fuchs. 1998. Desmoplakin is required early in development for assembly of desmosomes and cytoskeletal linkage. *J Cell Biol.* 143:2009-22.
- Garcia-Alvarez, B., A. Bobkov, A. Sonnenberg, and J.M. de Pereda. 2003. Structural and functional analysis of the actin binding domain of plectin suggests alternative mechanisms for binding to F-actin and integrin beta4. *Structure.* 11:615-25.
- Garrod, D.R., and S. Fleming. 1990. Early expression of desmosomal components during kidney tubule morphogenesis in human and murine embryos. *Development.* 108:313-21.
- Garrod, D.R., A.J. Merritt, and Z. Nie. 2002. Desmosomal adhesion: structural basis, molecular mechanism and regulation (Review). *Mol Membr Biol.* 19:81-94.
- Gavazzi, I., M.V. Nermut, and P.C. Marchisio. 1989. Ultrastructure and gold-immunolabelling of cell-substratum adhesions (podosomes) in RSV-transformed BHK cells. *J Cell Sci.* 94 (Pt 1):85-99.
- Geerts, D., L. Fontao, M.G. Nievers, R.Q. Schaapveld, P.E. Purkis, G.N. Wheeler, E.B. Lane, I.M. Leigh, and A. Sonnenberg. 1999. Binding of integrin alpha6beta4 to plectin prevents plectin association with F-actin but does not interfere with intermediate filament binding. *J Cell Biol.* 147:417-34.
- Gilles, C., M. Polette, M. Mestdagt, B. Nawrocki-Raby, P. Ruggeri, P. Birembaut, and J.M. Foidart. 2003. Transactivation of vimentin by beta-catenin in human breast cancer cells. *Cancer Res.* 63:2658-64.
- Gilles, C., M. Polette, J.M. Zahm, J.M. Tournier, L. Volders, J.M. Foidart, and P. Birembaut. 1999. Vimentin contributes to human mammary epithelial cell migration. *J Cell Sci.* 112 (Pt 24):4615-25.

Gimona, M., K. Djinovic-Carugo, W.J. Kranewitter, and S.J. Winder. 2002. Functional plasticity of CH domains. *FEBS Lett.* 513:98-106.

Givant-Horwitz, V., B. Davidson, and R. Reich. 2005. Laminin-induced signaling in tumor cells. *Cancer Lett.* 223:1-10.

Godsel, L.M., S.N. Hsieh, E.V. Amargo, A.E. Bass, L.T. Pascoe-McGillicuddy, A.C. Huen, M.E. Thorne, C.A. Gaudry, J.K. Park, K. Myung, R.D. Goldman, T.L. Chew, and K.J. Green. 2005. Desmoplakin assembly dynamics in four dimensions: multiple phases differentially regulated by intermediate filaments and actin. *J Cell Biol.* 171:1045-59.

Goldfinger, L.E., S.B. Hopkinson, G.W. deHart, S. Collawn, J.R. Couchman, and J.C. Jones. 1999. The alpha3 laminin subunit, alpha6beta4 and alpha3beta1 integrin coordinately regulate wound healing in cultured epithelial cells and in the skin. *J Cell Sci.* 112 (Pt 16):2615-29.

Goldman, R.D. 1971. The role of three cytoplasmic fibers in BHK-21 cell motility. I. Microtubules and the effects of colchicine. *J Cell Biol.* 51:752-62.

Gong, T.W., C.G. Besirli, and M.I. Lomax. 2001. MACF1 gene structure: a hybrid of plectin and dystrophin. *Mamm Genome.* 12:852-61.

Gonzales, M., B. Weksler, D. Tsuruta, R.D. Goldman, K.J. Yoon, S.B. Hopkinson, F.W. Flitney, and J.C. Jones. 2001. Structure and function of a vimentin-associated matrix adhesion in endothelial cells. *Mol Biol Cell.* 12:85-100.

Goto, M., H. Sumiyoshi, T. Sakai, R. Fassler, S. Ohashi, E. Adachi, H. Yoshioka, and S. Fujiwara. 2006. Elimination of epiplakin by gene targeting results in acceleration of keratinocyte migration in mice. *Mol Cell Biol.* 26:548-58.

Green, K.J., S.G. Guy, P.B. Cserhalmi-Friedman, W.H. McLean, A.M. Christiano, and R.M. Wagner. 1999. Analysis of the desmoplakin gene reveals striking conservation with other members of the plakin family of cytolinkers. *Exp Dermatol.* 8:462-70.

Green, K.J., and J.C. Jones. 1996. Desmosomes and hemidesmosomes: structure and function of molecular components. *Faseb J.* 10:871-81.

Green, K.J., D.A. Parry, P.M. Steinert, M.L. Virata, R.M. Wagner, B.D. Angst, and L.A. Nilles. 1990. Structure of the human desmoplakins. Implications for function in the desmosomal plaque. *J Biol Chem.* 265:2603-12.

Gregor, M., A. Zeold, S. Oehler, K.A. Marobela, P. Fuchs, G. Weigel, D.G. Hardie, and G. Wiche. 2006. Plectin scaffolds recruit energy-controlling AMP-activated protein kinase (AMPK) in differentiated myofibres. *J Cell Sci.* 119:1864-75.

Grille, S.J., A. Bellacosa, J. Upson, A.J. Klein-Szanto, F. van Roy, W. Lee-Kwon, M. Donowitz, P.N. Tsichlis, and L. Larue. 2003. The protein kinase Akt induces epithelial mesenchymal transition and promotes enhanced motility and invasiveness of squamous cell carcinoma lines. *Cancer Res.* 63:2172-8.

- Groot, K.R., L.M. Sevilla, K. Nishi, T. DiColandrea, and F.M. Watt. 2004. Kazrin, a novel periplakin-interacting protein associated with desmosomes and the keratinocyte plasma membrane. *J Cell Biol.* 166:653-9.
- Gross, S.P., M. Vershinin, and G.T. Shubeita. 2007. Cargo transport: two motors are sometimes better than one. *Curr Biol.* 17:R478-86.
- Gu, L.H., and P.A. Coulombe. 2007. Keratin function in skin epithelia: a broadening palette with surprising shades. *Curr Opin Cell Biol.* 19:13-23.
- Gu, L.H., and P.A. Coulombe. 2007. Keratin expression provides novel insight into the morphogenesis and function of the companion layer in hair follicles. *J Invest Dermatol.* 127:1061-73.
- Guo, L., L. Degenstein, J. Dowling, Q.C. Yu, R. Wollmann, B. Perman, and E. Fuchs. 1995. Gene targeting of BPAG1: abnormalities in mechanical strength and cell migration in stratified epithelia and neurologic degeneration. *Cell.* 81:233-43.
- Guo, W., and F.G. Giancotti. 2004. Integrin signalling during tumour progression. *Nat Rev Mol Cell Biol.* 5:816-26.
- Guttman, J.A., D.J. Mulholland, and A.W. Vogl. 1999. Plectin is concentrated at intercellular junctions and at the nuclear surface in morphologically differentiated rat Sertoli cells. *Anat Rec.* 254:418-28.
- Hayot, C., O. Debeir, P. Van Ham, M. Van Damme, R. Kiss, and C. Decaestecker. 2006. Characterization of the activities of actin-affecting drugs on tumor cell migration. *Toxicol Appl Pharmacol.* 211:30-40.
- Helfand, B.T., L. Chang, and R.D. Goldman. 2004. Intermediate filaments are dynamic and motile elements of cellular architecture. *J Cell Sci.* 117:133-41.
- Hendrix, M.J., E.A. Seftor, Y.W. Chu, R.E. Seftor, R.B. Nagle, K.M. McDaniel, S.P. Leong, K.H. Yohem, A.M. Leibovitz, F.L. Meyskens, Jr., and et al. 1992. Coexpression of vimentin and keratins by human melanoma tumor cells: correlation with invasive and metastatic potential. *J Natl Cancer Inst.* 84:165-74.
- Hendrix, M.J., E.A. Seftor, Y.W. Chu, K.T. Trevor, and R.E. Seftor. 1996. Role of intermediate filaments in migration, invasion and metastasis. *Cancer Metastasis Rev.* 15:507-25.
- Hendrychova, J., M. Vitova, K. Bisova, G. Wiche, and V. Zachleder. 2002. Plectin-like proteins are present in cells of *Chlamydomonas eugametos* (Volvocales). *Folia Microbiol (Praha).* 47:535-9.
- Herrmann, H., Fourquet, B., Franke, W.W. 1989. Expression of intermediate filament proteins during development of *xenopus laevis*. I. cDNA clones encoding different forms of vimentin. *Development* 105:279-298.

Herrmann, H., and U. Aebi. 2000. Intermediate filaments and their associates: multi-talented structural elements specifying cytoarchitecture and cytodynamics. *Curr Opin Cell Biol.* 12:79-90.

Herrmann, H., and G. Wiche. 1987. Plectin and IFAP-300K are homologous proteins binding to microtubule-associated proteins 1 and 2 and to the 240-kilodalton subunit of spectrin. *J Biol Chem.* 262:1320-5.

Hesse, M., T.M. Magin, and K. Weber. 2001. Genes for intermediate filament proteins and the draft sequence of the human genome: novel keratin genes and a surprisingly high number of pseudogenes related to keratin genes 8 and 18. *J Cell Sci.* 114:2569-75.

Hieda, Y., Y. Nishizawa, J. Uematsu, and K. Owaribe. 1992. Identification of a new hemidesmosomal protein, HD1: a major, high molecular mass component of isolated hemidesmosomes. *J Cell Biol.* 116:1497-506.

Hijikata, T., T. Murakami, M. Imamura, N. Fujimaki, and H. Ishikawa. 1999. Plectin is a linker of intermediate filaments to Z-discs in skeletal muscle fibers. *J Cell Sci.* 112 (Pt 6):867-76.

Hijikata, T., T. Murakami, H. Ishikawa, and H. Yorifuji. 2003. Plectin tethers desmin intermediate filaments onto subsarcolemmal dense plaques containing dystrophin and vinculin. *Histochem Cell Biol.* 119:109-23.

Homan, S.M., R. Martinez, A. Benware, and S.E. LaFlamme. 2002. Regulation of the association of alpha 6 beta 4 with vimentin intermediate filaments in endothelial cells. *Exp Cell Res.* 281:107-14.

Hopkinson, S.B., and J.C. Jones. 2000. The N terminus of the transmembrane protein BP180 interacts with the N-terminal domain of BP230, thereby mediating keratin cytoskeleton anchorage to the cell surface at the site of the hemidesmosome. *Mol Biol Cell.* 11:277-86.

Hynes, R.O. 2002. A reevaluation of integrins as regulators of angiogenesis. *Nat Med.* 8:918-21.

Impola, U., V.J. Uitto, J. Hietanen, L. Hakkinen, L. Zhang, H. Larjava, K. Isaka, and U. Saarialho-Kere. 2004. Differential expression of matrilysin-1 (MMP-7), 92 kD gelatinase (MMP-9), and metalloelastase (MMP-12) in oral verrucous and squamous cell cancer. *J Pathol.* 202:14-22.

Inada, H., H. Togashi, Y. Nakamura, K. Kaibuchi, K. Nagata, and M. Inagaki. 1999. Balance between activities of Rho kinase and type 1 protein phosphatase modulates turnover of phosphorylation and dynamics of desmin/vimentin filaments. *J Biol Chem.* 274:34932-9.

Inagaki, N., H. Goto, M. Ogawara, Y. Nishi, S. Ando, and M. Inagaki. 1997. Spatial patterns of Ca²⁺ signals define intracellular distribution of a signaling by Ca²⁺/Calmodulin-dependent protein kinase II. *J Biol Chem.* 272:25195-9.

Ivaska, J., H.M. Pallari, J. Nevo, and J.E. Eriksson. 2007. Novel functions of vimentin in cell adhesion, migration, and signaling. *Exp Cell Res.* 313:2050-62.

Ivaska, J., H. Reunanen, J. Westermarck, L. Koivisto, V.M. Kahari, and J. Heino. 1999. Integrin alpha2beta1 mediates isoform-specific activation of p38 and upregulation of collagen gene transcription by a mechanism involving the alpha2 cytoplasmic tail. *J Cell Biol.* 147:401-16.

Ivaska, J., K. Vuoriluoto, T. Huovinen, I. Izawa, M. Inagaki, and P.J. Parker. 2005. PKCepsilon-mediated phosphorylation of vimentin controls integrin recycling and motility. *Embo J.* 24:3834-45.

Izawa, I., and M. Inagaki. 2006. Regulatory mechanisms and functions of intermediate filaments: a study using site- and phosphorylation state-specific antibodies. *Cancer Sci.* 97:167-74.

Jacinto, A., and L. Wolpert. 2001. Filopodia. *Curr Biol.* 11:R634.

Jefferson, J.J., C. Ciatto, L. Shapiro, and R.K. Liem. 2007. Structural analysis of the plakin domain of bullous pemphigoid antigen1 (BPAG1) suggests that plakins are members of the spectrin superfamily. *J Mol Biol.* 366:244-57.

Jefferson, J.J., C.L. Leung, and R.K. Liem. 2004. Plakins: goliaths that link cell junctions and the cytoskeleton. *Nat Rev Mol Cell Biol.* 5:542-53.

Jefferson, J.J., C.L. Leung, and R.K. Liem. 2006. Dissecting the sequence specific functions of alternative N-terminal isoforms of mouse bullous pemphigoid antigen 1. *Exp Cell Res.* 312:2712-25.

Jiang, W.G. 1996. E-cadherin and its associated protein catenins, cancer invasion and metastasis. *Br J Surg.* 83:437-46.

Jones, J.C., and R.D. Goldman. 1985. Intermediate filaments and the initiation of desmosome assembly. *J Cell Biol.* 101:506-17.

Jones, J.C., and K.J. Green. 1991. Intermediate filament-plasma membrane interactions. *Curr Opin Cell Biol.* 3:127-32.

Jones, J.C., S.B. Hopkinson, and L.E. Goldfinger. 1998. Structure and assembly of hemidesmosomes. *Bioessays.* 20:488-94.

Jones, J.C., M.A. Kurpakus, H.M. Cooper, and V. Quaranta. 1991. A function for the integrin alpha 6 beta 4 in the hemidesmosome. *Cell Regul.* 2:427-38.

Kalendar R. 2007. FastPCR: a PCR primer and probe design and repeat sequence searching software with additional tools for the manipulation and analysis of DNA and protein. (www.biocenter.helsinki.fi/bi/programs/fastpcr.htm)

Kalinin, A., L.N. Marekov, and P.M. Steinert. 2001. Assembly of the epidermal cornified cell envelope. *J Cell Sci.* 114:3069-70.

- Kartenbeck, J., U. Haselmann, and N. Gassler. 2005. Synthesis of junctional proteins in metastasizing colon cancer cells. *Eur J Cell Biol.* 84:417-30.
- Kazerounian, S., and S. Aho. 2003. Characterization of periphilin, a widespread, highly insoluble nuclear protein and potential constituent of the keratinocyte cornified envelope. *J Biol Chem.* 278:36707-17.
- Kazerounian, S., J. Uitto, and S. Aho. 2002. Unique role for the periplakin tail in intermediate filament association: specific binding to keratin 8 and vimentin. *Exp Dermatol.* 11:428-38.
- Kiosses, W.B., R.H. Daniels, C. Otey, G.M. Bokoch, and M.A. Schwartz. 1999. A role for p21-activated kinase in endothelial cell migration. *J Cell Biol.* 147:831-44.
- Kirchner, J., Z. Kam, G. Tzur, A.D. Bershadsky, and B. Geiger. 2003. Live-cell monitoring of tyrosine phosphorylation in focal adhesions following microtubule disruption. *J Cell Sci.* 116:975-86.
- Kodama, A., I. Karakesisoglou, E. Wong, A. Vaezi, and E. Fuchs. 2003. ACF7: an essential integrator of microtubule dynamics. *Cell.* 115:343-54.
- Kokkinos, M.I., R. Wafai, M.K. Wong, D.F. Newgreen, E.W. Thompson, and M. Waltham. 2007. Vimentin and epithelial-mesenchymal transition in human breast cancer--observations in vitro and in vivo. *Cells Tissues Organs.* 185:191-203.
- Koretz, K., S. Bruderlein, C. Henne, T. Fietz, M. Laque, and P. Moller. 1994. Comparative evaluation of integrin alpha- and beta-chain expression in colorectal carcinoma cell lines and in their tumours of origin. *Virchows Arch.* 425:229-36.
- Koster, J., S. van Wilpe, I. Kuikman, S.H. Litjens, and A. Sonnenberg. 2004. Role of binding of plectin to the integrin beta4 subunit in the assembly of hemidesmosomes. *Mol Biol Cell.* 15:1211-23.
- Kowalczyk, A.P., P. Navarro, E. Dejana, E.A. Bornslaeger, K.J. Green, D.S. Kopp, and J.E. Borgwardt. 1998. VE-cadherin and desmoplakin are assembled into dermal microvascular endothelial intercellular junctions: a pivotal role for plakoglobin in the recruitment of desmoplakin to intercellular junctions. *J Cell Sci.* 111 (Pt 20):3045-57.
- Kowalczyk, A.P., T.S. Stappenbeck, D.A. Parry, H.L. Palka, M.L. Virata, E.A. Bornslaeger, L.A. Nilles, and K.J. Green. 1994. Structure and function of desmosomal transmembrane core and plaque molecules. *Biophys Chem.* 50:97-112.
- Kreis, S., H.J. Schonfeld, C. Melchior, B. Steiner, and N. Kieffer. 2005. The intermediate filament protein vimentin binds specifically to a recombinant integrin alpha2/beta1 cytoplasmic tail complex and co-localizes with native alpha2/beta1 in endothelial cell focal adhesions. *Exp Cell Res.* 305:110-21.
- Kron, S.J., D.G. Drubin, D. Botstein, and J.A. Spudich. 1992. Yeast actin filaments display ATP-dependent sliding movement over surfaces coated with rabbit muscle myosin. *Proc Natl Acad Sci U S A.* 89:4466-70.

- Ku, N.O., J. Liao, and M.B. Omary. 1998. Phosphorylation of human keratin 18 serine 33 regulates binding to 14-3-3 proteins. *Embo J.* 17:1892-906.
- Ku, N.O., S.A. Michie, R.M. Soetikno, E.Z. Resurreccion, R.L. Broome, and M.B. Omary. 1998. Mutation of a major keratin phosphorylation site predisposes to hepatotoxic injury in transgenic mice. *J Cell Biol.* 143:2023-32.
- Kurose, K., O. Mori, H. Hachisuka, H. Shimizu, K. Owaribe, and T. Hashimoto. 2000. Cultured keratinocytes from plectin/HD1-deficient epidermolysis bullosa simplex showed altered ability of adhesion to the matrix. *J Dermatol Sci.* 24:184-9.
- Laemmli, U.K. 1970. Cleavage of structural proteins during the assembly of the head of bacteriophage T4. *Nature.* 227:680-5.
- Lane, E.B., B.L. Hogan, M. Kurkinen, and J.I. Garrels. 1983. Co-expression of vimentin and cytokeratins in parietal endoderm cells of early mouse embryo. *Nature.* 303:701-4.
- Le Borgne, R., A. Alconada, U. Bauer, and B. Hoflack. 1998. The mammalian AP-3 adaptor-like complex mediates the intracellular transport of lysosomal membrane glycoproteins. *J Biol Chem.* 273:29451-61.
- Lechler, T., and E. Fuchs. 2007. Desmoplakin: an unexpected regulator of microtubule organization in the epidermis. *J Cell Biol.* 176:147-54.
- Lee, J.M., S. Dedhar, R. Kalluri, and E.W. Thompson. 2006. The epithelial-mesenchymal transition: new insights in signaling, development, and disease. *J Cell Biol.* 172:973-81.
- Lemieux, P., S. Oesterreich, J.A. Lawrence, P.S. Steeg, S.G. Hilsenbeck, J.M. Harvey, and S.A. Fuqua. 1997. The small heat shock protein hsp27 increases invasiveness but decreases motility of breast cancer cells. *Invasion Metastasis.* 17:113-23.
- Lesniewicz, K., J. Luscher-Firzlaff, E. Poreba, P. Fuchs, G. Walsemann, G. Wiche, and B. Luscher. 2005. Overlap of the gene encoding the novel poly(ADP-ribose) polymerase Parp10 with the plectin 1 gene and common use of exon sequences. *Genomics.* 86:38-46.
- Leung, C.L., K.J. Green, and R.K. Liem. 2002. Plakins: a family of versatile cytolinker proteins. *Trends Cell Biol.* 12:37-45.
- Leung, C.L., R.K. Liem, D.A. Parry, and K.J. Green. 2001. The plakin family. *J Cell Sci.* 114:3409-10.
- Leung, C.L., D. Sun, M. Zheng, D.R. Knowles, and R.K. Liem. 1999. Microtubule actin cross-linking factor (MACF): a hybrid of dystonin and dystrophin that can interact with the actin and microtubule cytoskeletons. *J Cell Biol.* 147:1275-86.

- Li, K., G.J. Guidice, K. Tamai, H.C. Do, D. Sawamura, L.A. Diaz, and J. Uitto. 1992. Cloning of partial cDNA for mouse 180-kDa bullous pemphigoid antigen (BPAG2), a highly conserved collagenous protein of the cutaneous basement membrane zone. *J Invest Dermatol.* 99:258-63.
- Lie, A.A., R. Schroder, I. Blumcke, T.M. Magin, O.D. Wiestler, and C.E. Elger. 1998. Plectin in the human central nervous system: predominant expression at pia/glia and endothelia/glia interfaces. *Acta Neuropathol (Berl).* 96:215-21.
- Lin, C.M., H.J. Chen, C.L. Leung, D.A. Parry, and R.K. Liem. 2005. Microtubule actin crosslinking factor 1b: a novel plakin that localizes to the Golgi complex. *J Cell Sci.* 118:3727-38.
- Linder, S. 2007. The matrix corroded: podosomes and invadopodia in extracellular matrix degradation. *Trends Cell Biol.* 17:107-17.
- Linder, S., and M. Aepfelbacher. 2003. Podosomes: adhesion hot-spots of invasive cells. *Trends Cell Biol.* 13:376-85.
- Linder, S., D. Nelson, M. Weiss, and M. Aepfelbacher. 1999. Wiskott-Aldrich syndrome protein regulates podosomes in primary human macrophages. *Proc Natl Acad Sci U S A.* 96:9648-53.
- Litjens, S.H., J.M. de Pereda, and A. Sonnenberg. 2006. Current insights into the formation and breakdown of hemidesmosomes. *Trends Cell Biol.* 16:376-83.
- Litjens, S.H., J. Koster, I. Kuikman, S. van Wilpe, J.M. de Pereda, and A. Sonnenberg. 2003. Specificity of binding of the plectin actin-binding domain to beta4 integrin. *Mol Biol Cell.* 14:4039-50.
- Litjens, S.H., K. Wilhelmsen, J.M. de Pereda, A. Perrakis, and A. Sonnenberg. 2005. Modeling and experimental validation of the binary complex of the plectin actin-binding domain and the first pair of fibronectin type III (FNIII) domains of the beta4 integrin. *J Biol Chem.* 280:22270-7.
- Liu, C.G., C. Maercker, M.J. Castanon, R. Hauptmann, and G. Wiche. 1996. Human plectin: organization of the gene, sequence analysis, and chromosome localization (8q24). *Proc Natl Acad Sci U S A.* 93:4278-83.
- Long, H.A., V. Boczonadi, L. McInroy, M. Goldberg, and A. Maatta. 2006. Periplakin-dependent re-organisation of keratin cytoskeleton and loss of collective migration in keratin-8-downregulated epithelial sheets. *J Cell Sci.* 119:5147-59.
- Loranger, A., S. Gilbert, J.S. Brouard, T.M. Magin, and N. Marceau. 2006. Keratin 8 modulation of desmoplakin deposition at desmosomes in hepatocytes. *Exp Cell Res.* 312:4108-19.
- Lorenz, M., H. Yamaguchi, Y. Wang, R.H. Singer, and J. Condeelis. 2004. Imaging sites of N-wasp activity in lamellipodia and invadopodia of carcinoma cells. *Curr Biol.* 14:697-703.

Lotz, M.M., I. Rabinovitz, and A.M. Mercurio. 2000. Intestinal restitution: progression of actin cytoskeleton rearrangements and integrin function in a model of epithelial wound healing. *Am J Pathol.* 156:985-96.

Lunter, P.C., and G. Wiche. 2002. Direct binding of plectin to Fer kinase and negative regulation of its catalytic activity. *Biochem Biophys Res Commun.* 296:904-10.

Lyons, A.J., and J. Jones. 2007. Cell adhesion molecules, the extracellular matrix and oral squamous carcinoma. *Int J Oral Maxillofac Surg.* 36:671-9.

Maatta, A., T. DiColandrea, K. Groot, and F.M. Watt. 2001. Gene targeting of envoplakin, a cytoskeletal linker protein and precursor of the epidermal cornified envelope. *Mol Cell Biol.* 21:7047-53.

Maatta, A., C.J. Hutchison, and M.D. Watson. 2004. Spectraplakins and nesprins, giant spectrin repeat proteins participating in the organization of the cytoskeleton and the nuclear envelope. *Symp Soc Exp Biol:*265-77.

Machesky, L.M., and Gould, K.L. 1999. The Arp2/3 complex: a multifunctional actin organizer. *Curr. Opin. Cell Biol.* 11:117-121
Magin, T.M., P.

Mandelkow, E., and E.M. Mandelkow. 1995. Microtubules and microtubule-associated proteins. *Curr Opin Cell Biol.* 7:72-81.

Manton, I., and Clarke, R. 1952. An electron microscopy study of the spermatozoid of sphagnum. *J. Exp. Bot.* 3 pp. 265-275.

Mercurio, A.M., I. Rabinovitz, and L.M. Shaw. 2001. The alpha 6 beta 4 integrin and epithelial cell migration. *Curr Opin Cell Biol.* 13:541-5.

Mareel, M., K. Vleminckx, S. Vermeulen, M. Bracke, and F. Van Roy. 1992. E-cadherin expression: a counterbalance for cancer cell invasion. *Bull Cancer.* 79:347-55.

Mareel, M., K. Vleminckx, S. Vermeulen, G. Yan, M. Bracke, and F. van Roy. 1994. Downregulation in vivo of the invasion-suppressor molecule E-cadherin in experimental and clinical cancer. *Princess Takamatsu Symp.* 24:63-80.

Mareel, M.M., and R. Crombez. 1992. Biology of cancer invasion and metastasis. *Acta Otorhinolaryngol Belg.* 46:107-15.

Marekov, L.N., and P.M. Steinert. 1998. Ceramides are bound to structural proteins of the human foreskin epidermal cornified cell envelope. *J Biol Chem.* 273:17763-70.

Marinkovich, M.P., G.P. Lunstrum, D.R. Keene, and R.E. Burgeson. 1992. The dermal-epidermal junction of human skin contains a novel laminin variant. *J Cell Biol.* 119:695-703.

- Martys, J.L., C.L. Ho, R.K. Liem, and G.G. Gundersen. 1999. Intermediate filaments in motion: observations of intermediate filaments in cells using green fluorescent protein-vimentin. *Mol Biol Cell*. 10:1289-95.
- McInroy, L., and A. Maatta. 2007. Down-regulation of vimentin expression inhibits carcinoma cell migration and adhesion. *Biochem Biophys Res Commun*.
- McIntosh, J.R., E.L. Grishchuk, and R.R. West. 2002. Chromosome-microtubule interactions during mitosis. *Annu Rev Cell Dev Biol*. 18:193-219.
- McLean, W.H., L. Pulkkinen, F.J. Smith, E.L. Rugg, E.B. Lane, F. Bullrich, R.E. Burgeson, S. Amano, D.L. Hudson, K. Owaribe, J.A. McGrath, J.R. McMillan, R.A. Eady, I.M. Leigh, A.M. Christiano, and J. Uitto. 1996. Loss of plectin causes epidermolysis bullosa with muscular dystrophy: cDNA cloning and genomic organization. *Genes Dev*. 10:1724-35.
- Mejillano, M.R., S. Kojima, D.A. Applewhite, F.B. Gertler, T.M. Svitkina, and G.G. Borisy. 2004. Lamellipodial versus filopodial mode of the actin nanomachinery: pivotal role of the filament barbed end. *Cell*. 118:363-73.
- Mese, G., Richard, G. and White, T. 2007. Gap junctions: basic structure and function. *J Invest Dermatol* 127:25162524/
- Minard, M.E., L.M. Ellis, and G.E. Gallick. 2006. Tiam1 regulates cell adhesion, migration and apoptosis in colon tumor cells. *Clin Exp Metastasis*. 23:301-13.
- Mitchison, T., and M. Kirschner. 1984. Dynamic instability of microtubule growth. *Nature*. 312:237-42.
- Mizutani, K., H. Miki, H. He, H. Maruta, and T. Takenawa. 2002. Essential role of neural Wiskott-Aldrich syndrome protein in podosome formation and degradation of extracellular matrix in src-transformed fibroblasts. *Cancer Res*. 62:669-74.
- Morino, M., T. Tsuzuki, Y. Ishikawa, T. Shirakami, M. Yoshimura, Y. Kiyosuke, K. Matsunaga, C. Yoshikumi, and N. Saijo. 1997. Specific expression of HSP27 in human tumor cell lines in vitro. *In Vivo*. 11:179-84.
- Mullins, R.D., Heuser, J.A., and Pollard, T.D. 1998. The interaction of Arp2/3 complex with actin: nucleation, high affinity pointed end capping, and formation of branching networks of filaments. *Proc. Natl. Acad. Sci. USA*. 95:6181-6186
- Ngan, C.Y., H. Yamamoto, I. Seshimo, T. Tsujino, M. Man-i, J.I. Ikeda, K. Konishi, I. Takemasa, M. Ikeda, M. Sekimoto, N. Matsuura, and M. Monden. 2007. Quantitative evaluation of vimentin expression in tumour stroma of colorectal cancer. *Br J Cancer*. 96:986-92.
- Niessen, C.M., F. Hogervorst, L.H. Jaspars, A.A. de Melker, G.O. Delwel, E.H. Hulsman, I. Kuikman, and A. Sonnenberg. 1994. The alpha 6 beta 4 integrin is a receptor for both laminin and kalinin. *Exp Cell Res*. 211:360-7.

Niessen, C.M., E.H. Hulsman, L.C. Oomen, I. Kuikman, and A. Sonnenberg. 1997. A minimal region on the integrin beta4 subunit that is critical to its localization in hemidesmosomes regulates the distribution of HD1/plectin in COS-7 cells. *J Cell Sci.* 110 (Pt 15):1705-16.

Nikolic, B., E. Mac Nulty, B. Mir, and G. Wiche. 1996. Basic amino acid residue cluster within nuclear targeting sequence motif is essential for cytoplasmic plectin-vimentin network junctions. *J Cell Biol.* 134:1455-67.

Nishizawa, M., I. Izawa, A. Inoko, Y. Hayashi, K. Nagata, T. Yokoyama, J. Usukura, and M. Inagaki. 2005. Identification of trichoplein, a novel keratin filament-binding protein. *J Cell Sci.* 118:1081-90.

Nishizawa, Y., J. Uematsu, and K. Owaribe. 1993. HD4, a 180 kDa bullous pemphigoid antigen, is a major transmembrane glycoprotein of the hemidesmosome. *J Biochem (Tokyo).* 113:493-501.

Norgett, E.E., S.J. Hatsell, L. Carvajal-Huerta, J.C. Cabezas, J. Common, P.E. Purkis, N. Whittock, I.M. Leigh, H.P. Stevens, and D.P. Kelsell. 2000. Recessive mutation in desmoplakin disrupts desmoplakin-intermediate filament interactions and causes dilated cardiomyopathy, woolly hair and keratoderma. *Hum Mol Genet.* 9:2761-6.

Ochoa, G.C., V.I. Slepnev, L. Neff, N. Ringstad, K. Takei, L. Daniell, W. Kim, H. Cao, M. McNiven, R. Baron, and P. De Camilli. 2000. A functional link between dynamin and the actin cytoskeleton at podosomes. *J Cell Biol.* 150:377-89.

O'Keefe, E.J., H.P. Erickson, and V. Bennett. 1989. Desmoplakin I and desmoplakin II. Purification and characterization. *J Biol Chem.* 264:8310-8.

Okuda, T., S. Matsuda, S. Nakatsugawa, Y. Ichigotani, N. Iwahashi, M. Takahashi, T. Ishigaki, and M. Hamaguchi. 1999. Molecular cloning of macrophin, a human homologue of *Drosophila kakapo* with a close structural similarity to plectin and dystrophin. *Biochem Biophys Res Commun.* 264:568-74.

Okumura M, Uematsu J, Hirako Y, Nishizawa Y, Shimizu H, Kido N, Owaribe K. 1999. Identification of the hemidesmosomal 500 kDa protein (HD1) as plectin. *J Biochem (Tokyo).* Dec;126(6):1144-50.

Orian-Rousseau, V., D. Aberdam, L. Fontao, L. Chevalier, G. Meneguzzi, M. Kedinger, and P. Simon-Assmann. 1996. Developmental expression of laminin-5 and HD1 in the intestine: epithelial to mesenchymal shift for the laminin gamma-2 chain subunit deposition. *Dev Dyn.* 206:12-23.

Oshima, R.G. 2007. Intermediate filaments: a historical perspective. *Exp Cell Res.* 313:1981-94.

Osiak, A.E., G. Zenner, and S. Linder. 2005. Subconfluent endothelial cells form podosomes downstream of cytokine and RhoGTPase signaling. *Exp Cell Res.* 307:342-53.

Osmanagic-Myers, S., M. Gregor, G. Walko, G. Burgstaller, S. Reipert, and G. Wiche. 2006. Plectin-controlled keratin cytoarchitecture affects MAP kinases involved in cellular stress response and migration. *J Cell Biol.* 174:557-68.

Osmanagic-Myers, S., and G. Wiche. 2004. Plectin-RACK1 (receptor for activated C kinase 1) scaffolding: a novel mechanism to regulate protein kinase C activity. *J Biol Chem.* 279:18701-10.

O'Toole, E.A. 2001. Extracellular matrix and keratinocyte migration. *Clinical and experimental dermatology.* 26:525-530.

O'Toole, E.A., Marinkovich, M.P., Warren, K., Hoeffler, K., Furthmayr, H., Woodley, D.T. 1997. Laminin-5 inhibits human keratinocyte migration. *Exp. Cell Res.* 233:330-339.

Owaribe K., Y. Nishizawa, and W. W. Franke. 1991. Isolation and characterization of hemidesmosomes from bovine corneal epithelial cells. *Exp. Cell Res.* 192:622-630.

Pankov, R., E. Cukierman, B.Z. Katz, K. Matsumoto, D.C. Lin, S. Lin, C. Hahn, and K.M. Yamada. 2000. Integrin dynamics and matrix assembly: tensin-dependent translocation of alpha(5)beta(1) integrins promotes early fibronectin fibrillogenesis. *J Cell Biol.* 148:1075-90.

Perez-Moreno, M., C. Jamora, and E. Fuchs. 2003. Sticky business: orchestrating cellular signals at adherens junctions. *Cell.* 112:535-48.

Pfendner, E., F. Rouan, and J. Uitto. 2005. Progress in epidermolysis bullosa: the phenotypic spectrum of plectin mutations. *Exp Dermatol.* 14:241-9.

Prout, M., Z. Damania, J. Soong, D. Fristrom, and J.W. Fristrom. 1997. Autosomal mutations affecting adhesion between wing surfaces in *Drosophila melanogaster*. *Genetics.* 146:275-85.

Pytela, R., and G. Wiche. 1980. High molecular weight polypeptides (270,000-340,000) from cultured cells are related to hog brain microtubule-associated proteins but copurify with intermediate filaments. *Proc Natl Acad Sci U S A.* 77:4808-12.

Rabinovitz, I., A. Toker, and A.M. Mercurio. 1999. Protein kinase C-dependent mobilization of the alpha6beta4 integrin from hemidesmosomes and its association with actin-rich cell protrusions drive the chemotactic migration of carcinoma cells. *J Cell Biol.* 146:1147-60.

Rash, J.E., J.W. Shay, and J.J. Biesele. 1970. Preliminary biochemical investigations of the intermediate filaments. *J Ultrastruct Res.* 33:399-407.

Raymond, K., M. Kreft, J.Y. Song, H. Janssen, and A. Sonnenberg. 2007. Dual Role of {alpha}6{beta}4 Integrin in Epidermal Tumor Growth: Tumor-suppressive Versus Tumor-promoting Function. *Mol Biol Cell.*

Reimann, J., W.S. Kunz, S. Vielhaber, K. Kappes-Horn, and R. Schroder. 2003. Mitochondrial dysfunction in myofibrillar myopathy. *Neuropathol Appl Neurobiol.* 29:45-51.

Reipert, S., F. Steinbock, I. Fischer, R.E. Bittner, A. Zeold, and G. Wiche. 1999. Association of mitochondria with plectin and desmin intermediate filaments in striated muscle. *Exp Cell Res.* 252:479-91.

Rezniczek, G.A., C. Abrahamsberg, P. Fuchs, D. Spazierer, and G. Wiche. 2003. Plectin 5'-transcript diversity: short alternative sequences determine stability of gene products, initiation of translation and subcellular localization of isoforms. *Hum Mol Genet.* 12:3181-94.

Rezniczek, G.A., J.M. de Pereda, S. Reipert, and G. Wiche. 1998. Linking integrin alpha6beta4-based cell adhesion to the intermediate filament cytoskeleton: direct interaction between the beta4 subunit and plectin at multiple molecular sites. *J Cell Biol.* 141:209-25.

Rezniczek, G.A., L. Janda, and G. Wiche. 2004. Plectin. *Methods Cell Biol.* 78:721-55.

Roper, K., and N.H. Brown. 2003. Maintaining epithelial integrity: a function for gigantic spectraplakins in adherens junctions. *J Cell Biol.* 162:1305-15.

Roth, A.L., and D.K. Berg. 2003. Large clusters of alpha7-containing nicotinic acetylcholine receptors on chick spinal cord neurons. *J Comp Neurol.* 465:195-204.

Rouan, F., L. Pulkkinen, G. Meneguzzi, S. Laforgia, P. Hyde, D.U. Kim, G. Richard, and J. Uitto. 2000. Epidermolysis bullosa: novel and de novo premature termination codon and deletion mutations in the plectin gene predict late-onset muscular dystrophy. *J Invest Dermatol.* 114:381-7.

Ruhrberg, C., Hajibagheri, M.A., Simon, M., Dooley, T.P., Watt, F.M. 1996. Envoplakin a novel precursor of the cornified envelope that has homology to desmoplakin. *J Cell Biol* 134(3):715-29.

Ruhrberg, C., Hajibagheri, M.A., Parry, D.A., Watt, F.M., Periplakin a novel component of cornified envelopes and desmosomes that belongs to the plakin family and forms complexes with envoplakin *J Cell Biol* 29:139(7)1835-49.

Ruhrberg, C., and F.M. Watt. 1997. The plakin family: versatile organizers of cytoskeletal architecture. *Curr Opin Genet Dev.* 7:392-7.

Sabeh, F., I. Ota, K. Holmbeck, H. Birkedal-Hansen, P. Soloway, M. Balbin, C. Lopez-Otin, S. Shapiro, M. Inada, S. Krane, E. Allen, D. Chung, and S.J. Weiss. 2004. Tumor cell traffic through the extracellular matrix is controlled by the membrane-anchored collagenase MT1-MMP. *J Cell Biol.* 167:769-81.

Sahai, E. and Marshall C.J. 2003. Differing modes of tumour cell invasion have distinct requirements for Rho/ROCK signalling and extracellular proteolysis. *Nat Cell Biol.* Aug 5(8):690-2.

Sahai, E. 2005. Mechanisms of cancer cell invasion. *Curr Opin Genet Dev.* 15:87-96.

Sanchez-Aparicio, P., A.M. Martinez de Velasco, C.M. Niessen, L. Borradori, I. Kuikman, E.H. Hulsman, R. Fassler, K. Owaribe, and A. Sonnenberg. 1997. The subcellular distribution of the high molecular mass protein, HD1, is determined by the cytoplasmic domain of the integrin beta 4 subunit. *J Cell Sci.* 110 (Pt 2):169-78.

Sawin, K.E., and S.A. Endow. 1993. Meiosis, mitosis and microtubule motors. *Bioessays.* 15:399-407.

Schaapveld, R.Q., L. Borradori, D. Geerts, M.R. van Leusden, I. Kuikman, M.G. Nievers, C.M. Niessen, R.D. Steenbergen, P.J. Sniijders, and A. Sonnenberg. 1998. Hemidesmosome formation is initiated by the beta4 integrin subunit, requires complex formation of beta4 and HD1/plectin, and involves a direct interaction between beta4 and the bullous pemphigoid antigen 180. *J Cell Biol.* 142:271-84.

Schaapveld, R. Q., Herrmann, H., Schultess, J., Markl, J., 2001. Vimentin and desmin of a cartilaginous fish, the shark *Scyliorhinus stellaris*: sequence, expression patterns and in vitro assembly. *Eur. J. Cell Biol.* 80:692-702

Schmelz, M., R. Moll, C. Kuhn, and W.W. Franke. 1994. Complexus adhaerentes, a new group of desmoplakin-containing junctions in endothelial cells: II. Different types of lymphatic vessels. *Differentiation.* 57:97-117.

Schmidt, A., and M.N. Hall. 1998. Signaling to the actin cytoskeleton. *Annu Rev Cell Dev Biol.* 14:305-38.

Schmidt, A., and S. Jager. 2005. Plakophilins--hard work in the desmosome, recreation in the nucleus? *Eur J Cell Biol.* 84:189-204.

Schroder, R., B. Goudeau, M.C. Simon, D. Fischer, T. Eggermann, C.S. Clemen, Z. Li, J. Reimann, Z. Xue, S. Rudnik-Schoneborn, K. Zerres, P.F. van der Ven, D.O. Furst, W.S. Kunz, and P. Vicart. 2003. On noxious desmin: functional effects of a novel heterozygous desmin insertion mutation on the extrasarcomeric desmin cytoskeleton and mitochondria. *Hum Mol Genet.* 12:657-69.

Schroder, R., W.S. Kunz, F. Rouan, E. Pfendner, K. Tolksdorf, K. Kappes-Horn, M. Altenschmidt-Mehring, R. Knoblich, P.F. van der Ven, J. Reimann, D.O. Furst, I. Blumcke, S. Vielhaber, D. Zillikens, S. Eming, T. Klockgether, J. Uitto, G. Wiche, and A. Rolfs. 2002. Disorganization of the desmin cytoskeleton and mitochondrial dysfunction in plectin-related epidermolysis bullosa simplex with muscular dystrophy. *J Neuropathol Exp Neurol.* 61:520-30.

Schroder, R., I. Warlo, H. Herrmann, P.F. van der Ven, C. Klasen, I. Blumcke, R.R. Mundegar, D.O. Furst, H.H. Goebel, and T.M. Magin. 1999. Immunogold EM reveals a close association of plectin and the desmin cytoskeleton in human skeletal muscle. *Eur J Cell Biol.* 78:288-95.

Schweizer, J., P.E. Bowden, P.A. Coulombe, L. Langbein, E.B. Lane, T.M. Magin, L. Maltais, M.B. Omary, D.A. Parry, M.A. Rogers, and M.W. Wright. 2006. New consensus nomenclature for mammalian keratins. *J Cell Biol.* 174:169-74.

Schwende, H., E. Fitzke, P. Ambs, and P. Dieter. 1996. Differences in the state of differentiation of THP-1 cells induced by phorbol ester and 1,25-dihydroxyvitamin D3. *J Leukoc Biol.* 59:555-61.

Seals, D.F., E.F. Azucena, Jr., I. Pass, L. Tesfay, R. Gordon, M. Woodrow, J.H. Resau, and S.A. Courtneidge. 2005. The adaptor protein Tks5/Fish is required for podosome formation and function, and for the protease-driven invasion of cancer cells. *Cancer Cell.* 7:155-65.

Seifert, G.J., D. Lawson, and G. Wiche. 1992. Immunolocalization of the intermediate filament-associated protein plectin at focal contacts and actin stress fibers. *Eur J Cell Biol.* 59:138-47.

Sevcik, J., L. Urbanikova, J. Kost'an, L. Janda, and G. Wiche. 2004. Actin-binding domain of mouse plectin. Crystal structure and binding to vimentin. *Eur J Biochem.* 271:1873-84.

Simon, M., and H. Green. 1984. Participation of membrane-associated proteins in the formation of the cross-linked envelope of the keratinocyte. *Cell.* 36:827-34.

Simon-Assmann, P., B. Duclos, V. Orian-Rousseau, C. Arnold, C. Mathelin, E. Engvall, and M. Kedinger. 1994. Differential expression of laminin isoforms and alpha 6-beta 4 integrin subunits in the developing human and mouse intestine. *Dev Dyn.* 201:71-85.

Simon-Assmann, P., C. Leberquier, N. Molto, T. Uezato, F. Bouziges, and M. Kedinger. 1994. Adhesive properties and integrin expression profiles of two colonic cancer populations differing by their spreading on laminin. *J Cell Sci.* 107 (Pt 3):577-87.

Singh, S., S. Sadacharan, S. Su, A. Belldegrun, S. Persad, and G. Singh. 2003. Overexpression of vimentin: role in the invasive phenotype in an androgen-independent model of prostate cancer. *Cancer Res.* 63:2306-11.

Sjoblom, T., S. Jones, L.D. Wood, D.W. Parsons, J. Lin, T.D. Barber, D. Mandelker, R.J. Leary, J. Ptak, N. Silliman, S. Szabo, P. Buckhaults, C. Farrell, P. Meeh, S.D. Markowitz, J. Willis, D. Dawson, J.K. Willson, A.F. Gazdar, J. Hartigan, L. Wu, C. Liu, G. Parmigiani, B.H. Park, K.E. Bachman, N. Papadopoulos, B. Vogelstein, K.W. Kinzler, and V.E. Velculescu. 2006. The consensus coding sequences of human breast and colorectal cancers. *Science.* 314:268-74.

Skerrow, C.J., and A.G. Matoltsy. 1974. Isolation of epidermal desmosomes. *J Cell Biol.* 63:515-23.

Skerrow, C.J., and A.G. Matoltsy. 1974. Chemical characterization of isolated epidermal desmosomes. *J Cell Biol.* 63:524-30.

Small, J.V. 1995. Getting the actin filaments straight: nucleation-release or treadmilling? *Trends Cell Biol.* 5:52-5.

Small, J.V., M. Herzog, and K. Anderson. 1995. Actin filament organization in the fish keratocyte lamellipodium. *J Cell Biol.* 129:1275-86.

Smith, F.J., Eady, R.A., Leigh, I.M., McMillian, J.R., Rugg, E.L., Kellsell, D.P., Bryant, S.P., Spurr, N.K., Geddes, J.F., Kirtschig, G., Milana, G., deBono, A.G., Wiche, G., Pulkkinen, L., Uitto, J., McLean, W.H., Lane, E.B., 1996. Plectin deficiency results in muscular dystrophy with epidermolysis bullosa. *Nat Genet.* 13:450-457

Sonnenberg, A., J. Calafat, H. Janssen, H. Daams, L.M. van der Raaij-Helmer, R. Falcioni, S.J. Kennel, J.D. Aplin, J. Baker, M. Loizidou, and et al. 1991. Integrin alpha 6/beta 4 complex is located in hemidesmosomes, suggesting a major role in epidermal cell-basement membrane adhesion. *J Cell Biol.* 113:907-17.

Sonnenberg, A., and R.K. Liem. 2007. Plakins in development and disease. *Exp Cell Res.* 313:2189-203.

Sonnenberg, A., A.M. Rojas, and J.M. de Pereda. 2007. The structure of a tandem pair of spectrin repeats of plectin reveals a modular organization of the plakin domain. *J Mol Biol.* 368:1379-91.

Spazierer, D., P. Fuchs, V. Proll, L. Janda, S. Oehler, I. Fischer, R. Hauptmann, and G. Wiche. 2003. Epiplakin gene analysis in mouse reveals a single exon encoding a 725-kDa protein with expression restricted to epithelial tissues. *J Biol Chem.* 278:31657-66.

Spazierer, D., P. Fuchs, S. Reipert, I. Fischer, M. Schmuth, H. Lassmann, and G. Wiche. 2006. Epiplakin is dispensable for skin barrier function and for integrity of keratin network cytoarchitecture in simple and stratified epithelia. *Mol Cell Biol.* 26:559-68.

Spinardi, L., Y.L. Ren, R. Sanders, and F.G. Giancotti. 1993. The beta 4 subunit cytoplasmic domain mediates the interaction of alpha 6 beta 4 integrin with the cytoskeleton of hemidesmosomes. *Mol Biol Cell.* 4:871-84.

Spinardi, L., J. Rietdorf, L. Nitsch, M. Bono, C. Tacchetti, M. Way, and P.C. Marchisio. 2004. A dynamic podosome-like structure of epithelial cells. *Exp Cell Res.* 295:360-74.

- Stanley, J.R., P. Hawley-Nelson, S.H. Yuspa, E.M. Shevach, and S.I. Katz. 1981. Characterization of bullous pemphigoid antigen: a unique basement membrane protein of stratified squamous epithelia. *Cell*. 24:897-903.
- Stanley, J.R., T. Tanaka, S. Mueller, V. Klaus-Kovtun, and D. Roop. 1988. Isolation of complementary DNA for bullous pemphigoid antigen by use of patients' autoantibodies. *J Clin Invest*. 82:1864-70.
- Stappenbeck, T.S., J.A. Lamb, C.M. Corcoran, and K.J. Green. 1994. Phosphorylation of the desmoplakin COOH terminus negatively regulates its interaction with keratin intermediate filament networks. *J Biol Chem*. 269:29351-4.
- Stegh, A.H., H. Herrmann, S. Lampel, D. Weisenberger, K. Andra, M. Seper, G. Wiche, P.H. Krammer, and M.E. Peter. 2000. Identification of the cytolinker plectin as a major early in vivo substrate for caspase 8 during CD95- and tumor necrosis factor receptor-mediated apoptosis. *Mol Cell Biol*. 20:5665-79.
- Steinboeck, F., and D. Kristufek. 2005. Identification of the cytolinker protein plectin in neuronal cells - expression of a rodless isoform in neurons of the rat superior cervical ganglion. *Cell Mol Neurobiol*. 25:1151-69.
- Sterk, L.M., C.A. Geuijen, L.C. Oomen, J. Calafat, H. Janssen, and A. Sonnenberg. 2000. The tetraspan molecule CD151, a novel constituent of hemidesmosomes, associates with the integrin alpha6beta4 and may regulate the spatial organization of hemidesmosomes. *J Cell Biol*. 149:969-82.
- Stossel, T.P. 1993. On the crawling of animal cells. *Science*. 260:1086-94.
- Stradal, T., W. Kranewitter, S.J. Winder, and M. Gimona. 1998. CH domains revisited. *FEBS Lett*. 431:134-7.
- Strelkov, S.V., H. Herrmann, and U. Aebi. 2003. Molecular architecture of intermediate filaments. *Bioessays*. 25:243-51.
- Sun, D., C.L. Leung, and R.K. Liem. 2001. Characterization of the microtubule binding domain of microtubule actin crosslinking factor (MACF): identification of a novel group of microtubule associated proteins. *J Cell Sci*. 114:161-172.
- Sun, Y., J. Zhang, S.K. Kraeft, D. Auclair, M.S. Chang, Y. Liu, R. Sutherland, R. Salgia, J.D. Griffin, L.H. Ferland, and L.B. Chen. 1999. Molecular cloning and characterization of human trabeculin-alpha, a giant protein defining a new family of actin-binding proteins. *J Biol Chem*. 274:33522-30.
- Suzuki, S., Z.S. Huang, and H. Tanihara. 1990. Cloning of an integrin beta subunit exhibiting high homology with integrin beta 3 subunit. *Proc Natl Acad Sci U S A*. 87:5354-8.
- Suzuki, S., and Y. Naitoh. 1990. Amino acid sequence of a novel integrin beta 4 subunit and primary expression of the mRNA in epithelial cells. *Embo J*. 9:757-63.

Svitkina, T.M., and G.G. Borisy. 1999. Arp2/3 complex and actin depolymerizing factor/cofilin in dendritic organization and treadmilling of actin filament array in lamellipodia. *J Cell Biol.* 145:1009-26.

Svitkina, T.M., A.B. Verkhovsky, and G.G. Borisy. 1996. Plectin sidearms mediate interaction of intermediate filaments with microtubules and other components of the cytoskeleton. *J Cell Biol.* 135:991-1007.

Szent-Gyorgyi, A.G. 2004. The early history of the biochemistry of muscle contraction. *J Gen Physiol.* 123:631-41.

Takeichi, M. 1991. Cadherin cell adhesion receptors as a morphogenetic regulator. *Science.* 251:1451-5.

Tatin, F., C. Varon, E. Genot, and V. Moreau. 2006. A signalling cascade involving PKC, Src and Cdc42 regulates podosome assembly in cultured endothelial cells in response to phorbol ester. *J Cell Sci.* 119:769-81.

Tennenbaum, T., A.K. Weiner, A.J. Belanger, A.B. Glick, H. Hennings, and S.H. Yuspa. 1993. The suprabasal expression of alpha 6 beta 4 integrin is associated with a high risk for malignant progression in mouse skin carcinogenesis. *Cancer Res.* 53:4803-10.

Tian, R., M. Gregor, G. Wiche, and J.E. Goldman. 2006. Plectin regulates the organization of glial fibrillary acidic protein in Alexander disease. *Am J Pathol.* 168:888-97.

Towbin, H., T. Staehelin, and J. Gordon. 1979. Electrophoretic transfer of proteins from polyacrylamide gels to nitrocellulose sheets: procedure and some applications. *Proc Natl Acad Sci U S A.* 76:4350-4.

Tsuboi, S. 2007. Requirement for a complex of Wiskott-Aldrich syndrome protein (WASP) with WASP interacting protein in podosome formation in macrophages. *J Immunol.* 178:2987-95.

Tsuruta, D., and J.C. Jones. 2003. The vimentin cytoskeleton regulates focal contact size and adhesion of endothelial cells subjected to shear stress. *J Cell Sci.* 116:4977-84.

Tucker, J. 1992. The microtubule-organizing center. *Bioessays.* 14:861-7.

Uematsu, J., Y. Nishizawa, A. Sonnenberg, and K. Owaribe. 1994. Demonstration of type II hemidesmosomes in a mammary gland epithelial cell line, BMGE-H. *J Biochem (Tokyo).* 115:469-76.

Uitto, J., and L. Pulkkinen. 1996. Molecular complexity of the cutaneous basement membrane zone. *Mol Biol Rep.* 23:35-46.

Uitto, J., G. Richard, and J.A. McGrath. 2007. Diseases of epidermal keratins and their linker proteins. *Exp Cell Res.* 313:1995-2009.

- Valster, A., N.L. Tran, M. Nakada, M.E. Berens, A.Y. Chan, and M. Symons. 2005. Cell migration and invasion assays. *Methods*. 37:208-15.
- van den Heuvel, A.P., A.M. de Vries-Smits, P.C. van Weeren, P.F. Dijkers, K.M. de Bruyn, J.A. Riedl, and B.M. Burgering. 2002. Binding of protein kinase B to the plakin family member periplakin. *J Cell Sci*. 115:3957-66.
- Van Waes, C. 1995. Cell adhesion and regulatory molecules involved in tumor formation, hemostasis, and wound healing. *Head Neck*. 17:140-7.
- Van Waes, C., D.M. Surh, Z. Chen, M. Kirby, J.S. Rhim, R. Brager, R.B. Sessions, J. Poore, G.T. Wolf, and T.E. Carey. 1995. Increase in suprabasilar integrin adhesion molecule expression in human epidermal neoplasms accompanies increased proliferation occurring with immortalization and tumor progression. *Cancer Res*. 55:5434-44.
- Vasiliev, J.M. 2004. Cytoskeletal mechanisms responsible for invasive migration of neoplastic cells. *Int J Dev Biol*. 48:425-39.
- Vasiliev, J.M., T. Omelchenko, I.M. Gelfand, H.H. Feder, and E.M. Bonder. 2004. Rho overexpression leads to mitosis-associated detachment of cells from epithelial sheets: a link to the mechanism of cancer dissemination. *Proc Natl Acad Sci U S A*.
- Vasioukhin, V., C. Bauer, L. Degenstein, B. Wise, and E. Fuchs. 2001. Hyperproliferation and defects in epithelial polarity upon conditional ablation of alpha-catenin in skin. *Cell*. 104:605-17.
- Vikstrom, K.L., G.G. Borisy, and R.D. Goldman. 1989. Dynamic aspects of intermediate filament networks in BHK-21 cells. *Proc Natl Acad Sci U S A*. 86:549-53.
- Vita, G., M.C. Monici, K. Owaribe, and C. Messina. 2003. Expression of plectin in muscle fibers with cytoarchitectural abnormalities. *Neuromuscul Disord*. 13:485-92.
- Vijayaraj, and R.E. Leube. 2007. Structural and regulatory functions of keratins. *Exp Cell Res*. 313:2021-32.
101:12526-30.
- Walsh, E.P., and N.H. Brown. 1998. A screen to identify *Drosophila* genes required for integrin-mediated adhesion. *Genetics*. 150:791-805.
- Waterman-Storer, C.M., and E.D. Salmon. 1997. Actomyosin-based retrograde flow of microtubules in the lamella of migrating epithelial cells influences microtubule dynamic instability and turnover and is associated with microtubule breakage and treadmilling. *J Cell Biol*. 139:417-34.
- Waterman-Storer, C.M., and E.D. Salmon. 1997. Microtubule dynamics: treadmilling comes around again. *Curr Biol*. 7:R369-72.

- Webb, B.A., R. Eves, and A.S. Mak. 2006. Cortactin regulates podosome formation: roles of the protein interaction domains. *Exp Cell Res.* 312:760-9.
- Webb, D.J., J.T. Parsons, and A.F. Horwitz. 2002. Adhesion assembly, disassembly and turnover in migrating cells -- over and over and over again. *Nat Cell Biol.* 4:E97-100.
- Weed, S.A., Karginov, A.V., Schafer, D.A., Weaver, A.M., Kinley, A.W., Cooper, J.A. and Parsons, J.T. 2000. Cortactin localization to sites of actin assembly in lamellipodia requires interactions with F-actin and the Arp2/3 complex. *J Cell Biol.* 2;151(1):29-40.
- Weiss, P., and W. Ferris. 1954. Electronmicrograms of larval amphibian epidermis. *Exp Cell Res.* 6:546-9.
- Weiss, P., and W. Ferris. 1954. Electron-Microscopic Study of the Texture of the Basement Membrane of Larval Amphibian Skin. *Proc Natl Acad Sci U S A.* 40:528-40.
- Wiche, G. 1998. Role of plectin in cytoskeleton organization and dynamics. *J Cell Sci.* 111 (Pt 17):2477-86.
- Wiche, G., and M.A. Baker. 1982. Cytoplasmic network arrays demonstrated by immunolocalization using antibodies to a high molecular weight protein present in cytoskeletal preparations from cultured cells. *Exp Cell Res.* 138:15-29.
- Wiche, G., D. Gromov, A. Donovan, M.J. Castanon, and E. Fuchs. 1993. Expression of plectin mutant cDNA in cultured cells indicates a role of COOH-terminal domain in intermediate filament association. *J Cell Biol.* 121:607-19.
- Wiche, G., R. Krepler, U. Artlieb, R. Pytela, and W. Aberer. 1984. Identification of plectin in different human cell types and immunolocalization at epithelial basal cell surface membranes. *Exp Cell Res.* 155:43-9.
- Wiche, G., R. Krepler, U. Artlieb, R. Pytela, and H. Denk. 1983. Occurrence and immunolocalization of plectin in tissues. *J Cell Biol.* 97:887-901.
- Wicki, A., and G. Christofori. 2007. The potential role of podoplanin in tumour invasion. *Br J Cancer.* 96:1-5.
- Wicki, A., F. Lehenbre, N. Wick, B. Hantusch, D. Kerjaschki, and G. Christofori. 2006. Tumor invasion in the absence of epithelial-mesenchymal transition: podoplanin-mediated remodeling of the actin cytoskeleton. *Cancer Cell.* 9:261-72.
- Wijnhoven, B.P., W.N. Dinjens, and M. Pignatelli. 2000. E-cadherin-catenin cell-cell adhesion complex and human cancer. *Br J Surg.* 87:992-1005.

Wilhelmsen, K., S.H. Litjens, I. Kuikman, N. Tshimbalanga, H. Janssen, I. van den Bout, K. Raymond, and A. Sonnenberg. 2005. Nesprin-3, a novel outer nuclear membrane protein, associates with the cytoskeletal linker protein plectin. *J Cell Biol.* 171:799-810.

Williams, J.F. 1989. Optimization strategies for the polymerase chain reaction. *Biotechniques.* 7:762-9.

Winder, S.J., L. Hemmings, S.J. Bolton, S.K. Maciver, J.M. Tinsley, K.E. Davies, D.R. Critchley, and J. Kendrick-Jones. 1995. Calmodulin regulation of utrophin actin binding. *Biochem Soc Trans.* 23:397S.

S.J. Winder, T.J. Gibson and J. Kendrick-Jones. 1995. Dystrophin and utrophin: the missing links!. *FEBS Lett.* 369:27-33

Winsor, B., and E. Schiebel. 1997. Review: an overview of the *Saccharomyces cerevisiae* microtubule and microfilament cytoskeleton. *Yeast.* 13:399-434.

Wolf, K., I. Mazo, H. Leung, K. Engelke, U.H. von Andrian, E.I. Deryugina, A.Y. Strongin, E.B. Brocker, and P. Friedl. 2003. Compensation mechanism in tumor cell migration: mesenchymal-amoeboid transition after blocking of pericellular proteolysis. *J Cell Biol.* 160:267-77.

Wong, M.K., and A.I. Gotlieb. 1988. The reorganization of microfilaments, centrosomes, and microtubules during in vitro small wound reendothelialization. *J Cell Biol.* 107:1777-83.

Wozniak, M.A., K. Modzelewska, L. Kwong, and P.J. Keely. 2004. Focal adhesion regulation of cell behavior. *Biochim Biophys Acta.* 1692:103-19.

Wright, M.D., S.M. Geary, S. Fitter, G.W. Moseley, L.M. Lau, K.C. Sheng, V. Apostolopoulos, E.G. Stanley, D.E. Jackson, and L.K. Ashman. 2004. Characterization of mice lacking the tetraspanin superfamily member CD151. *Mol Cell Biol.* 24:5978-88.

Xie, Z., W. Su, Z. Guo, H. Pang, S.R. Post, and M.C. Gong. 2006. Up-regulation of CPI-17 phosphorylation in diabetic vasculature and high glucose cultured vascular smooth muscle cells. *Cardiovasc Res.* 69:491-501.

Yamada, K.M., and S. Miyamoto. 1995. Integrin transmembrane signaling and cytoskeletal control. *Curr Opin Cell Biol.* 7:681-9.

Yamaguchi, H., M. Lorenz, S. Kempiak, C. Sarmiento, S. Coniglio, M. Symons, J. Segall, R. Eddy, H. Miki, T. Takenawa, and J. Condeelis. 2005. Molecular mechanisms of invadopodium formation: the role of the N-WASP-Arp2/3 complex pathway and cofilin. *J Cell Biol.* 168:441-52.

Yang, Y., C. Bauer, G. Strasser, R. Wollman, J.P. Julien, and E. Fuchs. 1999. Integrators of the cytoskeleton that stabilize microtubules. *Cell.* 98:229-38.

- Yarrow, J.C., Z.E. Perlman, N.J. Westwood, and T.J. Mitchison. 2004. A high-throughput cell migration assay using scratch wound healing, a comparison of image-based readout methods. *BMC Biotechnol.* 4:21.
- Yoon, M., R.D. Moir, V. Prahlad, and R.D. Goldman. 1998. Motile properties of vimentin intermediate filament networks in living cells. *J Cell Biol.* 143:147-57.
- Young, K.G., M. Pool, and R. Kothary. 2003. Bpag1 localization to actin filaments and to the nucleus is regulated by its N-terminus. *J Cell Sci.* 116:4543-55.
- Zamir, E., and B. Geiger. 2001. Molecular complexity and dynamics of cell-matrix adhesions. *J Cell Sci.* 114:3583-90.
- Zernig, G., and G. Wiche. 1985. Morphological integrity of single adult cardiac myocytes isolated by collagenase treatment: immunolocalization of tubulin, microtubule-associated proteins 1 and 2, plectin, vimentin, and vinculin. *Eur J Cell Biol.* 38:113-22.
- Zhang, T., P. Haws, and Q. Wu. 2004. Multiple variable first exons: a mechanism for cell- and tissue-specific gene regulation. *Genome Res.* 14:79-89.
- Zhou, X., A. Stuart, L.E. Dettin, G. Rodriguez, B. Hoel, and G.I. Gallicano. 2004. Desmoplakin is required for microvascular tube formation in culture. *J Cell Sci.* 117:3129-40.
- Ziegler, W.H., R.C. Liddington, and D.R. Critchley. 2006. The structure and regulation of vinculin. *Trends Cell Biol.* 16:453-60.

